Tryptophanyl-tRNA Synthetase And Its Role In The Incorporation Of New Intrinsic Fluorescent Probes Into Proteins.

Christopher Warren Victor Hogue

Thesis submitted to
the School of Graduate Studies and Research
in partial fulfillment of the requirements for the degree of
Doctor of Philosophy in Biochemistry

University of Ottawa

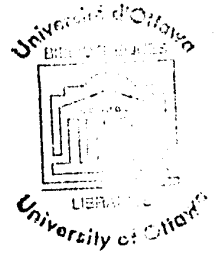

People are generally better persuaded by the reasons which they have themselves discovered than by those which have come into the minds of others.

Blaise Pascal 1623-1662

Abstract

TRYPTOPHANYL-TRNA SYNTHETASE AND ITS ROLE IN THE INCORPORATION OF NEW INTRINSIC FLUORESCENT PROBES INTO PROTEINS.

Christopher Warren Victor Hogue
Department of Biochemistry, University of Ottawa, 1994

Fluorescence spectroscopy can reveal insights into the structure, function and dynamics of proteins using the intrinsic fluorescence of tryptophan (Trp) residues. Time-resolved fluorescence is uniquely sensitive to the local microenvironment of Trp residues. This methodology is widely used, yet extensions allowing the further study of protein interactions are desired. Tryptophan analogs are targeted as new intrinsic probes, since their structures may camouflage them sufficiently to trick the relevant protein synthesis mechanisms to allow their incorporation into proteins. The specificity of a single enzyme, tryptophanyl-tRNA synthetase (TrpRS; E.C. 6.1.1.2), is the key to success for biosynthetic Trp analog incorporation. TrpRS catalyzes the ATP activation of Trp, and the subsequent aminoacylation of $tRNA^{Trp}$, prior to ribosomal protein synthesis.

Bacillus subtilis TrpRS has a single conserved and essential Trp-92 residue in each of its symmetrical α-2 subunits. The fluorescence of this Trp was very useful for investigating the TrpRS mechanism, together with the nonfluorescent isomorphous analog 4-fluorotryptophan as substrate. A tryptophanyl-5'-adenylate dependent quenching of Trp-92 fluorescence was observed, consistent with a local α-helix formation, placing a conserved Cys residue in quenching proximity to the Trp-92 fluorophore. This corresponds with the recent crystal structure of the homologous *B. stearothermophilus* TrpRS. Titrations while monitoring Trp-92 fluorescence revealed that the TrpRS dimer undergoes a concerted conformational change, virtually complete with the reaction of one subunit. This change seems necessary since this very small enzyme could only bind the relatively large $tRNA^{Trp}$ substrate through interactions with both subunits.

Potentially useful Trp analogs for fluorescence studies were examined to determine if they were TrpRS substrates. 5-hydroxytryptophan (5HW) and 7-azatryptophan (7AW) were studied both as TrpRS substrates, and as biosynthetically incorporated replacements of Trp-92. Methodology for efficient incorporation of these normally toxic Trp analogs is demonstrated. 7AW was shown to be very sensitive to solvent exposure, as its inclusion into a buried region of the protein causes large increases in its fluorescence yield. 7AW is recognized as having particular utility for the study of protein folding. Observations of the time-resolved fluorescence behaviour of Trp and 5HW in the same protein microenvironment are of consequence for fluorescence theory, as they indicate that the current assumptions regarding radiative properties may require modification.

By combining insights from both the crystal structure and these intrinsic fluorescence studies with both Trp and the analogs, a clearer picture of the mechanism of TrpRS was obtained. Prior to this study, the role of the essential Trp-92 was not understood in terms of the mechanism of TrpRS. This study demonstrates Trp-92 is crucial for both TrpRS conformational stability and for its very dynamic mechanism which involves large, substrate-dependent conformational changes.

To Marylka and the wee one.

Acknowledgements

Together, Dr. Arthur G. Szabo and Dr. John P. MacManus got me out of a bad spot in life, and provided me with the opportunity to work at the National Research Council of Canada as a technician in 1988. They somehow overlooked the fact that I had not yet obtained my B.Sc. when they hired me. Without that opportunity I would not have become a scientist. My thesis project formed in those early days as a technician. Dr. Szabo kindly provided me with the opportunity to return to the NRC to do graduate studies, after encouraging me to go back to Windsor and finish my B.Sc.

Persons in Dr. Szabo's group over the years who spent time teaching me fluorescence techniques included Dr. Cindy Hutnik and Dr. Kevin Willis. Without Don Krajcarski's excellent technical support, keeping equipment operating, and teaching the subtleties of time-resolved fluorescence, this would be a much less substantial work. Ms. Tanya Dahms provided that essential graduate student camaraderie that is hard to obtain in an off-campus setting.

Over the years, Dr. MacManus and his group, Rita Ball, Ingrid Rasquinha and Karen Shank, were of important assistance in this effort, performing some of the original biological sleight-of-hand to get the original oncomodulin expression systems to work which later proved that this business of analog incorporation would indeed work.

Dr. Jeffrey T. Wong has been instrumental in getting this project started by providing the original expression systems. Other people working on tryptophanyl-tRNA synthetase have provided very helpful discussions and enthusiasm for this work, including Dr. Hong Xue, and Dr. Roger E. Koeppe II. Dr. Charles W. Carter Jr. and his graduate student, Silvie Doublié performed a miracle and solved the structure of the tryptophanyl-tRNA synthetase complex right before I started writing my thesis, providing an otherwise unattainable interpretational viewpoint. Many thanks go to Dr. Makato Yaguchi and his technician Pat Lanthier for providing mass spectrometry and amino acid analysis services. Thanks are also in order to Mrs. R. To and Dr. C. Chen for their efforts at crystallizing the enzyme.

I would also like to acknowledge the people who helped me feel confident in my abilities by letting me help them; Irene Hill, Ian Clark, John Brennan, Jacinta Drew, and our students; Claire Brown, Andromeda Bruckman, Dan Dufor, and Sonya Cyr.

I am sincerely grateful to those staff of the National Research Council of Canada dedicated to making opportunities for myself and other students to perform frontier generic research at the Institute for Biological Sciences. I earnestly hope that NRC will keep in mind its corporate goals and commitment to the training of future graduate students.

The financial support of this work over the last four years from both the Ontario Graduate Scholarship program and the Natural Sciences and Engineering Research Council are gratefully acknowledged.

Table of Contents

List of Tables

List of Figures

List of Abbreviations

Notations:

nAW ..... n-azatryptophan where n = 2,7

nFW ..... n-fluorotryptophan where n = 4-7

nMW ..... n-methyltryptophan where n = 1-7,ß,α

AaaRS ..... aminoacyl-tRNA synthetase for amino acid "Aaa", its three-letter code.

AnnB "protein" ..... With A or B one-letter amino acid codes, and nn a residue number for the specified protein. Indicates a protein with mutation of residue A in position nn to residue B.

Ann(xxx) "protein" ..... Indicates mutation of amino acid A of residue nn in the specified protein to an amino acid analog code xxx.

A $\rightarrow$ B ..... Energy transfer from species A to B.

Symbols For Fluorescence Spectroscopic Parameters, Often Used:

τ_s ..... singlet fluorescence lifetime

τ_r ..... radiative lifetime

τ_m ..... intensity weighted mean lifetime

$<\tau>$ ..... average lifetime

λ_{max} ..... spectral wavelength maximum

α_i ..... amplitude of decay component *i* (preexponential term)

c_i ..... concentration of decay component *i*

k_{nr} ..... sum of all non-radiative rates

J..... Spectral overlap integral for RET

Φ..... quantum yield

κ^2 ..... orientational dependence of Förster energy transfer.

ϵ_λ ..... Molar extinction coefficient at wavelength λ

Abbreviations:

..... (Some symbols used in tables and figures are defined in their accompanying captions.)

1M7AI 1-methyl-7-azaindole

2AW..... 2-azatryptophan; tryptazan

4FW..... 4-fluorotryptophan

4FW-AMP ..... 4-fluorotryptophanyl-5'-adenylate

5FW..... 5-fluorotryptophan

5HI 5-hydroxyindole

5HT ..... 5-hydroxytryptamine; serotonin

5HW 5-hydroxytryptophan

5HW-AMP..... 5-hydroxytryptophanyl-5'-adenlate

5MeOW..... 5-methoxytryptophan

6FW..... 6-fluorotryptophan

6MW..... 6-methyltryptophan

7AI 7-azaindole

7AW-AMP..... 7-azatryptophanyl-5'-adenylate

7M7AI 7-methyl-7-azaindole

aaRS..... aminoacyl-tRNA synthetase

AMP ..... adenosine monophosphate

Amp^r ..... ampicillin resistance gene

ATCase ..... aspartate transcarbamylase

ATP ..... adenosine-5'-triphosphate

BCA ..... bicinchoninic acid

CP1 ..... connective polypeptide 1

CRC ..... cyclic-AMP receptor

CTP..... cytosine triphosphate

CTP..... cytosine-5'-triphosphate

DAS ..... decay associated spectra

DNA..... deoxyribonucleic acid

DTNB ..... 5,5'dithiobis(2-nitrobenzoic acid)

DTT ..... dithiothreitol

E.C. ..... Enzyme Commission

EDTA ..... ethylenediaminetetraacetic acid

FWHM..... full width at half maximum

GdHCl ..... guanidine hydrochloride

HPLC ..... high performance liquid chromatography

IPTG ..... isopropyl-ß-D-thiogalactopyranoside

$LacI^q$ ..... lac repressor gene

mRNA..... messenger ribonucleic acid

NATA..... N-acetyl-tryptophanamide

NaTyrA ..... N-acetyl-tyrosoinamide

NMR ..... nuclear magnetic resonance

PMSF ..... phenylmethylsulfonylfluoride

PMT..... photomultiplier tube

PP_i..... inorganic pyrophosphate

PP_iase ..... inorganic pyrophosphatase

Ptac ..... tac promoter sequence

RET ..... resonance energy transfer

RNA ..... ribonucleic acid

RNAP ..... RNA polymerase

SDS ..... sodiumdodecylsulfate

SDS-PAGE ..... sodiumdodecylsulfate polyacrylamide gel electrophoresis

Spc^r/Sm^r ..... spectinomycin/streptomycin resistance gene

SVR ..... serial variance ratio

TCA ..... trichloroacetic acid

TCSPC ..... time-correlated single photon counting

tRNA ..... transfer ribonucleic acid

Trp-ATP ..... tryptophanyl-2'-adenosinde triphosphate

TrpRS ..... tryptophanyl-tRNA synthetase

TrpS ..... tryptophanyl-tRNA synthetase gene

UV ..... ultraviolet

WSSR ..... weighted sum of squares of residuals

Chapter 1

INTRODUCTION

INTRODUCTION

This work is concerned with the biosynthetic incorporation of alternative amino acids, selected to change the optical spectroscopic properties of proteins. These changes will enhance the study of protein structure, function, dynamics and interactions using fluorescence spectroscopic techniques. Bacterial protein synthesis can be used to incorporate some unnatural amino acids into recombinant proteins. The relevant portion of the protein synthesis pathway will be studied as it relates to the incorporation of these alternative amino acids. This introductory chapter provides a framework for understanding proteins, the machinery of protein synthesis, and how previous work with amino acid analogs relates to the current study. The next chapter will describe in detail the spectroscopic techniques and the spectroscopic features of the amino acids and analogs used in this work.

1.1 Proteins

Proteins are typically described by their characteristic roles as biological catalysts or enzymes. Yet proteins also serve organisms in other ways, to send signals, to store nutrients, to form supporting structures, and to provide defence mechanisms. In general, proteins posses properties and functions that are related to their structure. Protein structure is hierarchical in nature, therefore any understanding of protein structure begins with the structural elements held in common.

Proteins are linear biopolymers comprised of ordered sequences of the 20 naturally occurring amino acids (Fig. 1.1). A protein is formed as a condensation polymer of these monomer units. The α-carboxyl group of one amino acid forms an amide bond with the α-amino group of the next, with the elimination of water.

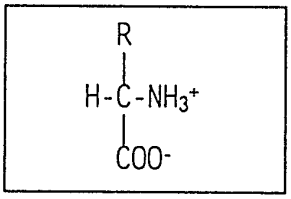

Figure 1.1: General structure of a zwitterionic L amino acid. R represents the amino acid side chain.

The 20 amino acids which are most frequently found in proteins show a diversity of chemical structures. Nature has provided this library of amino acids, Figure 1.2, with a variety of volumes, charge, polarity, and bonding forces. The properties of a functional protein are dominated by these side chains and their spatial organization. Proteins may also contain other organic or inorganic components, known as prosthetic groups or coenzymes.

The hierarchical nature of protein structure is best described by example. First, the sequence of amino acids (primary structure) is characteristic of a particular protein. Figure 1.3 shows the primary sequence for the enzyme tryptophanyl-tRNA synthetase (TrpRS) from *B. stearothermophilus* (Winter and Hartley, 1977; Barstow et al, 1986). Most of the covalent bonds in a protein are uniquely described by such a primary sequence. Different organisms may have similar proteins - with the same functions. These often have many similarities in primary sequence, and they will often share structural similarities and spatial organization.

The second level of hierarchy of protein structure comprises the organization of amino acids which are close neighbors in the linear sequence of the protein. These are classified by recognizable patterns. A right-handed coiled polypeptide chain stabilized by intrachain hydrogen bonding between backbone carbonyl and amide groups is known as an α-helix. The α-helix most often observed involves hydrogen bonding between the CO of residue N, and the NH of residue $N+4$. There are 3.6 amino residues in each turn of the α-helix, and its diameter is approximately 5 Å. A flat

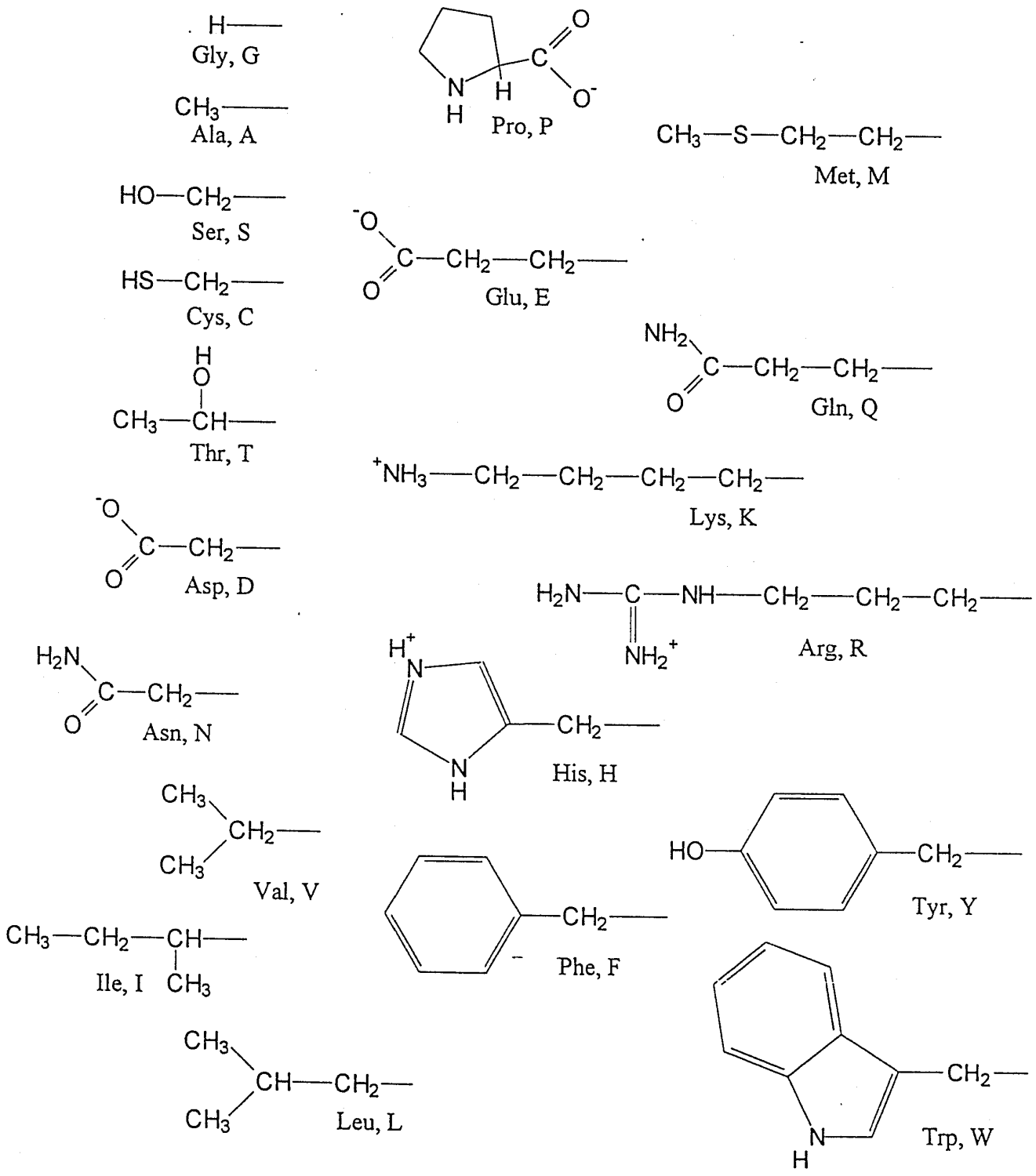

Figure 1.2: Side chain structures of the 20 common amino acids found in proteins. Shown beneath each amino acid is the corresponding IUPAC-IUPAB three-letter abbreviation and one-letter symbol.

```
1               5                  10                  15                  20
Met Lys Thr Ile Phe Ser Gly Ile Gln Pro Ser Gly Val Ile Thr Ile Gly Asn Tyr Ile

               25                  30                  35                  40
Gly Ala Leu Arg Gln Phe Val Glu Leu Gln His Glu Tyr Asn Cys Tyr Phe Cys Ile Val

               45                  50                  55                  60
Asp Gln His Ala Ile Thr Val Trp Gln Asp Pro His Glu Leu Arg Gln Asn Ile Arg Arg

               65                  70                  75                  80
Leu Ala Ala Leu Tyr Leu Ala Val Gly Ile Asp Pro Thr Gln Ala Thr Leu Phe Ile Gln

               85                  90                  95                 100
Ser Glu Val Pro Ala His Ala Gln Ala Ala Trp Met Leu Gln Cys Ile Val Tyr Ile Gly

              105                 110                 115                 120
Glu Leu Glu Arg Met Thr Gln Phe Lys Glu Lys Ser Ala Gly Lys Glu Ala Val Ser Ala

              125                 130                 135                 140
Gly Leu Leu Thr Tyr Pro Pro Leu Met Ala Ala Asp Ile Leu Leu Tyr Asn Thr Asp Ile

              145                 150                 155                 160
Val Pro Val Gly Glu Asp Gln Lys Gln His Ile Glu Leu Thr Arg Asp Leu Ala Glu Arg

              165                 170                 175                 180
Phe Asn Lys Arg Tyr Gly Glu Leu Phe Thr Ile Pro Glu Ala Arg Ile Pro Lys Val Gly

              185                 190                 195                 200
Ala Arg Ile Met Ser Leu Val Asp Pro Thr Lys Lys Met Ser Lys Ser Asp Pro Asn Pro

              205                 210                 215                 220
Lys Ala Tyr Ile Thr Leu Leu Asp Asp Ala Lys Thr Ile Glu Lys Lys Ile Lys Ser Ala

              225                 230                 235                 240
Val Thr Asp Ser Glu Gly Thr Ile Arg Tyr Asp Lys Glu Ala Lys Pro Gly Ile Ser Asn

              245                 250                 255                 260
Leu Leu Asn Ile Tyr Ser Thr Leu Ser Gly Gln Ser Ile Glu Glu Leu Glu Arg Gln Tyr

              265                 270                 275                 280
Glu Gly Lys Gly Tyr Gly Val Phe Lys Ala Asp Leu Ala Gln Val Val Ile Glu Thr Leu

              285                 290                 295                 300
Arg Pro Ile Gln Glu Arg Tyr His His Trp Met Glu Ser Glu Glu Leu Asp Arg Val Leu

              305                 310                 315                 320
Asp Glu Gly Ala Glu Lys Ala Asn Arg Val Ala Ser Glu Met Val Arg Lys Met Glu Gln

              325         328
Ala Met Gly Leu Gly Arg Arg Arg
```

Figure 1.3: The amino acid sequence of *B. stearothermophilus* TrpRS as an example of primary structure. (Winter and Hartley, 1977; Barstow et al, 1986). The underlined sequences correspond to sequences with homologies with other aminoacyl-tRNA synthetases.

stretch of protein chain stabilized by hydrogen bonds between neighboring chains is known as a ß-sheet. The directions of the polypeptide strands forming a ß-sheet can be oriented parallel or antiparallel to one another. Turns with recognizable patterns are also considered secondary structures. For example a hairpin turn with a hydrogen bond between the CO of residue N and the NH of residue $N+3$ is known as a ß-turn.

Efforts have been made to correlate amino acid sequences with a propensity to form certain types of secondary structure (Chou and Fasman, 1974a) and to predict protein secondary structure using the primary sequence and these data (Chou and Fasman, 1974b; Fasman, 1989). Webster and coworkers, (1987) have carefully considered the sequence of our example protein, *B. stearothermophilus* tryptophanyl-tRNA synthetases with homologous sequences from the same enzyme from *E. coli* (Hall et al., 1982) and *B. subtilis* (Chow and Wong, 1988). They predicted the secondary structure of a portion of this enzyme (Fig. 1.4) (1991 unpublished communication, T. Webster). However the overall three-dimensional structural organization and conformation of a protein cannot yet be inferred from this information alone (Fasman, 1989).

The third level of the protein structure hierarchy, the tertiary structure, is the functional three-dimensional configuration which the protein backbone and side chains adopt. Tertiary structure forms through a combination of covalent and noncovalent stabilizing bonds between the amino-acid side chains, including disulfide bonds, hydrophobic interactions, hydrogen bonds, and ionic pair interactions (Dill, 1990). This level of structural detail is obtained through painstaking and laborious experiments involving the formation of pure protein crystals. Carter Jr., and Carter (1979) were able to produce single protein crystals of *B. stearothermophilus* TrpRS. The x-ray crystallographic structure of this protein was reported in 1993 (Doublié and Carter Jr.). Different levels of detail of this tertiary structure are shown in Figure 1.5, together with a schematic showing how the secondary structure of the protein is organized.

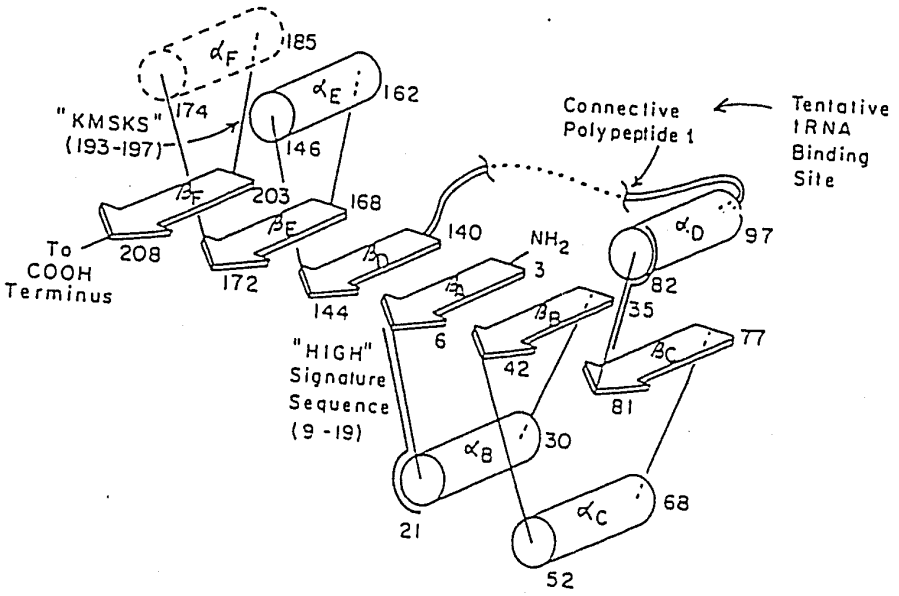

Figure 1.4: Schematic of Webster's predicted secondary structure of bacterial tryptophanyl-tRNA synthetase. Cylinders represent α-helicies, flat arrows represent ß-sheets. The assignment is based in part on sequence similarities with methionine-tRNA synthetase. Two consensus sequences common to some aminoacyl-tRNA synthetases, "HIGH" and "KMSKS" assist in orienting the prediction. These sequences and the secondary structural elements ßA, αB, ßB, and αC, form the Rossman nucleotide-binding fold, common to these proteins. The F-helix was not strongly predicted, hence it appears with dashed lines. The D α-helix was an unexpected prediction since it did not appear in other homologous enzymes. The structure of the Connective Polypeptide 1 region was not predicted, since this region varies amongst this family of proteins. (T. Webster, unpublished communication).

Figure 1.5: Tertiary structure of the monomer subunit of *B. stearothermophilus* tryptophanyl-tRNA synthetase. (Doublié and Carter Jr., 1993) A. Schematic showing the approximate arrangement of secondary structural elements in the tertiary fold. Some of the α-helicies and ß-sheets as predicted by Webster (Fig 1.4) are labelled. The α-F helix is missing from the tertiary structure, and the α-D helix is present, both as predicted by Webster. The consensus sequences "HIGH" and "KMSKS" are within the circle. These are neighbors in space, unlike the representation in the previous secondary structure schematic. B. The polypeptide backbone of the enzyme is shown, omitting the side chains for clarity. The substrate tryptophanyl-5'-adenylate is shown in bold with the adenine ring at left within the Rossman fold. C. Complete structure showing side chains, using a "stick" representation. D. Complete structure using a space-filling "sphere" representation.

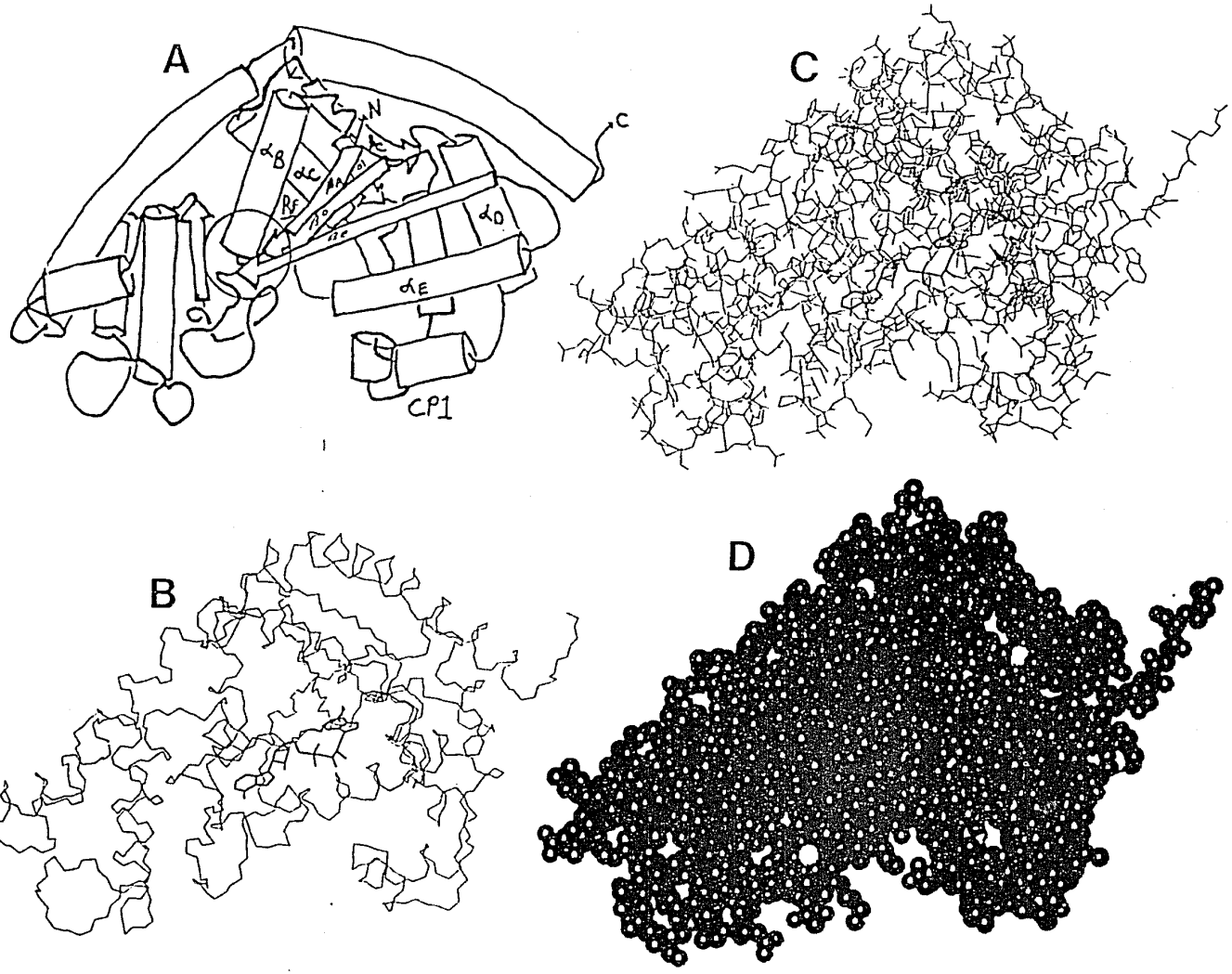
A
N
C
αB
αC
αF
αD
αE
CP1
C
B
D

A fourth level of protein structure is described for those proteins which consist of more than one polypeptide chain. How these chains fit together in the molecule is known as the quaternary structure. The forces stabilizing this association of polypeptides, or subunits are largely the same as those responsible for tertiary structure. The protein TrpRS exists as a functional enzyme through a noncovalent association of two identical polypeptide chains. Two views of this dimeric protein, together with its complexed substrate tryptophanyl-5'-adenylate, are shown in Figure 1.6.

In order to understand the role of any given protein and how its function relates to its structure, the protein must be purified, and interrogated by chemical and physical methods, such as sequencing and x-ray crystallography. These help establish its primary, secondary and tertiary structure. However finding an unknown function of a known protein may be more difficult to establish, even with the structural information. Since the structures obtained through crystallography are static, the dynamic information relating to how a protein may carry out its role is often missing. Information of how a protein interacts with substrate or other cellular components may also be missing from a static structure. Additional information can be obtained by other methods, such as kinetic studies, chemical modification, site-directed mutagenesis, optical and NMR spectroscopy. These are invaluable in integrating our understanding of the interrelationships of protein structure, function and dynamics.

1.2 Protein Synthesis

The flow of information from DNA to RNA to protein sequence has been well established over the last 30 years. The amino acid order; i.e. the primary sequence of a protein, is encoded in the sequence of the DNA for each gene. DNA and RNA are

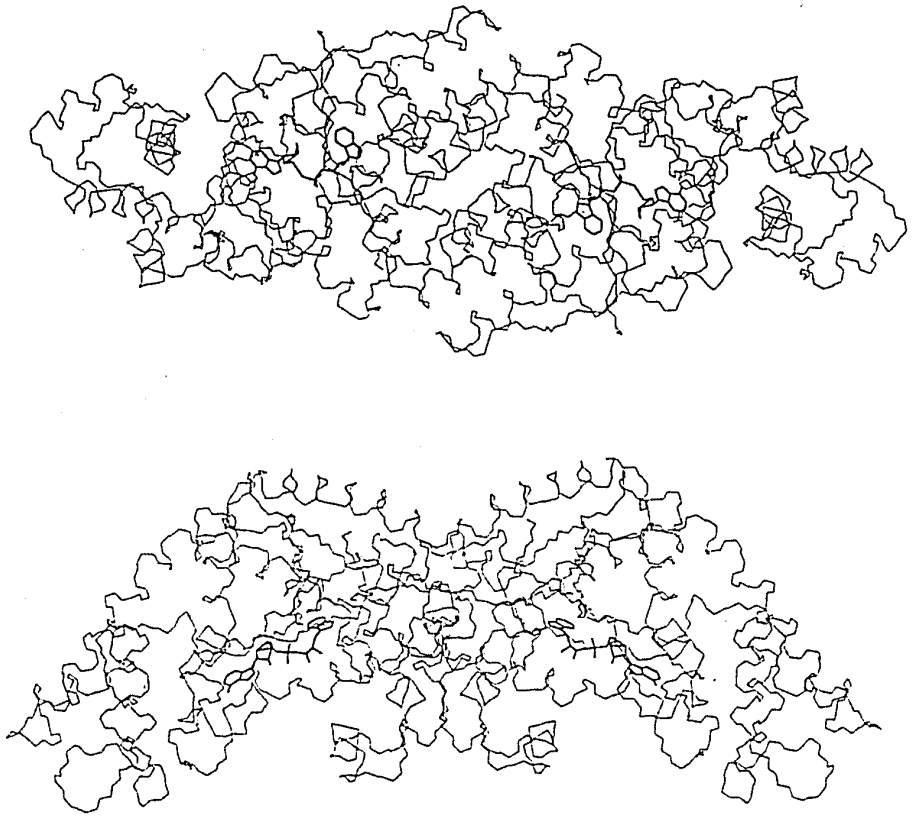

Figure 1.6: The quaternary structure of *B. stearothermophilus* tryptophanyl-tRNA synthetase as an α-2 symmetric dimer. (Doublié and Carter Jr., 1993). Top and side views. The substrate trytophanyl-5'-adenylate is depicted in bold, showing the active site of each monomer. The substrate Trp rings are closest to the center of the structure. Portions of each monomer interdigitate within each other. The dimer is 112 Å in length (Scale 1 mm = 1 Å).

linear biopolymers consisting of four monomeric nucleic acid bases (Adams et al., 1976) as depicted in Figure 1.7. DNA is composed of the deoxyribonucleotide derivatives of the purines adenine and guanine, and of the pyrimidines cytosine and thimine. These deoxyribonucleotides adenosine, guanosine cytidine and thymine comprise a condensation polymer which arranges itself for storage into a double helix formed by the pairing of the complementary deoxyribonucleotide bases, abbreviated A-T and G-C. These two strands are oriented in opposite directions, indicated by the numbering of the ribose ring 5' and 3' positions (Figure 1.7). The DNA sequence encodes each amino acid in a protein by means of a code of three deoxyribonucleotides - known as a triplet codon. This triplet codon is transcribed by enzymes to RNA (Table 1.1), using the DNA sequence as a template. RNA, is similar to DNA , but is comprised of ribonucleotide derivatives, with the substitution of the pyrimidine uracil in place of thymine. Messenger RNA, copied from DNA, serves as the template from which the protein sequence is translated.

It is simplest to describe protein synthesis within a cell as the ordered polymerization of activated amino acids. The translation of sequence information from the code of mRNA into a protein polymer is carried out in a ribosomal complex. Amino acids are carried to the ribosome attached to transfer-RNA molecules. tRNA molecules with specific anticodons carry their specific amino acid, complementing the mRNA codons detailed in Table 1.1. Hence tRNA molecules provide the physical translation from each mRNA codon to its corresponding amino acid. Stop and start signals, which vary amongst different organisms, punctuate the reading frame of the mRNA.

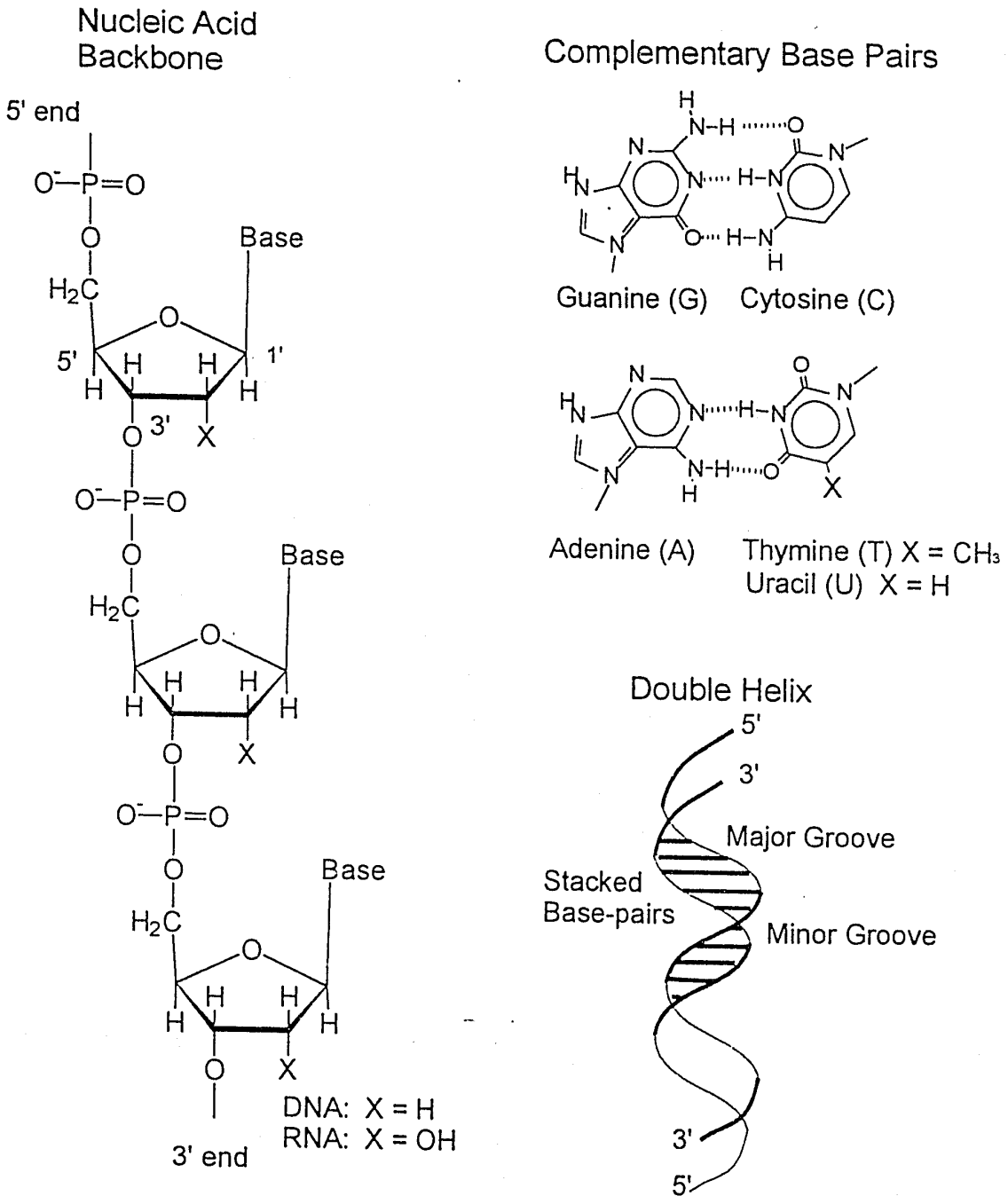

Figure 1.7: Structural components of DNA and RNA.

Table 1.1: The Genetic Code (mRNA).

Stop	UAA	Gly	GGU	Pro	CCU
	UAG		GGC		CCC
	UGA		GGA		CCA
Ala	GCU		GGG		CCG
	GCC	His	CAU	Ser	AGU
	GCA		CAC		AGC
	GCG	Ile	AUU		UCU
Arg	CGU		AUC		UCC
	CGC		AUA		UCA
	CGA	Leu	UUA		UCG
	CGG		UUG	Thr	ACU
	AGA		CUU		ACC
	AGG		CUC		ACA
Asn	AAU		CUA		ACG
	AAC		CUG	Trp	UGG
Asp	GAU	Lys	AAA	Tyr	UAU
	GAC		AAG		UAC
Cys	UGU	Met	AUG	Val	GUU
	UGC	Phe	UUU		GUC
Gln	CAA		UUC		GUA
	CAG				GUG
Glu	GAA				
	GAG				

1.2.1 The Ribosome - Site of Protein Synthesis

The ribosome is a complex molecular assembly, consisting of a small and large subunit (Prince et al, 1983). The prokaryotic ribosome is made up of three RNAs and 52 proteins. The ribosome has been considered too large to determine its structure from techniques used for globular proteins. However the structure of the ribosome has been revealed by many different experiments including chemical crosslinking, electron

microscopy and neutron diffraction techniques. A recent model of the ribosome complex is shown in Figure 1.8 (Lim et al., 1992). Most recently functional crystals of ribosomes from halophilic bacteria have been found suitable for X-ray crystallograpic studies (Evers et al., 1994), and more detailed structural elucidation is in progress.

Initiation of prokaryotic protein synthesis begins with the ribosome's recognition of the mRNA initiation site. In prokaryotes, the protein begins with an initiation codon specifying formyl-Methionine, recognized by a special tRNA, fMet-$tRNA_2^{Met}$ (Hunt, 1980). This amino acid may be later cleaved from the protein after synthesis by the enzyme methionine-aminopeptidase.

Ribosomal protein synthesis proceeds by the addition of amino acid residues to the c-terminal end of the growing polypeptide. mRNA in the ribosomal complex is translated to protein from the 5' to 3' direction. At least two binding sites for tRNA exist in the ribosome. The elongation of the polypeptide is performed in a three-stage cycle requiring elongation factor proteins and GTP hydrolysis (Clark, 1980). First the A site binds the incoming aminoacyl-tRNA. The P site binds the previous molecule of tRNA that was formerly bound in the A site, and to which the growing polypeptide is attached. Then the nascent polypeptide is transferred to the aminoacyl-tRNA in the A site, with the condensation of the new amino acid, lengthening the chain. Finally the tRNA in the P site is released, proceeding through an E or exit site, and the new peptidyl-tRNA in the A site is translocated to the P site, together with the translocation of the mRNA. The accuracy of the translation in the ribosome has been explained in part by a kinetic proofreading mechanism involving GTP hydrolysis and an elongation factor, EF-Tu, which binds the incoming aminoacyl-tRNA (Thompson, 1988, Weijland and Parmeggiani, 1994). This mechanism assures correct complementary base pairing prior to polypeptide chain elongation.

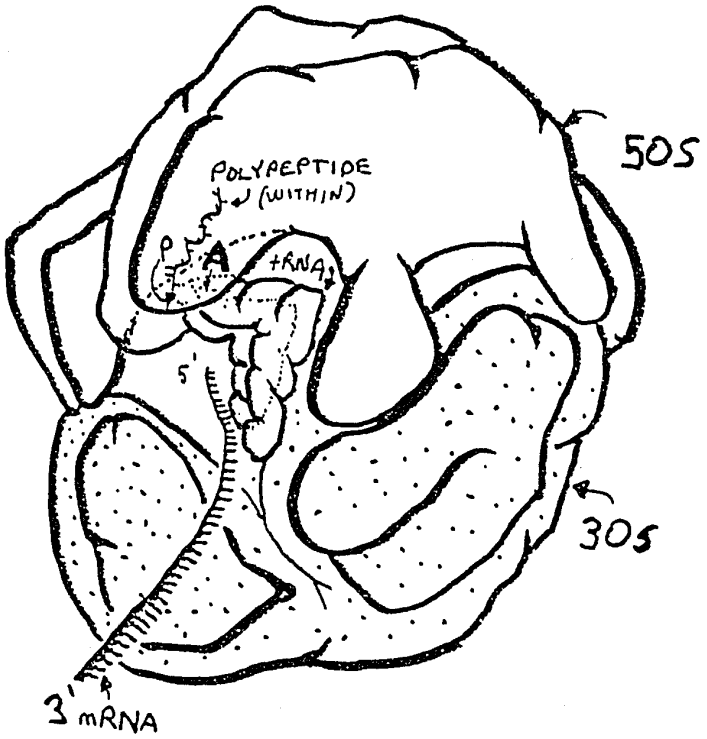

Figure 1.8: A model for the prokaryotic ribosomal complex. (After Lim et al., 1992). Two subunits, (unstippled) 50S and (stippled) 30S comprise a complex together with mRNA and two molecules of tRNA, occupying the A site and the P site. The polypeptide has been shown to pass through a large cavity within the 50S subunit before emerging (Yonath, 1993). The tRNA and mRNA are represented here in one of two possible orientations relative to the ribosome, but these orientations are still in dispute.

Termination of the growing protein is complete when a stop codon is reached. This causes the binding of factors inducing the hydrolysis of the peptidyl-tRNA (Caskey, 1980). A single mRNA can be simultaneously translated by several ribosomes, a structure known as a polysome.

1.2.2 Transfer Ribonucleic Acids

Transfer RNA is the translating element, relating mRNA sequence to a particular amino acid. tRNAs are small RNA molecules, typically 73-93 nucleic acid bases in length. Up to 10% of bases may be modified after tRNA synthesis. tRNA carries its cognate amino acid covalently on the amino acid acceptor end, linked through an ester bond between the carboxylate of the amino acid and either the 2' or 3' ribose hydroxyl of the 3' end of the tRNA.

Like proteins, RNA has a structural hierarchy. The secondary structural elements comprise nucleotide base-pairing interactions. The secondary structure of tRNA is often described as a cloverleaf shape, and a consensus sequence of tRNA has been described (McClain, 1993) shown in Figure 1.9. tRNA molecules posses three bases comprising the anticodon, roughly in the center of the sequence. These form base pairs with the codon of mRNA during protein synthesis. The third base pair formed of the codon-anticodon interaction, can be in a orientation somewhat different and more flexible as compared to those base-pair structures depicted in Figure 1.7. This is often called a "wobble" base pair and it allows a single tRNA to bind to multiple codons which can vary in the third base position, but represent the same amino acid (Table 1.1).

All the tRNA molecules in an organism require some similar structural features for the interactions shared in common. These include binding to EF-Tu and to

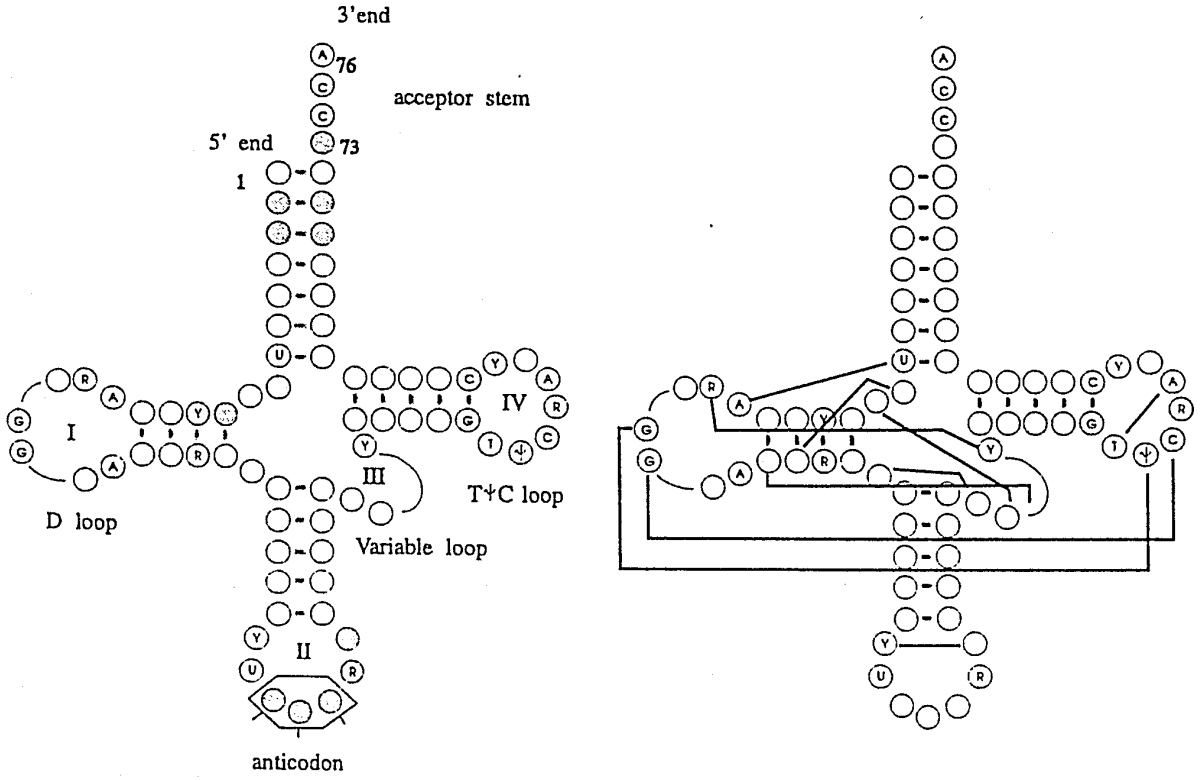

Figure 1.9: Secondary structure schematic of tRNA. (Left) Generalized structure with invariant or semivariant bases named (R = purine; Y = pyrimidine; ψ Pseudouridine) others represented by open circles. Lines in the D loop and Variable loop represent variable numbers of nucleotides. Shaded circles represent bases that have often been experimentally demonstrated to be important determinants for tRNA recognition by aminoacyl-tRNA synthetases. Base 73 has been found important for the specificity of most of these interactions. (Adapted from McClain, 1993) (Right) Schematic showing the arrangement of tertiary hydrogen-bonding interactions from the structure of $tRNA^{Phe}$, illustrating the involvement of invariant and semi-variant nucleotides in adopting the final tertiary structure. (Adapted from Quigley and Rich, 1976).

the ribosomal tRNA binding sites. Differences in structural features must be present so that tRNA can undergo specific interactions which ensure the fidelity of protein synthesis. These specific interactions include the recognition and covalent attachment of the correct amino acid to the tRNA, and the proper alignment and pairing of the tRNA's anticodon with the mRNA codon during translation.

The relationship between the structure and the shared interactions of tRNA became more clear after the elucidation of the tertiary structure. tRNA adopts a distinctive tertiary fold (Sussman et al., 1978). Most bases are stacked and base-paired, and the secondary structure is distorted, as depicted schematically in Figure 1.9, into the narrow L-shaped three-dimensional structure of Figure 1.10. Some tRNA molecules, such as mammalian mitochondrial tRNA, contain significant deletions in the D stem or pseudouridine stem. Experimental studies (Hou and Schimmel, 1992) and computational modelling (Steinberg et al., 1994) suggest the overall L-shaped bend in the tRNA molecule is flexible in nature. tRNAs with deletions can form a "boomerang" like structure to stretch to a normal anticodon-acceptor helix distance.

The structural elements responsible for the specific interactions of tRNA have proved more difficult to identify. The anticodon has been shown the only determinant for the specific interaction with mRNA. Single point mutations of tRNA sequences have revealed several bases responsible for tRNA recognition during the aminoacylation step, clustered near the acceptor stem and anticodon region (Rogers and Soll, 1990; McClain, 1993), depicted as shaded circles in Figure 1.9.

1.2.3 The Role of the Amino Acid

The question of the role of the amino acid in directing protein synthesis was addressed in early experiments by Chapeville et al. (1962) in which

Figure 1.10: Tertiary structure of yeast $tRNA^{Phe}$. (Sussman et al., 1978) (Left) Overall fold of phosphate backbone, depicting elements of secondary structure identified in Fig. 1.9. (Center) Detailed crystal structure showing base pairing, stick representation. (Right) Space-filling sphere representation. Note that the helical regions of tRNA have major and minor grooves like DNA (Fig. 1.7). Structure is approximately 80 angstroms in height.

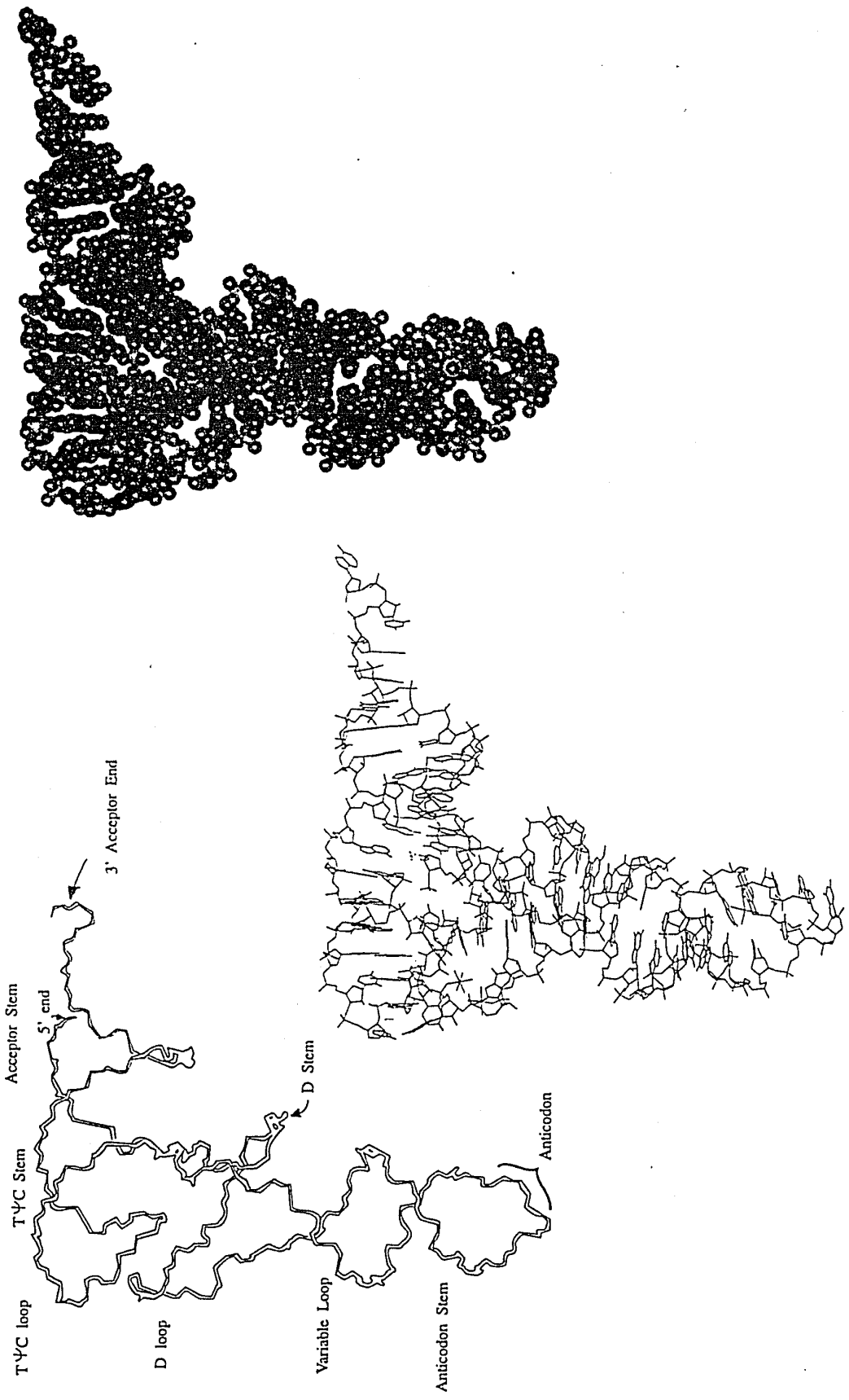
3' Acceptor End
Acceptor Stem
5' end
TΨC Stem
D Stem
Anticodon
TΨC loop
D loop
Variable Loop
Anticodon Stem

Cys-tRNA^{Cys} was chemically converted to Ala-tRNA^{Cys}. Subsequent analysis of the proteins synthesized demonstrated that Ala was put in place of Cys. It was concluded that the amino acid itself played no role in directing protein synthesis after tRNA aminoacylation. Later, Johnson (1974) found similar results after acetylating the ε-amino nitrogen of Lys-tRNA^{Lys} and recovering ε-N-acetyl-lysine in tetrameric hemoglobin.

Schultz and coworkers, (Mendel et al., 1992; Judice et al., 1993) have recently prepared proteins with a variety of unnatural amino acids (e.g O-methylserine; tert-leucine; L-4-nitro-2-aminobutyric acid - a nitro analog of Glu; and aminoethylhomocysteine and citrulline, both monoamine analogs of Arg). This was achieved through an in-vitro protein synthesis approach using suppressor tRNAs chemically acylated with the unnatural amino acids. The success of this technique with a wide variety of unnatural amino acids has demonstrated the passive role for amino acids in protein synthesis after tRNA aminoacylation.

One important exception is the recognition by chloroplast EF-Tu between misacylated Glu-tRNA^{Gln} and properly acylated Glu-tRNA^{Glu} (Stanzel et al., 1994). Chloroplasts, mitochondria, archaebacteria and Gram-positive bacteria lack an enzyme which attaches Gln to tRNA^{Gln}, and instead form Gln-tRNA^{Gln} from Glu-tRNA^{Gln} with an amidotransferase. Hence misacylated Glu-tRNA^{Gln} is abundant in chloroplasts, and requires further enzymatic processing. This specific form of amino acid discrimination is not observed with the EF-Tu of *E. coli*, a Gram-negative bacteria possessing the glutamine attaching enzyme, glutaminyl-tRNA synthetase.

1.2.4 Aminoacyl-tRNA Synthetases

Considering 20 possible amino acids and more than 20 possible tRNA molecules which could be aminoacylated, there are at least 400 different possible combinations. The class of enzymes comprising aminoacyl-tRNA synthetases maintains the fidelity of protein synthesis by the specific aminoacylation of cognate tRNA with cognate amino acid. Similar amino acids, such as the isomorphous Cys and Ser, or Val and Ile which differ by a methylene group, must be discerned by the individual aaRS enzymes without error. Most organisms contain twenty different aaRS enzymes which perform these tasks, one for each of the twenty protein amino acids.

The generally accepted mechanism for the formation of aminoacyl-tRNA is described by two reaction steps (Friest, 1989), first the formation of an activated aminoacyl-adenylate:

$$\text{aaRS} + \text{aa} + \text{ATP} \rightleftarrows \text{aaRS}\cdot\text{aa-AMP} + \text{PP}_i \qquad \text{(I)}$$

This step is driven to completion by the rapid intracellular degradation of PP_i by inorganic pyrophosphatase (Dignam and Deutscher 1979). The second step is the transfer of the amino acid onto tRNA, known as the aminoacylation step:

$$\text{aaRS}\cdot\text{aa-AMP} + \text{tRNA}^{aa} \rightleftarrows \text{aaRS} + \text{aa-tRNA}^{aa} + \text{AMP} \quad \text{(II)}$$

However there can be differences in the staging of the mechanism amongst aaRS enzymes (Friest, 1989). These include differences in the order of substrate binding, conformational changes and additional pretransfer hydrolytic proofreading mechanism which eliminate noncognate amino acids.

Table 1.2: Aminoacyl-tRNA Synthetase Classes.

	Class I	Class II
Aminoacyl Bond Site On Terminal Ribose	2' OH	3' OH (except PheRS)
Sequence Motifs[a]	...HIGH... ...KMSKS...	+G(F/Y)xx(V/L/I)xxPϕϕ (a) and (b) only +ϕϕxϕxxxFRx(E/D)... ...(R/H)xxxF... ϕGϕGϕGϕϕERϕϕϕϕ
Subclass Members	(a) LeuRS, IleRS, ValRS, CysRS, MetRS (b) TyrRS, TrpRS (c) ArgRS, GlnRS, GluRS	(a) HisRS, ProRS, SerRS, ThrRS (b) AspRS, AsnRS, LysRS (c) GlyRS, AlaRS (d) PheRS

[a] Bold type indicates conserved residues; normal type indicates consensus residues. Notation (x/y) indicates optional residues in one location. ϕ indicates hydrophobic residues, + indicates positively charged residues. Adapted from Cusack (1993) and Carter Jr. (1994).

The aaRS enzymes differ widely in their size and number of subunits (Mirande, 1991). Subunit organization has been shown to differ for some aaRS enzymes across species boundaries. Eukaryotic aaRS enzymes have been found in large multienzyme complexes of M_r 1.2×10^6, containing nine aaRS activities together with other proteins lacking aaRS activity. Amongst *E. coli* aaRS enzymes, AlaRS and GlyRS have the largest protomers and oligomeric size, while TrpRS has the smallest (Schimmel, 1987). There is an apparent inverse relationship between enzyme size and amino acid ligand size, as observed with other enzyme-substrate pairs (Goodsell and Olson, 1993).

At the time of writing, considerable new information about aminoacyl-tRNA synthetases has appeared in the literature, including new sequences, crystal structures, and mechanistic details. The subdivision of the known aminoacyl-tRNA synthetases into two classes (Eriani et al., 1990; Burbaum and Schimmel, 1991) has been a watershed event in the study of these enzymes. A few general trends relating to the

chemical nature of the amino acid and its volume can be related to the class and subclasses (Eriani et al., 1990) of these proteins, shown in Table 1.2. One observation is that several like pairs of amino acids which differ in size are partitioned between the two classes: i.e. Asp/Glu; Asn/Gln; Lys/Arg; Ser/Cys Phe/Tyr, with the larger of the two always in Class I. However no obvious correlation has been made between the aaRS class designation and the tRNA sequences or discriminator nucleotides shown in Figure 1.9, e.g. base 73. This implies that the structure of both the aaRS and the tRNA are important determinants in establishing their mutual identity and recognition.

1.2.4.1 Class I

Class I aminoacyl-tRNA synthetases share two primary structure motifs, as shown in Table 1.2. The amino acids acted upon by Class I enzymes contain more hydrophobic members than those acted on by Class II enzymes. Crystal structures of four members of Class I, TyrRS (Brick et al., 1988), MetRS (Brunie et al., 1990), TrpRS (Doublié and Carter Jr., 1993) and the GlnRS·$tRNA^{Gln}$ (Rould et al., 1989) complex, all show a common nucleotide-binding fold at the aminoacyl-adenylate binding site (Carter, Jr., 1993). This comprises parallel ß-strands and connecting α-helices in a structure known as the Rossmann fold (Rossmann et al., 1974). The two primary structure motifs H-I-G-H and K-M-S-K-S are near the ATP binding site (Figs. 1.5 and 1.6). While the regions conferring adenosine and amino acid binding have some structural homologies, there are no similarities with the $tRNA^{Gln}$ 3' end binding domains of GlnRS and structural domains in the other three enzymes. This suggests these all bind their cognate tRNA using different structural configurations.

A portion of Connective Polypeptide 1 (Fig. 1.4) has been implicated in binding a portion of the tRNA 3'-terminus in Class I aaRS enzymes (Rould et al., 1989; Burbaum and Schimmel, 1991). Connective polypeptide (CP1) links the N-terminal portion of the Rossman α/β nucleotide fold to the C terminal portion, identified in Figure 1.4. CP1 varies in length amongst Class I enzymes. A portion of the large CP1 in IleRS has been shown to be dispensable (Burbaum et al., 1990). The CP1 of GlnRS binds to the acceptor helix of $tRNA^{Gln}$ with a five-stranded antiparallel ß-sheet flanked by α-helicies (Rould et al., 1989) The dimeric enzymes TrpRS and TyrRS have CP1 regions which participate in inter-subunit stabilizations.

Mechanisms vary widely amongst Class I enzymes. MetRS, ValRS and IleRS have pretransfer hydrolytic proofreading mechanisms to eject noncognate aminoacyl-adenylates (Carter Jr., 1993) prior to step II. The order of substrate binding can also differ. The monomeric enzyme GlnRS will not perform reaction I unless it is first in a complex with $tRNA^{Gln}$ (Bhattacharyya et al., 1991; Perona et al., 1993). However the dimeric enzyme TyrRS, has an ordered mechanism, binding the amino acid Tyr first, then ATP, completing reaction I in the absence of $tRNA^{Tyr}$ (Brick and Blow, 1987). A third substrate order is shown in TrpRS from prokaryotic sources, which bind ATP first, then the amino acid, (Penneys and Muench, 1974; Xu et al., 1989) opposite to the order of TyrRS.

Unspecified conformational changes have been attributed to TrpRS and TyrRS (Fersht and Jakes, 1975) upon binding different substrates. TrpRS conformational changes were revealed by intrinsic fluorescence techniques (Andrews et al., 1985) and substrate-dependent changes in crystal morphology (Carter Jr. and Carter, 1979; Carter Jr. et al., 1994). Similarly sensitive experiments, using extrinsic fluorescence probes (Bhattacharyya et al., 1991) or experiments involving reactants diffusing into reactive crystals (Perona et al., 1993) show the bulk of the structure of GlnRS does not change conformation throughout its mechanism. This variety of mechanistic strategies

undertaken by Class I aaRS enzymes highlights their diverse approaches to ensuring the fidelity of protein synthesis.

1.2.4.2 Class II

Class II aminoacyl-tRNA synthetases can be designated by three conserved sequence motifs, as shown in Table 1.2. The amino acids controlled by Class II enzymes include more small, neutral molecules than Class I. From this observation, it has been suggested that Class II has more primitive origins than Class I (Carter Jr., 1993). However the relatively even distribution of 64 codons used (32 Class II and 29 Class I, ± 3 stop codons) between the two classes argues that they could be equally ancient. Functionally Class II enzymes differ from Class I by aminoacylating tRNA on the 3'OH (with the exception of PheRS). The sequence motifs of Class II are not strictly conserved. Motif 1 is found only in dimeric Class II enzymes (Moras, 1992) (with the exception that it is also found in PheRS - a tetramer). A principal difference between Class I and Class II is the location of the active site, which is usually in the C-terminal portion of Class II enzymes, wherein motifs 2 and 3 reside (except GlyRS and AlaRS).

Two crystal structures of Class II enzymes, SerRS (Cusack et al., 1990) and the AspRS·$tRNA^{Asp}$ (Ruff et al., 1991) complex, have confirmed the tertiary structural differences compared to Class I. Class II enzymes are missing the Rossman fold of Class I enzymes, and have instead an antiparallel ß-sheet nucleotide binding fold (Cusak, 1990). The amino acid binding pockets of AspRS and SerRS also seem to be more deeply buried than the pockets of the Class I enzymes.

The mode of tRNA binding between Class I and Class II enzymes may be fundamentally different, based on the comparison of the GlnRS·$tRNA^{Gln}$

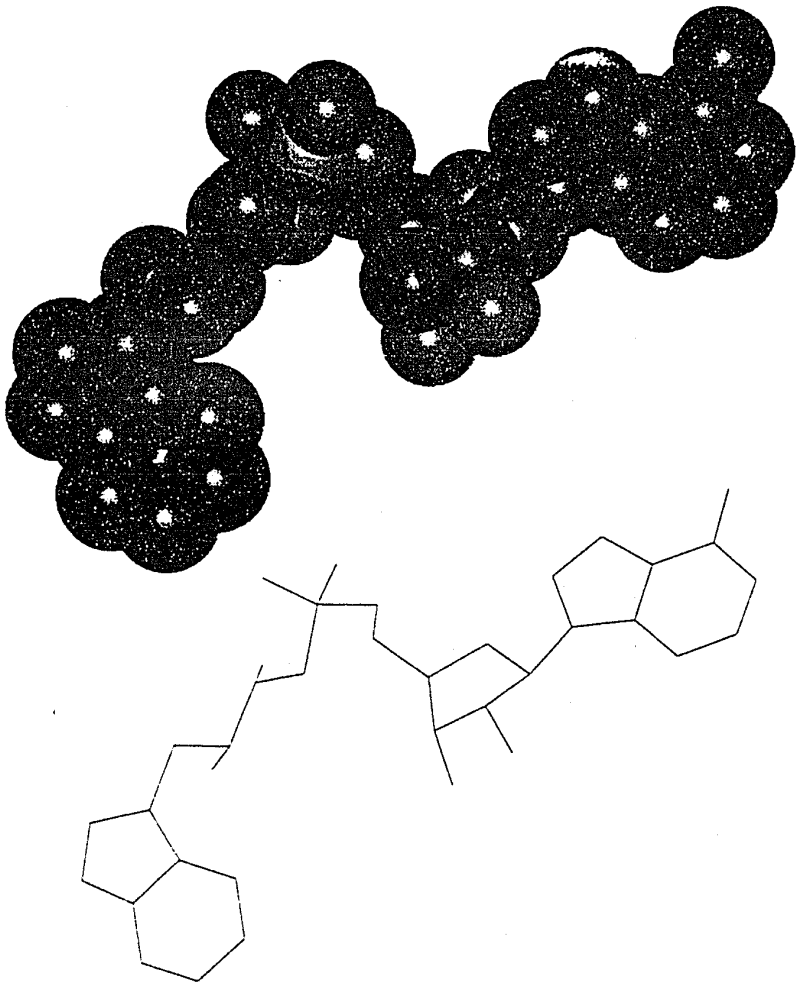

Figure 1.11: Structure of tryptophanyl-5'-adenylate as found in the active site of *B. stearothermophilus* TrpRS (Doublié and Carter Jr., 1993). (Top) Space-filling and (Bottom) stick views, with the indole ring to the left.

(Perona et al., 1993) and AspRS·tRNA^{Asp} complexes (Ruff et al., 1991). These show the tRNA binding on its minor groove side to GlnRS, and on its major groove side to AspRS. This relates to the functional difference in the site of tRNA aminoacylation between the two classes, i.e. the 3' or 2' ribose hydroxyl (Carter Jr. 1993). Based on these differences, Moras (1992) has suggested that the tRNA molecule is more passive partner in the binding and recognition process. Clearly the mode of recognition of cognate tRNA by each aaRS enzyme is idiosyncratic.

1.2.5 Tryptophanyl-tRNA synthetase

Tryptophanyl-tRNA synthetase (E.C. 6.1.1.2), like all aminoacyl-tRNA synthetases, plays a crucial role in protein synthesis. TrpRS was historically the second aminoacyl-tRNA synthetase discovered, first isolated and characterized from bovine pancreas (Davie et al., 1956). Since then TrpRS has been one of the most studied members of the family of aaRS. As other aaRS mechanisms, tRNA^{Trp} is aminoacylated with Trp by TrpRS in two reactions:

$$\text{TrpRS} + \text{Trp} + \text{ATP} \rightleftarrows \text{TrpRS·Trp-AMP} + \text{PP}_i \qquad \text{(III)}$$

$$\text{TrpRS·Trp-AMP} + \text{tRNA}^{Trp} \rightleftarrows \text{TrpRS} + \text{Trp-tRNA}^{Trp} + \text{AMP} \qquad \text{(IV)}$$

The first step, (III), involves the formation of the high energy tryptophanyl-5'-adenylate, shown in Figure 1.11, which is complexed in the enzyme's active site, one site per monomer (Figures 1.5, 1.6). Uncomplexed tryptophanyl-5'-adenylate is very unstable in water at pH $>$ 5 (Kingdon et al., 1958). It is also an efficient acylating

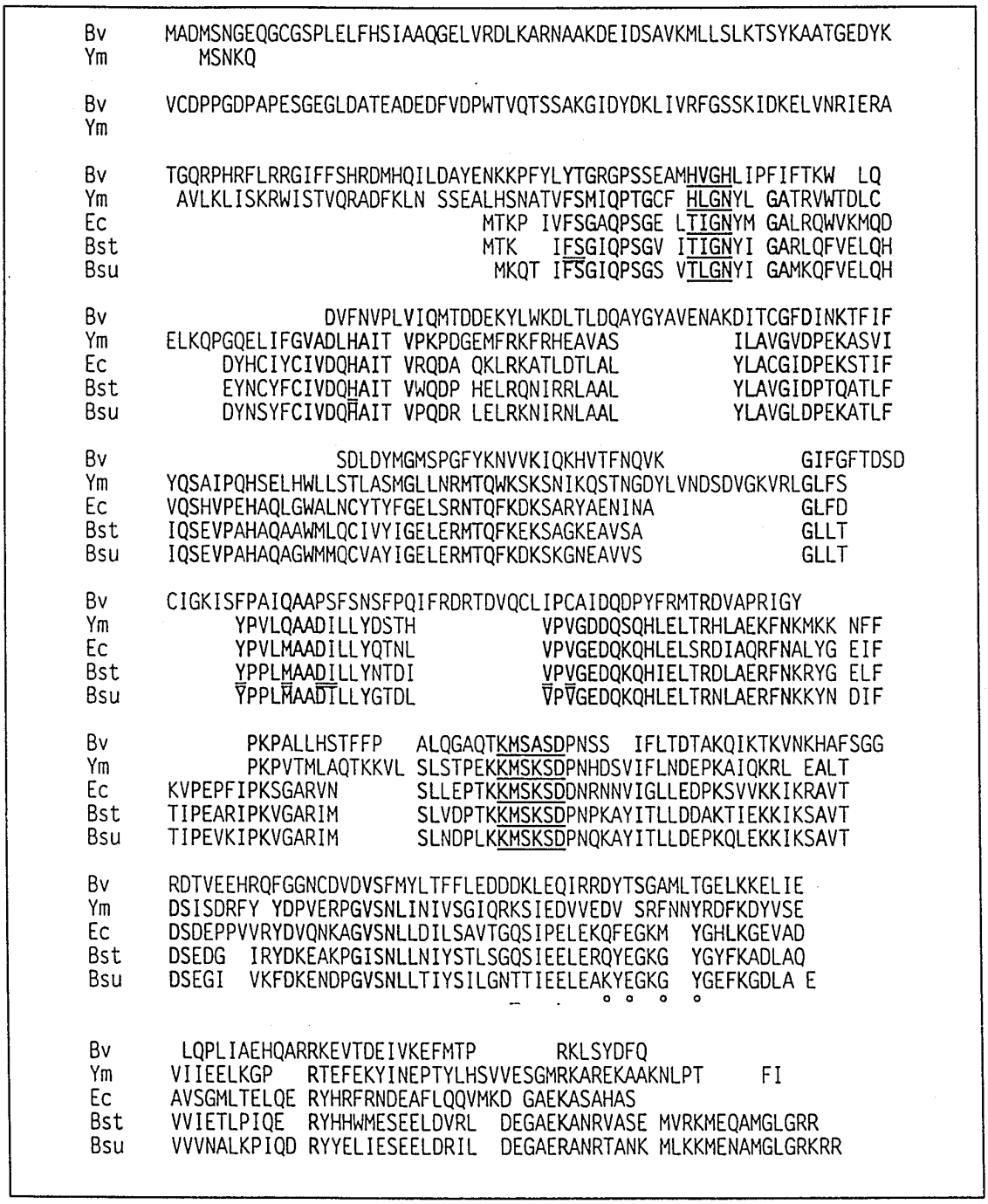

Figure 1.12: Amino acid sequences of TrpRS from Bv = bovine (Garret et al., 1991); Ym = yeast (Myers and Tzagoloff, 1985); Ec = *E. coli* (Hall et al., 1982); Bst = *B. stearothermophilus* (Barstow et al., 1986) and Bsu = *B. subtilis* (Chow and Wong, 1988). Strongly conserved residues are bold. Class I consensus sequences are underlined. Crystallographic nearest neighbors to substrate Trp are double underlined in the Bst sequence. Homologous sequences to anticodon binding sites are indicated with ° underneath (Doublié et al., 1994). Manual alignment shown here is based on 6 additional TrpRS sequences not shown. Mammalian sequences have very high homology, and are all similar to the bovine sequence.

agent (Wong et al., 1959; Krishnaswamy and Meister, 1960). The acylating activity of tryptophanyl-5'-adenylate is not completely contained in the enzyme's active site (Joseph, and Muench, 1971ab), as it will acylate the 2' ribose hydroxyl of excess ATP *in vitro*:

$$\text{TrpRS·Trp-AMP} + \text{ATP} \rightleftarrows \text{TrpRS·Trp-ATP} + \text{AMP} \qquad \text{(V)}$$

This forms tryptophanyl-2'-adenosinetriphosphate in a manner analogous to its natural substrate, the 3' end of tRNA (Coleman and Carter Jr., 1984). This reaction is believed to be an *in vitro* artefact. The formation of tryptophanamide in the presence of ammonium carbonate buffer (Andrews et al., 1985) also demonstrated the acylating reactivity of the TrpRS·Trp-AMP complex. Merle and coworkers (1986) showed a careful preparation of stoichiometric amounts of TrpRS complexed with tryptophanyl-5'-adenylate could be performed, avoiding the acyl-transfer byproduct tryptophanyl-2'-adenosinetriphosphate.

Tryptophanyl-tRNA synthetases have demonstrated significant differences in structure and mechanism between enzymes from prokaryotes, yeasts and vertebrates. The sequences of their cognate $tRNA^{Trp}$ also vary (Xue et al., 1993).

1.2.5.1 Prokaryotic TrpRS

Prokaryotoic TrpRS show high homology to one another, as can be seen in Fig. 1.12. *E. coli* TrpRS was the first prokaryotic TrpRS characterized (Joseph and Muench, 1971ab). It was found to be an $\alpha 2$ dimer of 37 kDa subunits. The enzyme had one DTNB titratable sulfhydryl group reported essential for activity (Kuehl et al., 1976), later identified as Cys-71. An ordered mechanism with ATP binding first was

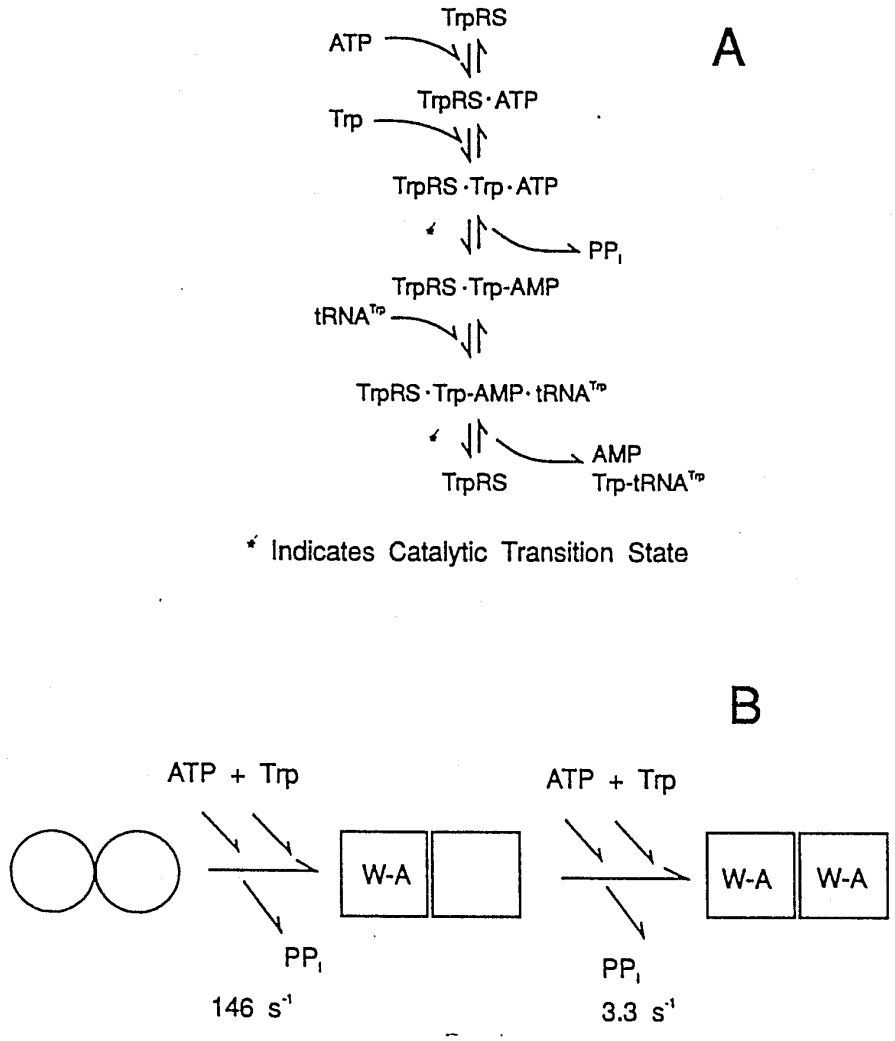

Figure 1.13: Mechanism of *E. coli* TrpRS A. Experiments using inhibition kinetics demonstrated the ordering of the reaction (Penneys and Muench 1974). B. Schematic of the concerted conformational change and positive cooperativity (Andrews et al., 1985; Merle et al., 1986) of *E. coli* TrpRS. In sharp contrast, the dimeric bovine pancreatic TrpRS only undergoes one half of the reaction because negative cooperativity can prevent the second subunit from being filled.

established using inhibition kinetics (Penneys and Muench 1974), depicted in Figure 1.13. The binding of two $tRNA^{Trp}$ per dimer was established using density gradient centrifugation (Muench 1976). Positive cooperativity for this TrpRS was identified using stopped-flow kinetics (Merle et al., 1986).

Spectroscopic and kinetic studies of this TrpRS (Andrews et al., 1985) concluded that a large conformational change occurred upon formation of tryptophanyl-5'-adenylate. This conclusion was made based on an assumption of the change in fluorescence due to the substrate Trp. However it was not possible to separate the spectral contributions from the substrate Trp and the enzyme's Trp residues.

The gene for *E. coli* TrpRS has been cloned (Hall and Yanofsky, 1981) and sequenced (Hall et al., 1982). The prokaryotic TrpRS sequences have a "TIGN" or "TLGN" rather than the Class I consensus sequence "HIGH" (Fig. 1.12). Recent site-directed mutagenesis and kinetic experiments have demonstrated that the *E. coli* TIGN sequence acts in the same capacity as HIGH (Chan and Koeppe, 1993; Fersht et al., 1987), stabilizing the substrate and transition state of the first part of the TrpRS reaction. Studies with *E. coli* $tRNA^{Trp}$ have demonstrated that the tryptophan anticodon bases CCA as well as G73 on the acceptor stem are important recognition elements for TrpRS (Pak et al., 1992).

B. stearothermophilus TrpRS was the first TrpRS sequenced (Winter and Hartley, 1977). Studies of this variant of TrpRS have centered largely on obtaining crystals suitable for x-ray crystallography, carried out in the laboratory of C.W. Carter Jr. (Carter Jr. and Carter, 1979; Coleman and Carter Jr., 1984; Carter Jr., 1988). This work culminated in a low-resolution structure of TrpRS complexed with Trp (Carter Jr. et al., 1990) and a high-resolution structure, as described earlier in this chapter. Various attempts at crystallization of this TrpRS with substrates have resulted in different crystal isomorphs (Carter Jr. and Carter, 1979). A thorough analysis of these crystal isomorphs indicates that the different crystal packing of TrpRS is a result

of different conformations associated with its catalytic mechanism (Carter Jr. et al., 1994). The most obvious difference between the two structures of *B. stearothermophilus* TrpRS at comparable resolutions is in the orientation of the C-terminal portion (Carter Jr. et al., 1994).

As noted earlier, prokaryotic TrpRS has the smallest CP1 sequence of the Class I aaRS enzymes. The structure of the TrpRS·Trp-AMP complex (Doublié and Carter Jr., 1993) shows part of the CP1 segment has a prominent protruding structure, which can be seen in the bottom center of the TrpRS structure in Figure 1.6. In this position, the TrpRS CP1 would be positioned close enough to the tryptophanyl-adenylate site to accommodate an interaction with the acceptor stem of $tRNA^{Trp}$.

Mutational experiments with tRNA have shown that $tRNA^{Trp}$ binds to TrpRS at the anticodon and acceptor ends (Pak et al., 1992). The binding of 2 $tRNA^{Trp}$ per dimer simultaneously (Muench, 1976) was previously mentioned. The geometry from the $tRNA^{Phe}$ structure (Figure 1.10) requires an approximately 50-70 Å distance between the anticodon and acceptor ends which must be bridged by TrpRS to bind at both sites. Yet the TrpRS·Trp-AMP complexed dimer itself is only 112 Å long (Figure 1.6; Doublié and Carter Jr., 1993). A 60 Å distance from the reactive phosphate of a Trp-AMP substrate reaches the far end of the opposite monomer, but does not intersect the same monomer. These geometric constraints indicate $tRNA^{Trp}$ *must straddle the TrpRS dimer interface* in order to simultaneously bind at both ends. This is also the case for TyrRS.

The TrpRS C-terminal end may also bend to accommodate the binding of $tRNA^{Trp}$ at both ends. As previously mentioned, a low-resolution structure of *B. stearothermophilus* TrpRS clearly shows a loosely tethered c-terminal end bending outward (Carter Jr. et al., 1994). Conformational changes in both the $tRNA^{Trp}$ and TrpRS could be very important in their binding and recognition.

B. subtilis Tryptophanyl-tRNA synthetase was identified, sequenced and expressed from its gene (Chow and Wong, 1988). The protein (330 amino acids) exhibits 78% homology to the *B. stearothermophilus* enzyme (328 amino acids), and 56% homology to the *E. coli* enzyme (334 amino acids). It was cloned and overexpressed in *E. coli* (Shi et al., 1989). This enzyme exhibits an ordered mechanism (Xu et al., 1989) binding ATP before the amino acid, like the *E. coli* enzyme. *B. subtilis* TrpRS has a single, conserved tryptophan and only 2 cysteine residues in each subunit. Conventional mutagenesis of this conserved Trp-92 to Phe, Ala or Gln has resulted in an inactive enzyme, implicating the conserved Trp-92 as an essential residue (Chow et al, 1992). Because this Trp was identified in the CP1 region, there was speculation that it was directly involved in tRNA binding, perhaps through intercalation with tRNA bases (Chow et al, 1992). However the crystal structure of the highly homologous *B. stearothermophilus* enzyme shows this Trp is a well-buried residue, residing at the subunit interface, which is discussed further in Chapter 3. The identity elements for $tRNA^{Trp}$ interaction were identified by site directed mutagenesis of the *B. subtilis* $tRNA^{Trp}$ (Xue et al., 1993), and found to be the same as for *E. coli* including the anticodon bases CCA and G73 on the acceptor stem.

1.2.5.2 Yeast TrpRS

Yeast TrpRS was sequenced by Myers and Tzagoloff (1985). A signal sequence for mitochondrial localization is present on the N-terminal end of the enzyme, which is not found in prokaryotic TrpRS (Fig. 1.12). Yeast TrpRS has not been as widely studied as prokaryotic or bovine TrpRS. The tRNA of halophilic bacteria, yeast and other eukaryotes use the discriminator base A73, rather than G73 of prokaryotes (Xue et al., 1993). This divergence in discriminator base is expected to be paralleled by

alterations in the structure of the TrpRS. Interestingly, yeast TrpRS will cross-react with mammalian $tRNA^{Trp}$ which also shares discriminator base A73, but not with prokaryotic $tRNA^{Trp}$. This is despite the sequence similarity of yeast TrpRS to the prokaryotic TrpRS as shown in Figure 1.12. A plant aaRS study (Jakubowski and Pawelkiewicz, 1975) identified TrpRS from yellow-Lupin seeds as having 37,000 *Mr* subunits, which would make this plant TrpRS more similar in size to prokaryotic and yeast TrpRS than to the mammalian TrpRS.

1.2.5.3 Mammalian TrpRS

Mammalian TrpRS species have been isolated as $\alpha 2$ dimers, consisting of two 58 kDa subunits (Lemaire et al., 1969; Gros et al., 1972), making them much larger enzymes than the prokaryotic or yeast variants. Bovine TrpRS was found to be a zinc metalloenzyme (Kisselev et al., 1981), unlike the prokaryotic TrpRS. Mammalian TrpRS does not cross-react well with prokaryotic $tRNA^{Trp}$ (Xue et al., 1993; $<$ 0.03%). This may correspond to species differences in the $tRNA^{Trp}$ discriminator bases, as noted for yeast. *E. coli* TrpRS does not cross react with polyclonal antibodies from bovine pancreatic TrpRS (Merle et al., 1986) indicating these enzymes share no similarities in structures that form antigens.

Bovine TrpRS was shown to bind one tryptophanyl-5'-adenylate per subunit (Graves et al., 1980). Kinetic studies showed anticooperativity in the formation of Trp-AMP (Merault et al., 1981; Mazat et al., 1982). This anticooperativity is opposite to the behavior in prokaryotic TrpRS, described in Figure 1.12. A conformational change of the enzyme, after the binding the first Trp-AMP, that prevents the second Trp-AMP binding in the opposite dimer (Favorova et al., 1981) is implied. Optical spectroscopic studies, including fluorescence and absorbance, indicated a possible

perturbation (Graves et al., 1980), but they could not specify whether the perturbation originated from protein or substrate. Far-UV circular dichroism spectroscopy, which is sensitive to the amount of secondary structure in the protein, showed no change within the enzyme after forming the Trp-AMP complex. Hence if conformational changes occurred in TrpRS, they did not alter the relative proportions of secondary structure.

Despite its early isolation in quantity, (Davie et al., 1956; Lemaire et al., 1968) the sequence of bovine pancreatic TrpRS was only recently determined (Garret et al., 1991). In addition, the sequence from human TrpRS (Frolova et al., 1991) has been obtained, which is 90% homologous to bovine TrpRS (Kisselev et al., 1993). The majority of the difference in size with prokaryotic TrpRS can be attributed to the larger N-terminus of the mammalian TrpRS, based on sequence alignment (Fig. 1.12). Of the two mammalian TrpRS sequences identified, only 20% homology with prokaryotic or yeast TrpRS is seen (Garret et al., 1991). This is unusually low homology considering TrpRS is assumed to be a "housekeeping" enzyme of prehistoric origin.

Mammalian TrpRS expression is γ- interferon inducible in cell culture (Kisselev et al., 1993), suggesting it may be involved in an immune response or defensive activity. Upon sequencing bovine TrpRS, Garret and coworkers found high homology (90%) with rabbit peptide chain release factor eRF previously cloned in the laboratory of Caskey (Lee et al., 1990). This generated some interesting speculation regarding a dual role for TrpRS. However it was convincingly demonstrated by Frolova and coworkers (1993) that the putative eRF sequence of Lee et al. was mistaken, and was rather the rabbit TrpRS sequence, with some incorrect sequence assignments (Kisselev et al., 1993). No other activity for TrpRS has been demonstrated that might be related to an immune response.

Early experiments suggest that bovine TrpRS excludes Trp analogs which have substituents at the 5-carbon of Trp (Sharon and Lipmann, 1957). Prokaryotic TrpRS including *B. subtilis*, (Barlati and Cifferi, 1970) and *E. coli* (Hogue et al., 1992) do not

exclude these analogs, nor does yeast (J.B.A Ross, personal communication). A physiological consideration of these organisms suggests that this discrimination of 5-carbon substituents by mammalian TrpRS may have an evolutionary basis. 5-hydroxytryptophan (5HW) is a naturally occurring amino acid, a precursor to serotonin (5-hydroxytryptamine, 5HT), derived from Trp in higher eukaryotes. Since some vertebrate cells will produce 5HW in the biosynthesis of 5HT, the vertebrate TrpRS should have sufficient specificity to prevent $tRNA^{Trp}$ from misacylation with 5HT. This specificity may be unnecessary in simple eukaryotes and prokaryotes which do not produce serotonin. The diversification of the natural amino acids for cell signalling may thus require greater substrate selectivity in vertebrate aaRS enzymes.

Much remains to be learned from TrpRS of mammalian or vertebrate origins. The differences in mechanism and substrate specificity should be reflected in the structure of bovine TrpRS. Sequence alignment shows a 15 amino acid insert in the bovine enzyme (Fig. 1.12: QIFRDRTDVQCL) into the region where Trp binding in the *B. stearothermophilus* enzyme is localized. Despite identities amongst surrounding residues, not one of the nearest neighbors of the substrate Trp are conserved between the sequence alignment of bovine and the four other TrpRS sequences. However 7 of these 8 residues are identical amongst the four other TrpRS sequences. These sequence differences may account for many of the observed differences in mechanism and substrate specificity. Application of any conclusions drawn from this work, involving *B. subtilis* TrpRS, to mammalian or vertebrate TrpRS are difficult to justify, as these are very different enzymes.

1.3 Incorporation Of Analogs Into Proteins

Despite their ability to discriminate against protein amino acids, several aminoacyl-tRNA synthetases will activate nonprotein amino acids and allow their biosynthetic incorporation into proteins (Schlesinger, 1968; Barlati and Ciferri, 1970; Sykes et al., 1974; Kohno et al., 1990; Koide et al., 1988). Miyazawa and coworkers (Koide et al., 1988) have used the term *alloprotein* to describe proteins with incorporated nonprotein amino acids. Although amino acid analogs have been used since the mid-1950's they have not been reviewed in light of their utility in studying proteins.

1.3.1 Early Trp Analog Experiments

Amino acid analogs of Phe, Tyr and Trp played an important role in the elucidation of pathways by which amino acids were incorporated into protein in the 1950's (Halvorson et al., 1955). There exist several early reports regarding tryptophan analog incorporation and its relation to tryptophanyl-tRNA synthetase. The purification and initial study of bovine TrpRS (Davie et al., 1956) included experiments with tryptophan analogs. A hydroxamic acid reaction was used as a colorimetric test for the presence of an acyl-adenylate. Tryptazan (2-azatryptophan, 2AW) was demonstrated as a substrate for TrpRS by this hydroxamic acid test.

The first report of tryptophan analog incorporation into proteins (Pardee et al., 1956) detailed the growth of a tryptophan deficient auxotroph of *E. coli* in media containing 7AW, 2AW or 5MW. Only 7AW and 2AW sustained bacterial growth. They concluded these azatryptophans, but not 5MW, are incorporated into proteins.

Sharon and Lipmann (1957) compared the reactivity of various Trp analogs with bovine TrpRS to the results of bacterial growth experiments like those of Pardee et al.,

(1956). They concluded that only those analogs which are first enzymatically activated by TrpRS are incorporated into protein. They suggested that analog toxicity was a result of erroneous protein synthesis. Sharon and Lipmann also reported a failure of 5MW, 6MW and 5HW to be activated by the bovine TrpRS. These early results were taken as evidence that larger substituents of the 5 position of Trp, i.e. 5MW and 5HW, rendered the analog incapable of biosynthetic incorporation in both bacteria and mammals.

These early conclusions regarding the ability to incorporate 5HW and 5MW were overstated. In later experiments, protein synthesis was experimentally kept separate from cell growth. Lark (1969) demonstrated that 5MW is incorporated into proteins of a Trp auxotroph of *E. coli*, during Trp starvation. Hence although 5MW would not sustain cell growth, it was incorporated into proteins in place of Trp. Other workers (Barlati and Ciferri, 1970) showed radiolabelled 5HW and 5MW incorporation into the proteins of *B. subtilis*. No particular protein was purified or studied in these early experiments, but is was clear that analog incorporated proteins could be made.

1.3.2 Analog Incorporated Proteins

Incorporation of unusual amino acids into proteins was recognized by only a few workers as a convenient method to study the influence of individual amino acids on enzyme kinetics. Schlesinger (1968) prepared and studied alkaline phosphatase with 2AW and 7AW incorporated in place of its multiple Trp residues. She found that there was little effect on enzymatic activity, but a much larger effect on the enzyme's absorbance and fluorescence properties. The value of this finding has only recently been appreciated and has lead to significant interest in such experiments (Négrerie et al., 1990; Hogue and Szabo, 1993).

Fluorotryptophans, were the first Trp analogs to offer a spectroscopic utility for use with NMR. Pratt and Ho (1975) studied the effect of 4- 5- and 6- fluorotryptophan incorporated into the *E. coli* enzymes lactose permease, ß-galactosidase, and D-lactate dehydrogenase, citing the potential for use in ^{19}F NMR. One of the first ^{19}F NMR studies of proteins used fluorotryptophan to demonstrate the proximity of two tryptophan residues in dihydrofolate reductase (Kimber et al., 1978). In Pratt and Ho's work, (1975) 4FW showed the smallest effects on enzymatic activity and growth rate, even increasing the activity of D-lactate dehydrogenase twofold. Pratt and Ho concluded that they could not predict the effect of fluorotryptophan analog incorporation into individual enzymes, due to the variability observed. ^{19}F NMR following the incorporation of fluoroanalogs of Trp has been used to study many other enzymes, recently summarized by Lian and coworkers (1994).

Aspartate transcarbamylase (ATCase) kinetics were studied with incorporated 7-azatryptophan (7AW) (Foote et al., 1980). The allosteric modulation of ATCase; ATP activation and CTP inactivation, was enhanced in the 7AW substituted enzyme. The kinetics were correlated to the crystal structure of ATCase, and it was suggested that 7AW-199, a part of the catalytic chain, was interacting with the carbamyl phosphate binding site via a hydrogen bond through the aza-nitrogen.

This earlier work provided demonstrations of the potential of a kind of tryptophan analog "mutagenesis" for studying enzymes. It is most interesting that this "analog mutagenesis" predates site-directed mutagenesis (Zoller and Smith, 1982) for the study of protein structure and function. The cited unpredictability of analog mutagenesis (Pratt and Ho, 1975) may be the reason the method has been overlooked until recently. But the large body of site-directed mutagenesis experiments performed to-date have confirmed the general unpredictability of the effects of altering the amino acid sequence (Fersht et al., 1987). The *in-vitro* preparation of enzymes with analog amino acids by Schultz and coworkers, described in Section 1.2.3. (Mendel et al.,

1992; Judice et al., 1993) represents renewed interest in this analog mutagenesis approach to study proteins.

1.3.3 Incorporated Trp Analogs As Intrinsic Fluorescent Probes

It is noteworthy that both protein fluorescence studies, tryptophan analog incorporation, and tryptophanyl-tRNA synthetase have a common historical origin. Shore and Pardee (1956) made many of the original significant conclusions about the fluorescence of proteins (Longworth, 1971), while simultaneously studying protein synthesis (Pardee et al., 1956) using tryptophan analogs. The latter reference indicated that the altered fluorescence of proteins with 7-azatryptophan could be detected apart from normal proteins. Independently of these workers, tryptophanyl-tRNA synthetase was first isolated in 1956 by Davie et al., who also used tryptophan analogs to characterize TrpRS.

The work of Schlesinger (1968) on 7-azatryptophan fluorescence in proteins was largely an isolated curiosity until very recently, but helps to bridge the gap in time and in fluorescence methodology from the early work to the present. The inferences of the utility for 7-azatryptophan can be made by re-examining Schlesinger's early experiments.

The use of incorporated Trp analogs to study protein structure, function and dynamics with modern fluorescence methodology was suggested by Hudson and coworkers (1986). However the strategies they proposed have not been undertaken, and they seem to have overlooked the earlier relevant work of Schlesinger (1968). The laboratory of Petrich has been enthusiastic in their support for the use of incorporated 7-azatryptophan in biological fluorescence studies of proteins (Négrerie et al., 1990). Yet they have not reported data from any biosynthetically prepared 7-azatryptophan

proteins, despite publishing a series of papers concerning the photophysics of 7-azatryptophan and 7-azaindole (7AI). Some of these reports include contradictory claims of the nature of 7-azatryptophan photophysics, which are discussed in detail in the next chapter.

The incorporation of 5HW for the study of proteins and protein-protein interactions using fluorescence was first demonstrated by this author at the onset of this thesis work (Hogue et al., 1992, in Appendix B). The techniques required for tryptophan analog incorporation are well within the repertoire of most labs which currently make and study proteins using recombinant protein expression techniques. Since the first demonstration in 1992 of the utility of 5HW fluorescence as an intrinsic fluorescence probe, (Appendix B) these techniques have been embraced by several other groups for studying a diversity of protein-protein and protein-DNA interactions with fluorescence.

5HW has already proved very useful in studies of protein-DNA interactions (Ross et al., 1992; Laue et al., 1993; Sato et al., 1994) including the revelation of some important oligomeric states of λ *c*I repressor protein (Senear et al., 1993). In another study, 5HW was incorporated into cAMP receptor (CRP) protein and the α and ß-subunits of RNA polymerase (RNAP) (Heyduk et al., 1993; Heyduk and Callaci, 1994) for further spectroscopic investigations of the protein-protein and protein-nucleic acid interactions between RNA, RNAP, and CRP. These workers reported that the 5HW-incorporated cAMP receptor protein (CRP) retained 100% of the specific cAMP binding and specific DNA binding activity. They also reported that multimeric RNAP could be reconstituted with either or both of the 5HW-incorporated α or ß subunit and that RNAP retained enzymatic activity in each case.

Soluble tissue factor is important in the blood coagulation cascade as it binds to factor VIIa. Tissue factor has also been prepared with 5HW (Hasselbacher et al., 1994) and 7AW, although the latter had poor to no activity. 5HW has also been used

to demonstrate the flexibility of the transcription activator domain of herpesvirus protein VP16 (Shen et al., 1994). These examples illustrate a growing interest in the topic of this research.

Chapter 2

FLUORESCENCE SPECTROSCOPY OF PROTEINS

FLUORESCENCE SPECTROSCOPY OF PROTEINS

2.1 Interaction of light with matter

Spectroscopy includes a variety of techniques which obtain information from matter through interactions with electromagnetic radiation. The range of energies of electromagnetic radiation have been classified into the electromagnetic spectrum, Figure 2.1 (Atkins, 1986). For an electromagnetic oscillator of frequency ν, its quantum-mechanically permitted energies are multiples of $h\nu$, where h = Planck's constant (6.626×10^{-34} Js). Light is a form of electromagnetic radiation which can be described as either a particle, called a photon, or as a wave with orthogonal electric and magnetic fields, propagating with mutually perpendicular orientations in the same direction. The wavelength (λ) of light is inversely proportional to the frequency (ν)

$$\lambda = c/\nu \qquad (1)$$

where c = speed of light, and hence is inversely proportional to the energy of the radiation.

For the energy of light to affect matter, it must cause a change in the energy of atoms or molecules by an absorption process. Light can affect atomic or molecular electrons, causing them to enter the lowest unoccupied orbital of the atom or molecule.

2.1.1 Absorption Processes (Excitation)

Chromophoric substances are those atoms or molecules which have absorption interactions with visible and ultraviolet light. The transition of electrons from an initial state of low energy, the ground state, to a higher level of energy, the excited state, can be caused by the absorption of a photon with the correct trajectory. The photon must

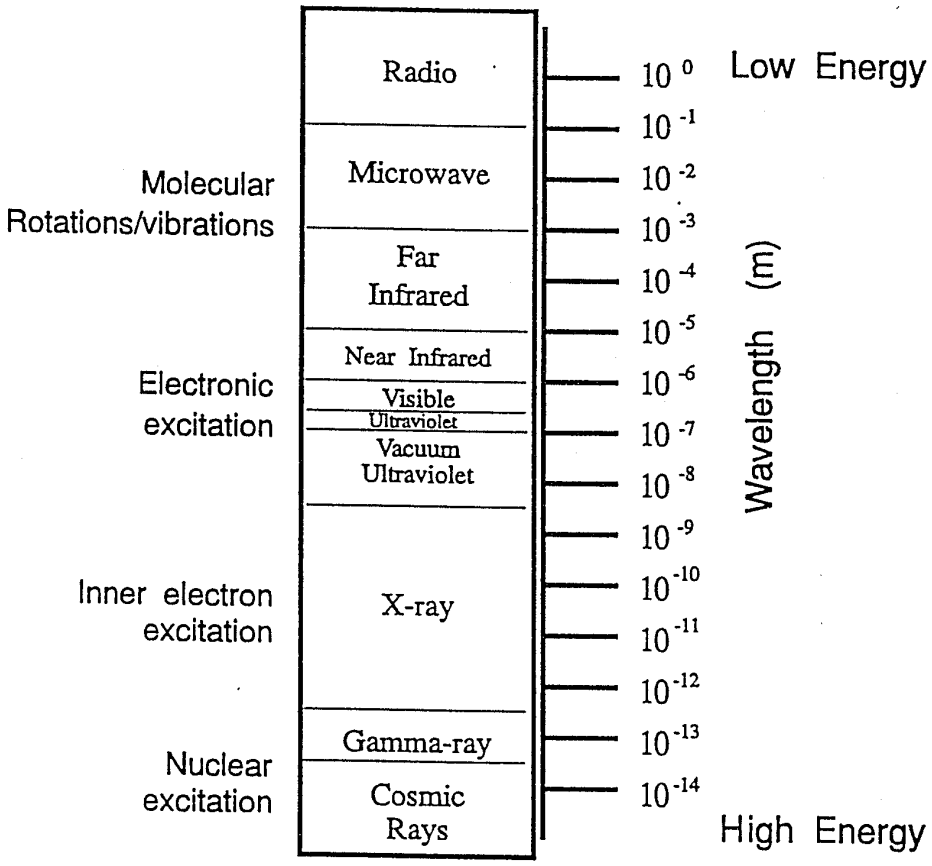

Figure 2.1: The electromagnetic spectrum (Atkins, 1986).

posses the same amount of energy $h\nu$ as the energy difference for the electron's transition to the excited state.

In molecules, electronic energy levels are complicated by the more intricate molecular orbitals, and by lower energy vibrational levels present in bonded structures. A picture of these superimposed electronic energy levels is shown in Figure 2.2. These are known as vibronic states. Electrons are capable of transitions into this multiplicity of higher energy levels after absorption of the required energy quanta. The number of molecules in the different vibronic states is described by a Boltzman distribution.

It is possible to observe absorbance from a double-bond containing solute in a non-double-bonded solvent, e.g. a protein in water. Molecules with single bonds have electrons in σ orbitals, those with double bonds have electrons in π orbitals. The specific low energy activation of the solute $\pi \rightarrow \pi^*$ transitions amongst solvent molecules with only higher energy $\sigma \rightarrow \sigma^*$ transitions is the basis for optical spectroscopy in solutions.

The energy of the $\pi \rightarrow \pi^*$ transitions of molecules is also affected by the extent of conjugated double bonds and by substitution of different atoms on the molecule (Pavia et al., 1979). For example, the amide backbones of proteins contain double bonds which absorb high energy UV light (205-220 nm). Conjugated double bonds as found in aromatic rings such as in the amino acids side chains of Phe, Tyr and Trp, absorb lower energy UV light then the amide backbone, at 240-300 nm.

The absorption of a photon is a very fast process (10^{-15} - 10^{-16} s) leading to an excited-state molecule. The return to the ground state is usually undertaken by slower processes. The general timescale in which a molecule resides in a excited state corresponds to some important molecular processes.

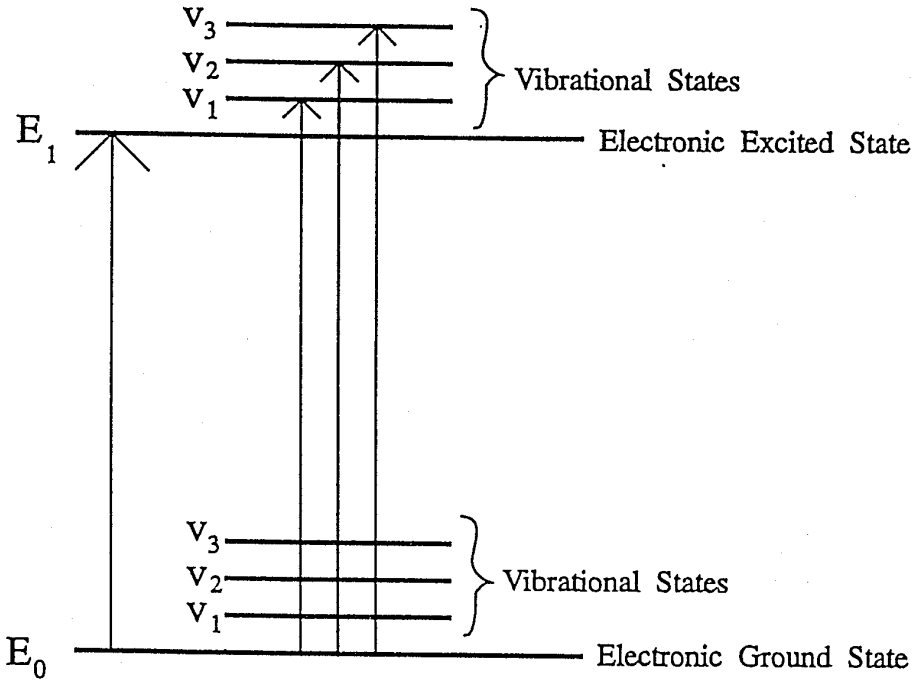

Figure 2.2: Schematic of the molecular energy levels upon superimposition of electronic and vibrational transitions (Pavia et al., 1979). Transitions representing absorbance are indicated, originating from the lowest vibrational state E_0v_0 at room temperature (Penzer, 1980) Note that the variations observed in absorbing transitions come from the distribution of vibronics levels in the excited state at these temperatures (Lakowicz, 1983).

2.1.2 Absorption Spectroscopy

Light passing through a chromophoric substance experiences an exponential decrease in intensity which depends upon both chromophore concentration and sample thickness. The Beer-Lambert Law:

$$I_t(\lambda) = I_i(\lambda)e^{-\alpha(\lambda)[J]l} \tag{2}$$

relates the intensity of transmitted light, I_t to the intensity of incident light I_i, and to the concentration of absorbing species J of thickness l. The proportionality constant $\alpha(\lambda)$ is an intrinsic property of the molecule. The fraction of light absorbed, A, can be determined with the equation:

$$A(\lambda) = 1 - \log \frac{I_t}{I_i} \tag{3}$$

The Beer-Lambert Law is often expressed as:

$$A(\lambda) = \epsilon_\lambda cl \tag{4}$$

where ϵ_λ is the molar extinction coefficient at wavelength λ of the chromophore, and c is the concentration (in this case c = [J]).¯ This form of the Beer-Lambert law is widely used in to determine concentration of various biochemical components which have known values of ϵ_λ.

Deviations from the Beer-Lambert relationship can originate from instrumental or sample effects. In practice, monochromatic light is not used in commercial spectrophotometers, but rather a bandwidth of light. Sampling with a large bandwidth of light near the edge of an absorbing feature can produce deviations (Montgomery and Swenson, 1976). This can be avoided with a narrow bandwidth. In addition, an

instrument's response to absorbance becomes non-linear as the absorbance increases above 1.

Changes in ϵ_λ can also appear from variations in pH, temperature, solvents, adsorption of sample onto vessel walls, sedimentation, aggregation, and light scattering by particulates. The scattered light from aggregate formation results in an absorbance-like signal that can be useful to monitor aggregation processes (Yoo and Albanesi, 1990) in the region where proteins usually have little absorbance e.g. 310-350 nm. This can also distort the determination of concentration of proteins, especially in the UV range since scattered light is proportional to $1/\lambda^4$

The absorbance from a protein arises primarily from the aromatic amino acids, Trp, Tyr and Phe, but there can also be contributions from any disulfide bonds or prosthetic groups associated with the protein (Creed 1984). The molar absorbance spectra (extinction coefficient versus wavelength) of the amino acids Trp, Tyr and Phe is shown in Figure 2.3 (Wetlaufer, 1962). The largest absorbance is that of Trp. The extinction coefficient of a protein can be predicted based on the number of chromophoric amino acids present and their relative extinction coefficients. This can be used to determine protein concentration reliably to within a 2% error (Gill and von Hippel, 1989). Alternatively the extinction coefficient can be experimentally determined by first measuring the absorbance, then determining the concentration of protein by a rigorous analytical procedure, such as quantitative amino acid analysis.

The absorbance of indoles have been examined in oriented crystals using polarized light (Yamamoto and Tanaka, 1972). This is used to distinguish individual dipoles absorbing light in a sample. Indole and its derivatives were shown to consist of two types of electronic transitions, designated as the ^1L_a and ^1L_b dipoles (after Platt notation; Figure 2.4). These transitions overlap across most of the absorption spectrum of Trp. There is observable fine structure in the overall absorbance spectrum of Trp owing to the ^1L_b transition which is sometimes seen as a peak near 289-292 nm. This

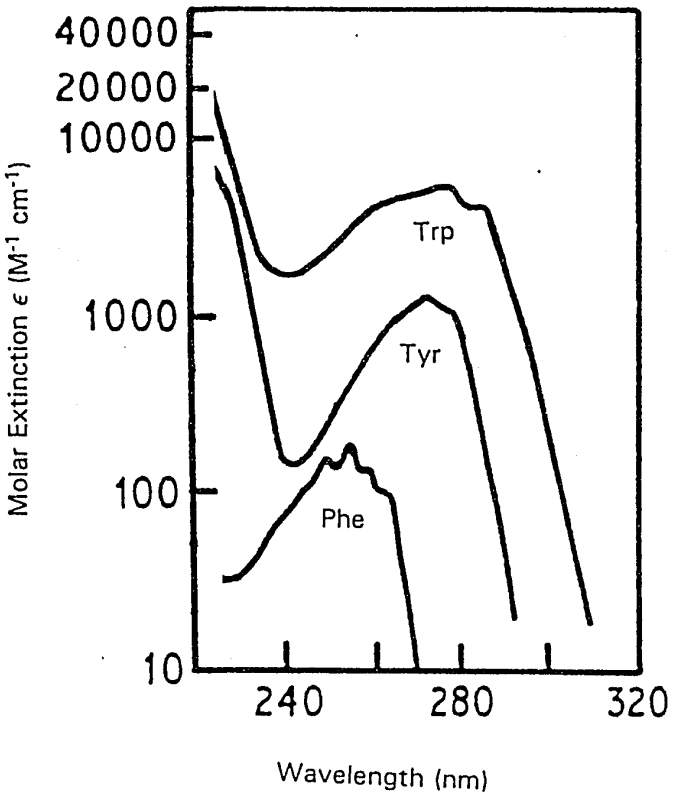

Figure 2.3: Molar absorbance spectra of Trp, Tyr and Phe. Extinction, ϵ at pH 6 (after Wetlaufer, 1962).

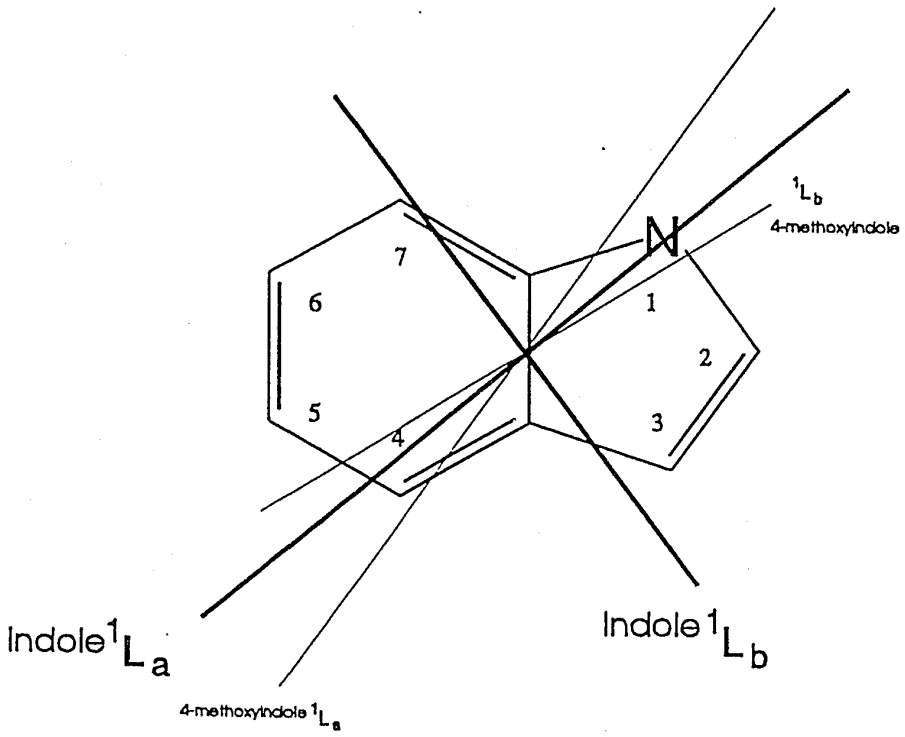

Figure 2.4: Transition moment directions of indole. The ^1L_a and ^1L_b states of 3-indolylacetic acid crystals (after Yamamoto and Tanaka, 1962) are shown. The directions of the moments of several substituted indoles were examined and found to have only small deviations in these directions, with the exception of 4-methoxyindole (Albinsson and Nordén, 1992). Numbering of the substitutable ring carbons of indole is also shown.

structure can be greatly enhanced in non-polar solvents. This feature is sensitive to charges in the environment of indole, Trp and Trp within proteins (Andrews and Forster, 1972).

2.1.3 Return to the Ground State (Emission)

The fate of the absorbed energy of an excited state molecule can be one of several pathways, most of which lead back to the original ground state molecule. Often this energy is transferred into vibrational, rotational or translational motion. Sometimes, the excited state molecules undergo chemical reactions or photochemistry, after which a new ground-state species is formed.

The excited state energy can be lost by the emission of radiation equal to the energetic separation between ground and excited states. The resulting radiation is called luminescence. Excited-state molecules with electrons with opposite spins are in singlet states, those with parallel spins are in triplet states. The transition from singlet to triplet excited state is called intersystem crossing (Figure 2.5), and it is quantum mechanically "forbidden", i.e. of low probability because it requires an inversion of electron spin. Forbidden transitions provide only weak spectral indications compared to allowed transitions. This probability can increase due to coupling between electronic and nuclear spins which causes electrons to become unpaired.

Luminescence originating from the transition from singlet excited state to singlet ground state, is known as fluorescence, which can occur on a timescale of around $10^{-(8-11)}$ s. The usually weaker luminescence from triplet excited state to singlet ground state, is called phosphorescence, and is a slower process of about $10^{(1--6)}$ s. The steps leading to fluorescence and phosphorescence emission are depicted in Figure 2.5, a modified Jablonski diagram (1935).

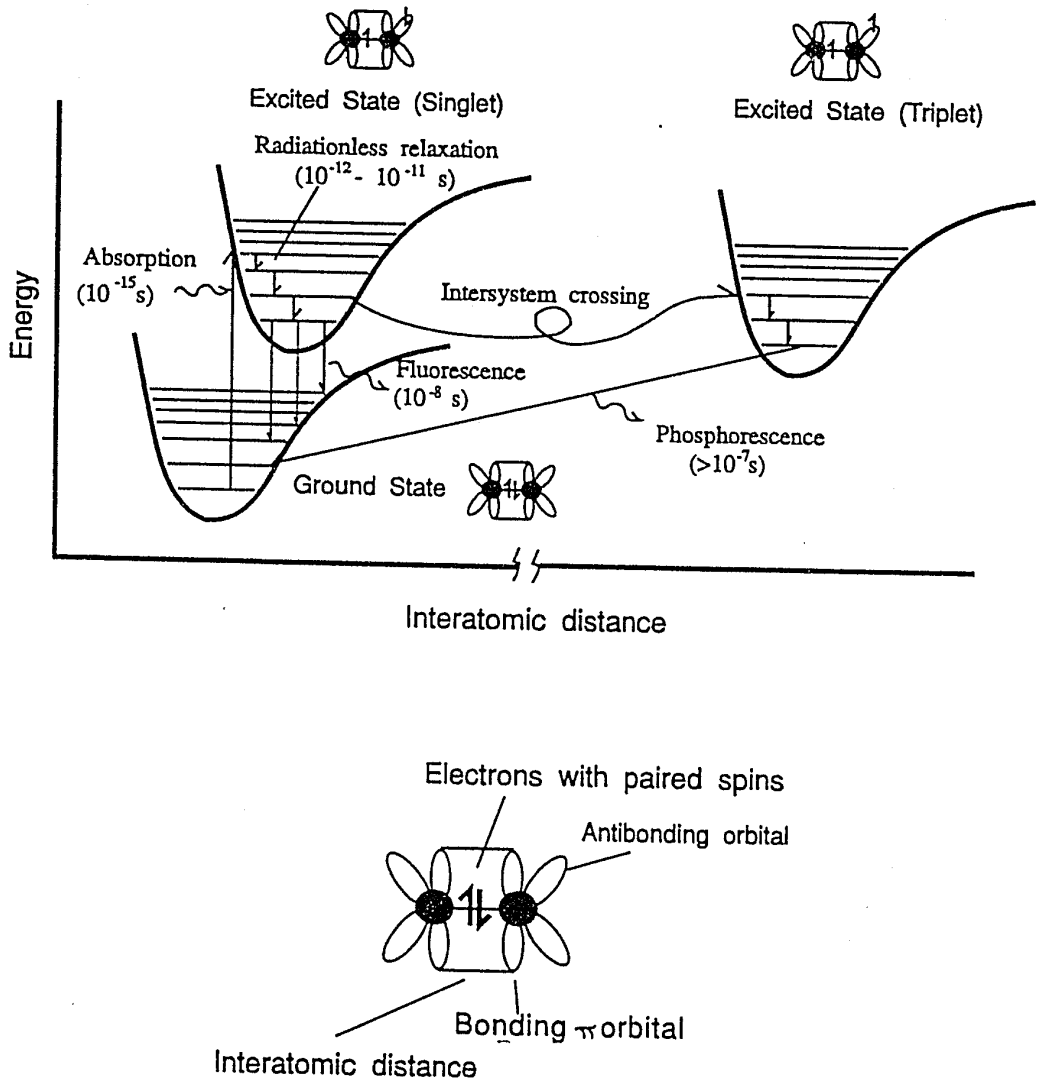

Figure 2.5: Schematic of some of the processes leading to luminescence. A modified Jablonski diagram. (1935). Timescales for each event are as indicated. The energy levels of ground and excited states are drawn in the style of a Morse curve (Penzer, 1980). These show the energy levels relative to the distance between nuclei (left = closer together, right = further apart). Note the rightward/downward progression of the vibronic transitions of electrons (arrows) in the excited state towards the energy minima of the Morse curve. These transitions are known as internal conversion.

During the timescale of fluorescence, other processes including molecular rotation, collisions, complexation and solvent motion can proceed. These processes can all affect the observed fluorescence. Fluorescence can be a sensitive indicator of these processes, all of which are important in the study of protein structure, function and dynamics.

The time a molecule remains in the excited state prior to emitting is the luminescence decay time. During this time several things can happen to the fluorophore which may in turn affect its luminescence. The decrease in energy caused by processes in the excited state, e.g. internal conversion or radiationless relaxation (Figure 2.5) causes the luminescent photons to be of lower energy compared to the photons absorbed. These processes occur on a $10^{-(11-12)}$ s timescale. The spectra in Figure 2.6 illustrates this effect, known as the Stokes' shift (Stokes, 1852).

The Franck-Condon principle maintains that electronic transitions are much faster than nuclear motions, since nuclei are much more massive. A near instantaneous change to an excited state electron density (10^{-15} s) leaves the nuclei in the same position in space in the initial excited state. If the ground and excited state molecular coordinates are largely unaffected by other processes, the absorption and emission should have shapes which are mirror images of one another, as shown in Figure 2.6. Correlations between the probability of absorbance and the reciprocal emission transitions exist (Franck-Condon factors), which explain this mirror image effect. Geometric differences, e.g. regarding the planarity of conjugated ring structures, can be correlated to differences in the shape and the Stokes shifts of the absorbance and fluorescence spectra (Berlman, 1970).

Solution studies of luminescent systems introduces further complications. Mobile solvent molecules with high dipole moments (e.g. water) are susceptible to reorienting themselves around a strong dipole moment. If the excited state molecule has a larger dipole moment than the ground state, then water or polar solvent can

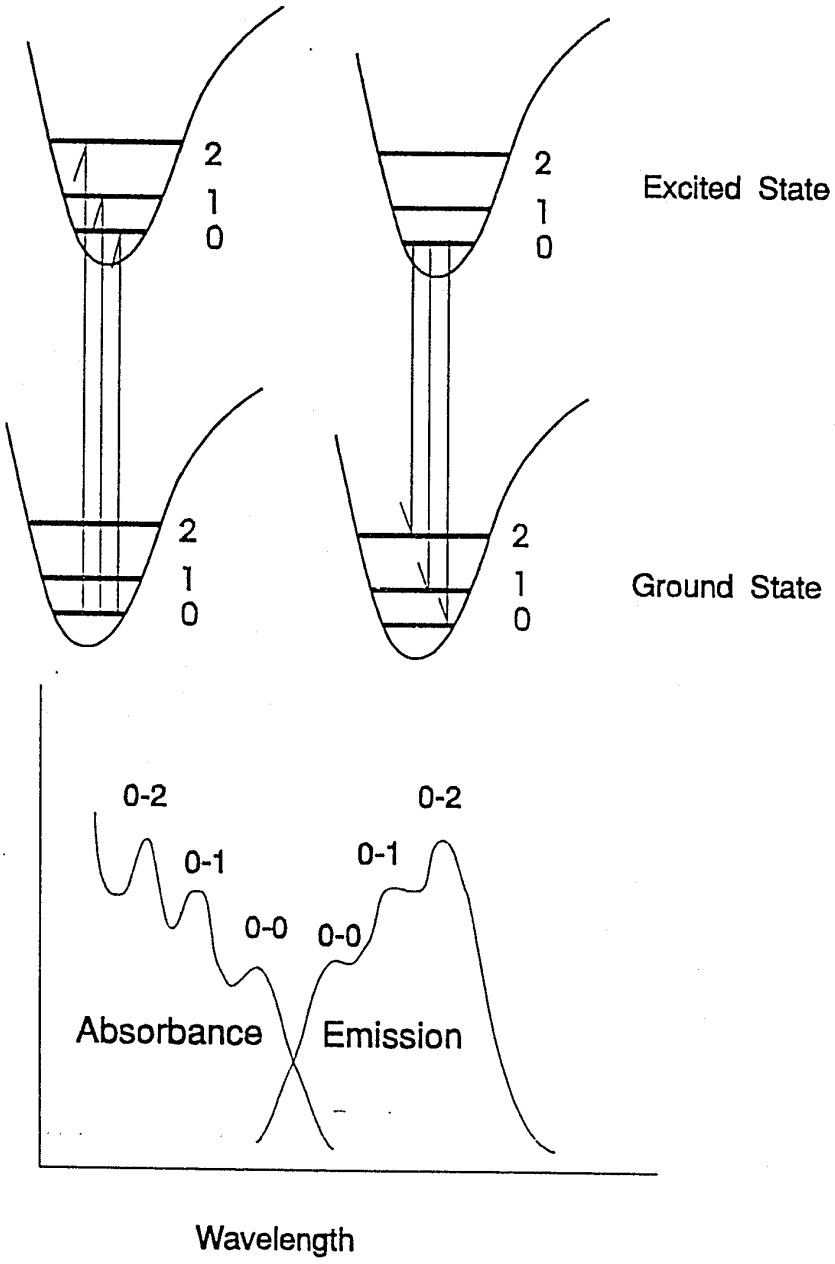

Figure 2.6: Schematic of absorbance and fluorescence transitions. (Lakowicz, 1983). The energy levels of ground and excited states are drawn in the style of a Morse curve (Penzer, 1980). The probabilities of absorbance transitions are related to the probabilities of the reciprocal emission transitions (Franck-Condon factors), hence the spectra appear as mirror images providing the excited-state and ground state geometries are similar.

reorganize around the direction of a new excited state dipole (Milton et al., 1978, Sun and Song, 1977). This results in a new equilibrium excited state of lower energy than the original one. This process is called solvent or dielectric relaxation and this can contribute to the magnitude of the Stokes' shift. Dipolar reorganization affects the Stokes' shift because of changes in transition energies in the ground and excited states. The alteration of the solvent dipole organization around the excited state molecule can also alter the vibronic energies of the ground state (Figure 2.5). This can result in a "smearing" of any fine structure that might be observed in luminescent emission spectra as shown in Figure 2.6. Hence not only is the geometry of a chromophore important in its fluorescence emission characteristics, but also the geometry from ground state and excited state interactions with external dipoles, such as those of dipolar solvents.

These solvent dipolar process are particularly relevant to indole, and to its amino acid derivative tryptophan (Skalski et al., 1980). In hexane, a non-polar solvent, indole fluorescence emission has a structured spectrum with a λ_{max} of 298 nm. In water, the structure is lost and the λ_{max} is at 347 nm (Sun and Song, 1977). The spectrum of indole in hexane is said to be blue-shifted relative to water. This large effect makes Trp fluorescence particularly sensitive to solvent exposure, and in general the fluorescence of Trp in a protein can be used to indicate whether it is buried within the protein or exposed to external solvent. Spectra from a buried and an exposed single Trp in mutants of the same protein are shown in Figure 2.7 to illustrate this solvent sensitivity. Tyrosine is not as sensitive to dipolar reorganization, as its λ_{max} is 304 $\pm$ 1 nm (Ross et al., 1992a). This is attributed to a lower dipole moment in the excited state than that of Trp, which does not promote a solvent reorganization in the excited state.

Collision with certain other molecules in solution can cause a physical transfer of energy from the excited state molecule to the colliding molecule. This process is called collisional or dynamic quenching. The fluorescence of tryptophan is efficiently

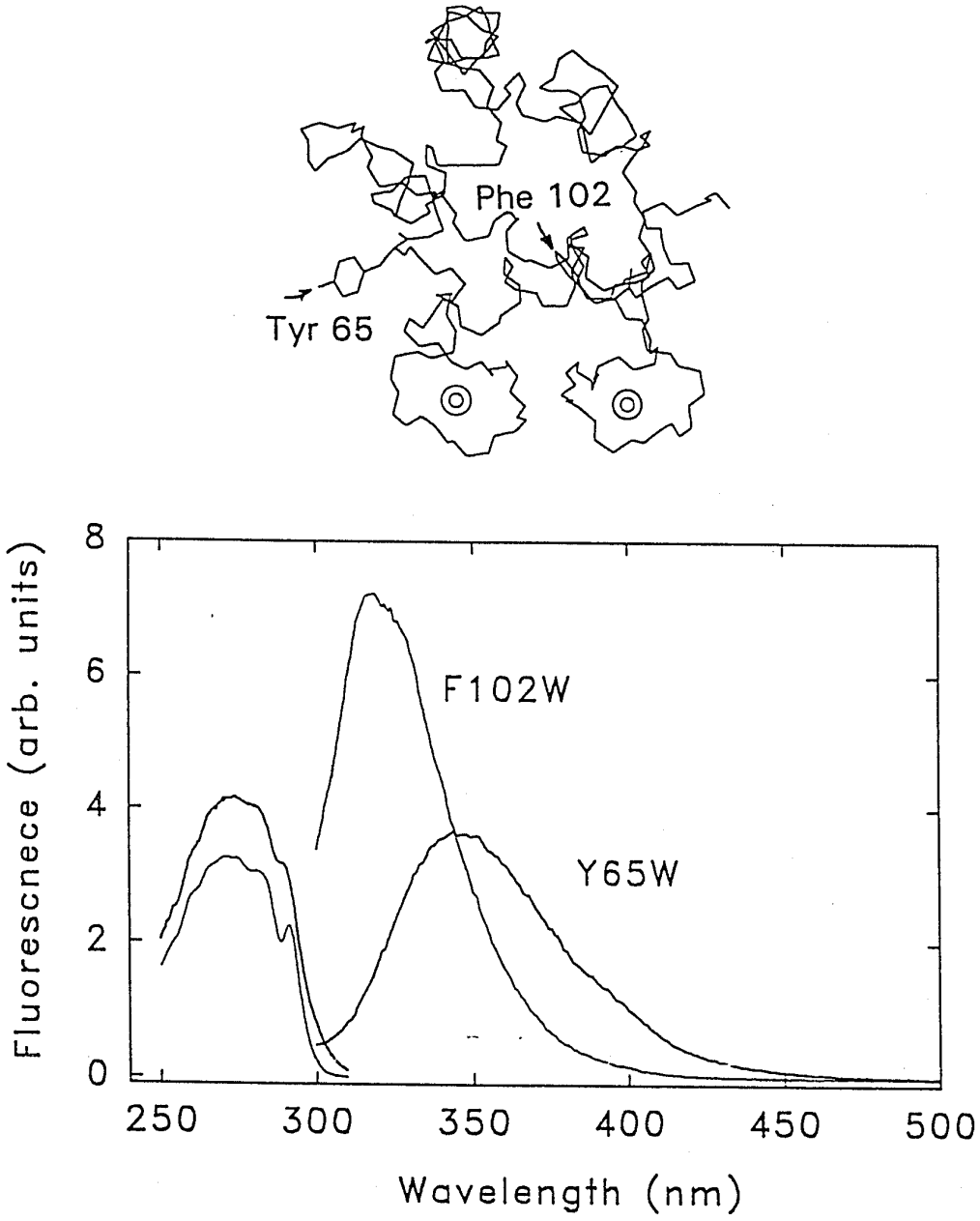

Figure 2.7: Fluorescence excitation and emission spectra of single Trp proteins. Corrected excitation spectra (left) at 350 nm emission, emission spectra at 285 nm excitation. The protein oncomodulin lacks Trp residues, but one was introduced in a solvent exposed position, replacing Tyr 65 (Y65W), and another was introduced in a buried position replacing Phe 102 (F102W). Their spectra show the effect of solvent, causing the exposed Trp-65 fluorescence to be red-shifted relative to the buried Trp-102 residue. Note also the prominent peak at 292 nm of F102W excitation, corresponding to the ^1L_b transition.

quenched by dissolved oxygen, I^- and acrylamide. Buried Trp residues within proteins can be physically shielded from these collisions by the rest of the protein, and hence their fluorescence may not be quenched to the same extent as an exposed Trp. Other molecular interactions can involve formation of excited state complexes, or exciplexes. Collectively these processes are concentration and diffusion dependent. Quenching of fluorescence from a pre-formed ground state complex is known as static quenching. A statically quenched fluorophore acts as a nonfluorescent chromophore.

It is possible to describe the rate of all these processes leading back to the ground state of the molecule. Consider the rate constant for the fluorescence radiative processes k_f and the rate constant for the sum of all the other nonradiative deactivation processes k_{nr}, for example:

$$k_{nr} = k_{rr} + k_{isc} + k_p + k_q[Q] \ldots \quad (2)$$

where k_{rr} is the rate of radiationless relaxation, k_{isc} is the rate of intersystem crossing, k_p is the rate of photoreaction, $k_q[Q]$ is the rate of concentration dependent collisional quenching from molecular species Q. The sum:

$$k_f + k_{nr} \quad (5)$$

accounts for the total rate for the depopulation of the excited singlet state. The lifetime of the singlet excited state is the average time the molecule remains in the excited state, defined as τ_s where:

$$\tau_s = 1 / (k_f + k_{nr}) \quad (6)$$

The rate of fluorescence depopulation of a molecule k_f is related to the radiative lifetime of the molecule, τ_r:

$$\tau_r = 1 / k_f \tag{7}$$

The fluorescence quantum yield, Φ_f, is defined as the ratio of photons emitted to photons absorbed. The quantum yield of a fluorophore Φ_f, is related by definition to both the singlet lifetime and the radiative lifetime:

$$\Phi_f = \tau_s / \tau_r \tag{8}$$

2.1.4 Fluorescence Spectroscopy

A schematic of the fluorescence spectrophotometer, (also known as a fluorimeter) used in these studies is provided in Figure 2.8. The fluorescence of a sample has an absorbance (excitation) component, and an emission component. Thus two types of spectra can be collected from a sample, an excitation and an emission spectrum. Spectra are collected with emission at 90° to the exciting light. The fluorescence spectrophotometer has two monochromators (or sometimes three as shown in Figure 2.8). One monochromator is used to select the excitation wavelength from the xenon-arc lamp source. The others select the wavelengths at which the emitted light is collected. A fluorimeter such as the one in Figure 2.8 with dual emission monochromators is in the "T-format", which is useful for monitoring the polarization of fluorescence, described later in this chapter. However for most spectra, only a single emission monochromator is used, in the "L-format".

In order to collect an emission spectrum, a wavelength for excitation is selected

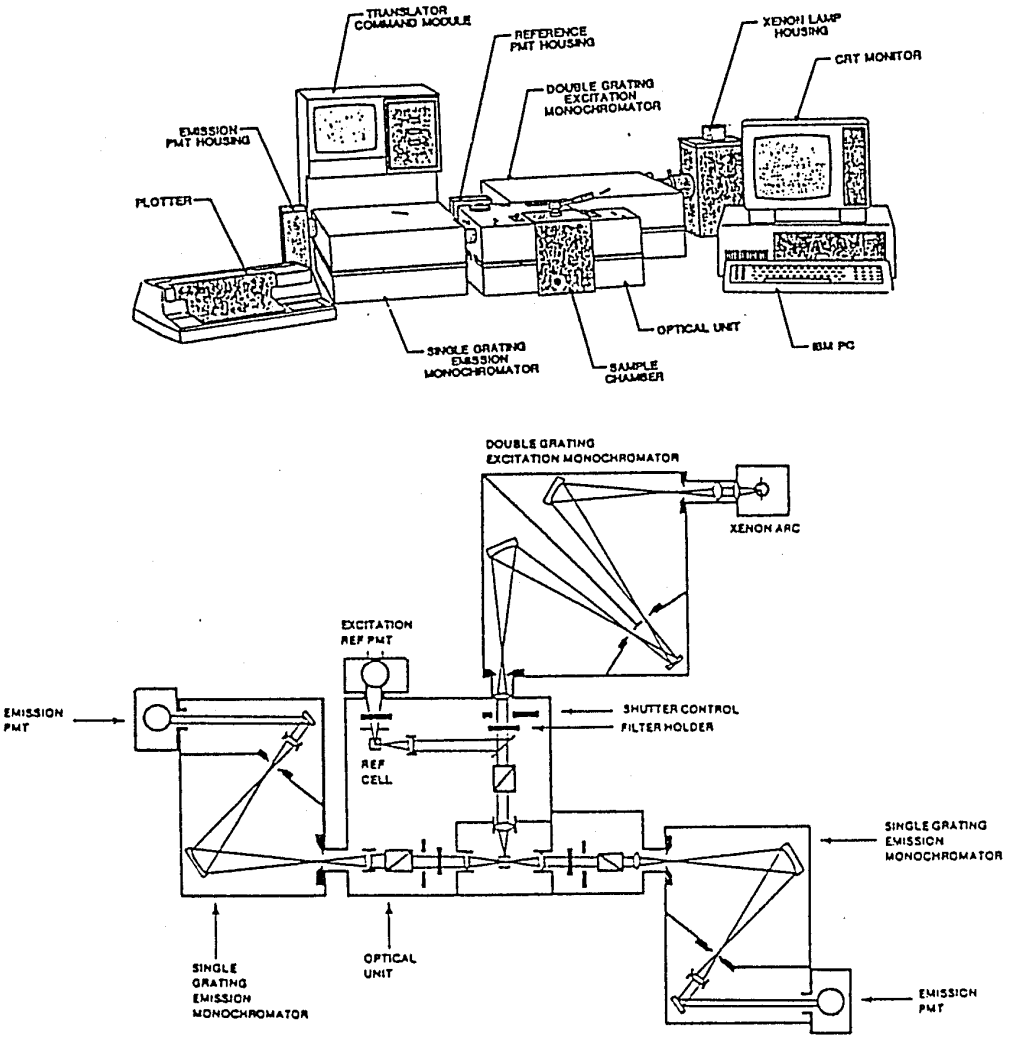

Figure 2.8: Schematic of a fluorimeter. (SLM Aminco Inc). (TOP) The fluorimeter components less the second emission monochromator in the L-format, together with the electronic modules not depicted in the lower optical schematic. (BOTTOM) T-format optical arrangement of the instrument used in this work. Excitation light originates from a xenon arc lamp and passes through a double grating monochromator for wavelength selection. A beam splitter shunts some of the excitation light to a reference cell and photomultiplier tube for ratio correction. Sample is contained in a cuvette in the Optical Unit. Adjustable polarizers are indicated in the light paths by small rectangles with diagonals. Emission is collected from either face of the sample cuvette at right angles to the excitation beam. Emission wavelength is selected by a single grating monochromator and fluorescent light is detected with a water-cooled red-sensitive emission PMT.

and fixed with the excitation monochromator. An excitation spectrum is collected by fixing the emission wavelength, and varying the excitation wavelength. An excitation spectrum can be compared to the absorbance spectrum of the same sample, as the excitation spectrum depicts only that absorbance of the sample which leads to fluorescence emission. Differences in these suggest a mixture of chromophores contribute to the fluorescence at the emission wavelength. Fluorescence of a sample can be considered a continuous three-dimensional surface with y-axis of intensity, and x and z axes of excitation and emission wavelengths, although these surfaces require long data collection times and are rarely shown.

Fluorescence intensity is described in arbitrary units of measurement since its value will depend on the response of the instrument. It is common practice to normalize the maximum of a fluorescence spectra to the value of 1, in order to compare spectral shapes between samples. However to obtain an accurate indication of the quantity of fluorescence that is emitted from a sample, the quantum yield should be determined with respect to a reference fluorophore, described later.

Accurate fluorescence measurements involve a careful set of procedures to eliminate errors. First, the absorbance of the sample solution at the excitation wavelength should be < 0.10 to minimize any inner-filter effects (Parker, 1968). In the range of absorbance below 0.10, the fluorescence emission should increase linearly as a function of fluorophore concentration. The effect of temperature on the fluorescence yield of some samples can be large, e.g $> 1\%$ per degree, therefore the sample chamber should be maintained at a constant temperature. A spectrum of a blank solution consisting of all components with the exception of the molecule of interest is measured, and subtracted from the sample fluorescence spectrum to eliminate low levels of contaminating signals from other components.

Fluctuations in the lamp can occur over the time of the collection period. Wavelength dependent variations in the intensity of the excitation beam exist due to the

nature of the optics of the fluorimeter. These are accounted for instrumentally by the simultaneous collection of fluorescence from a reference fluorophore (e.g. rhodamine 6G). The emission signal is divided by this reference signal while scanning, a process known as a ratio correction.

Prior to determining a quantum yield of the fluorophore, the spectrum should be corrected to represent the true sample fluorescence free of instrumental or procedural artefacts (Parker and Rees, 1960). Corrections to excitation and emission spectra are made by multiplying the spectrum by a set of correction factors which can be considered a "spectrum" of all the distortions of the particular instrument which have been combined and normalized.

2.1.4.1 Quantum Yields

Under steady-state conditions Φ_f can be expressed by definition as a ratio of rate constants described earlier:

$$\Phi_f = \frac{k_f}{(k_f+k_{nr})} \qquad (9)$$

This ratio can be related to the ratio of rates of emissive and absorptive processes and measured absolutely (Parker, 1968) with special apparatus.

Relative quantum yields are easier to obtain without a need for special instrumentation. Standard compounds of high purity are employed (Parker, 1968; Miller, 1981) as primary standards, measured, usually in the same time as the sample measurement, to eliminate errors from variations in the day-to-day operation of the instrument. In this work the standards NATA (Φ_f = 0.14) and acidic 2-aminopyridine (Φ_f = 0.66; Meech and Phillips, 1983) are used as primary standards.

The quantum yield of a sample s is calculated relative to a reference compound r, using the equation (Demas and Crosby, 1971):

$$\Phi_f(s) = \frac{1-10^{-A(r)}}{1-10^{-A(s)}} \times \frac{D_s}{D_r} \times \frac{I(\lambda_s)}{I(\lambda_r)} \times \left[\frac{\eta_d(s)}{\eta_d(r)}\right]^2 \times \Phi_f(r) \qquad (10)$$

The quantities measured are: the absorbancies at the excitation wavelength, A(s) and A(r); the intensity of exciting light at the excitation wavelengths used (if they differ) $I(\lambda_s)$ and $I(\lambda_r)$; the integrated, corrected fluorescence intensity over the same wavelength ranges, D_s and D_r; and the refractive indices of the solvent (if they differ) $\eta_d(s)$ and $\eta_d(r)$. The last two terms of equation 8 are 1 if the buffer is the same for both sample and reference.

The largest source of error in quantum yield measurements of proteins is typically the precision with which one can measure absorbance. Matching the excitation wavelength used for both the primary standard and the sample helps avoid errors introduced by the corrective terms in equation 10. The standard, 2-aminopyridine, is capable of excitation at wavelengths > 300 nm, and is used in this range instead of the standard N-acetyl-tryptophanamide (NATA) which has no useful absorbance > 300 nm. Typical values of Φ_f for single Trp proteins range from 0.05 to 0.3 (Eftink, 1991).

Quantum yields are useful for determining the sensitivity of a fluorophore. At excitation wavelength λ, the sensitivity of a fluorophore is defined as the product $\Phi_f \times \epsilon_\lambda$ with units M^{-1} cm^{-1}. If one obtains the value for Φ_f, through steady state measurements, and the value for τ_s by measuring the time dependence of the decay of the singlet excited state, it is possible to calculate the τ_r for the molecule with equation 10, and hence the rate of fluorescence for the molecule. This then permits the calculation of the sum of the rates of the nonradiative processes, k_{nr}.

2.1.4.2 Fluorescence Decay

In order to measure the singlet fluorescence decay time τ_s, the following derivations apply. Consider a population of fluorescent molecules in the excited state, $[F^*]$. The decay of this population to the ground state is a combination of random process:

$$\frac{d[F^*]}{dt} = (k_f + k_{nr})[F^*] \tag{11}$$

This follows first order kinetics due to the single term $[F^*]$. The integration of 11 with respect to time gives:

$$[F^*] = [F_o^*]e^{-t(k_f+k_{nr})} \tag{12}$$

which, when substituted with equation 6, can be rewritten:

$$[F^*] = [F_o^*]e^{-t/\tau_s} \tag{13}$$

The intensity of fluorescence I at time t and wavelength λ is proportional to this rate of excited state depopulation, hence

$$I(\lambda,t) = \alpha(\lambda)e^{-t/\tau_s} \tag{14}$$

If *i* species of unique fluorophores, or one fluorophore in *i* unique environments, are present, then the monoexponential decay function 14 becomes a sum of exponential decays:

$$I(\lambda,t) = \sum_{i=1}^{n} \alpha_i(\lambda) e^{-t/\tau_i} \qquad (15)$$

with an α and τ for each ith component. In this work, the term "multi-exponential" fluorescence decay refers to the applicability of equation 15 to a system where $i > 1$. Donzel et al. (1974) showed it is possible to estimate the relative ground state concentrations of the fluorescent components from the preexponential terms α_i.

A relationship exists between the steady-state spectrum and a time-resolved spectrum (Knutson et al., 1982). This can be used to extract i emission spectra associated with i individual decay time components, forming decay-associated spectra, or DAS:

$$I_i(\lambda) = I_{ss}(\lambda) [\alpha_i(\lambda)\tau_i / \sum_i \alpha_i(\lambda)\tau_i] \qquad (16)$$

where $I_i(\lambda)$ is the intensity spectrum (DAS) of the ith component, $I_{ss}(\lambda)$ is the intensity of the steady-state spectrum, and the preexponential term $\alpha_i(\lambda)$ is obtained from equation 15, normalized so that $\sum\alpha_i = 1$. The fractional fluorescence $f_i(\lambda)$ is related to $\alpha_i(\lambda)$:

$$f_i(\lambda) = (\alpha_i(\lambda)\tau_i) / \sum \alpha_i(\lambda)\tau_i \qquad (17)$$

The quantum yield of a mixture of n fluorophores, Φ_t, is a simple sum of their individual quantum yields, Φ_i multiplied by their normalized fractional concentration, c_i:

$$\Phi_t = \sum_{i=1}^{n} \Phi_i c_i \qquad (18)$$

If the fluorophore exhibiting i exponential fluorescence decays is a single species, the fractional concentration c_i can be estimated from the DAS. The fractional

area of the ith DAS component, A_i depends on the sensitivity product of the fluorophore, $\epsilon_{i\lambda} \times \Phi_i$, and the fractional ground state concentration c_i of the fluorophore producing the ith decay component:

$$A_i \propto \epsilon_{i\lambda} \Phi_i c_i \tag{19}$$

When the same fluorophore in different conformers is responsible for each decay component i, it is assumed that the values of $\epsilon_{i\lambda}$ are similar. Since equation 8 relates the singlet lifetime and quantum yield, $\Phi_i = \tau_i/\tau_r$, and assuming constancy of τ_r for the fluorophore in different conformers, equation 19 becomes $A_i \propto \tau_i c_i$. The validity of this assumption of the constancy of τ_r will be addressed in this work. The fractional concentration of ground-state species, c_i can be calculated from the DAS area and the decay time:

$$c_i = (A_i/\tau_i) / \sum_i A_i/\tau_i \tag{20}$$

(Willis and Szabo, 1992). This value is used to estimate the concentration of molecules giving rise to each decay component i. In the case where all DAS component spectra are identical in shape, $c_i = \alpha_i$. In the case where the DAS component shapes are different, α_i values will vary with wavelength. In this work, values of c_i derived from areas of DAS components are used instead of α_i when the underlying assumptions of equation 20 are reasonable for the system measured, i.e. fluorescence from a single species with the same $\epsilon_{i\lambda}$ and τ_r.

If the sample consists of a single chemical species with n unique environments (i.e. heterogeneity in the fluorescence decay), the value for τ_s is substituted with the average decay time $<\tau>$ where:

$$<\tau> = \sum_{i=1}^{n} \alpha_i \tau_i \tag{21}$$

The intensity-weighted or mean lifetime τ_m is used to compare lifetime with intensity data, whereas $<\tau>$ is used to compare lifetimes with quantum yield data. τ_m is derived from equation 15, and can be calculated from the decay data by the equation:

$$\tau_m = \sum_{i=1}^{n} \alpha_i \tau_i^2 \quad / \sum_{i=1}^{n} \alpha_i \tau_i \qquad (22)$$

2.1.4.3 Fluorescence Anisotropy and Energy Transfer

Fluorescence can provide parameters which describe the molecular motions of proteins which can occur on the ps-ns timescale. One such parameter is fluorescence anisotropy, which can resolve rotational motions of proteins (Weber, 1960). In addition, the transfer of electronic energy from one chromophore to another may be demonstrated in the fluorescence measurements. One type of energy transfer is known as resonance energy transfer (RET). This has a defined distance dependence and can be a useful "yardstick" for measuring distances in proteins and biomolecules (Stryer, 1978).

For a fluorophore, the probability of an absorption event is maximum at one relative orientation of the incident light. This is proportional to the resolved vector components of the absorption dipole oscillator on the electric field vector of the incident light. Since fluorescence involves the same electronic transitions as absorbance, the emitted light from an ordered chromophore, should have the same orientation and direction as the absorbed light. Polarized light can be generated by passing unpolarized light through a polarizing crystal, and can be used to excite a sample. If, during the excited-state lifetime and prior to fluorescence, the fluorophore undergoes motion, that motion can be detected by a depolarization of the emitted light.

The anisotropy of a fluorophore in solution is defined as:

$$R = (F_{\parallel} - F_{\perp})/ (F_{\parallel} + 2F_{\perp}) \quad (23)$$

where F are the fluorescence intensity parallel ($_{\parallel}$) and perpendicular ($_{\perp}$) to the plane of polarization of the excitation beam. The maximum value of R is 0.4 which would indicate no motion. Values near 0 indicate rapid molecular motion.

Given a pulse of excitation light, the anisotropy of the sample will decay with time, in a process analogous to fluorescence decay, but dependent on molecular motions. It is also possible to measure the rate of decay of anisotropy with time, and determine molecular parameters relating to global tumbling and local segmental motions (e.g. Royer et al., 1990; Bucci and Steiner, 1988; and references therein).

If the luminescent emission of one molecule A overlaps with the absorbance of a nearby chromophore B, the two can undergo resonance energy transfer (RET, indicated as A→B). Two types of RET predominate, a short range electron-exchange mechanism and a long range (> 10 Å) process known as Förster energy transfer. The Förster equation (1951) can be used to determine intramolecular distances in biological macromolecules from fluorescence data. To determine these distances, first the spectral overlap integral, J, between the normalized fluorescence donor emission, F_d and the molar absorbance spectrum of the acceptor, ϵ_a must be calculated:

$$J = \int F_d(\nu)\epsilon_a(\nu)\nu^{-4}d\nu \quad (24)$$

Here a wavenumber scale (cm^{-1}) is used instead of a wavelength scale (nm). The energy transfer rate k_t can be determined by:

$$k_t = (8.8 \times 10^{-25}\, \kappa^2\, \Phi_d\, J) / (\eta^4\, \tau_d\, r^6) \quad (25)$$

where Φ_d is the donor quantum yield, τ_d the donor lifetime, η the index of diffraction, r the donor-acceptor separation, and κ the orientation factor. The value κ^2 considers the orientations of the emissive dipole and the absorbing dipoles and is often estimated with $<\kappa^2> = 2/3$, which is the average κ^2 for a random orientation of two dipoles (Eisinger and Dale, 1976).

The distance R_o is the value of r at which the Förster transfer rate and the luminescence rate of the donor are equal, i.e. $k_t\tau_d = 1$, and the transfer efficiency is 50%:

$$R_o^6(\text{cm}) = 8.8 \times 10^{-25}\, \kappa^2\, n^{-4}\, \Phi_d\, J \qquad (26)$$

The transfer efficiency T is:

$$T = R_o^6/(r^6 + R_o^6) \qquad (27)$$

The value for T can be obtained from the fluorescence intensity data in the absence of energy transfer, I_f, and in the presence of energy transfer, I_t:

$$T = (1 - I_t) / I_f \qquad (28)$$

or from fluorescence lifetime data in a similar fashion. With T and R_o, the distance between donor and acceptor can be computed with equation 27.

The presence of two absorbance transitions are important to consider when using anisotropy. The ^1L_a and ^1L_b absorbance transitions of Trp can both contribute to Trp fluorescence Valeur and Weber (1977) were able to resolve the fluorescence excitation of indole and Trp into these absorbance transitions at low temperature. In

the region 305-310 nm the ^1L_a state is preferentially excited, although the extinction coefficient is very small. Fluorescence from indole was shown to originate primarily from the ^1L_a transition at -58° C, with the contribution from the ^1L_b state diminishing with higher temperatures. Hence Trp fluorescence in proteins can be largely considered to originate from the ^1L_a state. But the single ^1L_a state is also populated by $^1L_b \rightarrow {}^1L_a$ internal conversion. Because of this internal conversion the angle between these two transition moments can act to decrease the observed Trp fluorescence anisotropy. RET between like fluorophores, e.g. Trp→Trp, can have a similar effect, decreasing the observed anisotropy.

2.2 Time Correlated Single Photon Counting

The steady-state fluorimeter described previously (Figure 2.8) operates with a constant beam of light striking the sample and continuous emission collection. Time-resolved fluorescence is measured with an instrument that employs transient conditions. Time resolved fluorescence can be measured using two techniques. These include phase-modulation approaches (as reviewed by Lakowicz, 1983) and time-correlated single photon counting (TCSPC) methods (as reviewed by O'Connor and Phillips, 1984). This thesis work has employed TCSPC. In this method the time difference between excitation by a brief pulse of light and the opto-electronic measurement of the time of arrival of the first fluorescent photon to a detector is measured. TCSPC has developed over the last two decades with careful prior considerations for corrections to avoid instrumental and procedural artefacts in order to obtain the proper measurement of τ_s for biological samples (as reviewed by Szabo, 1988).

2.2.1 Operating Principle of TCSPC

In this technique an elaborate component-based instrument is used to measure the time between an excitation light pulse and the arrival of a fluorescence photon at a detector. The component optics and circuitry found in such instruments are described in detail in the review text of Demtröder (1988). A detailed schematic of the instrument used in this work is provided in Figure 2.9. This instrument has been described at length in previous thesis work originating from the same laboratory (Hutnik, 1990) but the instrumental operation is only briefly summarized here.

The instrument utilized in this work to measure fluorescence decays employs a mode-locked synchronously-pumped argon ion laser driving a cavity-dumped dye laser, frequency doubled for stable pulsed excitation. Excitation pulses at 825 kHz are generated by this laser, whose pulses are 10 ps FWHM. Light emerging at 50 mW power selected at a wavelength between 575-640 nm is frequency doubled by a KD^*P crystal into the ultraviolet range 284-320 nm.

The light intensity is attenuated with a neutral density filter prior to reaching the sample, such that the probability of a single emissive photon being detected per pulse is about 1% in order to obtain single photon counting (Coates, 1968). The wavelength of emissive photons are selected by monochromators with 4 nm bandpasses after passing through Glan-Taylor polarizers oriented at 54.7° to the vertical to eliminate anisotropic effects.

The electronic components of the instrument determine the time between the excitation pulse and the arrival of the emissive photon, at a microchannel plate-photomultiplier tube. This is digitized by the electronics and then output to a computer-controlled multichannel analyzer. This accumulates the photon counts in data channels assigned to different time points, typically 2048 channels at 10 ps / channel each. The overall width is selected to encompass the longest measured lifetime by at

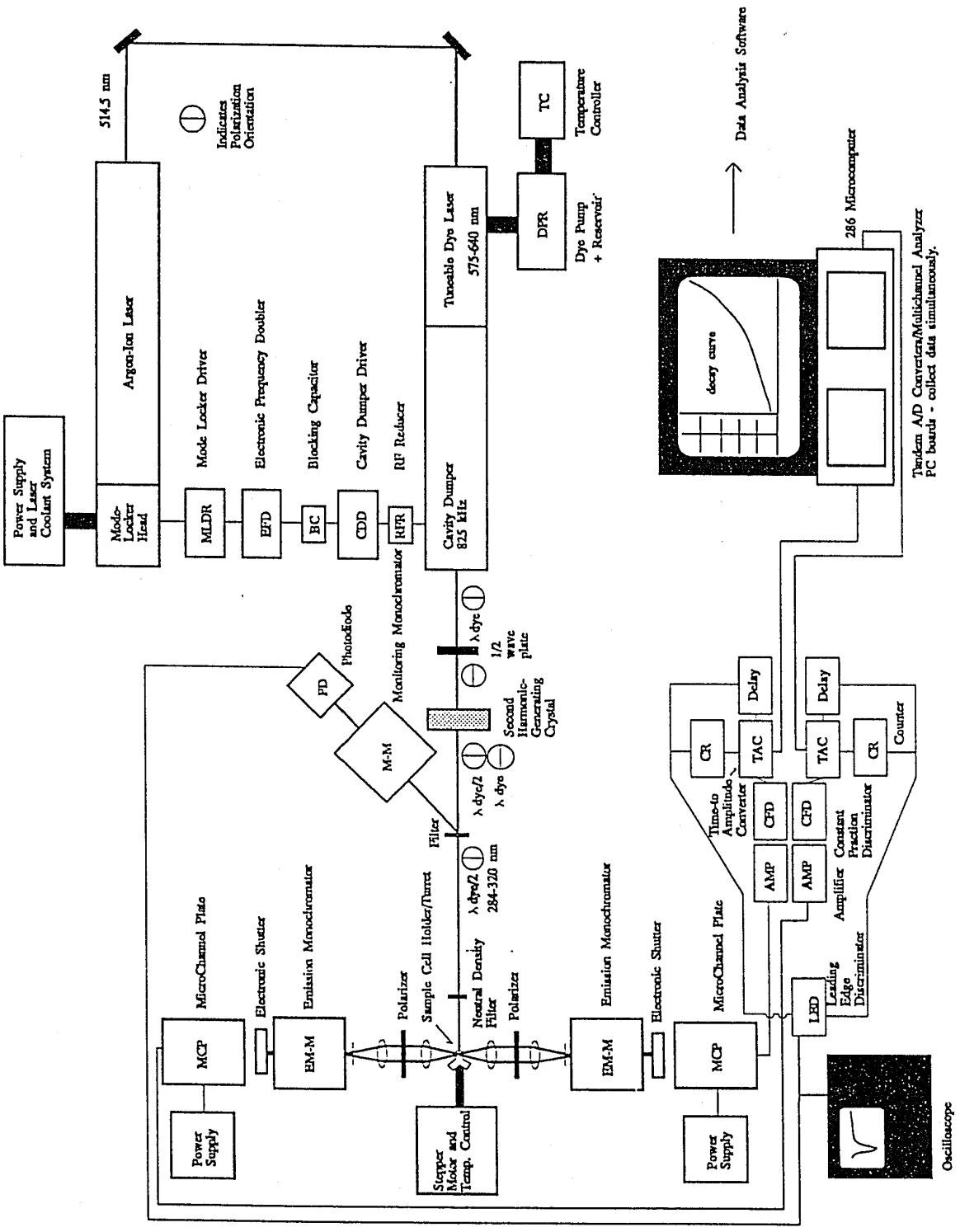

Figure 2.9: Schematic of the TCSPC apparatus used in this study.

least threefold to ensure a full representation of the decay curve. A total of 2×10^6 counts are collected in a typical curve to optimize the signal-to-noise ratio, rendering the subsequent decay data analysis statistically significant (McKinnon et al., 1977).

The sample is contained in an optical quartz cuvette within a thermostated compartment. A blank is measured for each sample, and the intensity-time profile of the blank is subtracted from that of the sample. The finite width of the laser pulse (10 ps FWHM) must be also accounted for in the data. A intensity-time profile of the laser pulse can be generated using the Stokes' Raman scattering of pure water at the appropriate wavelength (Willis et al., 1990). Typical fluorescence decay data from a single Trp protein is shown in Figure 2.10, along with the pulse profile.

2.2.2 Decay Data Analysis

Individual fluorescence decay curves are obtained from the TCSCP instrument, $D_S(t)$, at a single excitation/emission wavelength pair. These represent a convolution ($\otimes$) of the instrument's response function $D_L(t)$ originating in part from the finite excitation pulse width, together with the true decay of the sample, $F_s(t)$ (i.e. equation 15).

$$D_S(t) = D_L(t) \otimes F_s(t) \tag{29}$$

If the sample decay $D_S(t)$ and the instrument's response function $D_L(t)$ are measured at the same time (Figure 2.10) a convolution integral can be solved for $F_s(t)$ where $F_s(t)$ describes the excited state decay of the molecule under study:

$$F_s(t) = \int D_L(t') F_s(t-t')dt' \tag{30}$$

Solving this convolution involves a number of iterative trial fits of $F_s(t)$ using a non-linear least squares fit based on a Marquardt (1963) algorithm, which preferentially weights data points with more counts. The fitted $F_s(t)$ is used to generate data points corresponding to:

$$D_c(t_i) = D_L(t) \otimes F_s(t) \tag{31}$$

Noise is well characterized in this counting procedure to be Poissonian, allowing well-defined statistical parameters to be used to judge the quality of fit. A best fit is determined by the minimization of the weighted sum of squares of residuals (WSSR) between the experimental data $D_S(t_i)$ and the calculated convolution points $D_c(t_i)$:

$$WSSR = \sum_{i=1}^{n} w_i \, [D_s(t_i) - D_c(t_i)]^2 \tag{32}$$

where n is the number of data channels, t_i is the decay time at which the ith interval measurement was made, and w_i is the weight given to the square of the deviation between the experimental and fitted data points in the ith channel. The points for which variance is small are given greater weight:

$$\omega_i = \frac{1}{D_s(t_i)} \tag{33}$$

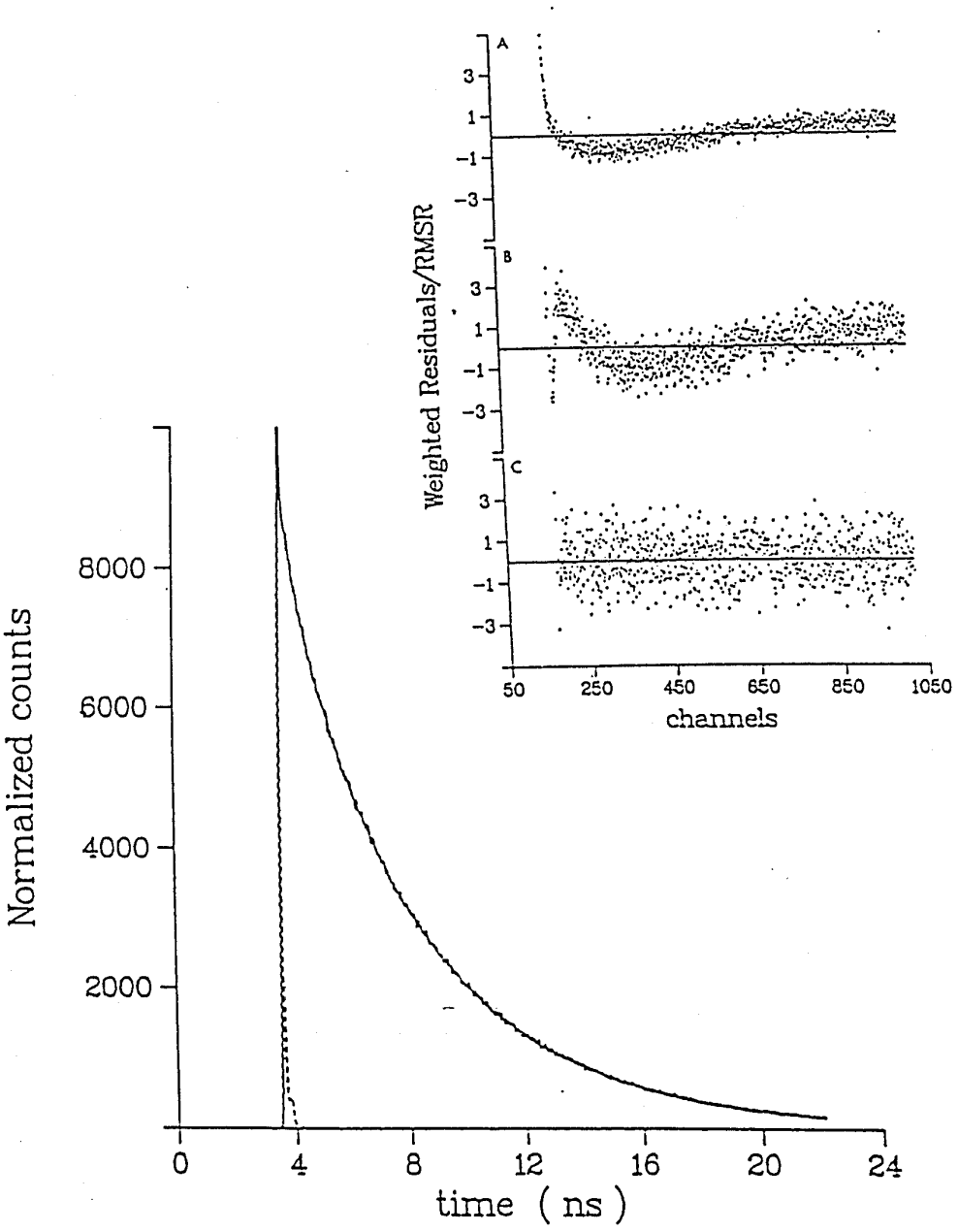

Figure 2.10: Typical fluorescence decay data. (Left) A fluorescence decay profile (solid line) together with the instrument response function (dashed line). (Right) Plots of weighted residuals fitting the decay curve at left to one, two, and three-exponential decay terms, from top to bottom.

The weighted residuals $r(t_i)$ for all i channels are:

$$WSSR = \sum_{i=1}^{n} \left[\frac{[D_s(t_i) - D_c(t_i)]^2}{D_s(t_i)} \right] = \sum_{i=1}^{n} [r(t_i)]^2 \qquad (34)$$

which is equivalent to the statistical parameter chi-square χ^2 (O'Connor and Phillips, 1984).

Three statistical parameters can be used to judge quality of fit, a σ value, a serial variance ratio (SVR) and a subjective examination of a plot of weighted residuals, $r(t_i)$ as shown in Figure 2.10.

The σ value is the square root of the reduced χ^2 or WSSR:

$$\sigma = (\chi^2_r)^{1/2} = \left[\frac{\chi^2}{n_2 - n_1 + 1 - p} \right]^{1/2} \qquad (35)$$

with n_1 as start and n_2 and ending channels, p the number of variable parameters. For a good fit, σ should be close to 1 but values between 0.9 and 1.2 are generally acceptable in combination with the other statistical tests (Phillips et al., 1985).

The SVR tests the independence of a successive series of observations, and unlike σ, it can provide a measure of the correlation between successive residuals:

$$SVR = \frac{\sum_{i=n_1+1}^{n_2} [r(t_i) - r(t_{i-1})]^2}{\sum_{i=n_1}^{n_2} [r(t_i)]^2} \times \frac{(n_2 - n_1)}{(n_2 - n_1 - 1)} \qquad (36)$$

An SVR between 1.7 and 2.0 corresponds to a good statistical fit of the data (McKinnon et al., 1977).

The subjective examination of the weighted residual plots, as shown in Figure 2.10 is combined with σ and SVR to judge goodness of fit. A properly fit decay curve will display a set of weighted residuals that behave as a random normal distribution with unit standard deviation because of the Poissonian nature of the noise. A complete randomness of these points indicates that the experimental decay curve was best fit by that trial function. By convention, if no further improvement in the statistical fit of TCSPC data is obtained by introducing one more exponential term, the fit with the fewest decay parameters is accepted as significant (Szabo 1988).

It is possible and desirable to combine the individual fluorescence decay curves, and instrument response curves corresponding to the various emission wavelengths monitored to obtain a simultaneous analysis of the parameters of the decay function in equation 14, provided that values of τ_s are similar at different wavelengths. This process is known as Global Analysis (Knutson, et al., 1983), and exploits relationships between individual decay curves to overdetermine values of α_i and τ_i. This can significantly aid in distinguishing between model decay functions that might vary amongst individual wavelength data. DAS and decay parameters reported in this work were all computed using global analysis, except when indicated.

2.3 Intrinsic and Extrinsic Protein Fluorescence Studies

The intrinsic fluorescence of proteins is dominated largely by Trp fluorescence, despite excitation of the other two potential fluorophores, Phe and Tyr (Teale and Weber, 1957). Reasons for this include its higher extinction coefficient and its ability to act as an energy transfer acceptor, depleting nearby Tyr fluorescence (Longworth, 1970). The particular sensitivity of Trp to its environment, undergoing changes in

intensity, spectral shape and λ_{max}, makes it a very useful probe for biological investigations of proteins.

One persistent difficulty in the study of intrinsic fluorescence of a protein is in the assignment of the overlapping fluorescence emission to individual Trp residues in proteins with more than one Trp. Fortunately Trp is typically present in low numbers in proteins (Klapper, 1977) compared to Tyr, and several proteins have only a single Trp residue (Grinvald and Steinburg, 1976).

In order to take advantage of the full range of fluorescence parameters including lifetime data, energy transfer and anisotropy decay, a single fluorophore is typically required to allow correlation of these parameters to structural and physical models.

In cases where a single intrinsic fluorophore is not available, extrinsic fluorescent probe molecules can be used. Often these are conjugated aromatic ring structures which are chemically attached to a protein through a functional group such as the side chain of Cys. These have an additional advantage of extending beyond the excitation and emission wavelength ranges of intrinsic fluorophores. Hence they can be monitored without interference from signals from the intrinsic fluorophores. Often the sensitivity of these molecules is much higher than that of Trp.

There are two main disadvantages of extrinsic fluorescence probes for studying biological molecules. Extrinsic molecules can interfere with biological function through steric effects or by the unwanted labelling of a required functional group. In addition, a multitude of potential functional groups as labelling sites can cause undesired heterogeneity in the labelling of the protein. In one example, Lindahl et al. (1991) remarked on the negative effect of extrinsic labelling on the dissociation constant of papain for the inhibitor protein cystatin. They also noted that changes in fluorescence could be explained by motions of the extrinsic probe, rather than conformational changes of the protein. As a result they had to limit their conclusions to titrations and stoichiometry.

An alternative to resorting to extrinsic fluorescence and chemical modification is the alteration of the number and type of intrinsic probes found in a protein by oligonucleotide-directed mutagenesis techniques (Zoller and Smith, 1982). With this technique it is feasible to eliminate the redundant Trp fluorescence by changing Trp residues into other amino acids at the genetic level, typically to Phe or Tyr (e.g. Royer et al., 1990; Harris and Hudson 1990; Smith et al., 1991). It is also possible to introduce single Trp residues into sites of interest in proteins lacking Trp (e.g. Hutnik et al., 1990; Hutnik et al., 1991; Chabbert et al., 1991), again with Trp usually replacing other aromatic amino acids, Tyr or Phe. This technique can provide large quantities of protein due to the high overexpression of recombinant proteins in the bacterial or yeast systems used.

Most often, these site-directed replacements involving Trp are without major consequence for the biological function of the protein. However the subject of this thesis, *B. subtilis* TrpRS, is an important exception (Chow et al., 1992). Site-directed mutagenesis to replace the single Trp-92 with a number of amino acids abolishes TrpRS activity.

The use of Trp analogs incorporated into proteins is put forth in this thesis as an alternative and an extension to these attempts to obtain active proteins with single fluorophores. It is hoped this strategy will combine the nondisruptive qualities of intrinsic fluorescence with the enhanced fluorescence selectivity and sensitivity usually attributed to extrinsic fluorophores. In addition, means for removing unwanted Trp fluorescence from a protein in a less disruptive manner are also provided by certain analogs of Trp, detailed later in this chapter.

2.3.1 Fluorescence Quenching of Trp in Proteins

There exist a number of conditions in which the fluorescence of Trp in proteins is diminished. Some of these include nearby cysteine or disulfides, (Cowgill, 1967); charged groups such as His, Asp or Glu (Cowgill, 1976; Willaert and Engelboroghs, 1991) or complexation with transition metals (as reviewed by Lakowicz, 1983). Molecules that act as energy transfer acceptors can also diminish Trp fluorescence through energy transfer via Förster or other energy transfer mechanisms (Birks, 1975).

Collisional quenching, as mentioned in section 2.1.3 provides additional nonradiative pathways for the decay of the Trp excited state. Common dynamic quenchers used to examine Trp fluorescence in proteins include I^-, O_2, and acrylamide. Impurities can also contribute to quenching.

The Stern-Volmer equation relates the loss of fluorescence intensity to the quencher concentration:

$$F_o/F = 1 + K_{SV}[Q] \tag{37}$$

A plot of the ratio of fluorescence intensity before and after quenching, F_o/F, versus $[Q]$ ideally produces a straight line, of slope K_{SV}. However nonlinearities can indicate additional processes, such as static quenching complexes (section 2.1.3) or multiple emitting centers (as reviewed by Eftink and Ghiron, 1981; and Laws and Contino, 1992).

For the heterogeneous fluorescence decay of a single Trp, the value of the average decay time τ_m (intensity weighted as per equation 22) can be used to derive the bimolecular quenching constant k_q (Eftink and Ghiron, 1976):

$$k_q = K_{SV}/\tau_m \tag{38}$$

(The τ_m value is used rather than the $<\tau>$ value if the K_{SV} is obtained from intensity data, rather than Φ_f data.)

Variations in the value of k_q can represent either the fractional exposure of a Trp residue to solvent (protein is static) or the rate of formation of "holes" through which quencher may access a Trp residue buried within a protein (protein is dynamic) (Eftink and Ghiron, 1977). A correlation between k_q and λ_{max} of Trp residues in proteins exists for acrylamide quenching (Eftink and Ghiron, 1976).

As previously mentioned in section 2.1.3, static quenching involves a nonfluorescent ground-state complex between the fluorophore and the quencher. According to Lakowicz (1983) the fluorescence lifetime is the most definitive method to distinguish between static and dynamic quenching. Since the static quenching completely removes fluorophores from the fluorescing pool, fluorescent lifetimes remain the same in the quenched state (τ) as the in the unquenched state (τ_0), thus the ratio $\tau/\tau_0 = 1$ for static quenching. Additionally, examination of the fluorophore's absorption spectra will reveal if any ground-state complexes are observed that would alter this spectra. In contrast, for dynamic quenching, fluorescence lifetimes are shortened, and the ratio $\tau/\tau_0 = \Phi/\Phi_0$ should exist. (In this case the average lifetime $<\tau>$ (equation 21) is used for heterogeneous Trp fluorescence decay data, in comparison with Φ). When both $\tau/\tau_0 \neq 1$ and $\tau/\tau_0 \neq \Phi/\Phi_0$, both static and dynamic quenching could be implicated in the quenching mechanism.

2.3.2 The Multi-Exponential Fluorescence Decay of Trp

The interpretation of the fluorescence decay of tryptophan is complex. This can be due to many different nonradiative rate parameters which have been documented for indole derivatives. In early time-resolved fluorescence studies, tryptophanyl

fluorescence was shown to exhibit multi-exponential fluorescence decays (Donzel et al., 1974; Grinvald and Steinberg, 1976). Tryptophan zwitterion was demonstrated to exhibit dual-exponential fluorescence decay behaviour which was first thought to be due to the solvent-relaxed ^1L_a and ^1L_b dipoles (Rayner and Szabo, 1978). However the demonstration of single-exponential fluorescence from related compounds such as indole and NATA indicate that the multi-exponential fluorescence could not possibly originate from these two states, as the ^1L_a was the dominant emission transition moment. These authors revised their rationalization in terms of a rotamer model (Szabo and Rayner, 1980).

Detailed lists of possible origins of the observed multi-exponential photophysics of Trp zwitterion have been presented (Szabo and Rayner, 1980; Beechem and Brand, 1985; Hudson et al., 1986; Eftink, 1991). These lists often include solvent dipolar relaxation, exciplex formation (Walker et al., 1967; Hershberger et al., 1981); Rydberg states and high-energy ionization (Lami, 1977); Trp rotamers (Szabo and Rayner, 1980) and combinations of rotamers which form charge-transfer pairs to nearby electronegative groups (Chang et al., 1983; Petrich et al., 1983).

Later, more elaborate studies using higher resolution fluorescence decay data have indicated that the Trp zwitterion undergoes excited-state reactions (Szabo, 1988; Willis et al., 1991) by virtue of a characteristic negative-prexponential term (α of equation 15) found in the fluorescence decay at long wavelengths (Birks, 1970; Laws and Brand, 1979). Possible excited-state reactions include solvent reorganization and conformer interconversion driven by interactions between the large dipoles of the zwitterionic side chain and the excited state indole ring (Willis et al., 1991). An excited-state proton transfer at the 4-position of the indole ring has been shown to occur in the excited-state of Trp zwitterion (Saito et al., 1984) in D_2O that can account for a nonradiative pathway of decay. In addition, deprotonation of the indole NH could also represent an excited-state reaction that could contribute to k_{nr}.

An excited-state reaction is the most likely origin of the observed multi-exponential decay behavior of zwitterionic Trp. Yet the origins of multi-exponential fluorescence of Trp zwitterion may have little to do with the nature of the origins of fluorescence decay observed in a protein. It is agreed that NATA and some other Trp derivatives appear to exhibit a single-exponential fluorescence decay behaviour (Szabo and Rayner, 1980; Lakowicz, 1983; Eftink, 1991), thus Trp zwitterion may be the exception, rather than the rule. Since NATA has its amino and carboxyl groups in amide bonds and no large side-chain dipole as found in Trp zwitterion, it should be a better model for Trp in proteins. NATA would be incapable of catalyzing the intramolecular C4 proton-transfer reaction, and the absence of the zwitterionic dipole would preclude excited-state reorientation of the alanyl side chain (Szabo, 1988). Furthermore the ^1L_a dipole dominates the fluorescence emission of Trp, mentioned earlier. These allow a rationalization that Trp fluorescence in a protein should originate from a fluorophore whose innate behavior is more like that of a single-exponential emitting species like NATA or indole rather than like that of Trp zwitterion. However Trp zwitterion illustrates the variety of quenching and non-radiative processes that could all somehow contribute to the observed Trp fluorescence in a protein environment.

An early comprehensive study of single-Trp proteins demonstrated that their time-resolved fluorescence could be described by two or three exponential decay terms (equation 15) (Grinvald and Steinberg, 1976). These were very often found, with the longest τ in the range 2-5 ns, the middle τ between 0.03 - 4 ns, and the shortest τ between 0.03 - 1 ns. Yet studies of multiple-Trp proteins and even whole protein extracts often exhibit the same decay characteristics. This is attributed to the determination of mean values of multiple fluorescence decays, due to the difficulties in the data analysis technique in resolving large numbers (i.e $>$ 4) of discrete exponential terms. Therefore it is crucial to extensively characterize the purity and composition of

a single-Trp protein to assure it is free from fluorescent contaminants. The observation of single, double and triple-exponential decay fluorescence in some highly-purified calcium-binding proteins with homologous single-Trp residues is an example verifying the assignment of a discrete set of multi-exponential decay terms to a pure, single-Trp protein (Pauls et al., 1993; Hutnik et al., 1990).

Conformational heterogeneity of Trp in proteins can be accounted for by different rotamers of the indole side chain of Trp (Szabo and Rayner, 1980). A growing body of experiments involving high-resolution fluorescence of pure protein samples suggests that conformational heterogeneity originating from rotamers is the most likely origin of the often-observed multi-exponential fluorescence decay of proteins. Other workers have fit decay data to distributions of lifetimes corresponding to distributions of conformational states. These may sometimes prove more applicable when discrete lifetime components fail to fit decay data satisfactorily (James and Ware, 1986; Alcala et al., 1987; Harris and Hudson, 1990). It is noted, however, that these models are susceptible to variations in the signal-to-noise ratio and the number of counts in decay data sets (Szabo, 1988). There are distinct differences between TCSPC and phase-modulation decay data in these two parameters, and continuous distribution models have failed to provide superior fits to data generated with TCSPC (Willis et al., 1994) compared with discrete component models.

Correlations have been presented to relate the preexponential terms of the fluorescence decay times, α_i or c_i which are assumed to relate to conformer concentrations, with the observed rotamer populations found by NMR (Ross et al., 1992c; Willis and Szabo, 1992). Rotamers of Trp on an α-helix are shown in Figure 2.11.

Experiments correlating rotamer structures of dipeptides containing Trp with the fluorescence decay behavior were reported (Chen et al., 1991). Computational simulations have demonstrated that the assumptions of energy minima associated with

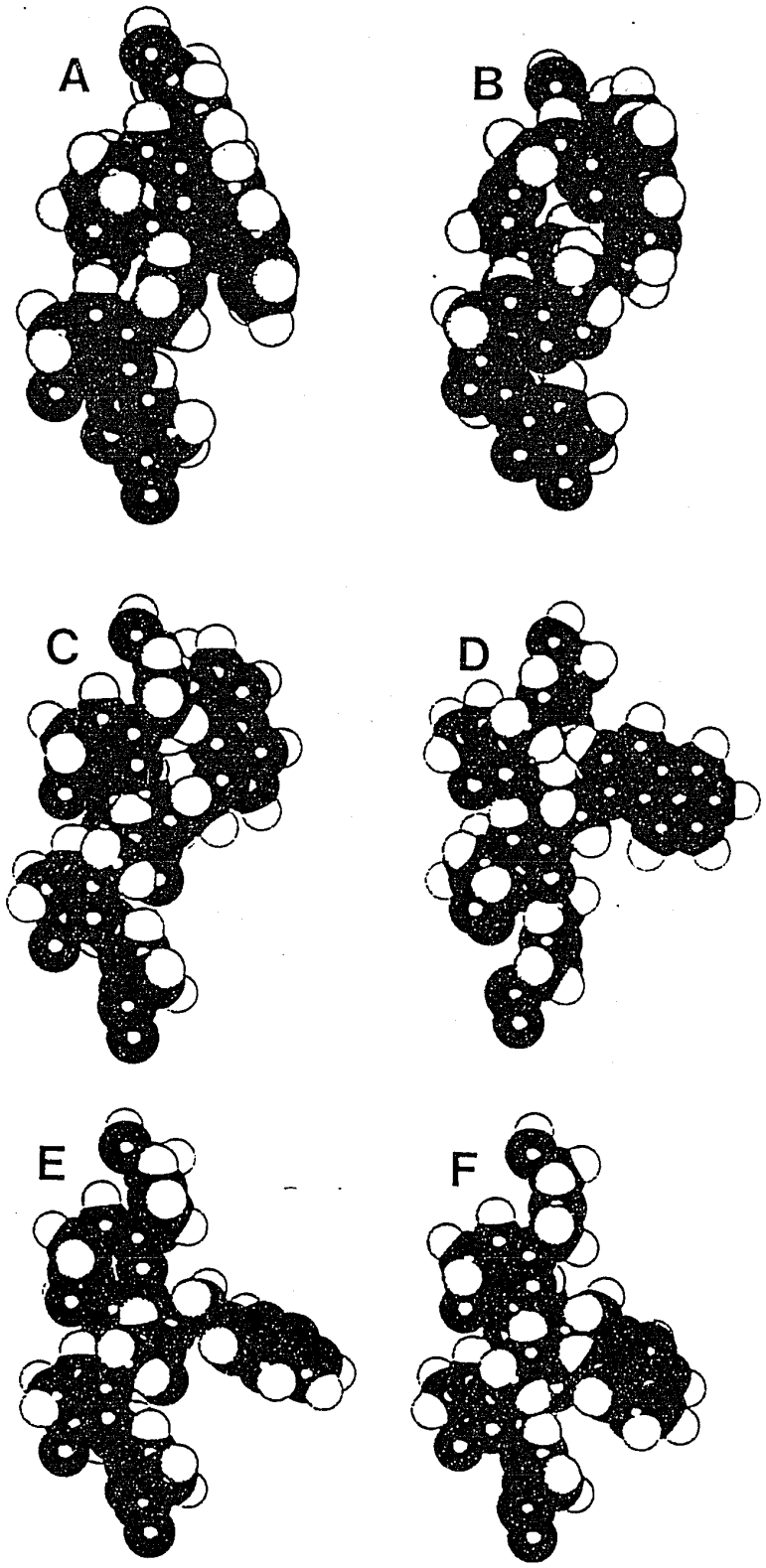

Figure 2.11: Rotamers of Trp on an α-helix. A) perp g+, B) anti g+, C) perp g-, D) anti g-, E) perp t, F) anti t.

rotameric states are reasonable for Trp zwitterions (Engh et al., 1986, Gordon et al., 1992) and for a Trp residue in a protein crystal structure (Haydock, 1993). However it was noted that the relative populations of Trp zwitterion rotamers calculated with molecular dynamics were not consistent with the experimental data assigned to rotamer populations from fluorescence decay data. These populations were shown to vary greatly when different molecular dynamics parameters were used in the calculations (Gordon et al., 1992).

The relative contributions of three fluorescence decay component α's of Trp were found to vary with amount of α-helical structure as determined by CD spectroscopy in single Trp peptides (Willis and Szabo, 1992; Willis et al., 1994). However the same observation was not found for a single Tyr peptide (Backlund and Gräslund, 1992) in a similar investigation. Willis et al. (1994) argued that a steric clash between the 6-membered portion of certain rotamers of the indole ring of Trp and the α-helical backbone was responsible for the observed variation. Such a steric clash may not be evident with the rotamers of the smaller Tyr ring and the α-helical backbone.

Important direct evidence supporting the rotamer model as the origin of multi-exponential fluorescence of Trp in proteins comes from the recent studies of the fluorescence decay of single protein crystals (Dahms et al., 1993). It was shown that the preexponentials, α_i corresponding to individual decay components, τ_i, vary as the orientation of the crystal axis is varied with the orientation of the exciting laser beam. This angular variation in decay component contributions α_i, but not decay time τ_i, is explained by the existence of populations of Trp rotamers within unit cells of the crystal. This observation is best explained by the rotamer hypothesis rather than any other mechanisms that have been advanced to explain the multi-exponential fluorescence decay of Trp in proteins.

Trp residues also clearly exhibit multi-exponential phosphorescence decays in proteins (Schlyer et al., 1994). These phosphorescence decay times are assigned to discrete ground-state conformers which interconvert on time-scales longer than the phosphorescence (Schlyer et al., 1994). Rotamers are thus a likely source of such ground-state heterogeneity of phosphorescence decay as well as fluorescence decay.

Clues towards a singular explanation for the observed fluorescence of Trp in proteins come from a now larger body of work which show patterns, not previously observed, are evident. Patterns of τ_s (long, medium, short decays) have been described earlier for the multi-exponential decay of single-Trp residues in proteins (Grinvald and Steinberg, 1976, Lakowicz, 1983). Yet patterns in DAS can also be observed; long decay components correspond to relatively red-shifted λ_{max}, intermediate components correspond to intermediate λ_{max}, and shortest decay components correspond to relatively blue-shifted λ_{max}. These patterns *dominate* DAS of proteins reported using both TCSPC and multifrequency phase fluorimetry techniques. Examples in addition to the work reported later in this thesis includes single Trp mutants of calmodulin (Chabbert et al., 1991); oncomodulin single Trp mutants (Hutnik et al., 1990 and 1991); lac repressor single Trp mutants (Royer et al., 1990); single Trp melanotropin peptides (Ito et al., 1993); single Trp subtilisin (Willis and Szabo, 1989); single Trp peptides of PTH (Willis and Szabo, 1992). Single Trp protein crystal fluorescence decays exhibit the same characteristic trends (Dahms, 1993, personal communication).

These DAS patterns persist, with only a few exceptions, even in the clear absence or presence of nearby solvent water. They suggest a singular common property of protein structure is responsible for the observed fluorescence decay. A multiplicity of mechanistic reasons to explain Trp fluorescence variations, each with a case-by-case application to different Trp microenvironments, is unlikely to provide such consistency of these patterns in the observed DAS data. An application of Occam's razor to the plurality of explanations for the variations in Trp fluorescence

observed in proteins seems necessary. It is anticipated that an understanding of the underlying structural basis for the observed Trp multi-exponential fluorescence is forthcoming, and it is hoped that experiments herein with Trp analogs in proteins will contribute to this understanding.

2.4 Tryptophan Analogs as Intrinsic Fluorophores

The basis of this thesis, the use of intrinsic probes in the form of Trp analogs, is made on the following suppositions: If one can use an *intrinsic* fluorescence probe with a fluorescence spectrum that does not overlap with Trp, it would enable the intrinsic fluorescence study of protein-protein interactions with those analogs without interference from Trp fluorescence. If such an intrinsic probe could be inserted using biosynthetic machinery, the technique could be relatively straightforward and of general applicability. If tryptophan analogs are largely benign and nondisruptive in their effects on protein structure and function, then there is greater likelihood of their success as fluorescence probes of biological phenomena. If, in addition, such an intrinsic probe had any special photophysical characteristics compared to Trp, they could have niches of utility currently not well served by Trp or extrinsic fluorescence probes.

Three Trp analogs are discussed here in terms of their photophysics and expected utility in studies of intrinsic fluorescence of proteins; 5HW, 7AW and 4FW, shown in Figure 2.12.

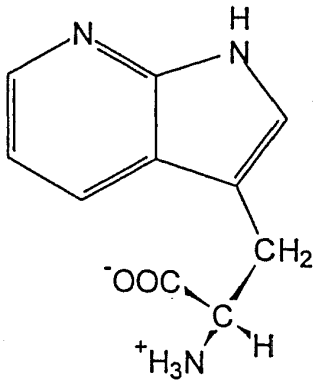

7-azatryptophan

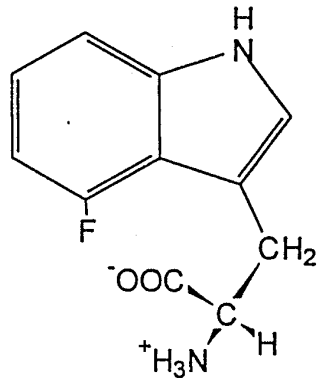

4-Fluorotryptophan

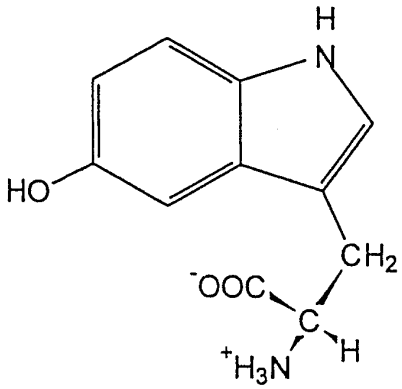

5-Hydroxytryptophan

Figure 2.12: Structures of Trp analogs 7AW, 4FW, and 5HW.

2.4.1 5-Hydroxytryptophan

5-Hydroxytryptophan is a naturally occurring amino acid, and is perhaps best known as an intermediate in the biosynthesis of serotonin (5HT, 5-hydroxytryptamine) from Trp. Despite records of 5HW incorporation into prokaryotic proteins residing in the literature since 1970 (Barlati and Cifferi), it was overlooked as an potential intrinsic fluorescence probe until recently. A mutant of the oncotrophoblastic calcium-binding protein, Y57W oncomodulin, was the first protein used to demonstrate the site-specific incorporation of 5HW in place of Trp-57 in an *E. coli* expression system (Hogue et al., 1992).

The absorbance spectra of both 5HW and 5HT have well-defined red-extended shoulders, compared to Trp (e.g. Figure 4.2 A). This red-extended shoulder in 5HT was shown to be primarily due to the absorbance of the single ^1L_b transition dipole in oriented crystals (Kishi et al., 1977). This is in contrast to the ^1L_a and ^1L_b dipole transitions of Trp which overlap across most of its absorbance spectrum (Yamomoto and Tanaka, 1972). The single ^1L_b transition dipole of 5-hydroxyindoles or 5-methoxyindoles is at a much reduced energy compared to that of indole (Lami, 1976), hence it can be selectively excited at wavelengths at 310 nm and above, while its extinction coefficient remains relatively high up to 320 nm. This red-extended absorbance comprises the primary utility of 5HW as a chromophore. This was demonstrated with two examples; in intrinsic fluorescence experiments using 5HW extended absorbance (Hogue et al., 1992), and recently with analytical ultracentrifugation experiments in which incorporated 5HW absorbance was used to distinguish protein from DNA (Laue et al., 1993) in a nondisruptive fashion.

The properties of ^1L_b fluorescence in 5-hydroxyindoles are expected to be very different from the ^1L_a fluorescence which is observed from Trp. Since the predicted oscillator strength of the ^1L_b state is less than half that of the ^1L_a state (Lami, 1976),

the effect of dipolar and solvent relaxation on 5HW fluorescence should be greatly diminished. This has been observed, as large variations exist in maxima of indole (^1L_a) fluorescence in different solvents (cyclohexane 298 nm; and water 342 nm) but only small variations are observed with 5-hydroxyindole (^1L_b) fluorescence maxima (cyclohexane 322 nm; water 331 nm) (Lami, 1976).

Consistent with these observations, 5HW fluorescence in proteins is not expected to exhibit the variations in λ_{max} as are observed with Trp in proteins (as reviewed by Eftink and Ghiron, 1976) and the 5HW λ_{max} is expected to be not as sensitive to solvent exposure as is the λ_{max} of Trp. The fluorescence maximum of Tyr is also relatively invariant, usually occurring between 303 and 305 nm, yet its quantum yield proves very sensitive to environmental changes (Ross et al., 1992a).

5HW has other distinct advantages as a fluorophore. As mentioned previously, the $^1L_b \rightarrow {}^1L_a$ internal conversion is a depolarization mechanism of Trp fluorescence. The ^1L_b transition of 5HI can be exclusively excited, and therefore in 5HI this depolarization mechanism can be avoided. This predicts higher fluorescence anisotropy values in proteins with 5HW, compared to Trp. This was observed in the single 5HW containing protein Y57(5HW) oncomodulin (Hogue et al., 1992). At 295 nm the steady-state anisotropy of the Y57W oncomodulin was 0.11, whereas at 315 nm the Y57(5HW) anisotropy was 0.188. In a complex with antibodies, steady-state fluorescence anisotropy values close to the theoretical limit of 0.4 were observed with 315 nm excitation of this 5HW residue. Therefore one would expect improved anisotropy measurements of proteins with 5HW replacing Trp.

Yet another utility for incorporated 5HW is found as a Förster energy transfer acceptor for Tyr fluorescence. 5HW absorbance between 300-320 nm has a significant overlap with Tyr fluorescence at 305 nm. Ross and coworkers (1992b) calculated the overlap integral for Förster energy transfer from Tyr to 5HW from the emission spectrum of NATyrA and the absorbance spectrum of 5-hydroxytryptophan. They

obtained a value of 2.2×10^{-12} $cm^6 \cdot mol^{-1}$ for Tyr → 5HW, compared with that for Tyr → Trp 6.6×10^{-13} $cm^6 \cdot mol^{-1}$. They concluded that for the same distance of separation and relative dipole orientation, the energy transfer rate from Tyr to 5HW should be about 3 times that of Tyr to Trp. Further the singular dipole orientation of 5HW compared to Trp, as discussed above, should render energy transfer from Tyr to 5HW more sensitive to the orientation factor κ in the Förster equation (26) (Mersol et al., 1992).

Hudson and coworkers (1986) have suggested that an amino acid chromophore with simpler photophysical properties compared to tryptophan, would make the interpretation of fluorescence decay in proteins less ambiguous. 5HW fits the criteria set out by Hudson because: (A) it has well-separated ^1L_a and ^1L_b dipoles; (B) its emission spectra is essentially invariant to changes in polarity; and (C) it has single-exponential fluorescence decay kinetics. 5HW fluorescence has monoexponential decay kinetics in aqueous solution in physiological pH ranges (Hogue et al., 1992; Ross et al., 1992b; Hogue and Szabo, 1993; Chen et al., 1994a). Using 5HW fluorescence from excitation wavelengths > 310 nm, contributions from dual emission states, as well as exciplex formation (Lami 1976), can be discounted as origins of any observed multi-exponential fluorescence decay behaviour in proteins. 5HW fluorescence can therefore help to resolve the origin of multi-exponential fluorescence decay of Trp in proteins. Conformational heterogeneity and the rotamer model may also be a better rationalization for any non-exponential fluorescence decay that might be observed with a simpler fluorophore such as 5HW in proteins.

One final utility of 5HW deals with the possibilities for further chemical modification of an incorporated 5HW residue. Tyrosine has a phenolic hydroxyl which can be nitrated with tetranitromethane (TMN) under very mild conditions. 3-nitrotyrosine is coloured with an absorption maximum at 428 nm (Imoto and Yamada, 1989), making it a useful nonradiative Förster energy transfer acceptor. For example

the distance between Trp-99 and nitrated Tyrosine-138 was determined in calmodulin to be consistent with the crystallographic distance (Steiner et al., 1991). Further investigations into the chemical modification of 5HW incorporated into proteins could determine whether this could be useful as a nonfluorescent Förster energy transfer acceptor for Trp fluorescence, or as a visible intrinsic chromophore for proteins which might have applications in vibrational spectroscopy.

2.4.2 7-Azatryptophan

7AW, as mentioned in section 1.3.3, was used in the early biochemical studies of protein synthesis (Shore and Pardee 1956) and later in studies of enzyme structure-function (Schlesinger, 1968; Foote et al., 1980). Schlesinger made the first study of the absorbance and fluorescence properties of a protein with incorporated 7AW. It is important to recognize this early contribution, as much of the useful properties of 7AW as a fluorescence probe can be identified in this early work, although these properties were not well understood at the time.

A reevaluation of Schlesinger's work (1968) with 7AW incorporated alkaline phosphatase demonstrates 7AW as an extremely sensitive probe of environment. She observed that the emission of 7AW fluorescence in this protein had intense, blue-shifted fluorescence (uncorrected λ_{max} = 370 nm). Schlesinger further demonstrated that, upon guanidine-HCl denaturation of the 7AW-incorporated enzyme, there was a dramatic quenching of 7AW fluorescence, much more so than observed with tryptazan (2AW) or Trp forms of the same protein. The observation of intense, long-lived, blue-shifted 7AW fluorescence in buried locations in proteins is duplicated in this thesis. These large fluorescence yield changes (10-fold or more) of proteins with incorporated 7AW can provide a useful and specific probe for the examination of protein folding,

conformational changes or ligand-protein binding. In order to understand the origin of this large fluorescence yield change, relevant studies of simpler systems need to be examined.

The parent chromophore, 7AI, has been the subject of much recent study. The relative fluorescence intensity of various azaindoles including 7AI was first reported by Adler (1962) who reported a low fluorescence yield of 7AI in water. The fluorescence of 7AI was examined in detail by Avouris et al. (1976) who made many important conclusions about the photophysics of 7AI. The possible photophysical pathways they attributed to 7AI are indicated in Figure 2.13. In the last 4 years, Petrich and co-workers have asserted that 7AW is a potent and novel noninvasive fluorescent probe of protein structure and dynamics, and have sought to reinvestigate 7AI and 7AW photophysics (Négrerie et al., 1990; Négrerie et al., 1991; Gai et al., 1992; Négrerie et al., 1993; Chen et al., 1993; Rich et al., 1993ab; Chen et al., 1994a,b; Gai et al., 1994; Rich et al., 1994). However none of these papers report fluorescence from biosynthetically incorporated 7AW in proteins, despite encouraging others to do so.

When the fluorescence of 7AI and 7AW was examined in solvents, remarkable differences were observed (Avouris et al,. 1976; Chapman and Maroncelli 1992). In water, 7AI exhibited very poor fluorescence with λ_{max} = 402 nm, Φ_f = 0.032, and dual-exponential fluorescence decay with an average decay time of 0.82 ns. This latter point is under some dispute, discussed later. In aprotic solvents these parameters are much different, e.g. 7AI in acetonitrile: λ_{max} = 362 nm, Φ_f = 0.38, average decay of 5.7 ns. This represents an order of magnitude increase in Φ_f from water to aprotic solvents. However in alcohols, 7AI exhibits two populations of fluorescence, F1 and F2, neither of which is efficient, (Avouris et al., 1976; Chapman and Maroncelli, 1992). The former was assigned to the normal 7AI (n-7AI) fluorescence, the latter was assigned to fluorescence arising from tautomer 7AI (t-7AI) as shown in Figure 2.13 (Avouris et al., 1976; Chou et al., 1992; Chapman and Maroncelli 1992). This

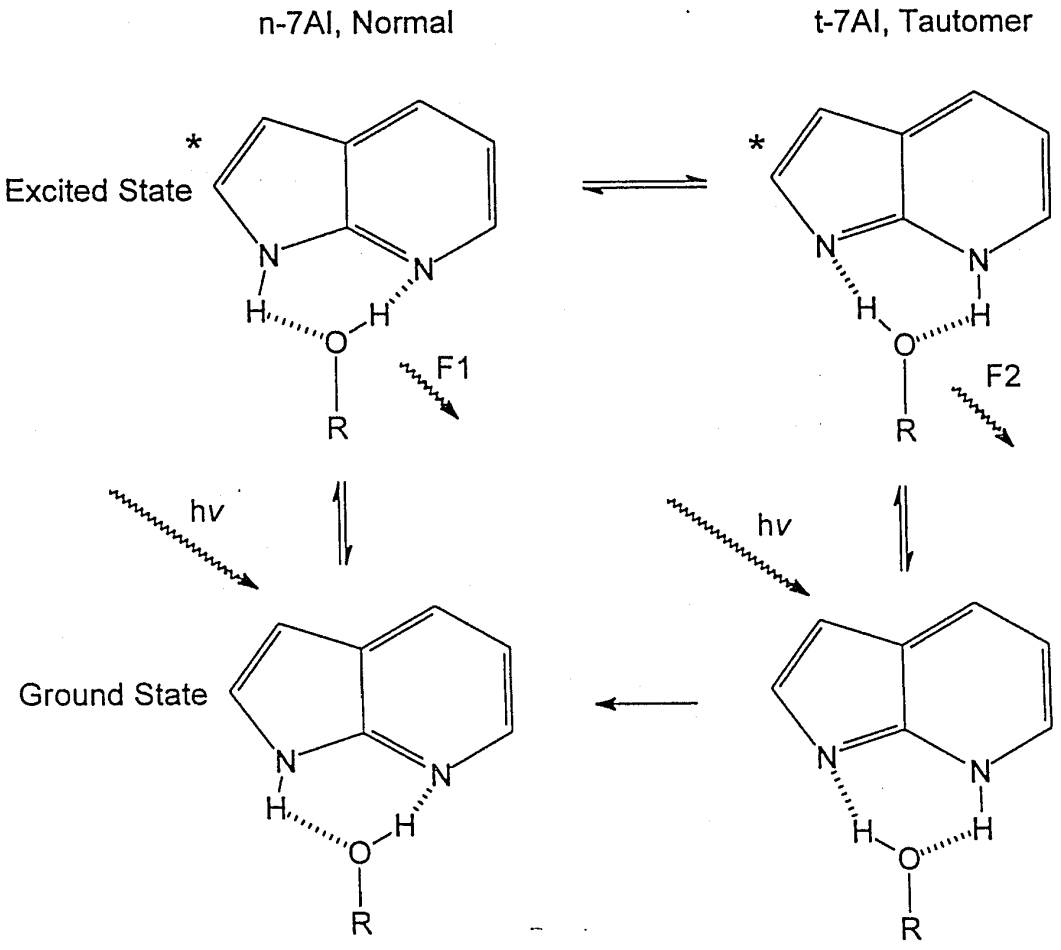

Figure 2.13: Tautomerization reactions of 7AI in protic solvents such as water or alcohols. F2 seems to be absent in water. (Avouris et al., 1976)

anomalous alcoholic fluorescence of 7AI has been the subject of competing photophysical theories, dealing with the tautomerization of 7AI.

A consensus mechanism for the tautomer fluorescence in alcohols involves a cyclic intermediate between the 7AI and the OH of the alcohol (Figure 2.13). This involves the hydrogen bonds $N^1H{\cdot}OR$ and $N^7{\cdot}HOR$ between the 7AI ring and the alcohol. Once this complex forms, tautomerization can produce two different bonds: $N^1{\cdot}HOR$ and $N^7H{\cdot}OR$. It is also important to note that the tautomer produced in the excited state does not accumulate in alcohol solutions, therefore there is a rapid reaction from t-7AI to form n-7AI via a ground-state double proton transfer mechanism (Avouris et al., 1976).

It is clear from these solvent studies that considerations must be made to describe 7AW fluorescence that include contributions from the following species: n-7AW, t-7AW, and protonated 7AW; and their possible excited-state reactions: e.g. double-proton transfer (tautomerization); single proton-transfer, and solvent reorganization. It is also clear there is a strong quenching of 7AI and 7AW that is absent with Trp, and the blocked analog 1M7AI (Chapman and Maroncelli, 1992).

For the observed quenching of 7AI from D_2O to H_2O, the ratio of Φ_0/Φ:τ_0/τ is unity ($\Phi_0/\Phi = 3.6$; $\tau_0/\tau = 3.5$ Chen et al., 1993). This ratio can be used to identify the protic quenching mechanism as having a dynamic character (Lakowicz, 1983). It must therefore be considered that H_2O and solvent hyroxyls act as very effective dynamic quenchers of 7AI and 7AW fluorescence, regardless of the mechanism.

In each of the reports by Petrich and coworkers, the authors have repeatedly stated that 7AW and 7AI in aqueous solution has a single-exponential fluorescence decay (e.g. Négrerie et al., 1990; Négrerie et al., 1991; Gai et al., 1992; Chen et al , 1993). Yet this is only observed in experiments in which filters are used to collect the fluorescence emission over a wide bandwidth. If discrete emission wavelengths are examined it is clear that 7AI and 7AW fluorescence exhibits multi-exponential

fluorescence decay (Chapman and Maroncelli, 1992; Hogue and Szabo, 1993). This also was demonstrated by Petrich and coworkers (Gai et al., 1992; Chen et al., 1993). The short decay component has a negative-preexponential term at long emission wavelengths, the signature of an excited-state reaction process. Single-exponential 7AW fluorescence is observed only in unresolved bandwidth conditions, as admitted by Petrich (Chen et al., 1993), and it is not likely to reflect the true nature of 7AW photophysics. Obviously this data cannot be compared to the accepted practice of collecting emission-wavelength resolved data and employing appropriate statistical analysis techniques.

The results of a study of 7AW in the tripeptide Lys-7AW-Lys (Brennan et al., 1994) indicate that 7AW is far more sensitive to changes of pH over the range of 3-4 than is Trp. This was also demonstrated in pH studies of 7AI (Négrerie et al., 1991) and methyl derivatives (Chen et al., 1993). This is expected based on the additional possibilities of protonating the N7 of the 7AI ring, which is not possible with indole.

A necessary conclusion is that there is no inherent advantage in any perceived simplicity of 7AW fluorescence decay behavior over that of Trp for biological systems, since it is clearly more complex. In contrast, 7AW should prove to be useful as a biological probe, not for any singular or simpler photophysical behavior, but rather for a myriad of responses to environment; a rich photophysical behavior which should fingerprint each environment in a protein uniquely. The extreme sensitivity of 7AW to water renders it a highly appealing probe for monitoring large conformational changes in proteins.

2.4.3 4-Fluorotryptophan

In contrast to the 5HW and 7AW analogs, 4FW is important not for its fluorescence behavior, but rather for its lack thereof. Fluorotryptophans have found previous uses in substrate studies of TrpRS (Knorre et al., 1971; Nevinsky et al., 1974;Xu et al., 1989); in studies of analog substituted enzymes (Pratt and Ho, 1975); and in studies of protein structure and function using ^{19}F NMR (Kimber et al., 1978; Li et al., 1989).

Bronskill and Wong (1988) demonstrated that 4-fluorotryptophan is nonfluorescent at room temperature, and that 4FW incorporation could be used as a general technique to avoid Trp fluorescence, allowing investigation of other chromophores in protein-protein interactions. They reported a tryptophan auxotroph of *B. subtilis* capable of growth on 4FW, (de-adapted away from Trp) and suggested this organism as a vehicle for preparation of functional proteins lacking Trp fluorescence. However, at the time of writing the nonfluorescent property of 4FW has not been applied to any studies of protein structure and function using fluorescence methods.

This may be due to the critical observations of Hott and Borkman, (1989), who showed that 4FW decomposes on exposure to UV light, and downplayed its potential uses for biological investigations. Their main conclusion was that the 4-fluoro-substituent rendered 4FW more photoreactive than Trp at room temperature. In their criticism, however, Hott and Borkman overlooked the blue-shifted nature of 4FW *absorbance*, compared to Trp. Trp fluorescence excitation at 300 nm will conveniently avoid the blue-shifted absorbance of 4FW, thereby minimizing the potential for 4FW photolysis. Most Trp fluorescence studies are already carried out using 295 nm and even greater excitation wavelengths, due to the absorbance of Tyr. The absorbance and subsequent photolysis of 4FW in a Trp fluorescence study is minimized, if the proper care is taken to avoid irradiation by wavelengths < 295 nm.

The low-fluorescence of other 4-substituted indole derivatives; 4-hydroxydimethyltryptamine (psilocin; a minor hallucinogenic component of some mushrooms) and 4-benzyloxyindole, have been previously reported (Bridges and Williams, 1968). It was shown that the quantum yield of these were 0.002 (314 nm emission) and 0.0001 (310 nm emission), respectively. Absorbance studies on indole derivatives in oriented films showed that the ^1L_a and ^1L_b dipoles of 4-methoxyindole are nearly parallel, and the vectors were close to the 4 and 1 carbons of indole as shown earlier in Figure 2.4 (Albinsson and Nordén, 1992). The position of the substituted C4 seems more relevant to observed low fluorescence yields, rather than the nature of the substituent.

Hott and Borkman (1989) also examined the low-temperature fluorescence and phosphorescence of 4-fluorotryptophan. They demonstrated a very structured blue-shifted fluorescence emission λ_{max} at 297 nm, (Trp λ_{max} = 313 nm under the same conditions) and blue shifted phosphorescence compared with Trp. The total emission yield from 4FW was of the same magnitude at 77 K as that of Trp, but the fluorescence yield was lower and the phosphorescence yield was higher, compared to Trp. Under these conditions, it seems that the 4-fluoro substituent increases the probability of intersystem crossing. The phosphorescence of 4-fluorotryptophan might be of some utility in protein studies, providing photolysis does not render the sample unusable.

The increase in photochemical pathways of 4FW can contribute to the nonfluorescent depopulation of the excited state (Hott and Borkman, 1989). However other possibilities should also be considered, as the complete 4FW photodegradation after a 20 minute irradiation time was not observed in their study. Increases in intersystem crossing can act to decrease the fluorescence. This can arise from coupling between electronic and fluorine nuclear spins causing electrons to become unpaired (Atkins 1986). Lami (1976) noted that the indole ^1L_a transition has a Rydberg-like character which can result in the photoejection of electrons. The very blue-shifted λ_{max}

of 4FW (264 nm in water) together with its photolability are consistent with the interpretation of Lami, although he did not consider any 4-substituted indoles in his work.

The crystal structure of 4FW (Xu et al., 1989) shows large alterations in bond distances compared to Trp (Fasman, 1988), with a 0.1 Å increase in the C5-C6 indole bond, a 0.05 Å increase in the N1-C9 bond, and decreases of between 0.02 - 0.06 Å in the N1-C2, C4-C5 and C6-C7 indole bonds. These are consistent with an alternate resonance structure as opposed to that depicted in Figure 2.4. The C-F bond of 4FW is calculated to be more highly polarized, compared with partial charges calculated for C-F bonds of 5FW, 6FW or 7FW (Xu et al., 1989). These workers also report ^{13}C NMR results which support their interpretation. Therefore the 4-position, and not the substituent, is related to the further polarization and thus redistribution of ground-state electrons consistent with new ground-state nuclear coordinates. Changes in bond length (Tonge and Carey, 1990) can also contribute to the higher observed photochemical reactivity of 4FW. In addition, the bond angles of the 4FW ring structure (Xu et al., 1989) show it is more planar than Trp, which could account for its more structured fluorescence spectrum at 77 K compared to Trp (Berlman, 1970).

The utility of 4FW to remove Trp fluorescence from proteins is wholly dependent on whether it can be *fully* incorporated in place of Trp so no fluorescence remains. Procedures involving the analogs, 5HW and 7AW are more forgiving, since one can avoid Trp fluorescence by the appropriate selection of excitation wavelength further into the red region of the spectrum. A small amount of Trp "leakage" into a population of protein which is supposed to have its fluorescence fully removed by 4FW will exhibit Trp fluorescence and diminish the usefulness of the technique. The incorporation of 5HW into oncomodulin Y57W was plagued by such "leakage" of the protein expression system, so that about 50% of the oncomodulin had Trp instead of 5HW (Hogue et al., 1992). These were separable using chromatographic techniques,

attributed to the solvent exposure of the 5HW and Trp residues and their different interactions with chromatographic matrices. But this separation may not always be possible, so it is important to maximize the incorporation of the analog at the outset. This problem is discussed in detail in Chapter 5.

Chapter 3

B. SUBTILIS TRYPTOPHANYL-tRNA SYNTHETASE

B. SUBTILIS TRYPTOPHANYL-tRNA SYNTHETASE

3.1 Introduction

As detailed in Chapter 1, TrpRS is responsible for recognizing Trp and catalyzing its reaction with ATP, and the subsequent acylation of $tRNA^{Trp}$. TrpRS catalyzes the aminoacylation of $tRNA^{Trp}$ in two steps. The first step is the formation of an activated tryptophanyl-5'-adenylate, driven to completion by inorganic pyrophosphate hydrolysis by pyrophosphatase:

$$\text{TrpRS} + \text{Trp} + \text{ATP} \rightleftarrows \text{TrpRS}\cdot\text{Trp-AMP} + PP_i \qquad \text{(III)}$$

The second step is the transfer of the Trp from tryptophanyl-5'-adenylate onto its cognate $tRNA^{Trp}$:

$$\text{TrpRS}\cdot\text{Trp-AMP} + tRNA^{Trp} \rightleftarrows \text{TrpRS} + \text{Trp-}tRNA^{Trp} + \text{AMP} \qquad \text{(IV)}$$

Each monomer of the symmetrical α-2 dimeric TrpRS enzyme from *B. subtilis* is a single Trp protein (Chow and Wong, 1988). TrpRS subunits from other prokaryotes have multiple Trp residues; two in *E. coli* TrpRS, and three in *B. stearothermophilus* TrpRS. The Trp-92 residue of *B. subtilis* TrpRS is the only conserved Trp residue of TrpRS (*B. stearothermophilus* Trp-91; *E. coli* Trp-93; yeast mitochondrial TrpRS Trp-129). The *B. subtilis* enzyme single Trp can be used as an unambiguous intrinsic fluorescence probe of substrate interactions and of conformational heterogeneity in its microenvironment. The location of this Trp is indicated in the center of the structure of *B. stearothermophilus* TrpRS in Figure 3.1.

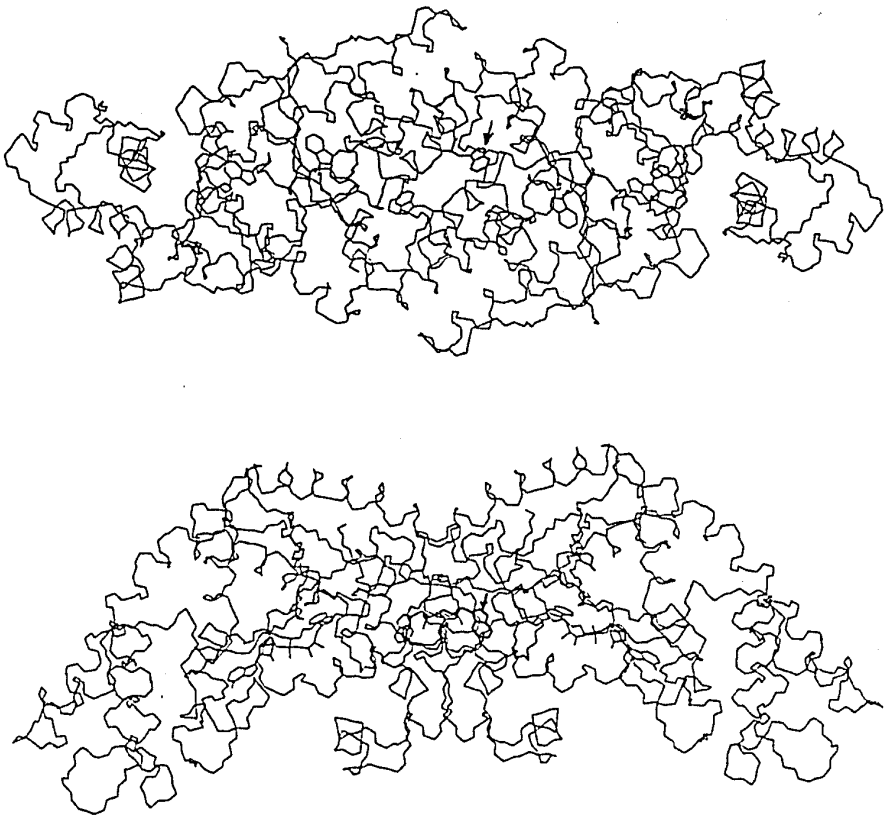

Figure 3.1: Structure showing conserved Trp of TrpRS The homologous *B. stearothermophilus* crystal structure shows Trp-91 (arrow) of the left subunit. It is located at the subunit interface, symmetrically interdigitated into the opposite subunit. It appears to be completely buried, as seen in these two orthogonal views (Doublié and Carter Jr., 1993).

In order to unambiguously observe the fluorescence of the Trp-92 residue, fluorescence contributions from any substrate Trp must be eliminated. The nonfluorescent Trp analog 4FW, has been demonstrated as a prokaryotic and eukaryotic TrpRS substrate by its *in-vivo* incorporation into proteins (Bronskill and Wong, 1988) as well as by *in-vitro* studies (Xu et al., 1989, Nevinsky et al., 1974). Hence the intrinsic fluorescence of Trp-92 together with 4FW as a substrate allows the study of the structure, function and dynamics of this enzyme system.

A by-product of the desired *in vitro* reaction involving a second molecule of ATP has been described in section 1.2.5, in which the 2' ribose hydroxyl of ATP is acylated in a manner analogous to the aminoacylation of the 3'-terminal adenosine of tRNA. This slow reaction:

$$\text{TrpRS·Trp-AMP} + \text{ATP} \rightarrow \text{TrpRS·Trp-ATP} + \text{AMP} \qquad \text{(V)}$$

requires a large excess of ATP. It was necessary to demonstrate that the TrpRS·Trp-AMP complex could be formed without contamination from this byproduct complex. Experiments with *E. coli* TrpRS, (Merle et al. 1986) using radiolabelled reagents demonstrated that a short incubation of TrpRS with ATP, Trp and pyrophosphatase would quickly fill the TrpRS active site with Trp-AMP. Sephadex G-25 chromatography could then be used to rapidly remove unreacted substrates, and stoichiometric amounts of TrpRS·Trp-AMP complex would elute. Similar conditions were used here for the preparation of adenylate complexes of *B. subtilis* TrpRS.

Site-directed mutagenesis of TrpRS was performed prior to this work (Chow et al., 1992) in order to substitute another amino acid for Trp-92 to prepare TrpRS free of intrinsic Trp-92 fluorescence. Their attempts at replacing Trp-92 with Phe, Ala and Gln proved unsuccessful at producing active enzyme. These workers concluded that Trp-92 was an essential residue, and they suggested the local structure of Trp-92 was

part of a $tRNA^{Trp}$ binding site. However the role of this "essential" Trp-92 is not understood as it relates to the mechanism of TrpRS. An unsuccessful attempt was made here to prepare the W92F TrpRS mutant for fluorescence studies. However the results were enlightening with respect to the role of Trp-92 in stabilizing the TrpRS structure and the nature of the enzyme.

This chapter examines TrpRS using the intrinsic fluorescence of Trp-92, with a combination of substrates including 4FW, ATP, PP_i and $tRNA^{Trp}$ to gain insight into the mechanism of TrpRS and $tRNA^{Trp}$ aminoacylation. Substrate titrations, quenching studies and thiol labelling experiments are also presented which help explain the nature of the fluorescence changes observed and their implications for the TrpRS mechanism. In addition, the fluorescence parameters of Trp-92 are critically examined to determine if correlations exist with TrpRS structure.

3.2 Methods and Materials

3.2.1 Materials

The following chemicals were obtained from Sigma Chemical Co., St. Louis, Missouri: ampicillin sodium salt, streptomycin sulfate, isopropyl-ß-D-thiogalactopyranoside (IPTG), chicken egg white lysozyme, Tris-HCl, disodium-EDTA, Hepes-HCl, dithiothreitol (DTT), casein (casamino acids), phenylmethylsulfonylfluoride (PMSF), scintillation fluid, DNase I, disodium-PIPES, *E. coli* strain W type XX tRNA, inorganic pyrophosphatase (PP_iase), disodium pyrophosphate (PP_i), Na_2ATP, DL-4FW, D-tryptophan, L-tryptophan, and urea; all were used without further purification. Sephadex G-25 fine, Sephadex G-50 superfine, DEAE Sephacel, Sephacryl S-200 HR, 10-15% acrylamide gradient precast PhastGels and SDS buffer strips were obtained from Pharmacia Canada Ltd., Dorval Quebec.

Th hydroxyapatite used, BioGel HTP, and sodium dodecylsulfate (SDS) were obtained fr BioRad Laboratories, Richmond California. N-acetyl-L-tryptophanamide (N TA) was obtained from Aldrich Chemical Co., Milwaukee, Wisconsin, and was pr iously recrystallized 3x from water. Dialysis was performed using Spectra-Por, 6, 0 or 12,000 molecular weight cutoff tubing, from Spectrum Medical Industries, L Angeles California. Water, with 18 MΩ resistance was used throughout, purified us a Milli-Q Water System, Millipore Canada Ltd., Mississauga Ontario. Reagents fo nicrobiological media, bacto tryptone, bacto-yeast extract, and agar were obtained fr DIFCO Corp., Detroit, Michigan. HCl, H_2SO_4, KCl, $CuCl_2$, glacial acetic ac MgAcetate, $MgCl_2$, NaCl, KI, acrylamide, K_2HPO_4, KH_2PO_4, trichloroacetic ac (TCA), glycerol, and spectral grade methanol were obtained from BDH Inc., To nto Ontario. L-[G-^{3}H]Trp was obtained from Amersham Canada Ltd., Oakville, O rio. Whatman 3MM or GF/A filter disks were obtained from Canadawide Sc ntific Co., Toronto Ontario. [γ-^{32}P]ATP and [α-^{32}P]ATP were obtained from A rican Radiolabelled Chemicals Inc, St. Louis Missouri. Sequanal grade Guanidine H was obtained from Pierce, Rockford Illinois.

B. subtilis TrpRS was purified to homogeneity from an *E. coli* expression sy m JM109 pKS /1 (Shi et al., 1989), and the mutant W92F from the strain JM109 pl W-F92 (Chow et al., 1992), both provided by Dr. J.T. Wong, University of T nto. Purified *B. subtilis* $tRNA^{Trp}$, expressed in *E. coli* was kindly provided by H g Xue from the laboratory of Dr. J.T. Wong, University of Toronto (Xue et al., 19 3a,b).

2.2 TrpRS Purification

JM109 pKS /1 cells (Shi et al., 1989) were cultured in 2 l of Terrific Broth (S nbrook et al., 1989) in 4 l erlenmeyer flasks, modified with aeration vanes, in a

constant temperature 37° C shaker. The Terrific Broth media was supplemented with twice the usual amount of glycerol as an enriched carbohydrate source, and with 0.5 g/l ampicillin to maintain the plasmid. Upon reaching an absorbance of 1.0 at 550 nm, the culture was induced with IPTG to a 1 mM final concentration. Cells were collected with centrifugation at 10,000 x g. 19 g of wet cell paste was obtained from 6 l of culture media.

Previous purifications schemes (Shi et al., 1989) employed acetone powder extracts of the bacteria, however an approach avoiding volatile solvents was used here, adapted from previous purifications of recombinant calcium-binding proteins (MacManus et al., 1989). Frozen cells (-80° C) were resuspended in a 40 ml (twice the volume (ml) of cell wet weight (g) of a warm solution (60° C) of 2.4 M sucrose with 40 mM Tris-HCl, 10 mM EDTA pH 8.0, and incubated for 30 min. Then, 160 ml (eight times the volume (ml) of cell wet weight (g) of a 0.1 mg/ml lysozyme solution in 50 mM Hepes-HCl, 100 mM KCl, 1 mM EDTA, 1 mM DTT, 0.5 mM PMSF, pH 8.0 was added. The cells were enzymatically lysed at room temperature for 1 h. 10 ml of a 1 M solution of streptomycin sulfate was injected with a syringe into the stirring lysate to aid precipitation. Lysed bacterial debris was then separated by centrifugation at 40,000 x g for 30 min in a Beckman LS65 ultracentrifuge with a Ti-60 rotor. The clarified extract was then digested with 180 Kunitz units/ml of DNAse I with $MgCl_2$ added to a final concentration of 3 mM.

A batch adsorption onto 25 g dry hydroxyapatite was performed after adjusting the extract to a total of 1 l volume containing 0.1 M K_2HPO_4, 10 mM EDTA, 1 mM DTT, and 1 mM PMSF, pH 6.8. After 10 minutes of gentle stirring, the hydroxyapatite was filtered out from the solution using a coarse sintered glass filter, and was washed with 200 ml of a solution of 0.1 M K_2HPO_4 pH 6.8. The remaining filtrate solutions were back extracted with a further 10 g of hydroxyapatite. TrpRS was eluted from the hydroxyapatite after soaking for 5 minutes with 300 ml of a 0.5 M

solution of K_2HPO_4 pH 6.8, then recovery of the solution by filtration. These were combined and dialyzed against 4 l of Milli-Q water, then into 2 changes of 4 l of a buffer containing 20 mM K_2HPO_4 50 mM KCl pH 6.8 (Buffer A). The dialysate was applied to a 2.5 × 10 cm column of DEAE Sephacel equilibrated with Buffer A. After a 500 ml wash with Buffer A, TrpRS was eluted with a linear gradient former filled with 250 ml each of Buffer A and a solution of 20 mM K_2HPO_4, 0.55 M KCl, pH 6.8. Fractions containing the major peak were pooled and concentrated to a volume of 3 ml using an Amicon stirred cell and a YM10 membrane. This was applied to a 1.1 m × 2.5 cm column of Sephacryl S-200 HR equilibrated with a buffer of 10 mM PIPES, 10 mM $MgCl_2$, 10 mM NaCl, 100 mM KCl at pH 7.0. A single peak eluted which was collected and dialyzed (12,000 molecular weight cutoff) against 4 changes of 4 l of Milli-Q water, in which the purified TrpRS formed a microcrystalline precipitate. This was allowed to settle, then lyophilized for storage.

Activity was assayed semiquantitatively by trapping radiolabelled Trp-tRNA^{Trp} on Whatman 3MM or GF/A filter disks (Bollum, F.J., 1966; Xu et al., 1989). Reactions were carried out at ambient temperature for 15 minutes in a buffer of 200 mM Tris-HCl, 20 mM MgAcetate pH 8.6. Controls included singular omissions of each reactant, previously characterized *B. subtilis* TrpRS obtained from the University of Toronto, and total radiolabelled reagent counts. 100 μl reaction mixtures were prepared from solutions of reactants made in Reaction Buffer: 40 μl of 16 mM ATP, 15 μl of a 5 mg/ml solution of *E. coli* strain W tRNA, 5 μl of a mixture of 5:1 L-Trp:L-[G-^{3}H]Trp, diluted to >10000 cpm in 5 μl, 2-5 μl of TrpRS (typically 10-15 μl), and the balance made up with Reaction Buffer. 50 μl duplicate aliquots were precipitated onto filter paper disks with a cold, 5% solution of trichloroacetic acid, 0.5% casein. The disks were washed with this solution three times, then twice with 95% ethanol. Disks were dried under a heat lamp and counted in a Beckman liquid scintillation system.

Nebulation-assisted electrospray ionization (ESI) mass spectrometry (API III quadrupole. Sciex, Mississauga Ontario, Canada), performed by Dr. M. Yaguchi of NRCC, confirmed protein composition and purity from a 0.5 mg/ml solution of TrpRS in 10% acetic acid. The monomeric extinction coefficient of purified TrpRS was experimentally determined by measuring the absorbance of a solution of TrpRS at 280 nm, which was then subjected to quantitative amino acid analysis, performed by Pat Lanthier of NRCC. The ϵ_{280} value determined was 24154 M^{-1} cm^{-1} per monomer. This was within 2.3% of the value expected from the Trp (1) and Tyr (14) content of the protein (Gill and von Hippel, 1989) and was used to determine TrpRS concentration.

3.2.3 Aminoacyl-Adenylate Complex Preparation

Preparations of TrpRS·Trp-AMP were made using the technique described by Merle and coworkers (1986). The stoichiometry of the adenylate and the extent of the acyl-transfer reaction (III) were examined using [γ-^{32}P]ATP and [α-^{32}P]ATP The reaction mixtures contained 26 μM TrpRS, 200 μM L-Trp and 400 μM labelled ATP. Samples of TrpRS complexed with aminoacyl-adenylates were prepared with a 500 μl reaction mixture containing 400 μM DL-4-fluorotryptophan or 200 μM L-tryptophan, 400 μM unlabeled ATP, 100 μM TrpRS in Reaction Buffer together with a dialysis button (6000 molecular weight cutoff) containing 5 units of inorganic pyrophosphatase. After 5 minutes of reaction at 23° C, 250 μl of reaction mixture was passed through a 15 × 1 cm column of Sephadex G-25 fine equilibrated with freshly prepared 10 mM K_2HPO_4, 100 mM KCl buffer, which was also the buffer used for all spectroscopic studies reported here.

3.2.4 Thiol Reactivity

TrpRS·Trp-AMP was prepared as described above, but with the addition of a 5 µl aliquot of ß-mercaptoethanol to reduce the enzyme fully prior to Sephadex G-25 chromatography. Unreacted TrpRS was prepared in a similar fashion, but omitting ATP and Trp. 100 µl of a 100 µM solution of TrpRS or TrpRS·Trp-AMP was added to 900 µl of a solution of 10 mM DTNB prepared in 10 mM K_2HPO_4, 100 mM KCl buffer. TrpRS was similarly diluted into 10 mM DTNB solution in the same buffer with 0.1% SDS in order to ensure that thiols were fully accessible to the DTNB reagent. The absorbance was followed at 412 nm subsequent to mixing, with the reaction maintained at 22° C. The extent of labelling was calculated (Imoto and Yagata, 1989) using the extinction coefficient of the product p-nitrophenylthiolate anion of 13,600 M^{-1} cm^{-1} at 412 nm and the initial concentration of TrpRS determined from its absorbance.

3.2.5 Spectroscopic Measurements

Solutions of TrpRS for fluorimetry were prepared from lyophilized enzyme dissolved at high concentrations (1-5 mg/ml) in Reaction Buffer (200 mM Tris-HCl, 20 mM MgAcetate, pH 8.6). This was then subjected to a 15 cm column of Sephadex G-25 fine equilibrated with freshly prepared 10 mM K_2HPO_4, 100 mM KCl, pH 7.5 (Spectroscopic Buffer). This step was necessary because without it, the redissolved TrpRS exhibited high levels of light scattering at $\lambda < 260$ nm. This light scattering could arise from molecular aggregates of TrpRS which are too small to see. The scattering was greatly reduced by the chromatographic step. This technique is supported by the recent demonstration that gel filtration is a facile means of refolding proteins (Werner et al., 1994). For fluorimetric measurements, solutions were assured to have a final absorbance less than 0.1 at the excitation wavelength of 290 nm, to

avoid any inner-filter effect. TrpRS concentration values throughout this work refer to the monomer concentration, unless otherwise indicated by $TrpRS_2$, referring to dimer concentration.

Recrystallized NATA was used as a quantum-yield standard. Absorbance spectra were collected using a Varian DMS 200 spectrophotometer with a 1 nm bandpass. For quantum-yield determinations, 5 cm pathlength cuvettes were used to obtain accurate absorbance measurements at 300 nm for TrpRS and TrpRS·4FW-AMP, and then the solution was transferred to a 1 cm square fluorescence cuvette. Other quantum-yields are relative to uncomplexed TrpRS. Fluorescence spectra and titration data were collected using an SLM 8000C instrument with 4 nm emission and excitation bandpasses, with Glan-Taylor polarizers oriented to eliminate anisotropic effects. Spectra of solutions without $tRNA^{Trp}$ were corrected for the buffer-only blank contribution, and for the wavelength dependence of the instrument response. Blanks for the $tRNA^{Trp}$-containing solutions had an equal concentration of $tRNA^{Trp}$ present to subtract the small fraction of its luminescence. These blanks were constructed by adding aliquots of $tRNA^{Trp}$ to the reference cell mounted together with the sample cell in a spectrophotometer, until the absorbance reading at 260 nm was zero. All measurements were performed at 20° C. Anisotropy measurements were performed with Glan-Taylor polarizers and in T-format detection, as the average of three measurements, each acquired over 15 seconds.

Time-correlated single photon counting (TCSPC) using laser/microchannel plate instrumentation was used for measuring fluorescence decay data and has been described earlier in Chapter 2. Decay curves contained 1-2 × 10^6 counts collected over a 3 minute data collection time. Experiments with $tRNA^{Trp}$ required 10 minutes to accumulate the desired number of counts owing to the low fluorescence yield from competing $tRNA^{Trp}$ absorbance. The instrument response was determined from the Raman scattering of water (at 332 nm for 300 nm excitation) (Willis et al., 1990).

3.2.6 Iodide and Acrylamide Quenching

For quenching studies, solutions of various concentrations of KI were prepared by mixing freshly prepared stock solutions of 500 mM KCl with solutions of 400 mM KI, 100 mM KCl buffered with 10 mM K_2HPO_4 pH 7.5. This was done to keep the overall ionic strength of the solutions constant. Similarly, acrylamide solutions were prepared from a stock of 400 mM acrylamide, 100 mM KCl, 10 mM K_2HPO_4 pH 7.5 diluted with the spectroscopic buffer. 6 M GdHCl solutions were prepared by dissolving solid GdHCl into the iodide or acrylamide solutions, taking into account the dilution of the quencher caused by the added denaturant. Stock solutions of 20-25 μM TrpRS or TrpRS·4FW-AMP, prepared as previously described, were diluted 1/10 into the iodide or acrylamide solution, and the fluorescence was measured at 300 nm excitation and 310-330 nm emission. The signal was integrated over this wavelength range to provide the intensity at each quencher concentration which was then adjusted for dilution by the sample added.

3.2.7 Substrate Titrations

Titration data were obtained by the stepwise addition of 2 or 4 μl aliquots of substrates with continuous stirring while monitoring the fluorescence emission at 320 and 340 nm with 300 nm excitation using a macrotitration programme (Hogue et al., 1992), correcting for the blank and incremental dilution. Two minutes separated each addition to allow for equilibration. To examine substrate specificity, 1.5 ml of a solution of 5.0 μM TrpRS with 21.1 μM ATP·Mg^{2+} was titrated with aliquots of 0.200 mM L-Trp or D-Trp. Inorganic pyrophosphatase enzyme was not included in these titrations. To titrate the reversal of reaction I, 1.5 ml of a solution of 22.6 μM TrpRS·4FW-AMP, prepared as described earlier, was titrated with aliquots of freshly

prepared 1.00 mM PP_i. To titrate reaction I and the formation of 4FW-AMP, 1.5 ml of a solution of 37.5 μM TrpRS, 0.400 mM DL-4FW, and 10 units of PP_iase (with negligible fluorescence) was titrated with aliquots of 1.95 mM ATP·Mg^{2+}. This titration was followed with an addition of an excess PP_i to a final concentration of 0.6 mM, immediately after which the fluorescence was monitored with time. This was to determine the efficacy of the PP_iase and PP_i exchange in the titration mixture.

3.3 Results

3.3.1 Protein Purification and Identity

The purification reported here draws on previous purification information (Joseph and Muench, 1971a; Chow et al., 1992; Chow and Wong, 1988; Xu et al., 1989). Previous purifications schemes for *B. subtilis* TrpRS (Shi et al., 1989; Chow et al., 1992) used an acetone powder extract as the first cellular fractionation method. This was then processed with ion-exchange chromatography (DEAE Sephacel) eluted in a stepwise fashion with increasing concentrations of phosphate, followed by hydroxyapatite chromatography, again eluted in a stepwise fashion with increasing concentrations of phosphate. The preliminary attempts at employing this purification methodology with the clarified extract described here were unsatisfactory and unnecessarily complex. The purification was altered to employ gradients, rather than the stepwise elution, as these gave superior results in the form of sharper protein peaks and required less column manipulation.

While attempting to purify the mutant TrpRS, W92F, with the scheme of Wong's group, it was observed that a significant amount of proteins with molecular weights of 11 kDa and 25 kDa appeared in SDS-PAGE gels corresponding to the

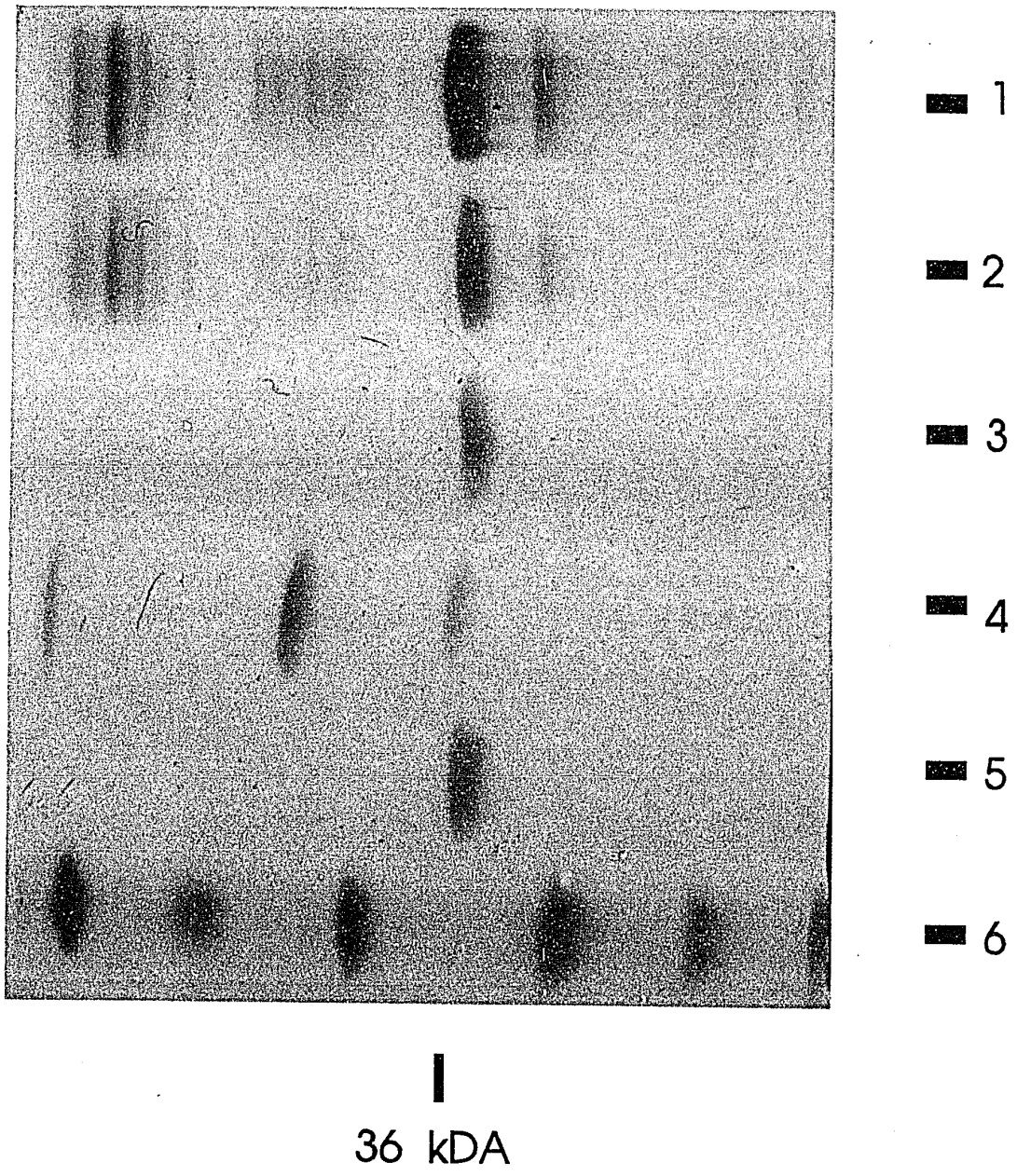

Figure 3.2: SDS PAGE of TrpRS and W92F Fragments. Pharmacia PhastGel 10-15% gradient. 1. W92F lysate. 2. wild-type TrpRS lysate. 3. W92F from Dr. J.T. Wong, U. of Toronto. 4. W92F fragments coeluted from DEAE column. 5. Authentic *B. subtilis* TrpRS. 6. Low Molecular weight markers.

TrpRS peak only after the DEAE chromatography step (Figure 3.2). These fragments appeared regardless of stepwise or gradient elution. These fragments also co-eluted with TrpRS under hydroxyapatite chromatography. Gel filtration using Sephadex G50 or Sephacryl S-200 HR demonstrated these fragments were associated with the single 72 kDa W92F TrpRS dimer peak. It appears that a proteolytic event during the DEAE chromatography step had nicked TrpRS, producing fragments that self-associated into a 72 kDa oligomer. The 72 kDa W92F TrpRS gel filtration peak could be resolved into 72, 36, 25 and 11 kDa peaks by first dissolving the sample in 8 M urea, then applying it to the Sephacryl S-200 HR column described previously, with the exception that the buffer contained 0.1% SDS (Figure 3.3). This provided a nonreducing, separation of the constituent fragments by molecular weight. The observation of 72 kDa and higher molecular weight sizes in the void volume (Figure 3.2) could represent disulfide-linked forms, as the two free thiol groups per subunit could, when denatured, form disulfide bonds with other monomers. Disulfide-linked dimers of TrpRS were also demonstrated by 72 kDa bands which appear on nonreducing SDS-PAGE gels after SDS denaturation of the enzyme or after addition of $CuCl_2$ (data not shown).

No fragmentation occurred in the wild-type TrpRS under the same purification conditions. W92F protein supplied by Dr. J.T. Wong's laboratory (University of Toronto) was also not fragmented. Further analyses with these W92F fragments were not attempted.

The TrpRS purification as described elsewhere, (Shi et al., 1989; Chow et al., 1992) was altered to take advantage of the very strong adsorbance of prokaryotic TrpRS onto hydroxyapatite (Fromant et al., 1981) in order to quickly remove TrpRS from other *E. coli* proteins and proteases. After the batchwise hydroxyapatite extraction and dialysis described in section 3.2.2, only the 36 kDa band of TrpRS could be visualized on silver-stained SDS-PAGE Pharmacia PhastGels (not shown). However UV spectra of the sample indicated nucleic acid absorbance at 260 nm. This

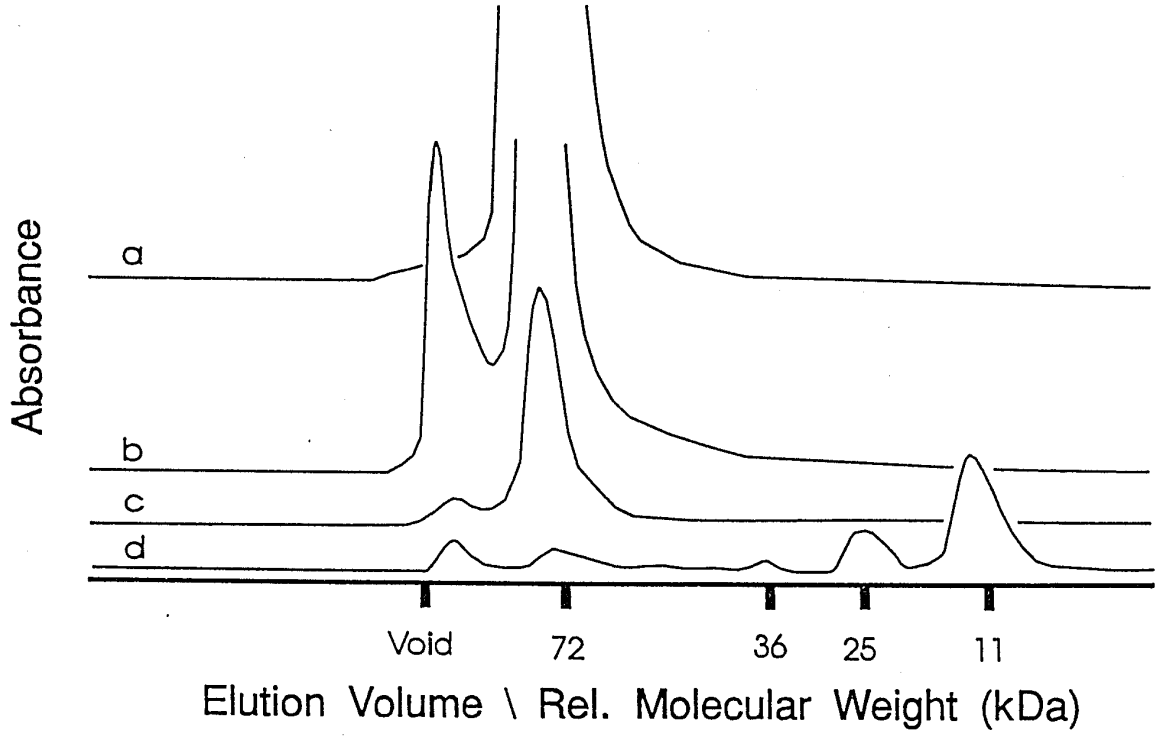

Figure 3.3: S-200 HR Gel Filtration of TrpRS, W92F fragments. a. Preparative gel filtration of TrpRS wild-type. b. Preparative gel filtration of W92F TrpRS, showing the void volume peak resulting from enzyme aggregation. This sample was purified following the protocol developed herein, and had no detectable fragmentation. c. Gel filtration of a fragmented W92F preparation, demonstrating association of the fragments to a size corresponding to the 72 kDa dimer. d. The same sample as in c, but urea denatured prior to application. The column was equilibrated and eluted as the others but with the addition of 0.1% SDS. This demonstrates resolution into smaller components as observed with SDS-PAGE in Figure 3.2. The presence of 72 kDa and/or higher aggregated species may be due to disulfide cross-linked forms.

UV signal was completely removed by DEAE Sephacel ion-exchange chromatography, eluted with a KCl gradient. The final gel filtration chromatography on Sephacryl S-200 HR produced a single peak corresponding to the 72 kDa dimer of TrpRS as previously reported (Shi et al., 1989), depicted in Figure 3.3. The final recovery of TrpRS was 122 mg from 6 l of culture, 2.8 fold more than that recovered by previous purifications (Ala et al., 1993). (Modifications to the expression system and growth conditions described later in Chapter 5 have further improved the yield of TrpRS.) Semi-quantitiative $tRNA^{Trp}$ aminoacylation activity assays using ^{3}H Trp demonstrated activity comparable to TrpRS from previous purifications, hence the additional steps (gel filtration, dialysis) were not in any way detrimental to the enzyme.

The gel filtration and dialysis steps were added to the purification scheme to ensure spectroscopic purity of the sample and to remove any small organic molecules or ions as well as any large aggregates. The formation of a TrpRS precipitate upon dialysis caused some initial concern. This TrpRS precipitate was examined under a microscope with a polarizing filter, and it was microcrystalline in nature. This precipitate could be concentrated by settling, prior to the lyophilization. The lyophilized TrpRS precipitate was found to dissolve readily into buffers.

Since a small amount of endogenous TrpRS from the JM109 *E. coli* parent strain is present, it is important here to maximize expression of the plasmid-encoded *B. subtilis* TrpRS (Carter Jr., 1988). Based on the purification of *E. coli* TrpRS from source (Kuehl et al, 1976; 280 mg from 18 kg cells) the amount of endogenous TrpRS from the host JM109 is estimated to be 0.3 mg or 0.2% of the total TrpRS recovered. ESI mass spectrometry characterization resulted in a measured molecular weight (M_w) of 37198.73 ($\pm$ 3.19) with contributions from 25 well-defined mass peaks. The expected M_w was 37197.99 for *B. subtilis* TrpRS and 37511.14 for *E. coli* TrpRS. These results indirectly indicate the composition and sequence were correct. They also indicate that no thiol oxidation had occurred in the course of purification. Mrs. R. To

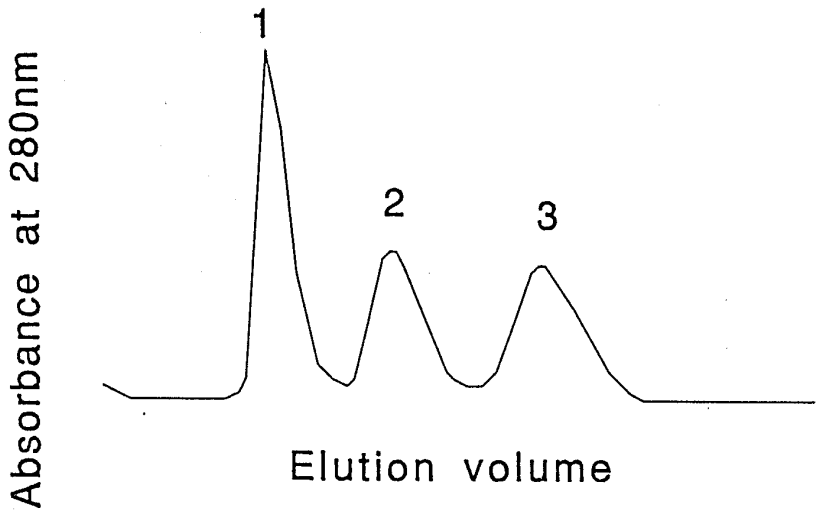

Figure 3.4: Sephadex G-25 Gel Filtration of Trp-AMP reaction with TrpRS Peak 1 contained the TrpRS complex, identified as tryptophanyl-5'-adenylate. Peak 2 contained ATP, and peak 3 contained Trp, as identified by their characteristic UV spectra.

of NRC was able to use this purified TrpRS to prepare single crystals of the uncomplexed enzyme. The crystals best formed with a hanging drop methodology under the following conditions: hanging drop consisting of 3.5 μl of 10 mg/ml solution of TrpRS eluted from S-200 HR in the column buffer, with 5 μl of reservoir buffer; reservoir buffer containing, 17% polyethyleneglycol-4000, 0.1 M ammonium sulfate, 0.1 M glycine buffer pH 8.75, 2% MPD at room temperature. A seed crystal could be added to the drop 24 hours later. Crystals grew to maximal size of 0.1 by 0.2 by 0.5 mm in a few days, but had poor X-ray diffraction (R. To, C. Chen, unpublished results). These also had a tendency to partially dissolve after a week or so, and were therefore not studied further. *B. subtilis* TrpRS crystals are currently being studied in the laboratory of Dr. D. Yang, McMaster University, (Ala et al., 1993). These workers, as well as Carter Jr. et al., (1990) have experienced similar difficulties with obtaining diffraction from uncomplexed or partially complexed TrpRS crystals.

The formation of the TrpRS·Trp-AMP complex was carried out, using gel-filtration to separate the large molecular weight complex from the smaller reactants. A chromatograph of this process is depicted in Figure 3.4. [γ-^{32}P]ATP and [α-^{32}P]ATP were used to characterize the adenylate complex. If the acylation by-product of reaction (V) was present in the complex, radioactivity from [γ-^{32}P]ATP would appear in the high molecular weight fraction. However no radioactivity (counts = background) eluted with the TrpRS peak when [γ-^{32}P]ATP was used. With [α-^{32}P]ATP, a 0.5 ml fraction of the first peak contained 2.1 ($\pm$ 0.3 μM) [α-^{32}P]ATP and 2.3 μM TrpRS. The absence of radioactivity from the [γ-^{32}P] of ATP indicated that no ATP was associated with the enzyme, and therefore no enzyme bound Trp-ATP acyl transfer by-product was formed under the conditions used herein to produce TrpRS·Trp-AMP and other analog-adenylate complexes.

3.3.2 Absorption Spectra and Thiol Reactivity.

The absorption spectra of TrpRS and the eluted TrpRS·4FW-AMP complex are shown in Figure 3.5 A, normalized to the same protein concentration. The spectrum of TrpRS was dominated by 14 Tyr residues, and had a λ_{max} at 277 nm. The spectrum is enhanced by the presence of the 4FW-AMP complex at the blue edge. The broad maxima in the complex arises from the spectral contribution of the substrate. The difference spectrum is shown in Figure 3.5 B. The λ_{max} of the difference spectrum is 261.5 nm, partway between that of 4FW at 264 nm and AMP at 259 nm. A smaller peak in the difference spectrum resides at 289 nm. This peak is consistent with the ^1L_b electronic transition of Trp-92, since that of 4FW would appear at 284 nm according to its UV spectrum.

Table 3.1 shows the results of DTNB titrations of both TrpRS and the TrpRS·4FW-AMP complex. Neither form of the enzyme exhibits DTNB reactivity, unless SDS was present to denature the protein and expose the Cys residues, in which case the expected stoichiometry of 2 Cys per subunit (Chow and Wong, 1988) was observed. This result indicated that the 1 essential Cys (of 4 per subunit) for *E. coli* TrpRS activity which could be titrated with DTNB (Kuehl et al., 1976; Joseph and Muench, 1971b) was not detected in the *B. subtilis* enzyme.

Table 3.1: Thiol Reactivity.

Sample	TrpRS (μM)	SH (μM)[a]	SH/TrpRS
TrpRS (0.1% SDS)	11.0	18.9	1.7
TrpRS	11.0	0	0
TrpRS(Trp-AMP)	6.5	0	0

[a] SH is thiol concentration determined with DTNB.

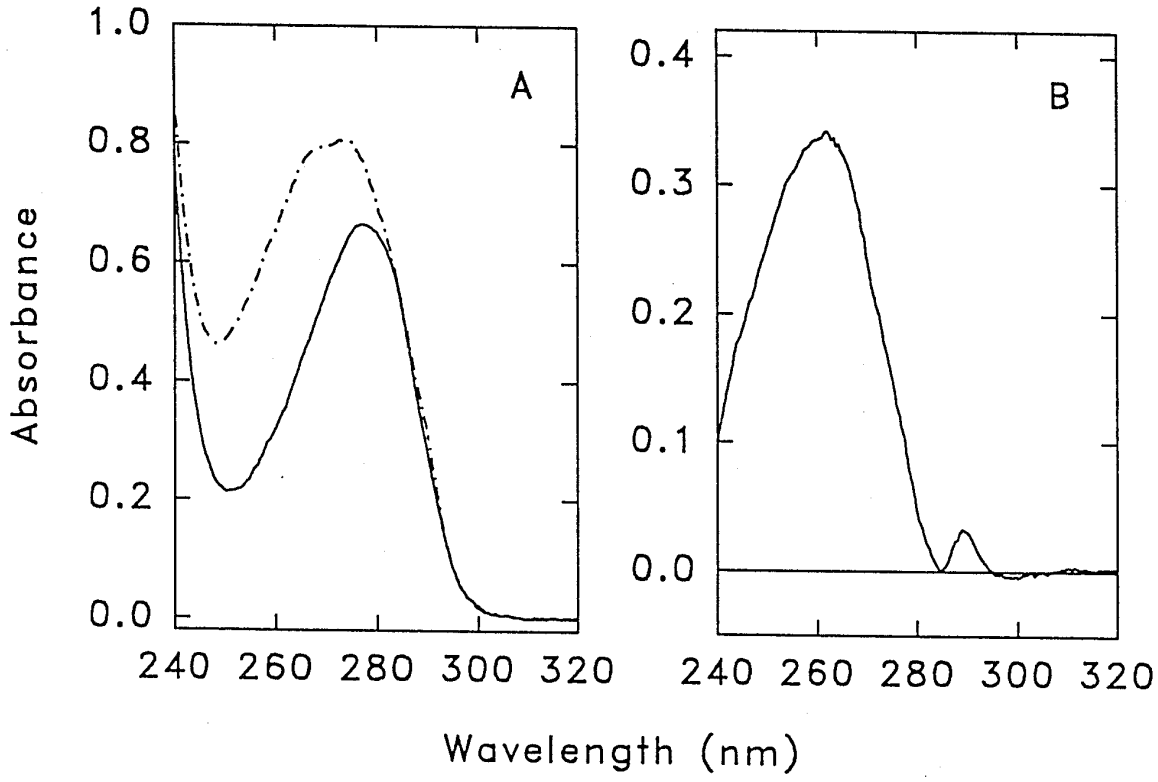

Figure 3.5: Ultraviolet Spectra of TrpRS and TrpRS·4FW-AMP A. Spectra of Normalized absorbance of (solid line) TrpRS; (dashed-dotted line) TrpRS·4FW-AMP complex. B. Difference spectrum derived from (A) with λ_{max} at 261.5 and 289 nm.

3.3.3 Steady-State Fluorescence.

In order to exclusively excite Trp-92 and avoid fluorescence from the 14 Tyr residues, it was necessary to use 300 nm excitation. No change in steady-state anisotropy occurred upon TrpRS dilution from 40 μM to 11 nM, suggesting that the dimer did not dissociate at the concentration ranges used in this study. Figure 3.6 illustrates the fluorescence of Trp-92 in free TrpRS and the complexed TrpRS·4FW-AMP. Trp-92 in the uncomplexed enzyme had a high quantum yield value of 0.18 (Table 3.2), which underwent a 70% decrease to 0.054 in the 4FW-AMP complexed enzyme. The λ_{max} of the emission of the uncomplexed TrpRS was 325 nm, while that of the TrpRS·4FW-AMP complex was 327 nm, demonstrating a slight red shift. It was possible to completely restore the fluorescence of Trp-92 by titration of the TrpRS·4FW-AMP complex by PP_i.

The fluorescence emission of a sample of TrpRS·4FW-AMP remained constant over a period of 8 hours. Since the fluorescence intensity change was so dramatic, it should be sensitive to any changes in the complex during this time period. This attested to the stability of the complex.

Table 3.2 lists the fluorescence quantum yields of TrpRS in combination with a number of substrates, including 4FW, ATP, PP_i and $tRNA^{Trp}$. The only individual substrates that appear to affect Trp-92 were ATP and PP_i, which only slightly increased the quantum yield of Trp-92. The large fluorescence quenching was observed only when both 4FW and ATP were present in conditions in which the TrpRS·4FW-AMP complex could form. There were no large shifts in λ_{max} of Trp-92 caused by the various substrates.

Some steady-state anisotropy values at 300 nm excitation, 325 nm emission are presented in Table 3.2.

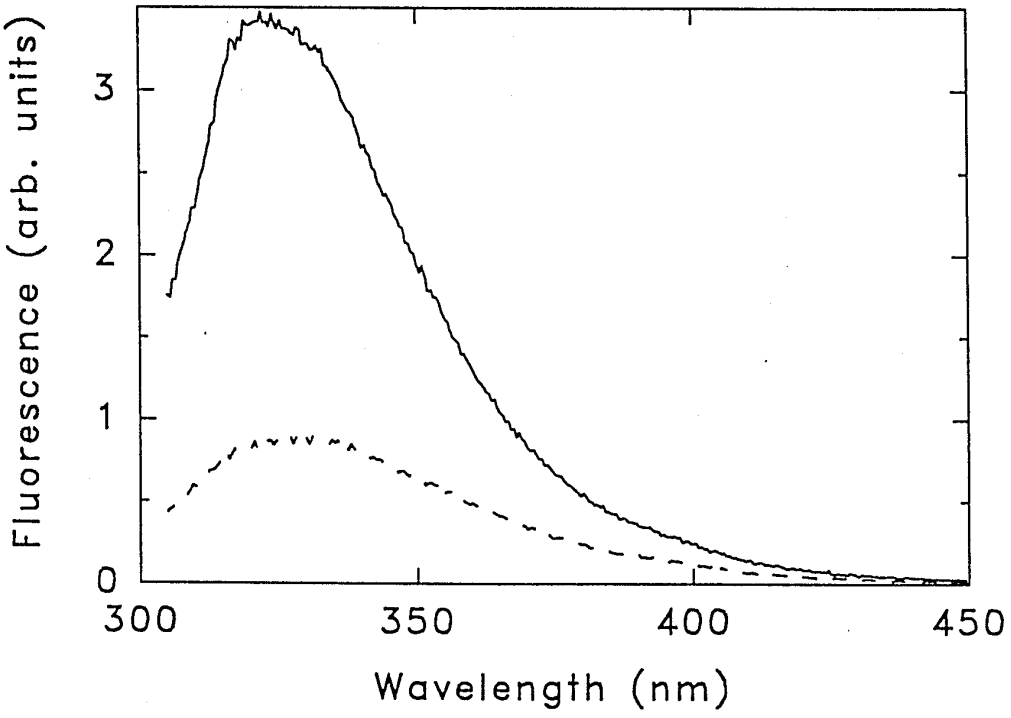

Figure 3.6: Trp-92 Fluorescence. Corrected steady-state emission spectra at 300 nm excitation of equal concentrations of (solid line) TrpRS; (dashed line) TrpRS·4FW-AMP complex.

Table 3.2: Steady-State Fluorescence Parameters.

Sample	Φ_f	λ_{max} (nm)	Anisotropy (± 0.01)
(1) TrpRS 22.1 μM	0.18 (±0.01)	325	0.19
(2) 22.1 μM + DL-4FW 364 μM	0.18 (±0.01)	325	nd[a]
(3) 22.1 μM + ATP 182 μM	0.19 (±0.01)	323	nd
(4) 3.1 μM + PP_i 182 μM	0.19 (±0.01)	325	nd
(5) TrpRS(4FW-AMP) 26.6 μM	0.054 (±0.001)	327	0.19
(6) TrpRS 3.1 μM + $tRNA^{Trp}$ 9 μM	0.18 (±0.01)	325	0.17
Following are (6) +...			
(7) ATP 20 μM	0.18 (±0.01)	325	0.19
(8) 4FW 20 μM	0.18 (±0.01)	325	0.19
(9) 4FW + ATP 20 μM each	0.084 (±0.001)	325	nd

[a] nd = not determined.

There was no detectable difference in the anisotropy of TrpRS or the 4FW-AMP complex. A perceptible increase occurred when ATP (Table 3.2 sample 7, 0.19) or 4FW (sample 8, 0.19) was added to TrpRS and $tRNA^{Trp}$ compared to the original solution (sample 6, 0.17). However the magnitude of these changes was not sufficient to conclusively demonstrate complex formation without other evidence.

3.3.4 Substrate Titrations.

Figure 3.7 A depicts the titrations in which D- and L-Trp were added to a sample of TrpRS in the presence of ATP and Mg^{2+}, while monitoring the total Trp fluorescence emission at 340 nm, after 300 nm excitation. The resulting fluorescence could originate from either substrate Trp or Trp-92. In the case of D-Trp there was a monotonic increase in fluorescence corresponding to the increase in D-Trp concentration. However the addition of L-Trp provoked an initial decrease in the fluorescence. Most of this decrease occurred with the first stoichiometric amount of added L-Trp. After a ratio of between 2-3 L-Trp to 1 TrpRS dimer, there was a

monotonic increase in fluorescence as observed with D-Trp. Figure 3.7 B shows the titration of the TrpRS·4FW-AMP complex by incremental addition of PP_i. Here, little increase occurred prior to the first stoichiometric amount of PP_i added. Between 1:1 and 7:1 the fluorescence increased steadily, reaching its plateau at close to a 8:1 excess of PP_i over TrpRS dimer. This may indicate the presence of multiple PP_i binding sites with similar affinity, together with the coopertive reaction reversal and displacement of 4FW-AMP..

Figure 3.8 shows the titration of ATP into a solution containing TrpRS, DL-4FW, Mg^{2+} and PP_iase. In this titration, a reproducible substoichiometric lag occurs after the initial addition of ATP. Immediately thereafter, the fluorescence decreases upon ATP addition, with the majority of the change nearly complete at 1:1 ATP to $TrpRS_2$. This could be a complication arising from the use of DL-4FW rather than L-4FW. There is no such lag in the titration using L-Trp.

In order to demonstrate the reversibility of the reaction and the activity of the PP_iase present, PP_i was added and the fluorescence monitored with time, depicted in Figure 3.8 B. A large excess of PP_i added caused the fluorescence to initially increase close to its original value in Fig. 3.8 A. This result is expected if PP_i exchange occurs, driving reaction (III) backwards. There was a subsequent rapid decrease in this fluorescence back to the intensity of the titration endpoint. This was also expected if PP_iase activity is present to drive reaction (III) towards formation of TrpRS·4FW-AMP by degrading PP_i. Therefore PP_iase prevented the reverse reaction throughout the titration with 4FW.

In all the titrations shown here, the fluorescence changes observed were consistent with a concerted (or fully cooperative) conformational change. The concerted nature of the Trp-92 fluorescence changes obviates its relation to concentration of species in solution, hence binding constants cannot be derived from these titrations.

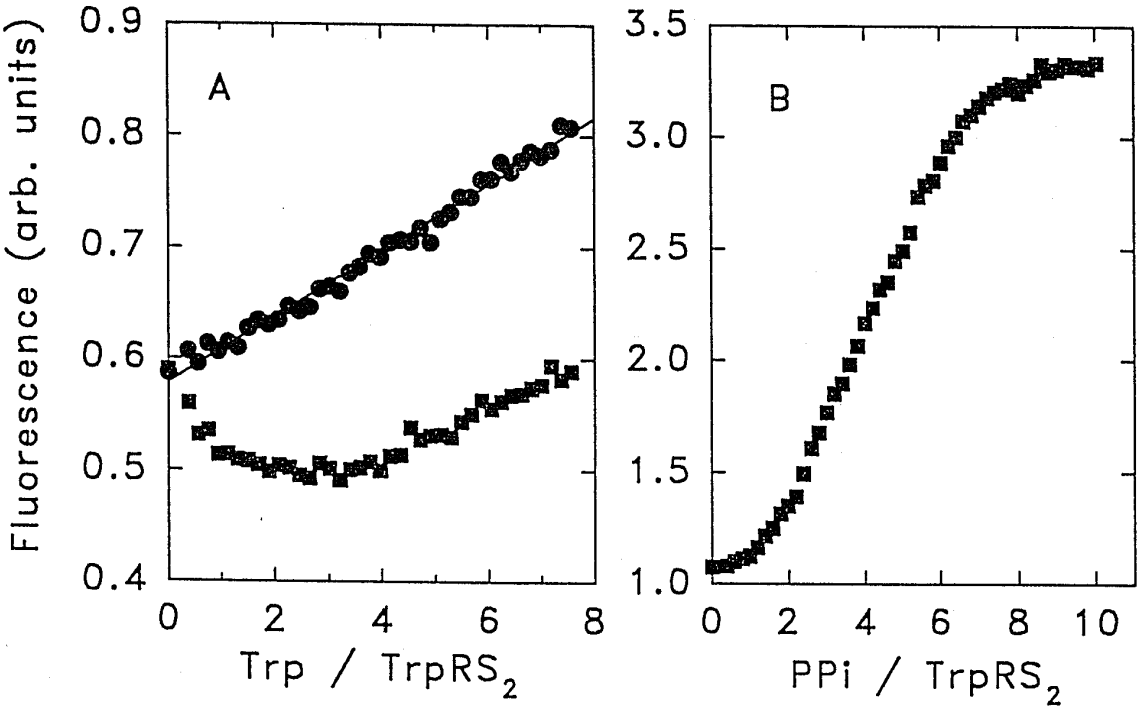

Figure 3.7: Titrations with Trp and PP_i. Duplicate fluorescence titrations monitored with 300 nm excitation, 340 nm emission. A. Titration of (•) D-Trp and (▪) L-Trp into a mixture of TrpRS and ATP. B. Titration of PP_i into a solution containing the TrpRS·4FW-AMP complex. Concentrations and conditions are described in Methods and Materials, section 3.2.7.

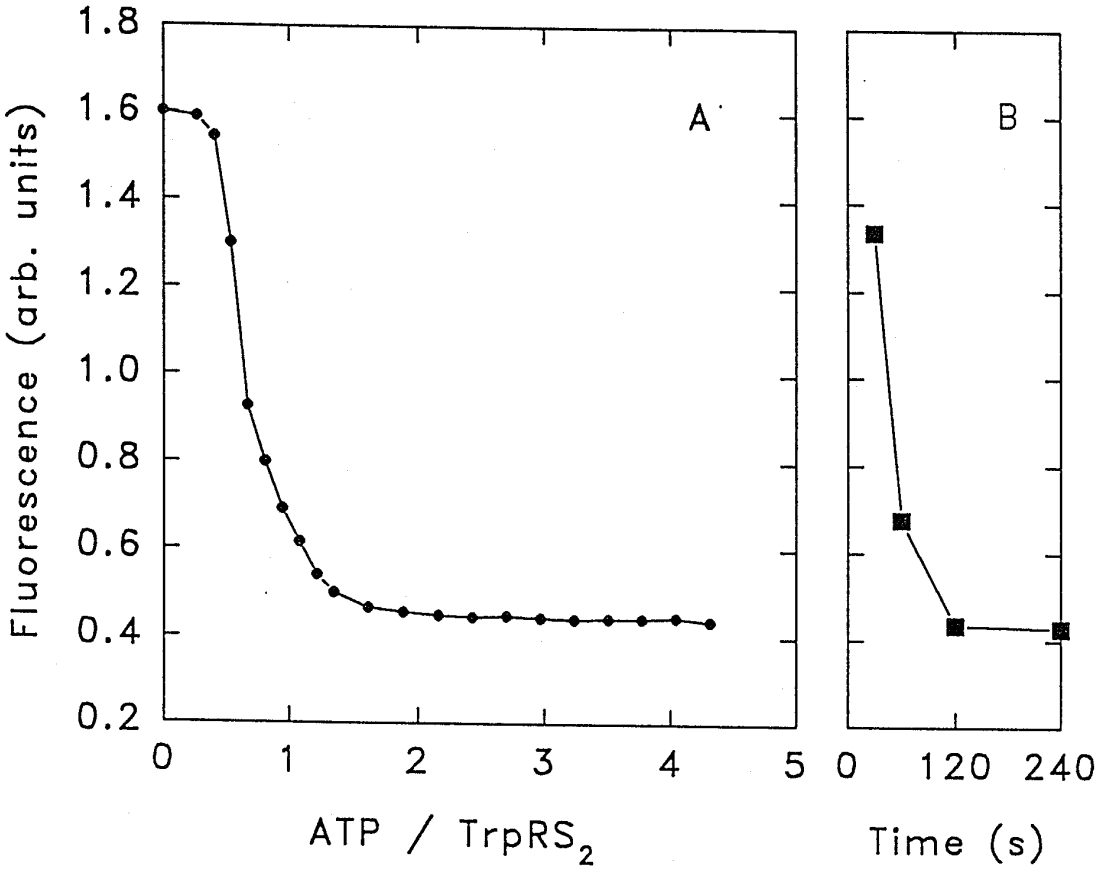

Figure 3.8: Titrations with ATP. A. Titration of ATP into a solution of TrpRS with 4FW and PP_iase enzyme present. Fluorescence at 300 nm excitation, 340 nm emission is monitored. B. Time course of fluorescence change after addition of PP_i to the titration endpoint, demonstrating the reversibility of reaction I, and the coupling of PP_iase in the titration to drive the reaction completely to the right. Concentrations and conditions are described in Methods and Materials, section 3.2.7. Lines connecting points have no physical significance.

3.3.5 Fluorescence Quenching

The data from iodide and acrylamide quenching experiments with TrpRS, denatured TrpRS and the TrpRS·4FW-AMP complex are depicted in Figure 3.9 as Stern-Volmer quenching plots. Table 3.3 lists the Stern-Volmer quenching constants, K_{sv}, obtained from the linear regression calculated line of best fit depicted in Figure 3.9, and the effective collisional rate constants, k_q, for the quenching process.

For TrpRS and the TrpRS·4FW-AMP complex, acrylamide quenching rates for Trp-92 were slightly higher than those of iodide. For both the iodide and acrylamide cases, the TrpRS·4FW-AMP complex exhibited decreased accessibility to quenching compared to uncomplexed TrpRS. This indicated less exposure of Trp-92 to small molecules upon forming the complex. For the case of TrpRS in 6 M GdHCl, the acrylamide K_{sv} of 4.15 M^{-1} was not as high as would be expected for a fully solvent exposed Trp (e.g. NATA = 17.5 M^{-1}; adrenocorticotropin = 13.5 M^{-1}, Eftink and Ghiron, 1977).

Table 3.3: Fluorescence Quenching Parameters.

Iodide Quenching	K_{sv} (M^{-1})[a]	τ_m (ns)[b]	k_q (x 10^{-9} $M^{-1}s^{-1}$)[c]
TrpRS	1.02	4.04	0.25
TrpRS(4FW-AMP)	0.482	3.77	0.13
TrpRS in 6 M GdHCl	2.51	nd[d]	nd
Acrylamide Quenching			
TrpRS	1.22	4.04	0.30
TrpRS(4FW-AMP)	0.823	3.77	0.22
TrpRS in 6 M GdHCl	4.15	nd	nd

[a] K_{sv} is the Stern-Volmer quenching constant derived from Fig. 5. [b] τ_m from Table 3.4. [c] kq is the bimolecular rate constant for the quenching process. [d] nd = not determined.

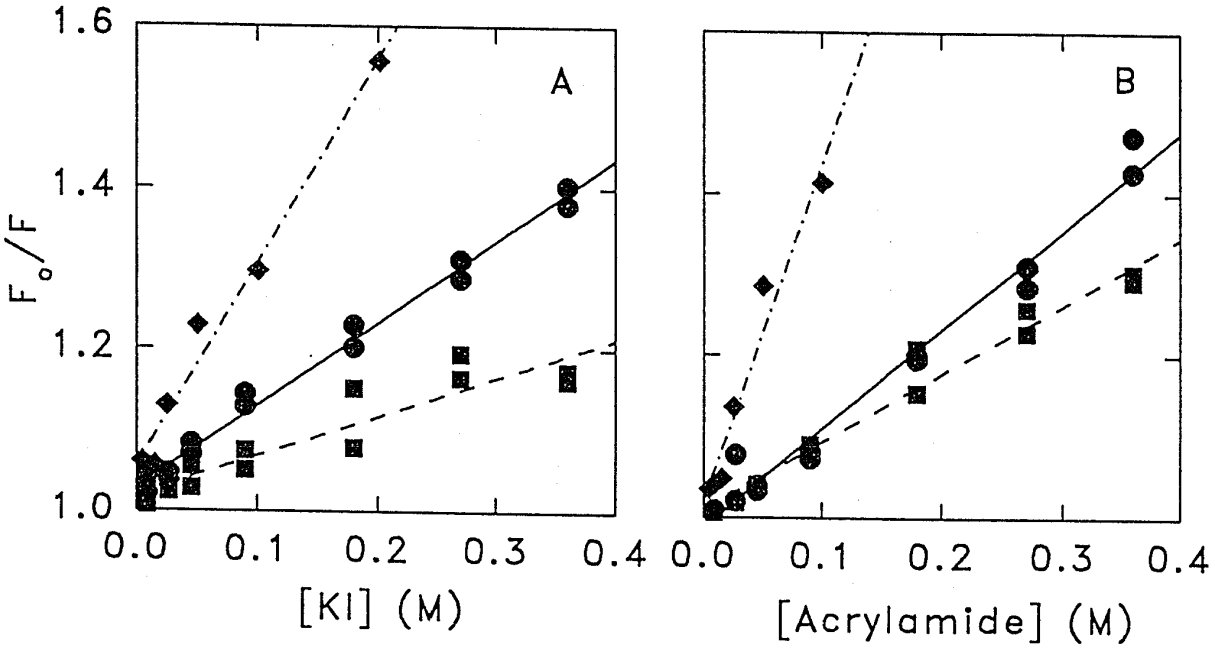

Figure 3.9: Stern-Volmer plots of fluorescence quenching. A. Iodide and (B.) Acrylamide quenching of (•) TrpRS, (▪) TrpRS·4FW-AMP and (◆) TrpRS in 6 M GdHCl.

The observed k_q value of 0.30×10^9 M^{-1} s^{-1} for acrylamide quenching of TrpRS and λ_{max} of 325 nm follows the relationship between bimolecular quenching constant and λ_{max} observed by Eftink and Ghiron (1976). These values were close to the acrylamide quenching parameters of the single Trp of RNase T_1 (0.1×10^9 M^{-1} s^{-1}) and were consistent with Trp-92 having limited solvent accessibility in the core of both the complexed and uncomplexed enzyme.

3.3.6 Time-resolved Fluorescence

Time-resolved fluorescence measurements of TrpRS alone or together with various substrates, or as the TrpRS·4FW-AMP complex all indicated that the fluorescence decay of Trp-92 was best fit by triple-exponential decay functions, indicated in Table 3.4. Samples in this Table 3.4 correspond to those in Table 3.2, with an additional TrpRS data set (Table 3.3 sample 10), provided for comparison with the data including $tRNA^{Trp}$, for which the TrpRS concentration was restricted to 3.1 μM. At 300 nm excitation, time-resolved fluorescence data from 3.1 μM TrpRS required 10 minute collection times to acquire the desired $1\text{-}2 \times 10^6$ counts.

Samples 1 and 10 of TrpRS illustrate significant differences only in the τ_1 lifetime. Global analysis of three different decay sets of TrpRS samples gave differing values of τ_1 ranging between the two values listed in Table 3.4, 5.99 and 7.17 ns. It was observed that τ_1 but not the shorter components, seemed to increase with increasing TrpRS concentration. Similar increases were observed in τ_1 by (Willis et al., 1994) upon formation of structure in a model peptide. This may be somehow related to the observation of low-wavelength light scattering in UV spectra which is suspected to result from higher-order oligomers or aggregates of TrpRS. Also, the slightly higher anisotropy for more concentrated TrpRS of 0.19 was evident compared

Table 3.4: Time-resolved Fluorescence Decay Parameters.[a]

Sample[b]	τ_1[c]	τ_2	τ_3	τ_m	$<\tau>$	τ_r	c_1[d]	c_2	c_3	F_1[e]	F_2	F_3	X^2	SVR
(1) TrpRS[f]	7.17 ± 0.07	3.40	0.77	4.0	3.1	17	0.092	0.661	0.246	0.213	0.726	0.061	1.05	1.92
(2) + DL-4FW	6.97 ± 0.09	3.38	0.75	4.0	3.0	17	0.088	0.652	0.260	0.205	0.731	0.064	1.03	1.96
(3) + ATP	6.71 ± 0.08	3.29	0.67	4.0	3.0	16	0.111	0.629	0.260	0.250	0.692	0.058	1.06	1.88
(4) + PP_i[g,h]	5.13 ± 0.10	2.99	0.63	3.5	2.7	14	0.166	0.572	0.261	0.313	0.627	0.060	1.08	1.83
(5) TrpRS·4FW-AMP	5.75 ± 0.02	1.87	0.53	3.8	2.0	36	0.181	0.359	0.460	0.531	0.344	0.125	1.05	1.89
(6) TrpRS + $tRNA^{Trp}$	6.22 ± 0.25	3.27	0.74	3.6	2.8	16	0.070	0.673	0.257	0.154	0.779	0.067	1.05	1.93
(7) + ATP	4.57 ± 0.07	2.70	0.61	3.5	2.8	16	0.303	0.467	0.230	0.497	0.453	0.050	1.05	1.93
(8) + 4FW	4.68 ± 0.07	2.63	0.58	3.4	2.6	14	0.244	0.488	0.268	0.443	0.497	0.060	1.05	1.84
(9) + ATP + 4FW[i]	5.19 ± 0.07	1.99	0.57	3.0	1.7	31	0.128	0.378	0.494	0.392	0.442	0.166	1.04	1.90
(10) TrpRS 3.1 μM	5.99 ± 0.21	3.26	0.77	3.5	2.8	16	0.074	0.669	0.257	0.158	0.772	0.070	1.07	1.90

[a] The excitation wavelength was 300 nm. Parameters are given for a global fit to data sets collected as a function of emission wavelength. Raman scattering at 332 nm from H_2O was used to determine the instrument response function. [b] Concentrations as in Table 3.2, except where indicated. [c] Fluorescence decay times in ns, recovered from global analysis, standard errors on $\tau_2 \leq \pm 0.05$; $\tau_3 \leq \pm 0.01$. [d] c_i is relative concentration and [e] F_i the fractional fluorescence of the decay components integrated across the decay spectrum. [f] Samples 1-3,5,6,9 and 10 had λ_{max} of 340 nm, 325 nm and ≤320 nm for decay times 1 to 3 respectively. [g] Samples 4, 7 and 8 had λ_{max} for all three decay components between 320 and 325 nm. [h] This sample was 3.1 μM in TrpRS and should be compared with sample 10 for the same conditions. [i] Sample 9 is capable of forming some TrpRS·4FW-AMP.

to dilute TrpRS of 0.17. Equilibrium amounts of higher-ordered oligomers may cause this apparent concentration-dependence of variation in τ_1.

Comparing those substrates involved in reaction I, ATP in sample 3 and 4FW in sample 2, there was little indication from either the fluorescence decay times, τ_i, or the relative concentrations of each decay component, c_i, that the substrates induced large changes in the fluorescence of Trp-92 over those of TrpRS alone. However a perceptible and reproducible increase in the c_1 values for the ATP and PP_i mixtures is observed, with a concomitant decrease in c_2 value. This would correspond to the slight increases in quantum yield observed in Table 3.2.

A change in all the fluorescence decay parameters of Trp-92 occurred with the formation of the TrpRS·4FW-AMP complex. The DAS of TrpRS and TrpRS·4FW-AMP are shown in Figure 3.10. The relative concentration of both τ_1 and τ_3 increased at the expense of τ_2 after formation of the 4FW-AMP complex. In addition, the fluorescence decay time of τ_2 was reduced by almost a factor of 2. In both cases, the λ_{max} of each of the decay components were very well separated and distinct, with λ_{max} of 340, 320-325, and $\leq$320 respectively for τ_1 - τ_3.

The increase in the τ_1 component, with a 340 nm λ_{max} together with the decrease in the τ_2 component seems to be the origin of the slight red shift observed from the TrpRS·4FW-AMP relative to uncomplexed enzyme. While this could be interpreted as increasing solvent exposure, this interpretation was not supported by the quenching data which clearly showed Trp-92 in the complexed enzyme is even less accessible to small molecules. Red shifts must therefore originate from dipolar relaxation from dielectric effects from within the protein, and not the solvent.

DAS of solutions of TrpRS and $tRNA^{Trp}$ alone or together with 4FW or ATP are shown in Figure 3.11, corresponding to samples 6-9 in Tables 3.2 and 3.4. In order to maintain a 3:1 excess of $tRNA^{Trp}$ over TrpRS monomer, and to avoid the inner-filter effect owing to $tRNA^{Trp}$ absorbance at 300 nm, it was necessary to work

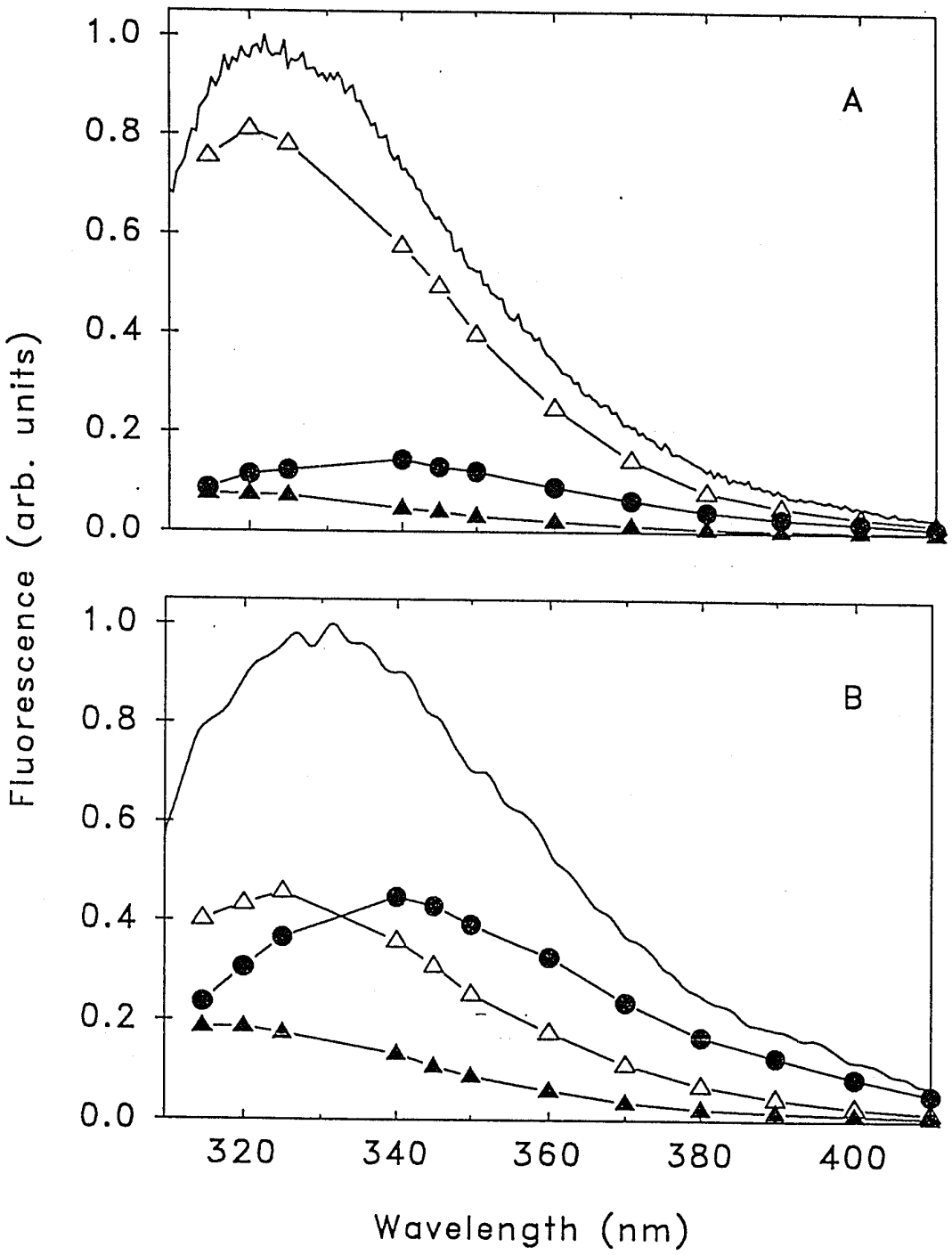

Figure 3.10: Decay-associated Spectra of TrpRS. A. TrpRS B. TrpRS·4FW-AMP. The decay component spectra (•) τ_1, (▲) τ_2, and (▲) τ_3 sum to the normalized steady-state spectra. Concentrations are listed in Table 3.2. Fluorescence decay parameters are listed in Table 3.4. Standard errors are within the contours of the plotted symbols.

with reduced TrpRS concentrations. Here only data from wavelengths between 320-360 nm were used owing to difficulties in obtaining adequate decay counts. Nonetheless, the concentrations used were in the range of those used for density gradient centrifugation (Muench, 1976), and were an order of magnitude higher than the K_m for $tRNA^{Trp}$ (Joseph and Muench, 1971a).

Figure 3.11 A , the sample of TrpRS with $tRNA^{Trp}$ present, is similar to Figure 3.10 A, TrpRS alone. The time-resolved fluorescence parameters listed in Table 3.4 were experimentally identical for samples 6 (TrpRS + $tRNA^{Trp}$) and 10 (TrpRS, same concentration and data collection conditions). These results suggest that $tRNA^{Trp}$ had no effect on Trp-92 fluorescence, and hence a complex involving only TrpRS and $tRNA^{Trp}$ either probably did not form, or at the least had no affect on Trp-92. The similarity of these DAS also attests to the validity of the method of blank-subtraction for these samples.

The addition of either 4FW or ATP to a solution of TrpRS and $tRNA^{Trp}$, causes distinct and similar changes to the fluorescence decay parameters as seen in Figure 3.11 B and C. Table 3.4 shows this change (samples 7 and 8) characterized by decreases in τ_1 (24%) and τ_2 (19%), and c_1 increased at the expense of c_2. Only small changes in the parameters for τ_3, or $<\tau>$ were observed. These results suggest that a ternary complex involving TrpRS, $tRNA^{Trp}$ and either 4FW or ATP forms, causing these changes in Trp-92 fluorescence. In the final sample (Fig. 3.11 D), both 4FW and ATP were added to TrpRS and $tRNA^{Trp}$. In this sample, the fluorescence decay parameters and DAS were similar to those of the TrpRS·4FW-AMP complex. This sample probably represents a mixture of the TrpRS·4FW-AMP together with uncomplexed forms, as the absence of pyrophosphatase enzyme could preclude the complete formation of the adenylate complex.

Differences in the patterns of the DAS λ_{max} for each of the three decay components were apparent in these DAS. Two patterns were observed. The first,

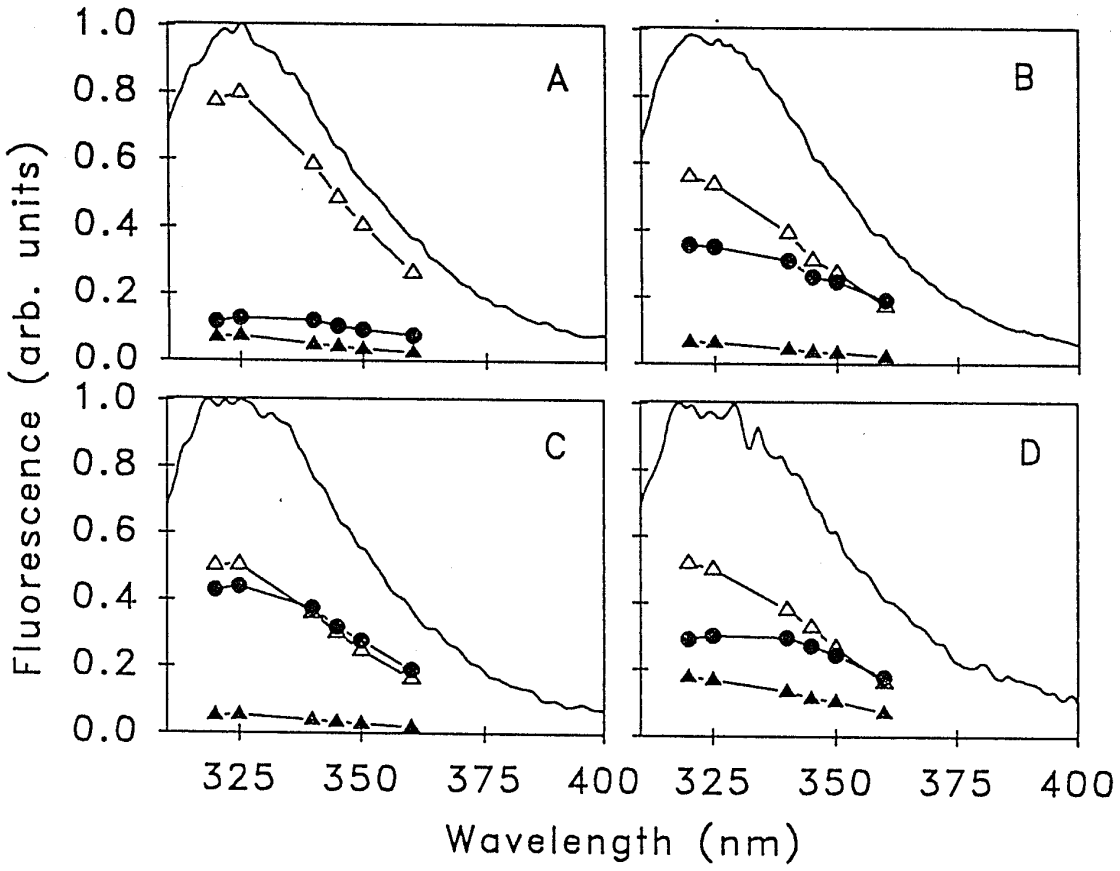

Figure 3.11: Decay-associated spectra of TrpRS with $tRNA^{Trp}$ Decay-associated spectra of: A. TrpRS + $tRNA^{Trp}$. B. TrpRS + $tRNA^{Trp}$ + 4FW. C. TrpRS + $tRNA^{Trp}$ + ATP. D. TrpRS + $tRNA^{Trp}$ + ATP + 4FW. The decay component spectra (•) τ_1, (▲) τ_2, and (▲) τ_3 sum to the normalized steady-state spectra. Concentrations are listed in Table 3.2. Fluorescence decay parameters are listed in Table 3.4. Standard errors are within the contours of the plotted symbols.

λ_{max} of 340, 325 and $\leq$ 320 nm for decay times $\tau_{1\text{-}3}$ respectively, was observed for all samples except the samples with the putative ternary complexes involving $tRNA^{Trp}$, and the sample including PP_i. These latter samples (Table 3.4 samples 4, 8 and 9) exhibited λ_{max} of between 320-325 nm for all three decay times $\tau_{1\text{-}3}$. The longer decay component λ_{max} underwent an unusual relative blue-shift, and were shorter, due to $tRNA^{Trp}$ ternary complexes or PP_i binding, a shift not apparent in the TrpRS·4FW-AMP complex.

The overall time-resolved fluorescence parameters show four distinct patterns. The first, represented by Figure 3.10 A, describes TrpRS without substrates. TrpRS alone or together with an individual substrate, ATP, 4FW, or $tRNA^{Trp}$ follows this pattern of fluorescence decay times, with slight changes to the long decay component arising from ATP. The second is the unique set parameters associated with the TrpRS·4FW-AMP complex, as depicted in Figure 3.10 B. The third is that involving a possible ternary complex, seen in Figure 3.11 B and C, involving TrpRS, $tRNA^{Trp}$ and either 4FW or ATP. The fourth pattern is associated with the presence of PP_i, which was first thought to be classified with the first DAS pattern. However it had important differences in both decay parameters (e.g. larger c_1, smaller τ_1) and in the values of DAS λ_{max}, making it unlike the other three. Qualitatively, the parameters of the TrpRS·PP_i complex were intermediate between those observed by TrpRS alone and those observed in ternary complexes with $tRNA^{Trp}$, which suggests interesting similarities of the effects of PP_i and $tRNA^{Trp}$ binding.

3.4. Discussion

3.4.1 Purification of TrpRS and the W92F Mutant.

The initial purification of the W92F mutant using the chromatographic scheme outlined by Wong's laboratory was unsuccessful, due to an inopportune proteolytic event on the DEAE column. Such fragments were not seen in the wild-type protein. This could be attributed to an unknown protease in the sample which was somehow activated on the DEAE column, despite the presence of the protease inhibitor PMSF. It is possible a protease was liberated from an inhibitor on this column. The W92F protein supplied by the laboratory of Dr. J.T. Wong did not suffer such fragmentation. This may be due to the acetone powder extracts used in their initial clarification which might have inactivated the offending protease. The batchwise hydroxyapatite extraction used in this work, was extremely efficient at removing other proteins from TrpRS, such that the only identifiable contaminants afterward were nucleic acids (this is shown later in section 5.3.1, Figure 5.4). It was expected that this step also removed the offending protease prior to its presumed activation on the DEAE column.

The W92F TrpRS polypeptide fragment sizes, 11 kDa and 25 kDa, could have resulted from a proteolytic event near the CP1 region or in the C-terminal region of W92F TrpRS. A fragmentation in the CP1 region might represent a local susceptibility to proteolysis of W92F TrpRS, perhaps due to a local structural anomaly at or near the mutation. A C-terminal cut would represent an even larger structural change due to the W92F mutation, as it would be much more distant. It is notable that the fragments were able to associate into a 72 kDa oligomer, as shown by gel filtration in Figure 3.3. The observations of the association of chymotrypsin proteolytic TrpRS fragments were reported earlier with *E. coli* TrpRS who reported a cut in the C-terminal region (Omnaas et al., 1979). Another Class I enzyme, IleRS, was demonstrated to self-associate after a proteolytic strand nick from trypsin (Lee, 1974) but the oligomer was

completely inactive. Shiba and Schimmel (1992) later reported that oligomeric IleRS could be reconstituted from three expressed fragments, with breaks at CP1 and further into the C-terminus. TrpRS would certainly lend itself to further studies with limited proteolysis, which were outside the intended scope of this thesis.

The subsequent purifications of W92F mutant using the purification detailed here demonstrated the suceptibility of the W92F protein to form higher molecular weight aggregates in buffers in which the wild-type protein did not. The gel-filtration chromatograph in Figure 3.3 demonstrated this, but aggregation phenomena were also observed at other times. For example, during the DNAse digestion step the W92F extract was observed to turn very cloudy, while a wild-type extract beside it remained clear. With the protocol detailed here, purification of W92F proceeded smoothly until the protein reached the fraction collector at the end of the S-200 HR gel filtration step. Almost immediately upon exit from the column, the eluted W92F TrpRS protein was observed to turn cloudy, forming aggregates. Urea and reducing agents were unable to resolubilize this material, and it was unacceptable for further studies. This was unfortunate, because it was hoped this enzyme could be used to observe Trp substrate fluorescence without interference from Trp-92 fluorescence.

The small amount of lyophilized W92F protein provided by Dr. J.T. Wong's lab had not been subjected to a final gel filtration step, as was the practice for this work. It also proved difficult to resuspend and showed similar aggregation in buffer. It is believed that similar aggregation problems may be the cause of the W92F inactivity reported by Chow et al. (1992). One reason for this belief is that their reported UV absorbance spectra does not correspond to the calculated extinction coefficients of TrpRS and the W92F mutant. If both proteins were at 0.73 mg/ml as cited, their estimated extinction coefficients, (TrpRS ϵ_{280} = 23610; W92F ϵ_{280} = 17920 M^{-1} cm^{-1}; Gill and Von Hippel, 1989) suggest absorbancies of 0.474 and 0.352. The figure of Chow et al. (1992) indicates absorbancies of 0.62 and 0.1 at 280 nm.

The predominant fluorescence expected from W92F from 14 Tyr residues at 280 nm excitation is similarly underrepresented in their report. If they had used an aggregated solution of W92F protein, and the aggregate settled, or was not transferred during pipetting, it would very likely result in a much lower W92F signal in spectroscopic samples. These workers measured concentrations with the Pierce BCA protein assay. This assay is dependent in part on the exposure of polypeptide backbone to reduce Cu(II) to Cu(I). According to the Pierce BCA reagent manual, different polypeptides could have as much as 50% variability in concentration but still provide the same assayed signal. An aggregated protein may expose a different amount of polypeptide backbone and hence react very differently to these reagents. Variation in reactivity to concentration-determining reagents could also account for the observed discrepancy in absorbance.

The inactivity of the mutant W92F, its susceptibility to proteolysis, and its observed propensity to aggregate indicate Phe is unable to replace the conserved Trp in this protein. This Trp is packed into the hydrophobic subunit interface in the crystal structure of *B. stearothermophilus* TrpRS (Figure 3.1). A Phe in this location may not completely fill the volume required, and this could disrupt the structure or expose a hydrophobic domain which nucleates aggregation. Irreversible aggregation could also have resulted from dissociated monomers, perhaps through the exposure of reactive thiol groups, such as the conserved Cys-96. The susceptibility of W92F TrpRS to aggregate and to proteolytic events clearly demonstrate the significance of Trp-92 in maintaining TrpRS structure.

3.4.2 The role of Cysteine in TrpRS

Previous DTNB titrations of *E. coli* TrpRS demonstrated 1 essential Cys per subunit, and a total of 3 or 4 Cys residues per subunit after SDS denaturation (Kuehl et al., 1976; Joseph and Muench, 1971b). The nucleotide sequence of *E. coli* TrpRS (Hall et al., 1982) reveals 4 Cys residues, two of which are conserved with the *B. subtilis* enzyme: Cys-39, and Cys-96. The DTNB reactive residue of *E. coli* TrpRS can be now identified from earlier experiments in which isolated Cys-labelled peptides were sequenced. This residue was Cys-71, unique to *E. coli* TrpRS (Figure 1.12), and to a homologous Cys-containing sequence in human placental TrpRS (Muench et al., 1975; Frolova et al., 1993). From the absence of a homologous Cys in other prokaryotic TrpRS, it could be concluded that it is probably not essential for TrpRS function. The DTNB reactive Cys in the *E. coli* enzyme was reported to be fully blocked by complexation with Trp-AMP (Muench et al., 1975). Labelling of *E. coli* Cys-71 with thiol-reactive groups probably interferes with substrate binding in a steric fashion. Other cysteine residues were clearly inaccessible in these two TrpRS variants.

3.4.3 Environment of Trp-92.

The enhancement of the Trp ^1L_b electronic transition between 289-293 nm (Yamamoto and Tanaka, 1972; Valeur and Weber, 1977) is a typical feature of the UV spectra of Trp residues in hydrophobic environments (e.g. Szabo et al., 1983; Hutnik et al., 1990). The absorbance difference spectra (Fig 3.5 B) suggests a change in the ^1L_b transition of Trp-92 so that it more closely resembles that observed from a hydrophobic core Trp. A similar change was observed in Trp absorbance when metal-free calcium-binding proteins: cod III parvalbumin or oncomodulin F102W were filled with calcium (Hutnik et al., 1990).

A small red-shift was observed in the emission spectra of Trp-92 upon forming the 4FW-AMP complex. This was at first interpreted as an increase in solvent exposure of Trp-92, and the red-shift was assumed to arise from solvent-based dipolar relaxation. The fluorescence quenching experiments were performed primarily to determine the extent of exposure of Trp-92 in the complexed and uncomplexed forms, as others had postulated that Trp-92 might be exposed to bind $tRNA^{Trp}$ (Chow et al., 1992). The quenching results indicated that Trp-92 was not exposed to small solute molecules, and resides in a solvent-inaccessible pocket in both the enzyme and complex. The dynamic quenching data suggests Trp-92 was even less accessible to solute quenchers in the TrpRS·4FW-AMP complex. The red shift is therefore attributed to an increase in the relative amount of the red-shifted decay component c_1, and not to solvent exposure of Trp-92.

The derived bimolecular quenching rate for Trp-92 in the presence of 6 M GdHCl was not as high as expected for a fully solvent exposed Trp. This might indicate that the protein had retained some structure or had somehow shielded Trp-92 from small molecule quenchers. Disulfide-linked dimers could also have contributed to preventing a more complete exposure of this residue to solvent.

Together, the quenching data, the UV absorbance data, and the inability to chemically label the nearby Cys-96, strongly suggest that Trp-92 was not exposed to solvent in the uncomplexed or complexed enzyme, and hence could not be directly involved in $tRNA^{Trp}$ recognition. This is strongly supported by the crystal structure which shows the homologous Trp-91 to be buried.

3.4.4 Trp-92 Fluorescence and Substrate Binding

The lack of any large effect of individual substrates, 4FW, ATP or $tRNA^{Trp}$ on Trp-92 fluorescence indicates either Trp-92 fluorescence was not affected by their binding, or they did not bind to the enzyme out of mechanistic order (Figure 1.13). Previous kinetic studies (Xu et al., 1989) of *B. subtilis* TrpRS showed behaviour of inhibition kinetics consistent with an ordered mechanism with ATP binding before Trp. This behaviour was opposite to that of the order of the closely related *B. stearothermophilus* TyrRS for reaction I, which binds the amino acid first, then ATP, owing to restricted access to the tyrosinyl-adenylate binding site (Fersht et al., 1987; Brick et al., 1988). It is unlikely that 4FW would bind to the active site at these concentrations. The dissociation constant determined for Trp using *E. coli* TrpRS was 0.12 mM (Muench, 1976), higher than the substrate amounts of 4FW used in these experiments.

The strong tendency of PP_i to displace Trp-AMP was probably due to its ability to first reverse the covalent reaction, and secondly to bind to the enzyme. Of the single substrates examined here, only ATP and PP_i had an affect on the fluorescence parameters of Trp-92, with the effect of PP_i being most notable. ATP could have exerted a long-range effect on Trp-92 from the negative charges of its polyphosphate group in the binding site.

The titration data with addition of PP_i to the TrpRS·4FW-AMP complex, shown in Figure 3.7, could be interpreted as the filling of 6 tight PP_i binding sites and 2 reverse reactions per dimer, each with equal probability (or equivalent binding affinity). The lack of a more gradual plateau over a large concentration range in this titration argues against a weak binding phenomena (Klotz, 1989). Two of the 6 binding sites are likely to be the same as the ATP polyphosphate binding sites (KKMSKS in the Rossman fold). Two additional tight PP_i bindings sites per monomer

are implied, and these could include sites which also bind to the phosphate backbone of $tRNA^{Trp}$.

One question that arises is why PP_i would bind to TrpRS, better than P_i, present in the buffer. The chelate effect, arising from the higher number of liganding sites for PP_i over P_i, as well as the higher charge density might explain this. Further evidence for the strong binding of inorganic forms of phosphate come from the unusually high affinity of TrpRS for hydroxyapatite, and the effectiveness of phosphate over chloride to elute TrpRS from DEAE Sephacel (Fromant et al., 1981; Shi et al., 1989). This is common to several aaRS enzymes of both Class I and Class II (Fromant et al., 1981). A multitude of Lys and Arg residues are presented to the surface of three conserved amphipathic helicies in the *B. stearothermophilus* TrpRS structure; comprising residues EDQKQHIELTRDLAERFNKRY, DDAKTIEKKIK, and on the last large helix EELDVRLDEGAEKANRVASEMVRKMEQAM. The larger two of these three helicies are covered with both positive (Lys,Arg) and negatively charged residues (Glu,Asp) in approximately equal numbers, and with few other residues represented. These structures are expected to be responsible for the strong hydroxyapatite binding which would require complementarity to a surface with equal numbers of opposite charges.

In an earlier chromatographic study of 12 aminoacyl-tRNA synthetases, 9 were very strongly bound to hydroxyapatite, requiring > 100 mM phosphate to elute (Fromant et al., 1981). Nucleic acids are also strongly bound by hydroxyapatite. The similarities of the surface charges of aaRS enzymes to hydroxyapatite may represent an important structural feature aiding in tRNA binding, one shared by both Class I and Class II aaRS enzymes. This also lends supports to the notion that inorganic material may have played a catalytic role in a prebiotic RNA-world (as reviewed by Orgel, 1994), to be later replaced by proteins.

Most of the samples exhibited a wide spread in DAS component λ_{max} values (> 20 nm). The redder of these λ_{max} could be attributed to nonsolvent dielectric relaxation, i.e. from the static dipoles *within* the protein. A dramatic effect on these λ_{max} values was observed with PP_i binding, effectively narrowing of the spread of DAS component λ_{max}, to within a 5 nm range. PP_i is very unlikely to diffuse into the protein and directly influence Trp-92 fluorescence. The blue shift of the reddest DAS component λ_{max} from PP_i binding is consistent with a decrease in nonsolvent dipolar relaxation experienced by Trp-92. This effect was also observed with putative ternary complexes involving $tRNA^{Trp}$ and either of 4FW or ATP. The chemical similarities of these two systems are their acidic phosphates. The binding of many negatively-charged species, such as the backbone of $tRNA^{Trp}$ or many PP_i molecules might decrease the dipole field strength of TrpRS as a whole, by offsetting the positive charges of the many exposed Lys and Arg side chains of TrpRS. If these interpretations are correct, it implies that the dipolar fields of proteins could be more important contributors to the observed heterogeneity of Trp fluorescence decay than previously recognized.

3.4.5 The Origin of Trp-92 Quenching

Strong fluorescence quenching was observed with the presence of the 4FW-AMP complex. This quenching could not be attributed to a fluorescence energy transfer mechanism to 4FW-AMP since there was no overlap between the 4FW or adenosine absorbance and Trp-92 fluorescence emission. The comparison of the decrease of Φ_f (70%) and $<\tau>$ (27%) from uncomplexed and complexed enzyme indicates the origin of the quenching could have been half dynamic and half static in character (Lakowicz, 1983). Quenching would arise from a conformational change

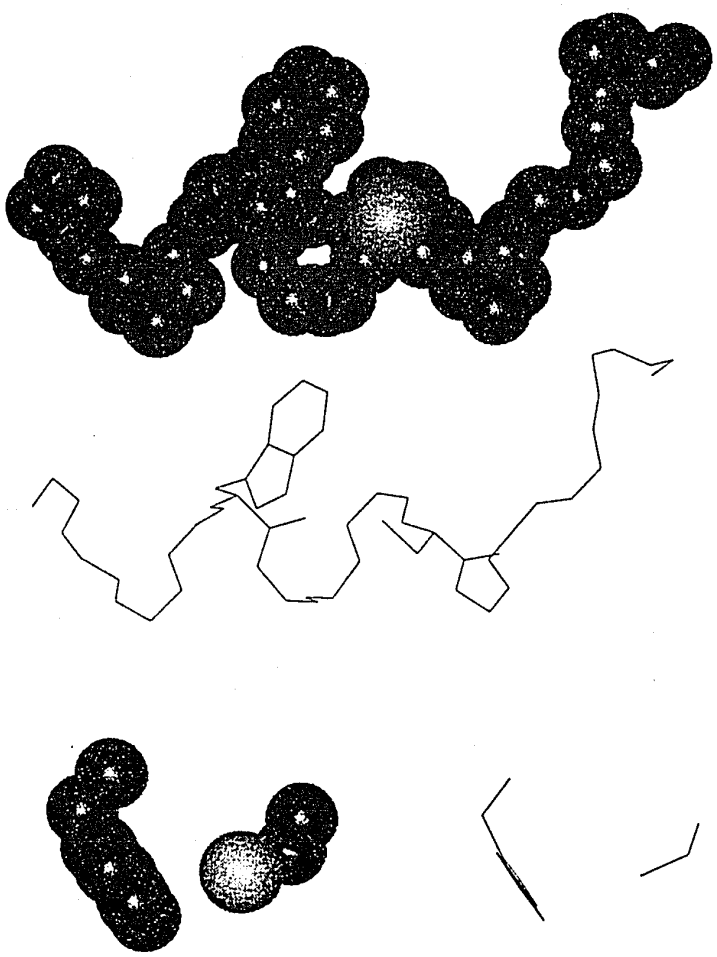

Figure 3.12: Local secondary structure of Trp-91 in *B. stearothermophilus* TrpRS. Space filling and stick models of the α-helix on which Trp-91 resides, with the side chains of Trp-91 and Cys-95 drawn. The structural views at the bottom show the close approach of Trp-91 and Cys-95, a distance of 3.58 Å between the N of the indole ring and the sulfur center, or 0.35 Å considering their respective radii.

which places Trp-92 close to a very strong quencher upon formation of the 4FW-AMP complex.

There are two possible rationalizations of the lack of proportional change of $<\tau>$ and Φ_f. One possibility is that both dynamic and static quenching of Trp-92 occurred upon complex formation, accounting for the drop in Φ_f. A second possibility is that there was only a dynamic quenching together with a variation of τ_r amongst different Trp conformers. This could have caused a disproportionate change in quantum yield as the conformer populations altered, appearing as static quenching. This explanation is detailed in Appendix A. However τ_r was assumed to be constant for a single Trp fluorophore in different conformations. If these τ_r were not constant for each conformer then the relative concentrations calculated from DAS would require adjustment, which cannot be done without *a priori* knowledge of the τ_r values.

The magnitude of fluorescence quenching of Trp-92 in the complexed enzyme is consistent with a strong quencher nearby. Since Cys-96 is four residues away, it would be capable of strong Trp-92 quenching (Cowgill, 1967) only if the local secondary structure was α-helical, which would place these residues adjacent to one another on one side of the α-helix. This geometry has been described for Tyr quenching by Asp or Glu carboxylates (Cowgill, 1976). The small molecule quenching studies and the change in the UV difference spectra indicate Trp-92 is buried in a hydrophobic pocket in the complexed enzyme. The lack of Cys-96 reactivity with DTNB (or its counterpart in *E. coli* TrpRS) is consistent with its inaccessibility to the surface. Hence experiments here strongly suggest Trp-92 and Cys-96 are both buried, and as such could be on the same side of an α-helix in the complexed enzyme. This conformation was proposed by the author prior to its observation in complexed *B. stearothermophilus* TrpRS, with the local α-helix indicated in Figure 3.12. The close approach of the indole N and the S of Cys in this structure is at the distance associated with S hydrogen bonding in proteins (Gregoret et al., 1991).

The high initial fluorescence of Trp-92 suggests the local conformation of Trp-92 and Cys-96 in the uncomplexed enzyme had these residues separated further than 10 Å apart to remove the quenching interaction. This structural criterion *eliminates the possibility that these residues reside on an α-helix in the uncomplexed enzyme conformer*. A necessary conclusion is that a large conformational change forms this local α-helix only upon Trp-AMP formation in a single subunit. Both subunits must form these α-helix structures in a concerted manner.

Formation of an α-helix in a segment containing Trp was shown to have had a profound affect on the preexponential terms of the fluorescence decay with model peptides (Willis et al., 1994). The strongest feature they observed upon helix formation was the increase in the value of α of the long decay time component, and the decrease in value of α of the intermediate decay time component. A similar pattern is observed here when Trp-92 time-resolved fluorescence changes from uncomplexed to 4FW-AMP complexed forms (Table 3.4 samples 1 and 5). Willis and coworkers further suggested that the fluorescent behavior of Trp in a ß-sheet would have a large intermediate decay component, as is the case for the uncomplexed enzyme, sample 1. While it may represent an oversimplification, a transition from ß-sheet to α-helix would certainly account for the appearance of quenching observed upon complex formation, by moving Trp-92 and Cys-96 from a conformation where they were well separated (ß-sheet) to one where they would be close together (α-helix).

Previous studies of *E. coli* TrpRS also demonstrated a decrease in the steady-state fluorescence (Andrews et al., 1985) with the formation of the Trp-AMP complex. In this system, 3 Trp fluorophores are present per subunit. A larger fluorescence quenching of *E. coli* TrpRS was observed with the first Trp-AMP formed (Merle et al., 1986) in the dimeric enzyme. This is similar to the result shown in Fig 3.5 A. *E. coli* has the conserved Trp-93 and Cys-97 residues (Figure 1.12). Andrews and coworkers attributed the 40% quench of Trp intensity to an 8% quenching due to Trp-AMP

substrate fluorescence, and a 32% quenching of enzyme Trp fluorescence. Trp-93 would have had to be quenched by 64% if it alone were responsible for the observed change of enzyme fluorescence. This value is close to the 70% quenching of *B. subtilis* Trp-92. Despite the presence of additional Trp fluorescence, these early results were consistent with and could be interpreted as a Trp-AMP dependent concerted rearrangement resulting in strong quenching of *E. coli* Trp-93 from the nearby conserved Cys residue. The conformational substates of these enzymes are therefore likely to be similar across bacterial species.

3.4.6 Concerted Conformational Change of TrpRS

At least 4 crystal morphologies of *B. stearothermophilus* TrpRS have been described, depending on substrate ATP or Trp presence (Carter Jr. and Carter, 1979). This earlier work suggests substrate-dependent conformational differences in TrpRS (Carter et al., 1990, Carter et al., 1994). Titrations with ATP and L-Trp presented here demonstrate that the fluorescence quenching observed with the formation of the aminoacyl-adenylate complex is dependent on a *single subunit* of the TrpRS dimer filling with the aminoacyl-adenylate. The stoichiometry indicates that the conformational change involving Trp-92 is concerted in nature. There must be substantial communication between the subunits for this to occur (Andrews et al., 1984).

The concerted conformational change was earlier suggested to relate to the cooperative binding and formation of Trp-AMP (Merle et al., 1986). The lack of a similarly large fluorescence quenching response of Trp-92 to the individual substrates 4FW, ATP and PP_i argues against a fluorescence-based conclusion that would localize Trp-92 within the Trp-AMP binding site. The conformational change of Trp-92

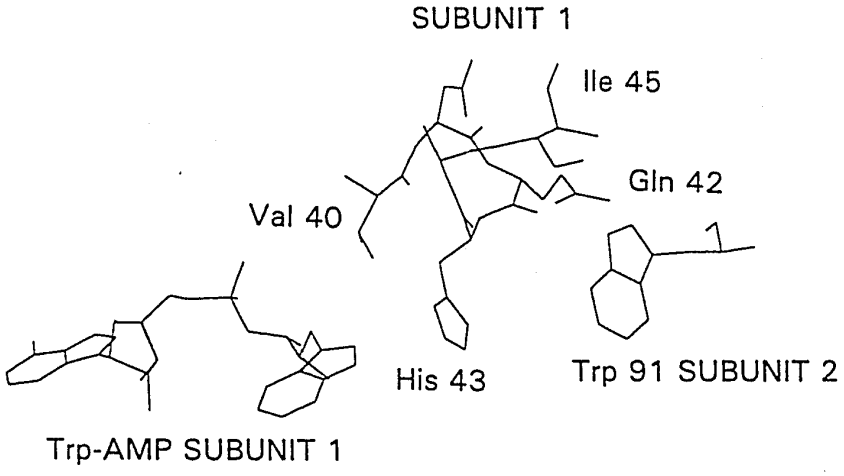

Figure 3.13: Substrate Trp and Trp-91 Near-Neighbors in *B. stearothermophilus* TrpRS The conserved short helical region comprising Val-40 to Ile-45 includes a near-neighbors to substrate Trp, His-43, sandwiched between two near-neighbors of Trp-91 from the opposite subunit, Ile-45 and Gln-42. This structure is probably involved in transmitting the conformational change of substrate binding across the dimer-interface.

probably results from a reorganization of the hydrophobic regions after binding the first Trp-AMP which could aid the cooperative binding of the next.

Figure 3.13 depicts a small conserved α-helical region consisting of residues Val 40 to Ile 45 between the Trp side chain of the substrate Trp-AMP in the left subunit, and the Trp-91 residue of the right subunit of the *B. stearothermophilus* structure. His-43, a near-neighbor of the substrate Trp, is between Gln-42 and Ile-45, near-neighbors of the opposite Trp-91 residue. This structure could account for the concerted nature of the observed conformational change by physically transmitting a substrate-based conformational change to the Trp-91 of the opposing subunit, consistent with these experiments.

3.4.7 Conformational States and TrpRS Mechanism

The experiments involving mixtures of $tRNA^{Trp}$ and TrpRS show no effect on the fluorescence of Trp-92, suggesting no complex forms between the two in the absence of other substrates. It may be mechanistically undesirable that $tRNA^{Trp}$ bind to TrpRS in the absence of Trp-AMP due to steric reasons. If the $tRNA^{Trp}$ aminoacylation site is topographically shared with the adenylate site, as it must be to undergo the reaction, the premature binding of $tRNA^{Trp}$ could sterically block the formation of Trp-AMP and behave as an unproductive complex. If TrpRS allows $tRNA^{Trp}$ binding only after Trp-AMP is present, then this could eliminate such unproductive complexes. The concerted conformational change could ensure the ordering of the mechanism in addition to providing the cooperativity of Trp-AMP binding (Merle et al, 1986). By presenting $tRNA^{Trp}$ binding sites in both subunits with only one Trp-AMP present, the enzyme may also be increasing the likelihood of

$tRNA^{Trp}$ binding and hence increasing the local $tRNA^{Trp}$ concentration with respect to the dimer.

The requirement for the high fluorescence of the Trp-92 residue prior to complex formation suggests this region has a much increased Trp to Cys distance. The disruption of the local α-helix of these residues could alter any $tRNA^{Trp}$ binding properties that might be associated with the remainder of the CP1 domain (Figure 3.14). Such a disruption could affect the conformation of the CP1 domain, a putative site for $tRNA^{Trp}$ acceptor-stem recognition. This helix could act like a spring which, upon "coiling", orients the CP1 domain exposing a $tRNA^{Trp}$ binding site. This may be how the mechanism ensures proper ordering of the reaction. Further evidence supporting this putative mechanism is given in Chapter 5.

3.4.8 The Role of the Essential Trp

This work resolves some earlier questions regarding the role of Trp-92. It is very unlikely that the indole ring is involved in initial $tRNA^{Trp}$ binding, since it remains buried even after forming the Trp-AMP complex, according to the data presented here. The observed ternary complexes involving TrpRS, $tRNA^{Trp}$ and either ATP or 4FW alter the fluorescence of Trp-92 and hence Trp-92 fluorescence may be affected in a $tRNA^{Trp}$ tryptophanylation transition state.

These experiments are consistent with the location of Trp-92 near the subunit interface. This could be rationalized by the concerted nature of its change in microenvironment, by the lack of evidence that it resides in the active site, and by the evidence that it remains a buried residue. This understanding is supported by the crystal structure. There is no clear evidence that Trp-92 binds directly to $tRNA^{Trp}$. To do this in such a transition state would require a major disruption involving

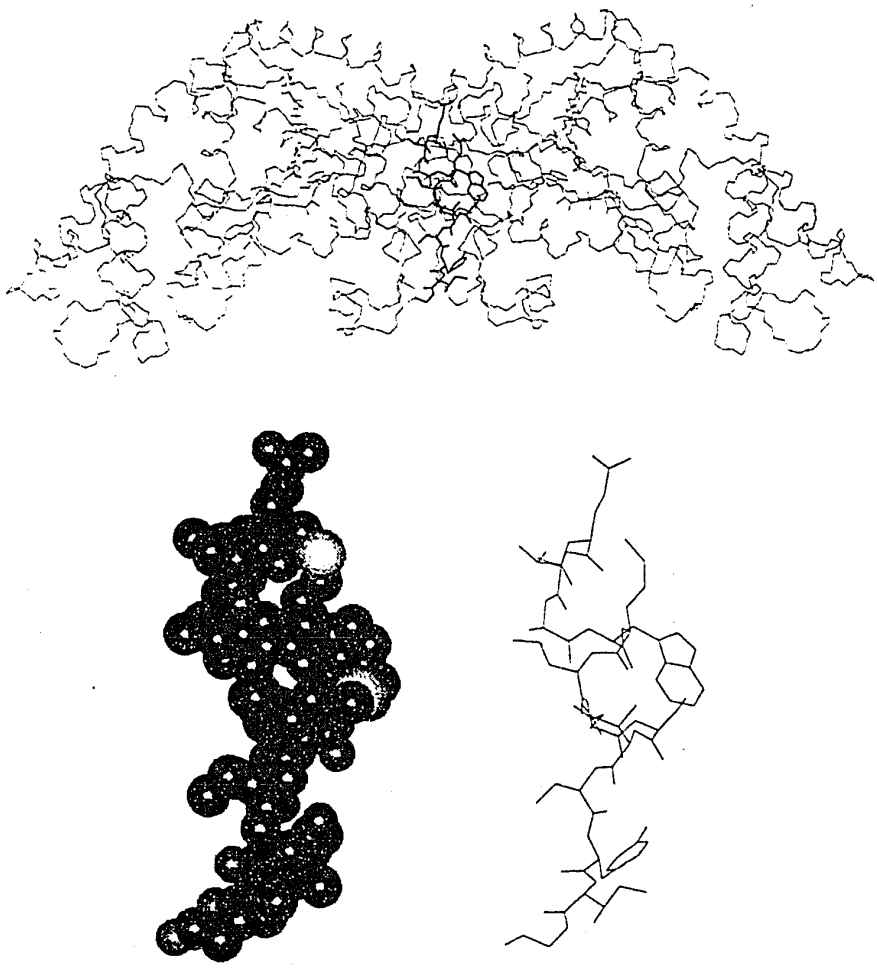

Figure 3.14: Trp-91 in *B. stearothermophilus* TrpRS (Top) bold residues indicate the local secondary structure of Trp-91 which proceeds into the protruding CP1 domain. (Bottom) Stick and sphere models of this structure. Considering the fluorescence data that requires that the Trp and Cys residues separate when the complex is removed, this helix will almost certainly form some longer structure, a conformational change which could propagate into and change the structure of the protruding domain.

exposing the subunit interface, which is unlikely. The fluorescence changes observed with the ternary complexes involving 4FW or ATP and $tRNA^{Trp}$ may be influenced by an induced-fit complex occurring due the combined presence of these three substrates. This could result in a change in the inter-subunit domain wherein Trp-92 resides.

The results described herein together with crystallographic information indicate the role of the essential Trp-92 is to act as a buried core residue that participates in inter-subunit communication and conformational changes associated with Trp-AMP formation. Mutagenesis of Trp-92 to Phe resulted in enzyme that was fundamentally unstable, however a failure to communicate subunit conformational changes could also account for its lack of $tRNA^{Trp}$ aminoacylation activity, reaction IV. But W92F did not catalyze reaction III (Chow et al., 1992), therefore the instability argument seems most applicable to account for its total lack of activity.

3.4.9 Relation to other Class I aaRS

The presence of domain similarity in Class I aaRS enzymes with variable insertions, designated CP1, suggested that tRNA acceptor helix specificity may be partially determined by CP1 structure (Burbaum and Schimmel, 1991). The interaction between the monomeric enzyme, GlnRS and its cognate $tRNA^{Gln}$ was depicted in the crystal structure of ternary complex involving GlnRS, $tRNA^{Gln}$ and ATP (Rould et al., 1989). The CP1 region of GlnRS binds to the acceptor helix of $tRNA^{Gln}$. This region is a five-stranded antiparallel ß-sheet flanked by three α-helicies (Rould et al., 1989), and is much larger than that identified as the CP1 region of TrpRS (Burbaum et al., 1990; Burbaum and Schimmel, 1991). The CP1 of TyrRS shares a role in binding the $tRNA^{Tyr}$ acceptor helix and in forming the subunit interface of the dimeric enzyme

(Brick et al., 1988; Burbaum and Schimmel, 1991). A similar role is expected of the CP1 of TrpRS, although it is also involved in the subunit interface.

In a fluorescence study of GlnRS, using extrinsic probes, Bhattacharyya et al. (1991) reported no evidence of a major conformational change of the enzyme upon binding $tRNA^{Gln}$. However ATP was shown to induce a conformational change of unknown character which altered the mode of $tRNA^{Gln}$ binding to GlnRS (Bhattacharyya and Roy, 1993). GlnRS requires the presence of cognate $tRNA^{Gln}$ in order to exhibit PP_i exchange activity. GlnRS thus catalyzes its two reaction steps (I and II) while $tRNA^{Gln}$ remains bound to the enzyme. GlnRS glutaminyl-adenylate formation is allowed only after $tRNA^{Gln}$ binding; a behaviour opposite to that observed for TrpRS. This implies that Gln is free to enter its binding site without any steric conflict with bound $tRNA^{Gln}$. On the other hand, the presence of $tRNA^{Trp}$ bound to TrpRS could be sufficiently bulky to sterically block the entry of the larger substrate Trp. This topographical consideration of whether an amino acid could bind in the presence of cognate tRNA may provide a partial explanation as to why the mechanisms of these related Class I aaRS enzymes differ.

3.5 Summary and Conclusions

Tryptophanyl-tRNA synthetase (TrpRS) of *B. subtilis* has a single conserved Trp-92 which is essential for its activity. 4FW can be used as a nonfluorescent substrate to unambiguously observe changes in Trp-92 fluorescence. Quenching studies of Trp-92 fluorescence indicated it was a highly buried residue. *B. subtilis* TrpRS formed a stable, nonfluorescent, enzyme-bound 4-fluorotryptophanyl-5'-adenylate. The presence of excesses of 4FW, ATP, or $tRNA^{Trp}$ did not greatly affect the fluorescence decay parameters of Trp-92, suggesting that either Trp-92 was not located

at sites involved in their binding or that TrpRS did not bind these individual substrates out of mechanistic order. A 70% decrease in Trp-92 fluorescence quantum yield was observed when the 4FW-AMP complex was formed, indicating a conformational change which introduced dramatic quenching in the Trp-92 microenvironment. Time-resolved measurements indicate this quenching was dynamic in nature. Titration of the TrpRS·4FW-AMP complex formation while monitoring Trp-92 fluorescence during the forward and backward reactions showed that the conformational change causing the quenching is concerted, and was complete after the formation of a single 4FW-AMP in the dimeric enzyme. Substantial subunit communication must exist to account for this change, and the fluorescence changes of Trp-92 reflect its proximity to the subunit interface. Ternary complexes were indicated by Trp-92 fluorescence in the presence of $tRNA^{Trp}$ and either Trp or ATP.

These results support an ordered mechanism for $tRNA^{Trp}$ aminoacylation by TrpRS, involving the formation of a conformation competent for $tRNA^{Trp}$ binding only after the formation of a Trp-AMP filled subunit. Structural considerations suggest that $tRNA^{Trp}$ binds across the dimer interface of TrpRS, and that the observed concerted conformational change might be involved in the presentation of a CP1 $tRNA^{Trp}$ binding domain. The presence of distinct substrate-dependent fluorescence decay patterns is evidence that TrpRS is a very dynamic enzyme, confirming the conformational differences implied by substrate-dependent crystal morphologies (Carter Jr. et al., 1994). The dynamic nature of the TrpRS mechanism is evident.

Chapter 4

ANALOGS OF TRP AS SUBSTRATES FOR TrpRS

ANALOGS OF TRP AS SUBSTRATES FOR TrpRS

4.1 Introduction

The Trp analogs 5HW (Barlati and Ciferri, 1970) and 7AW (Pardee et al., 1956) were identified as being capable of incorporation into bacterial proteins in early experiments. However the spectroscopic advantages of both 5HW (Hogue et al., 1992) and 7AW (Négrerie et al., 1990; Hogue and Szabo, 1993) have only recently been appreciated. As detailed in Chapter 2, these amino acids have red shifted absorbancies which would allow their selective fluorescence excitation in the presence of other proteins containing normal Trp.

The biosynthetic incorporation of 5HW and 7AW into proteins *in-vivo* implies that they would undergo $tRNA^{Trp}$ aminoacylation through an aminoacyl-adenylate intermediate in TrpRS. In this work the unique spectroscopic properties of selected Trp analogs was used to detect and characterize their *in-vitro* aminoacyl-adenylates in *B. subtilis* TrpRS.

From the perspective of finding new Trp analog candidates as intrinsic fluorescent probes, the demonstration of aminoacyl-adenylate complexes with TrpRS *in-vitro* is evidence that an analog should be biosynthetically incorporated into an expressed protein. Hence this *in-vitro* test could screen Trp analogs to find those that are promising for biosynthetic incorporation, without having to conduct a biosynthetic incorporation experiment. The active site of TrpRS has been shown experimentally by Shi and coworkers (1989) to be hydrophobic in character. It is expected that the fluorescence of complexes of Trp analogs would exhibit differences based on their inclusion into a hydrophobic site.

In addition to 5HW and 7AW, the analogs 5MeOW and 1MW, shown in Figure 4.1 were selected as candidates for their potential as intrinsic fluorescent probes from a number of commercially available Trp analogs. Both these analogs exhibit the

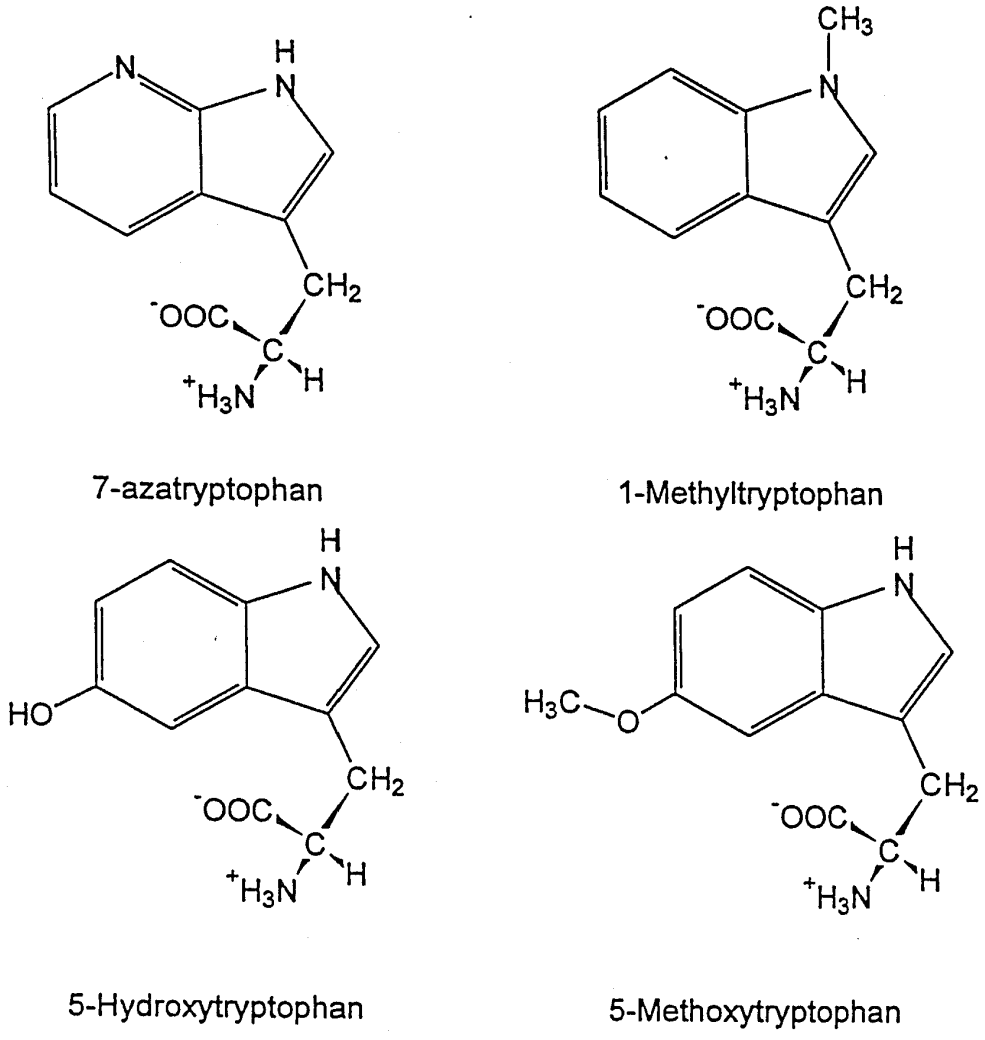

Figure 4.1: Trp Analogs Suitable as Spectroscopic Probes.

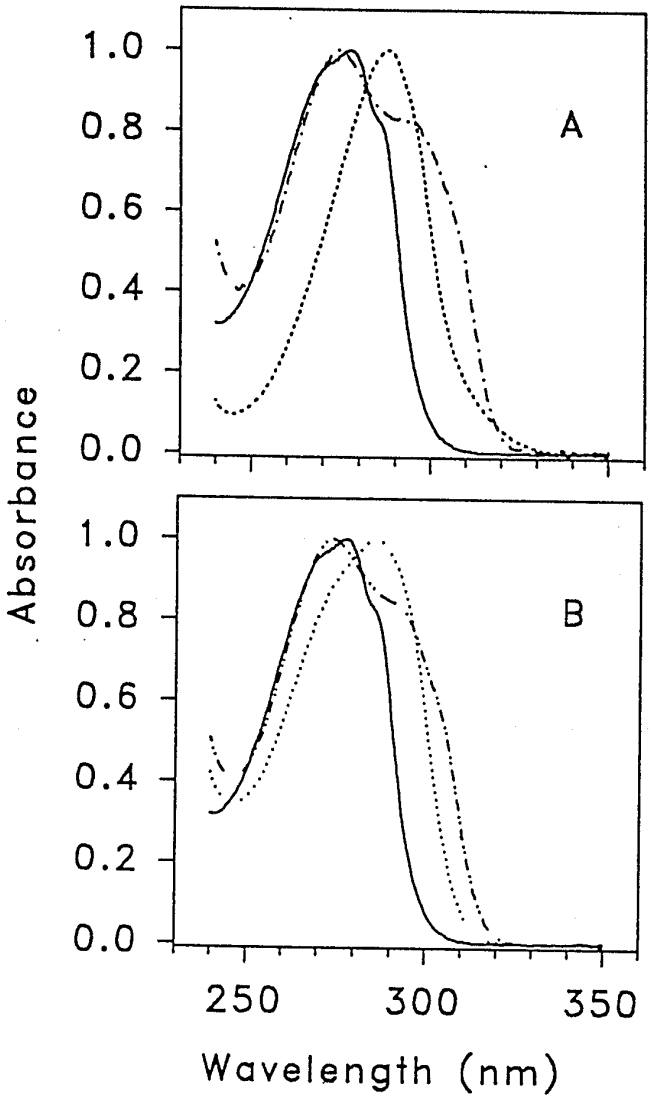

Figure 4.2: Peak normalized absorbance spectra of Trp analogs used in this study. A. (-) L-Trp, (-··-) L-5-hydroxytryptophan; and (···) DL-7-azatryptophan. B. (-) L-Trp; (-···-) DL-5-methoxytryptophan ; and (···) DL-1-methyltryptophan.

desired red-extended absorbance, compared to Trp, as shown in Figure 4.2. In addition, these analogs have the potential to eliminate pH dependent deprotonation that could affect the fluorescence. In 1MeW the indole N-H is blocked, in 5MeOW the hydroxyl of 5HW is blocked.

Since the enzyme-bound aminoacyl-adenylates could undergo rapid irreversible hydrolysis (Kingdon et al., 1958) after dissociation from the enzyme, any dissociation or hydrolytic processes of the aminoacyl-adenylate could be followed by changes in the fluorescence parameters of the Trp analog as it returns to solution.

4.2 Methods and Materials

4.2.1 Materials

Purification of *B. subtilis* TrpRS from an *E. coli* expression system followed the methods described in Chapter 3. Additional chemicals used to those listed in Chapter 3 are listed here. Subtilisin Carlsberg, NaAMP, D,L-7-azatryptophan, L-5-hydroxytryptophan, D,L-5-methoxytryptophan were all obtained from Sigma Chemical Co., St. Louis, Missouri. D,L-1-methyltryptophan was obtained from Aldrich Chemical Co., Milwaukee, Wisconsin. The quantum yield standard 2-aminopyridine was obtained from Eastman Kodak, Rochester New York. All these were analytical grade and used without further purification.

4.2.2 Preparation of Aminoacyl-adenylates

Solutions of TrpRS for fluorimetry were prepared from lyophilized enzyme dissolved at high concentrations (typically 5 mg/ml) in a pH 8.6 reaction buffer (200 mM Tris-HCl, 20 mM MgAcetate). Reactions to form the enzyme-bound aminoacyl-

adenylate were as described in Chapter 3. 500 μl of reaction mixture contained 100 μM TrpRS, 200 μM L- or 400 μM DL- Trp analog, and 400 μM ATP. After a 5 min. reaction time, 250 μl of the reaction mixtures was passed through a 15 cm column of Sephadex G-25 fine equilibrated with freshly prepared pH 7.5 10 mM K_2HPO_4, 100 mM KCl buffer, which was also the buffer used for all spectroscopic studies reported.

4.2.3 Spectroscopy

Solutions for fluorimetry were diluted (if required) to a final absorbance of 0.10 or less at the excitation wavelength to avoid any inner filter effect. 2-aminopyridine was used as a quantum-yield standard (0.66; Meech and Phillips, 1983) at 310 nm excitation in 0.1 N H_2SO_4 purged with nitrogen for 10 minutes prior to measurement. Absorbance spectra were collected using a Varian DMS 200 spectrophotometer with a 1 nm bandpass. Analytical-quality stock solutions of substrates were prepared in pH 7.5 10 mM K_2HPO_4, 100 mM KCl buffer, to derive the extinction coefficients listed in Table 4.1.

Steady-state fluorescence spectra were collected with Glan Taylor polarizers oriented to eliminate anisotropic effects, using an SLM 8000C instrument with 4 nm emission and excitation bandpass. Spectra were corrected for the blank contribution and for wavelength dependence of the instrument response.

Fluorescence decay data was measured using the method of time-correlated single photon counting (TCSPC) using laser/microchannel plate instrumentation. The instrument and data analysis techniques have been described in Chapter 2. All measurements were performed at 20^{o} C with 4 nm bandpass, and corrections were made for the blank containing buffer only. The instrument response function was determined from the Raman scattering of the excitation by water at 346 nm for 310 nm

excitation. Data were collected at 10 or 20 ps/channel in 2048 channels. Each decay curve contained 1-2 x 10^6 counts, except where indicated. The time-resolved data was combined with the corrected steady-state spectra to derive the Decay Associated Spectra (DAS), as detailed in Chapter 2.

4.3 Results

4.3.1 Analog Aminoacyl-Adenylates in TrpRS

The absorption spectra of the analogs are shown in Figure 4.2. Each analog has an extended low energy absorbance compared to Trp. Experiments were conducted with all these analogs to determine whether they associated with TrpRS in the form of aminoacyl-adenylates.

Each of the four Trp analogs was used in the aminoacyl-adenylate reaction with TrpRS and ATP and the reaction mixture was chromatographed with Sephadex G-25. The absorption spectra shown in Fig. 4.3 are those of the enzyme eluant of the reaction with 5HW and 7AW, as the eluants with 1MW and 5MeOW had no distinguishable spectral features indicating adenylates had formed.

The ratio of free enzyme to that of the TrpRS-aminoacyl-adenylate complex could be determined in the following way. The eluant mixture of enzyme and TrpRS-aminoacyl-adenylate complex was treated with PP_i which presumably hydrolyzed the complex to the original unreacted constituents of enzyme, ATP, and Trp analog. The concentration of ATP and the Trp analog were considered to be equal. Hence this comprised a mixture of chromophores with known extinction coefficients (Table 4.1). The absorption spectrum was then measured and from the extinction coefficients at 280 nm and 310 nm of each constituent (Table 4.1) the ratio could be determined. For TrpRS·7AW-AMP the ratio of unreacted enzyme monomer to complexed monomer

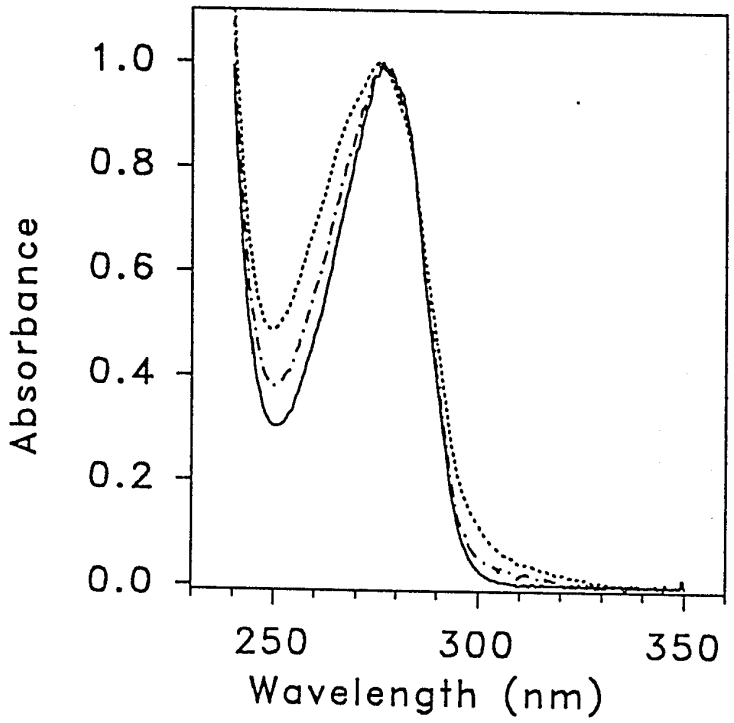

Figure 4.3: Peak normalized absorption spectra of TrpRS after reaction and chromatographic separation. TrpRS alone (-); 16 μM TrpRS with 10.5 μM 7AW-AMP bound (···); 17 μM TrpRS with 3.6 μM 5HW-AMP bound (-·-). Concentrations were obtained from linear combinations of individual absorbancies of TrpRS, 5HW, 7AW and AMP at 310 and 280 nm, together with the absorbancies of the complexes after pyrophosphate addition.

was 1.5:1, while for TrpRS·5HW-AMP the ratio was 4.7:1.

Table 4.1: Extinction Coefficients of Substrates.

Analog	ϵ_{310} M^{-1} cm^{-1}	ϵ_{280} M^{-1} cm^{-1}
L-5HW	2450	4900
DL-7AW	1205	5080
DL-5MeOW	1590	5140
DL-1MeW	340	3847
AMP	0	2310
TrpRS[a]	100	24154

[a] per monomer.

The absorption spectra and fluorescence spectra of the enzyme eluant of 1MW indicated that 1MW did not form a stable aminoacyl-adenylate complex with the enzyme. In the case of 5MeOW there was some weak evidence from the absorption and fluorescence spectra that there was an association of the 5MeOW with the enzyme. However absorbance that could be assigned to adenine at 260 nm was not present. When PP_i was added to the eluant in order to reverse the reaction there was no change in the fluorescence behaviour as was observed for the reactions with 7AW and 5HW.

An additional steady-state anisotropy experiment with 20 μM TrpRS and 10 μM DL-5MeOW gave a value of 0.025, which dropped upon the addition of excess ATP to 0.022. Conversely, the same experiment with 5 μM L-5HW had a starting value of 0.011 which rose to 0.022 with excess ATP addition. The initially higher value of anisotropy for 5MeOW, and its subsequent drop with ATP suggested it may have associated with TrpRS in the absence of ATP in a non-adenylate complex. However these low values of anisotropy, compared to the enzyme (Table 3.2) suggest most of DL-5MeOW and L-5HW remains in solution in these reaction mixtures. A similar experiment with DL-1MeW reported no change in anisotropy (0.005) after ATP

addition. An initial anisotropy value for DL-7AW was not able to be measured in this solution, owing to its low fluorescence yield, however the final anisotropy, after ATP addition was 0.01. Since both 5HI and 5MeOI have single ^1L_b excited-state dipoles which are excited at $\lambda > 310$ nm (Kishi et al., 1977) it was expected that these would have higher anisotropies compared to 7AW in which the ^1L_a and ^1L_b dipoles overlap (Chen et al., 1993).

4.3.2 7-Azatryptophanyl-Adenylate

The fluorescence spectrum of the TrpRS·7AW-AMP complex was dramatically different from that of an aqueous solution of 7AW itself. There was a 27 fold increase in the Φ_f changing from 0.013 in aqueous solution to 0.348 in the complex (Table 4.2) and a 10-fold increase in the fluorescence lifetime. A 40 nm blue shift of the spectral maximum (Figure 4.4 A) was also observed. After an excess of PP_i was added to the TrpRS·7AW-AMP complex, the fluorescence spectrum (Figure 4.4 A) resembled that of a mixture of the enzyme and the free amino acid, 7AW. Both excitation spectra at 400 nm emission and absorbance spectra showed a significant increase in 7AW absorbance at $\lambda > 300$ nm after forming the adenylate (not shown).

When the chromophore 7AW was exposed to aqueous solvent it had a very low Φ_f. As a result the fluorescence from a 4:1 mixture of TrpRS and DL-7AW showed that the fluorescence of TrpRS Trp-92 could be observed below 400 nm, even when excited at 310 nm. Figure 4.4 B shows the fluorescence of this mixture together with the individual fluorescence spectra of the enzyme and DL-7AW with 310 nm excitation. The absorbance of 20 μM TrpRS at 310 nm excitation was $\cong$ 0.002, but the quantum yield of the single Trp-92 residue under these conditions was at least 0.14. More precise measurements detailed in Chapter 3 show its quantum yield is 0.18. The absorbance of 80 μM DL-7AW was 0.100, and its quantum yield was 0.013. A

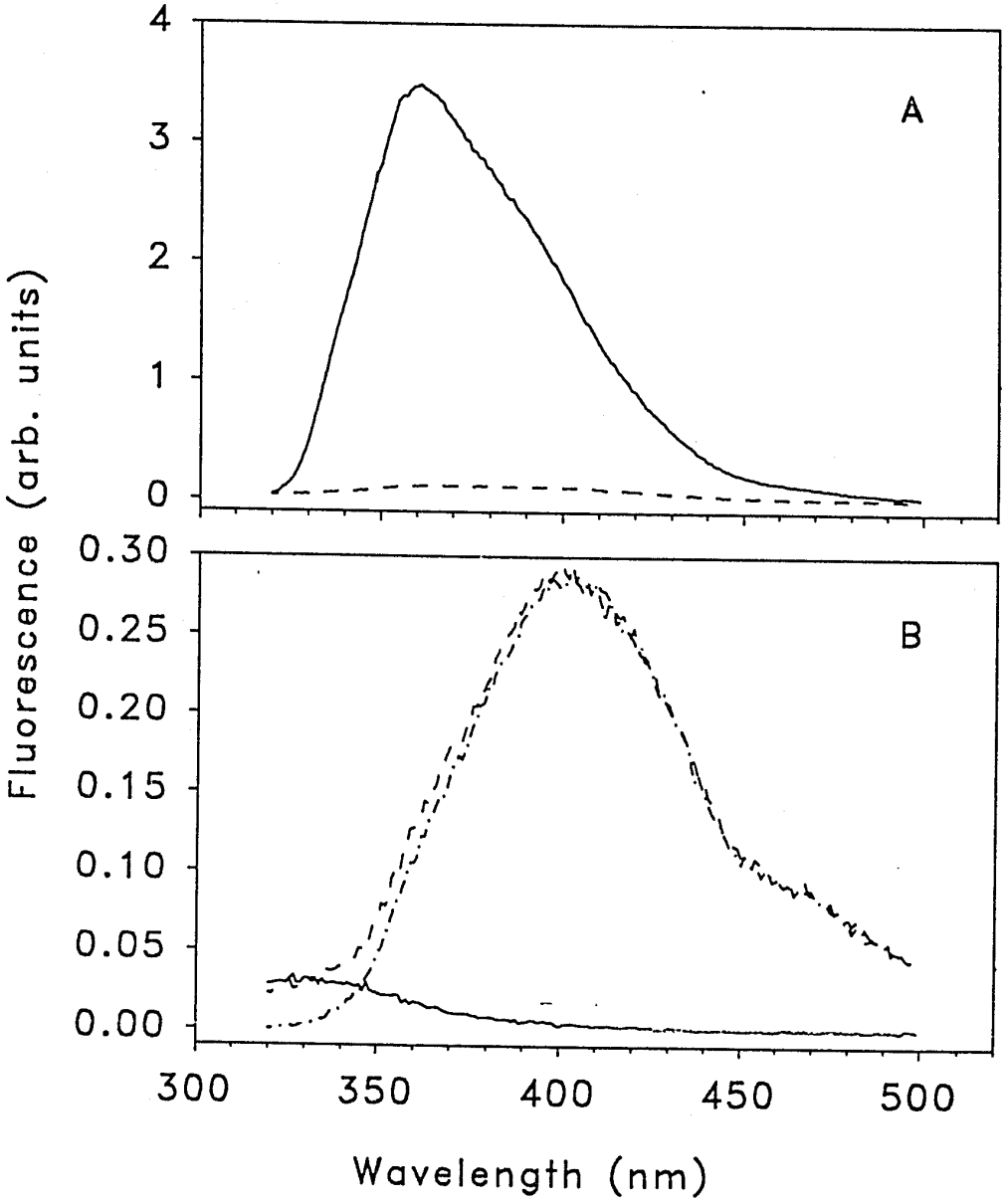

Figure 4.4: Fluorescence of TrpRS·7AW-AMP complex. Corrected steady-state fluorescence emission spectra at 310 nm excitation. A. (-) TrpRS·7AW-AMP; and (- -) the same material with a 2-fold excess of PP_i. B. (-) 20 μM TrpRS; (-·-) 80 μM DL-7-azatryptophan; (- -) Mixture of 20 μM TrpRS and 80 μM DL-7-azatryptophan.

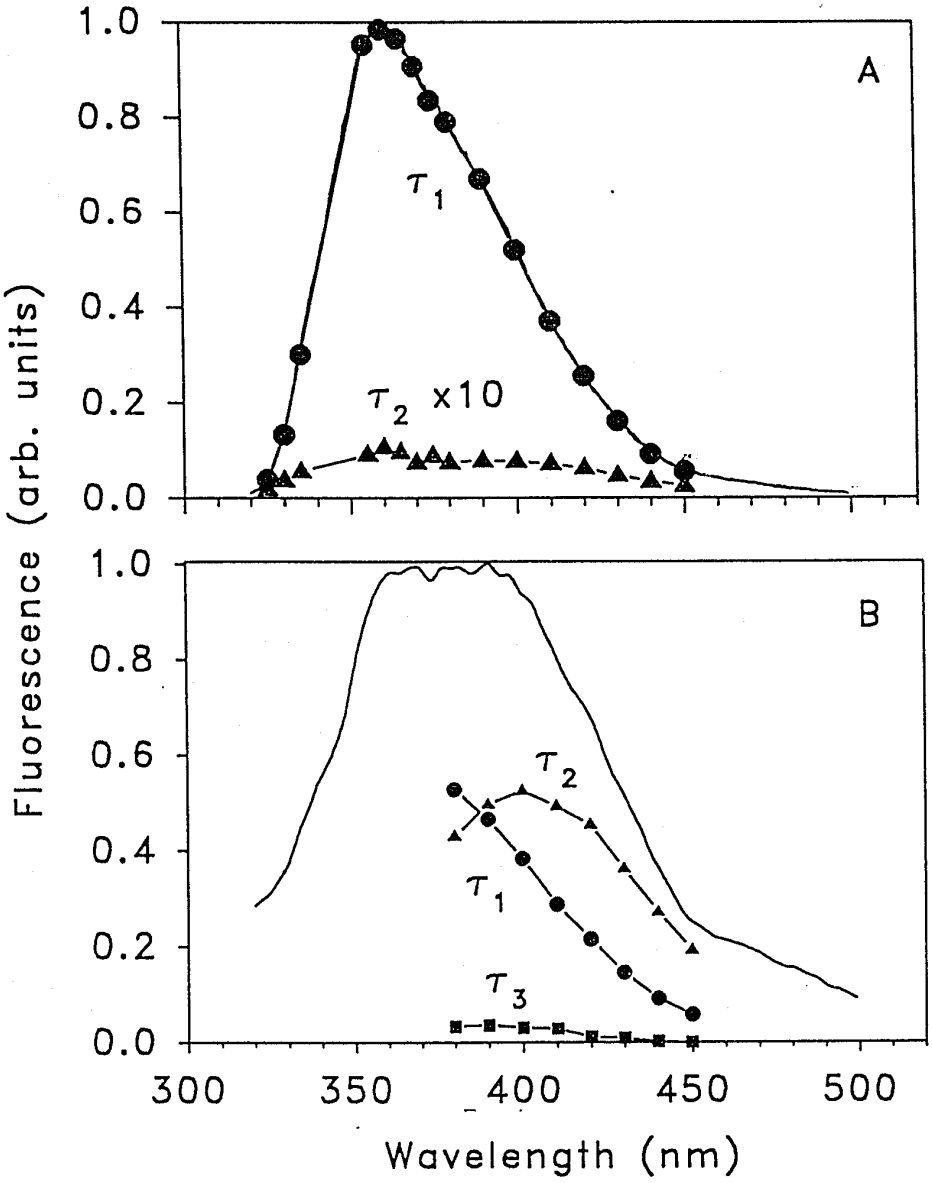

Figure 4.5: Decay-associated spectra of the TrpRS·7AW-AMP complex. A. TrpRS·7AW-AMP. B. TrpRS·7AW-AMP after an addition of a 2-fold excess of PP_i.

Table 4.2: Steady-state and Time-resolved Fluorescence Decay Parameters.[a]

Sample	τ_1 (ns)	τ_2 (ns)	τ_3 (ns)	α_1	α_2	α_3	SVR	Φ_f	λ_{max}
TrpRS·7AW-AMP[b]	10.5 ± 0.004	1.06 ±0.01		0.925	0.075		1.69	0.35	361
TrpRS·7AW-AMP[c]	10.6 ± 0.004	0.92 ±0.01		0.855	0.145		1.91		
TrpRS·7AW-AMP + PP_i	10.0 ± 0.019	0.83 ±0.002	0.26 ±0.007	0.048	0.803	0.149	1.78	0.017	391[d]
7AW		0.76 ±0.001	0.24 ±0.003		0.977	0.023[e]	1.33		401
TrpRS·5HW-AMP[f]	3.8 ±0.004	1.15 ±0.008		0.623	0.377		1.84	0.15	334
TrpRS·5HW-AMP +PP_i[g]	3.8 ±0.004	1.25 ±0.02		0.830	0.170		1.91	0.18	336
TrpRS·5HW-AMP[h]	3.8 ±0.003	1.13 ±0.007					1.92		
5HW	3.60 ±0.001			1			1.87	0.25	336
TrpRS[i]	4.5	1.20	0.072	0.045	0.038	0.917	1.68		325

[a]Excitation at 310 nm, α at 400 nm for 7AW samples, 330 nm for 5HW samples. [b] Global analysis of complete data set of spectrum from 325-400 nm. [c] Global analysis of spectrum from 360-450 nm avoiding enzyme fluorescence. [d] Broad maxima centred at 375 nm (Figure 4.5 B). [e] Pre-exponential became negative at wavelengths > 400 nm. [f] Sample undergoing hydrolysis during data acquisition. [g] Decay parameters of sample hydrolyzed after 3 h without PPi were the same. [h] Global analysis of fluorescence decay at 330 nm vs. time depicted in Figure 4.9. [i] See weak emission spectra (Figure 4.4 B). Noise was high owing to less than 350000 counts/decay curve.

measure of the sensitivity of a fluorophore was approximated by the product of the extinction coefficient and the quantum yield. At 310 nm, this value is 16 M^{-1} cm^{-1} for 7AW, and at least 14 M^{-1} cm^{-1} for TrpRS. Owing to the high sensitivity of TCSPC fluorescence decay measurements it is possible to resolve decay times that are due to Trp fluorescence at $\lambda < 380$ nm, even with 310 nm excitation.

The time-resolved fluorescence of the TrpRS·7AW-AMP complex (Table 4.2) measured shortly after Sephadex G-25 elution could best be fit to a biexponential decay process across the spectrum. At all wavelengths the majority of the fluorescence (> 98%) could be attributed to a long decay time, 10.5 ns component (Figure 4.5 A). The decay time of the second decay component, which accounted for the balance of the fluorescence intensity, was different at $\lambda < 360$ nm than from that found at $\lambda \geq 360$ nm. A global analysis which included all the datasets gave only a modest fit (SVR = 1.69) to two exponentials. When this analysis was extended to a fit to three exponential decay components, the decay times were 10.79 $\pm$ 0.02 ns, 5.9 $\pm$ 0.14 ns and 0.83 $\pm$ 0.01 ns (SVR = 1.95). The 5.9 ns component did not make a significant contribution to the fluorescence above 360 nm. Another global analysis which included only datasets measured at $\lambda \geq 360$ nm gave a fully satisfactory fit (SVR = 1.91) to two exponential decay components, with the shorter decay time being 0.915 ns. The 5.9 ns component is attributed the long decay time component of the Trp-92 fluorescence from the enzyme, which is poorly defined owing to its small contribution to the total fluorescence. The 0.83 ns component is assigned to the small amount of free 7AW which resulted from adenylate hydrolysis with low fluorescence. The long lifetime component is clearly that of 7AW in the TrpRS·7AW-AMP complex.

The steady-state fluorescence of the TrpRS·7AW-AMP decreased slowly with time from that found immediately after elution of the complexes from the G-25 column. This was unlike the complexes involving 4FW or Trp. A semilogarithmic plot of this loss of fluorescence intensity at 20° C is presented in Figure 4.6 (the

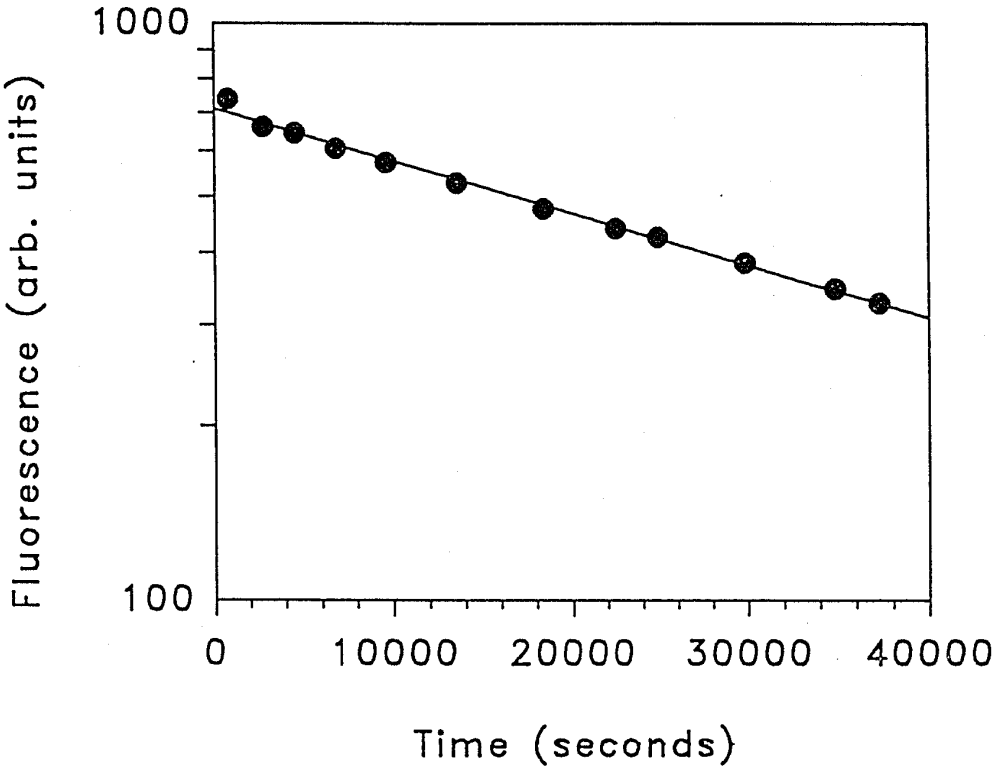

Figure 4.6: Rate of 7AW-AMP hydrolysis. Semilogarithmic plot of the decline in fluorescence intensity of enzyme bound 7AW-AMP with time. The half-life of TrpRS·7AW-AMP hydrolysis was 552 min.

sample was left in the dark between fluorescence readings). A straight line fit of this plot indicated first order kinetics. The fluorescence decrease is attributed to the slow rate of dissociation of the 7AW-AMP from the active site, followed by the rapid hydrolysis of the adenylate. The half-life of the TrpRS·7AW-AMP complex calculated from this plot (Segel 1976) was 9.2 hours.

When an excess of PP_i was added to the solution of the complex, three decay components were well defined (Table 4.2). In these experiments only data from the $\lambda > 380$ - 450 nm range were measured since it was known that the Trp-92 fluorescence made an important contribution to the fluorescence signal at $\lambda < 380$ nm. Global analysis (Table 4.2) of the data allowed the presentation of the DAS of the PP_i treated material in Figure 4.5 B. The two sub-nanosecond decay times were assigned to free 7AW, being very similar to decay times reported for 7AI in water (Chapman and Maroncelli, 1992). A long fluorescence decay time of 10 ns (only 0.56% of the fluorescence intensity of the intact complex) was still observed, contrary to expectations. It was thought that this long decay time would disappear after PP_i was added. While the majority of the fluorescence resulting from what was assigned to the TrpRS·7AW-AMP complex disappeared (> 99%), this long 10 ns lifetime component was not removed by the addition of an even larger excess of PP_i.

4.3.3 5-Hydroxytryptophanyl-Adenylate

The fluorescence spectra (excited at 310 nm) of the TrpRS·5HW-AMP complex was measured immediately after elution from G-25 chromatography, and after the addition of excess PP_i, as shown in Figure 4.7 A. The fluorescence of the freshly eluted TrpRS·5HW-AMP complex was slightly blue-shifted (2 nm) and quenched (Table 4.2) when compared to that of free 5HW. Figure 4.7 B shows that the emission

from the TrpRS·5HW-AMP is structured on the blue-edge of the spectrum, compared to the free 5HW. The PP_i treated fluorescence in Fig. 4.7 A is unstructured, like free 5HW.

The fluorescence of TrpRS·5HW-AMP complex changed rapidly with time and by analogy with the TrpRS·7AW-AMP complex this was attributed to the dissociation and hydrolysis of the 5HW-AMP. As a result, multiple experiments were performed, using freshly eluted adenylate complex each time. The time-resolved fluorescence of the TrpRS·5HW-AMP complex decayed with double exponential decay kinetics showing decay times of 3.80 ns and 1.15 ns (Table 4.2). This compares with single exponential decay kinetics for 5HW in aqueous solution (τ = 3.60 ns). The spectral maximum of the 1.15 ns component was found at 330 nm, which is significantly shifted from that of the 3.80 ns component (335 nm).

After the addition of excess PP_i, the shorter lifetime was not entirely removed (Table 4.2, Figure 4.8 C) but may be due to a small constant amount of enzyme fluorescence which may still result from excitation at 310 nm. The 3.80 ns decay time in this case may represent a weighted average of the 3.60 ns decay time of free 5HW and the 4.46 ns decay time of the enzyme (Table 4.2). This indicates that a small component of the fluorescence of the TrpRS·5HW-AMP complex may be due to that of the enzyme itself and hence the proportions of the decay components would require adjustment.

By measuring the time resolved fluorescence at 330 nm at time intervals after elution from the G-25 chromatogram the progress of the release of 5HW-AMP from the TrpRS·5HW-AMP complex could be monitored. The temporal change in fractional fluorescence of each of the two decay components together with the increase in the steady state fluorescence are shown in Figure 4.9. The dotted line in this figure represents the fractional fluorescence of the short decay time that could not be removed by excess PP_i and was attributed to TrpRS Trp-92 fluorescence. Analysis of a

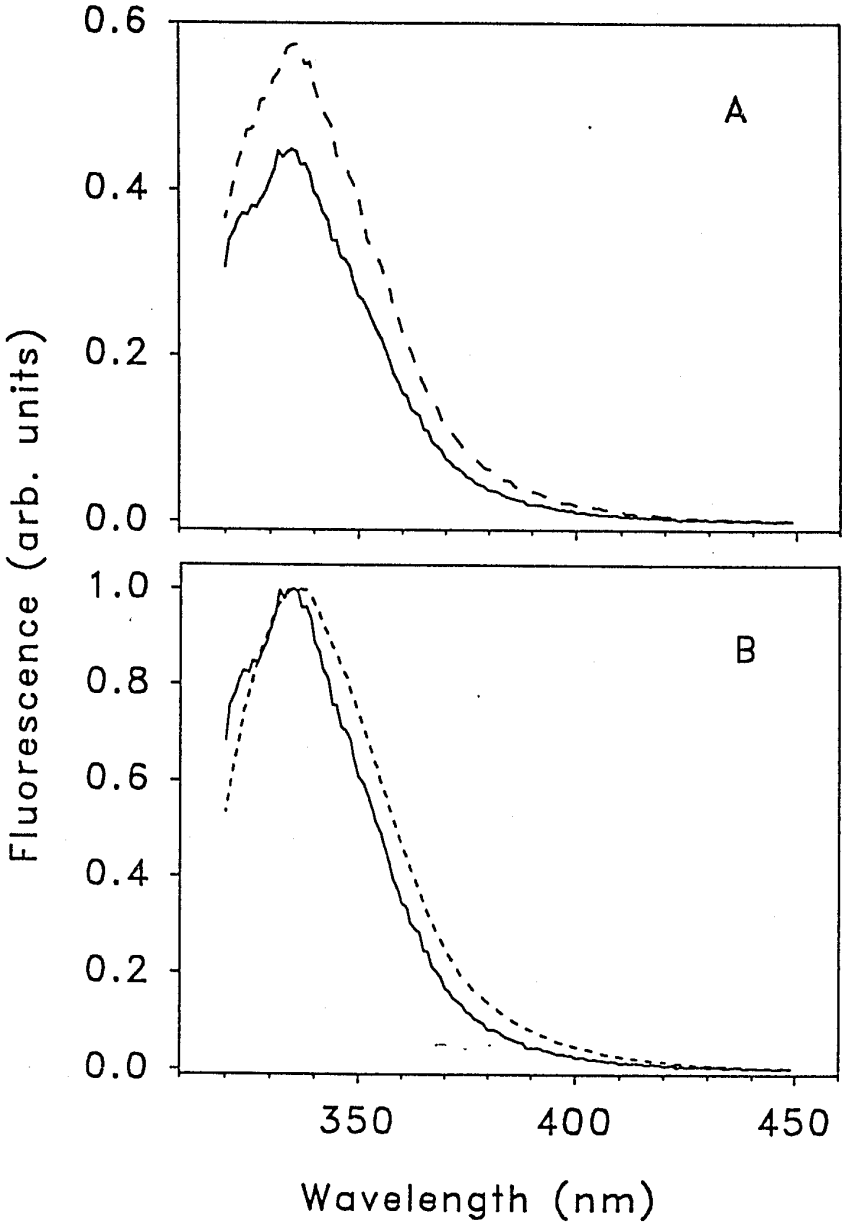

Figure 4.7: 5HW-AMP Fluorescence Corrected steady-state fluorescence emission spectra at 310 nm excitation. (-) TrpRS·5HW-AMP; and (- -) the same material with a 2-fold excess of inorganic pyrophosphate. A. Spectra prior to normalization. B. Normalized spectra highlighting the blue-shift and structured blue edge of the 5HW-AMP fluorescence.

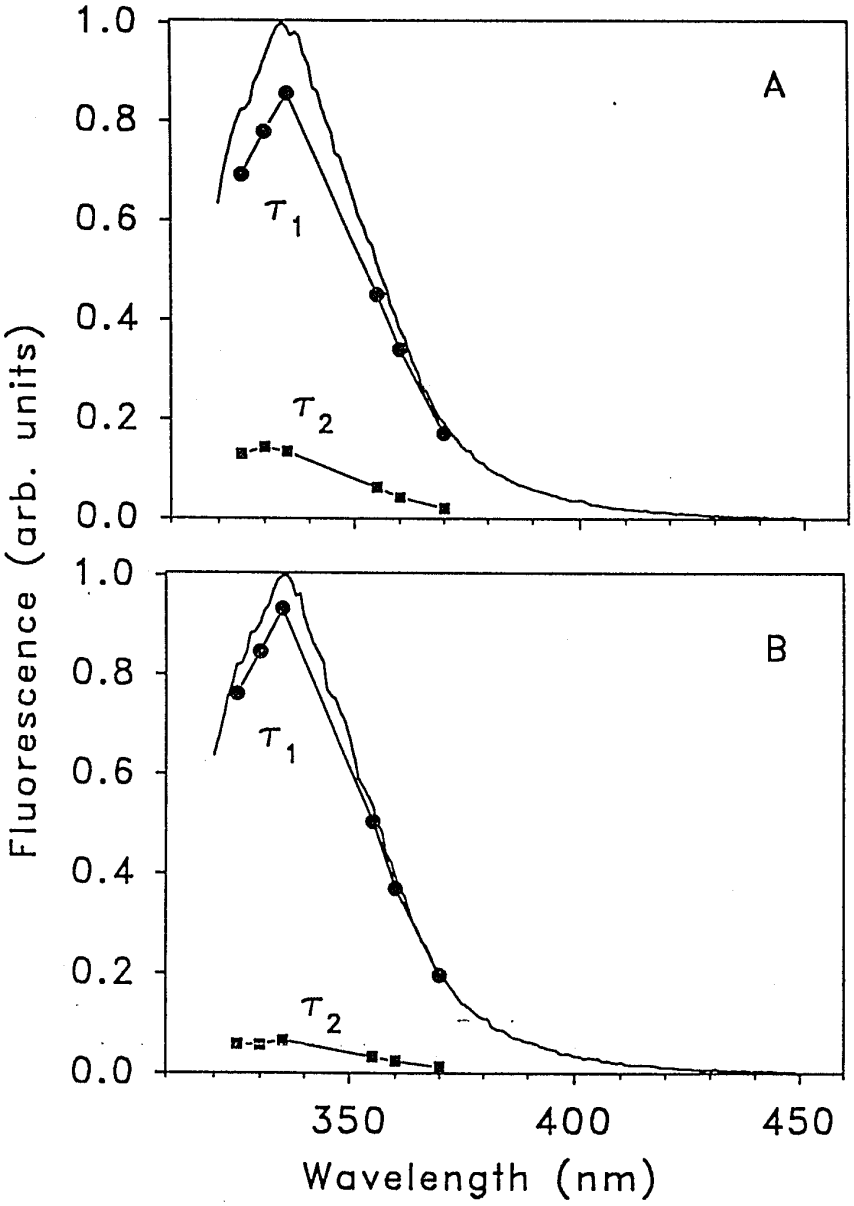

Figure 4.8: DAS of the TrpRS·5HW-AMP complex A. The decaying TrpRS·5HW-AMP complex. B. TrpRS·5HW-AMP after the addition of a 2-fold excess of PP_i.

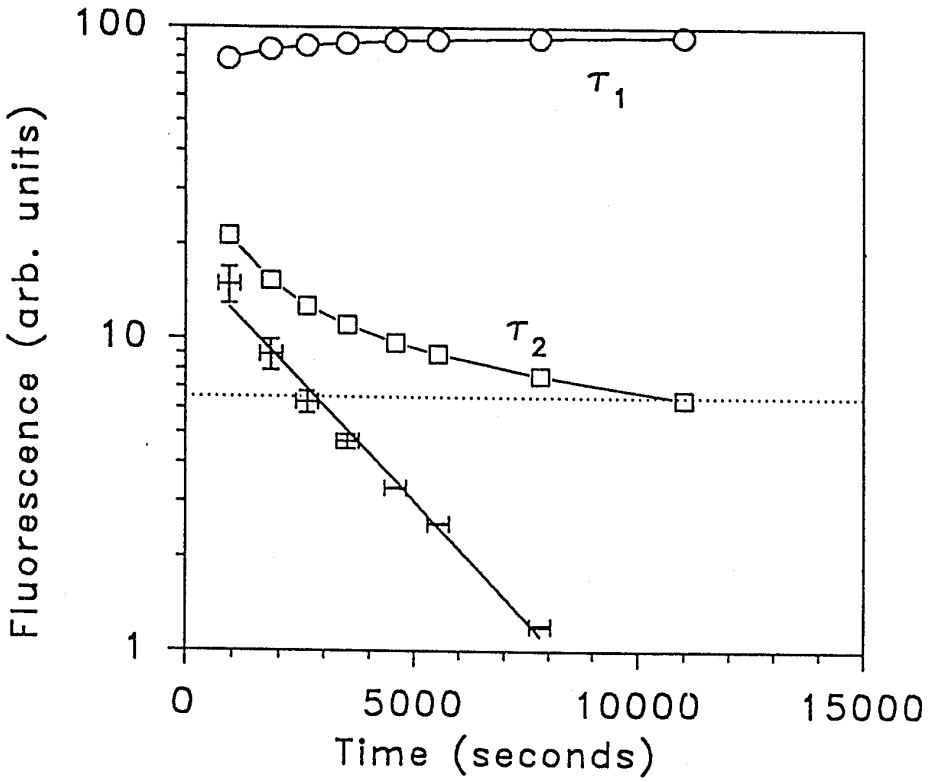

Figure 4.9: Rate of 5HW-AMP hydrolysis. Semi logarithmic plot of the change in 5HW-AMP fluorescence with time. Percent fractional contribution of (∘) the τ_1 component and (▫) the τ_2 component with time. Dotted line represents residual protein fluorescence contribution to τ_2. The dissociation of the TrpRS·5HW-AMP complex is assigned to the fractional fluorescence of τ_2 above that of the dotted baseline. Horizontal error bars represent the fluorescence decay collection time. Vertical error bars represent the change in steady-state fluorescence during the measurement period.

semilogarithmic plot of this data was performed. The final fractional fluorescence of τ_2 attributed to the enzyme was subtracted from the fractional fluorescence of the short decay time for each time point. Assuming first-order kinetics this analysis gave a half-life of 33 min for the TrpRS·5HW-AMP complex. This was very much shorter than that of the TrpRS·7AW-AMP complex.

4.4 Discussion

Tryptophan analogs have promising utility for studying protein-protein interactions, where one protein may contain a single tryptophan analog, and the other protein may contain one or many normal Trp residues. The TrpRS system could be considered a simple model of more ambitious studies of protein protein interactions. This system involves a protein with a Trp residue (TrpRS) interacting with the "minimalist" Trp analog entity: the amino acid itself. Hence it contains the same essential chromophores in similar proportions to those that would be observed in a protein-protein interaction.

4.4.1 Analog Aminoacyl-Adenylates in TrpRS

Column chromatography indicated that it was possible to prepare TrpRS bound aminoacyl-adenylates of 5HW and 7AW, but not of 5MeOW and 1MW. Compared to the absorbance of enzyme alone there was an increase at 310 nm due to the 5HW or 7AW and an increase at 260 nm due to the absorbance attributed to the adenine in the complex. Since 7AW has a lower extinction coefficient than 5HW at 310 nm (Table 4.1) it would be expected that the 310 nm shoulder of the TrpRS·5HW-AMP would be higher than that of TrpRS·7AW-AMP if both adenylates were present in equal

stoichiometric amounts. However, the absorbance at 310 nm and at 260 nm was greater for the TrpRS·7AW-AMP complex indicating that more of it formed than TrpRS·5HW-AMP. The lower amount of the TrpRS·5HW-AMP complex may be due to either its slower rate of formation and/or a faster rate of dissociation and subsequent hydrolysis of the released 5HW-AMP. The latter is most certainly a factor for 5HW-AMP, as it was much less stable than 7AW-AMP, or the aminoacyl-adenylates of Trp and 4FW described in Chapter 3.

It has already been shown that 7AW and 5HW are useful as new intrinsic fluorescence probes in proteins because they are both capable of exclusive excitation in the presence of Trp. Since 1MW and 5MeOW have significant absorbance at $\lambda > 300$ nm they are candidates for use as intrinsic fluorescent Trp analogs. An unreported previous failure to obtain a 5MeOW incorporated mutant of oncomodulin in earlier work (Hogue et al., 1992) demonstrated that 5MeOW was not capable of biosynthetic incorporation in *E. coli*. As a result, the failure to make an adenylate complex with 5MeOW in *B. subtilis* TrpRS is not surprising. The extended red edge of 5MeOW, like that of 5HW, is an enticing feature that could be exploited for intrinsic fluorescence studies. Any of these analogs may still be useful for the creation of synthetic peptides for similar studies.

4.4.2 7-Azatryptophanyl-Adenylate

As discussed in Chapter 2, the parent chromophore 7AI is capable of undergoing a tautomerization reaction catalyzed by solvent hydroxyl groups as found in water and alcohols (Chou et al., 1992; Chapman and Maroncelli, 1992). In aprotic solvents the quantum yield of 7-azaindole is large, e.g. 0.38 in acetonitrile (Chapman and Maroncelli, 1992). In water and in alcohols, the 7AI quantum yield is very small,

e.g. 0.032 in H_2O. In the experiments reported herein the significantly high level of 7AW fluorescence in the TrpRS·7AW-AMP complex was suggested to be due to the binding of 7AW-AMP into the hydrophobic (Shi et al., 1989) L-Trp specific binding pocket of the enzyme. The decay time, emission maximum and quantum yield of buried 7AW-AMP most closely matched those of 7AI and 1M7AI in aprotic solvents such as acetonitrile and diethyl ether (Chapman and Maroncelli, 1992), rather than those of 7AI in alcohols. The results, together with the failure of 1MW to form an adenylate complex, indicate that hydrogen bonding of the indole N-H of substrate Trp-AMP may be very important in the binding of the adenylate in the enzyme.

The half-life of the TrpRS·7AW-AMP complex calculated from Figure 4.6 is 9.2 hours. 7AW-AMP is thus held by TrpRS in the absence of PP_i, but not as tightly as Trp-AMP and 4FW-AMP, which showed no evidence of breakdown even after 8 hours. This shows that the high-energy activated amino acid is held for a extremely long time in the active site. This would preserve the energy of amino acid activation for a later reaction with $tRNA^{Trp}$.

A very small amount of the original long-lifetime 10 ns component, assigned to the bound 7AW-AMP, remained after PP_i treatment. Time-resolved fluorescence measurements of incubations of TrpRS with stoichiometric amounts of combinations of AMP, 7AW, Mg^{2+} and PP_i were performed to see if this component could be attributed to the equilibrium binding of 7AW into the active site. A long decay time component was never observed. Additional experiments were performed in order to try to account for this small amount of a 10 ns fluorescence component. It was shown that this was not due to any acyl-transfer products involving free AMP, as an excess of AMP added to the intact complex did not increase the amount of this 10 ns component remaining after PP_i treatment. The addition of subtilisin to the sample quickly removed this 10 ns component. This result suggested that the 10 ns component represents a very small amount of protein which had irreversibly "trapped" the 7AW-

AMP, possibly in an alternate conformation or perhaps in an aggregated state. Another important conclusion of these combination experiments is that there was no spectroscopic evidence of 7AW binding in the absence of ATP. This was consistent with the sequential mechanism of ATP binding before Trp, as shown by the inhibition studies of B. *subtilis* TrpRS kinetics of (Xu et al., 1989).

In an early report Schlesinger (1968) showed that 7AW incorporated in alkaline phosphatase had an intense, blue-shifted fluorescence in buffer. Upon denaturation in 6 M guanidine-HCl, the fluorescence intensity decreased, becoming more like the free amino acid. These results were consistent with the observations of 7AW seen here, a highly blue-shifted and intense fluorescent emission from a buried 7AW, and a much weaker red-shifted emission from a solvent exposed 7AW.

More recently, Petrich and coworkers (Négrerie et al. 1990) reported experiments with a peptide containing 7AW which was reported to interact with a protease resulting in a change in the fluorescence decay time from 870 ps to 675 ps and a blue shift of the fluorescence maximum when bound to the protein. These results were explained as being consistent with the similar changes observed for 7AI in a less polar alcohol. The decrease in decay time was attributed to the binding of the 7AI side chain into a hydrophobic pocket of the enzyme and the inability of forming hydrogen bonding complexes involving N1 and N7 with H_2O. The results here contradict this interpretation.

The observations reported herein, indicate that when 7AW is located in a hydrophobic pocket or core of protein, the formation of N1 and N7 hydrogen bonded complexes with water is prevented. This results in a significant increase of fluorescence intensity with a concomitant increase in the excited state decay time, and blue shift of the emission maximum. Our observations suggest that either H_2O is not entirely excluded from the binding pocket of *Streptomyces griseus* proteinase B, or this pocket contains polar residues which may hydrogen bond to the 7AW residue causing

tautomerization. It is known that this protease apparently indiscriminately binds several bulky hydrophobic amino acid side chains such as Trp, Tyr or Leu (Bryant et al., 1976) and the mM inhibition constants for both the D- and L-7AW peptides were not consistent with specific binding (Rich et al., 1993).

4.4.3 5-Hydroxytryptophanyl-Adenylate

The spectra of the complex of 5HW-AMP shows only a very small change in λ_{max} (Fig. 4.7). If the fluorescence of 5HW were sensitive to dipolar relaxation, a larger difference between its fluorescence spectra in the complex would be expected. However the λ_{max} of 5HW seems to be somewhat invariant, remaining in the range between 334-336 nm. This is similar to Tyr, which is also insensitive to dipolar relaxation, with emission λ_{max} values between 304-306 nm (Ross et al., 1992). Two decay spectra in Figure 4.8 show that the structured blue edge arises from the short decay component fluorescence of 5HW.

The double exponential decay behaviour of 5HW-AMP could be interpreted as originating from two conformational states within the enzyme complex. These may represent a bound conformation and hydrolytic conformation, as were implied by other proofreading aminoacyl-tRNA synthetases. Alternatively these might represent 5-hydroxyindole side chain rotamers within the active site, or possibly conformational heterogeneity of active site residues.

It is also conceivable that the 3.8 ns decay time observed arises only from hydrolyzed, free 5HW together with a contribution from the enzyme Trp-92 fluorescence. But this is not consistent with the overall blue shift of the spectrum in Figure 4.7 B. This would leave the 1.15 ns component assigned to the bound 5HW-AMP together with a contribution from enzyme fluorescence. From the DAS of the

TrpRS·5HW-AMP complex (Figure 4.8 A) and Table 3.3, the 3.8 ns component α represented 62% of the fluorescent species, and provided 85% of the total fluorescence, the remainder being associated with the 1.15 ns component. If this 62% represents previously hydrolyzed 5HW, this would necessarily imply an even faster hydrolytic process, in addition to that depicted in Figure 4.9, which could not possibly be observed with the methods used here. Such a process would have a half-life on the order of magnitude of the duration of the data collection time, 2 minutes, and would imply there is a cooperative effect, i.e. two hydrolytic rates. However, no such cooperativity was observed in the slower 7AW-AMP hydrolysis in Figure 4.6. In addition, the enzyme was not fully saturated upon elution, so it is unlikely that cooperativity would be observed. Only 1 out of every 5 monomers was filled, according to the absorbance of the eluted complex. These points argue in favor of conformational heterogeneity in the 5HW-AMP complex. Two exponential decay times could also be assigned to the Trp-AMP complex (section 5.4.4).

5HW is a natural amino acid but has not been reported to be found in the amino acid primary sequence of any natural protein. In higher eukaryotes 5HW is a precursor to serotonin (5-hydroxytryptamine). Early experiments with bovine pancreatic TrpRS showed that 5HW was not a substrate (Sharon and Lipman, 1957). A mammalian TrpRS could be expected to more strongly discriminate against 5HW due to the larger amounts of 5HW present from the production of serotonin.

Aminoacyl-tRNA synthetases could undergo editing or proofreading of noncognate amino acids (Friest, 1991). Pretransfer proofreading occurs when the noncognate aminoacyl-adenylate is hydrolyzed prior to tRNA aminoacylation. This is monitored indirectly by determining the ratio of AMP generated to tRNA aminoacylated (Xu et al., 1989). Excess AMP generated is evidence of hydrolytic proofreading. The spectral properties of 5HW and 7AW have allowed the direct monitoring of the loss of their TrpRS aminoacyl-adenylate complexes. The

TrpRS·5HW-AMP complex is 16 times more likely to dissociate and hydrolyze than the TrpRS·7AW-AMP complex.

Xu and coworkers (1989) showed that 5-fluorotryptophan is a better TrpRS substrate than Trp. They correlated substrate hydrophobicity with its kinetic behavior in TrpRS, demonstrating that the selectivity of the TrpRS active site is dependent on hydrophobicity. Other demonstrations of 5-methyltryptophan incorporation (Barlati and Cifferi, 1970) indicate there is sufficient room for substituents the size of a hydroxyl or methyl group on position 5 of the indole ring. Failure to accommodate a methoxyl group indicates there is a limit to the size of substituent that can be fit by the binding pocket.

It is possible that the bacterial tryptophanyl-tRNA synthetase has also experienced some evolutionary pressure against its reaction with 5HW. A kind of *in vivo* proofreading of *B. subtilis* TrpRS against 5HW could be inferred from early experiments with 5HW incorporation into a Trp auxotroph of *B. subtilis* (Barlati and Cifferi, 1970). In that study, 5HW incorporation halted with the addition of 1/10 the concentration of Trp. A pretransfer hydrolytic proofreading mechanism of TrpRS may serve to prevent mischarging of $tRNA^{Trp}$ with 5HW in the presence of Trp. The inefficient formation of the TrpRS·5HW-AMP complex and rapid loss of any 5HW-AMP adenylate which did form supports this understanding.

4.4.4 TrpRS Structural Specificity

Piel et al., (1983) have previously studied a series of derivatives of ATP and chemically synthesized tryptophanyl-adenylates in reactions with yeast TrpRS and $tRNA^{Trp}$. They demonstrated that aminoacylation of $tRNA^{Trp}$ and Trp-AMP formation are linked, and that the nucleotide binding pocket is identical for both ATP

and the adenylate. Only sporadic attempts at studying the Trp substrate specificity of TrpRS *in vitro* have so far been attempted. Many inferences on the substrate specificity of TrpRS could be made from *in-vivo* studies of analog incorporation.

Yeast undergoes inhibition of enzyme synthesis with Trp analogs, the effect of inhibition in the order: 2AW > 6MW > 5MW > 4MW > 4,6-dimethyltryptophan (Halvorston et al. 1955). Some of these effects were exerted on Trp biosynthetic pathways, others on TrpRS inhibition. It was shown that 4MW was a competitive inhibitor of yeast TrpRS and did not participate in tRNA aminoacylation *in-vitro* (Stäheli et al., 1981). This report also stated that 5MW did not inhibit the *in-vitro* TrpRS reaction with Trp; and that 5FW was incorporated into yeast protein, but 5MW and 4MW were not. However the strains of yeast used in this study were not Trp auxotrophs, and biosynthetic incorporation of these analogs would suffer from competition with Trp. Under these conditions, only the analogs that are capable of competing with Trp would show incorporation, in this case 5FW. 5FW was shown to be a superior substrate compared to Trp for both bovine (Nevinsky et al., 1974) and *B. subtilis* TrpRS (Xu et al., 1989). Using a Trp auxotroph, 5HW has been shown to be incorporated into expressed mating-factor peptides in yeast (J.B.A. Ross, personal communication). Hence incorporation experiments using yeast auxotrophs may also demonstrate the incorporation of other Trp analogs, such as 5MW.

Mammalian TrpRS specificity has also been studied. One early contribution (Sharon and Lipmann, 1957) compared the results of *in-vitro* bovine pancreatic TrpRS analog experiments with *in-vivo* studies using *E. coli* auxotrophs. However problems in interpretation arise from their assumption that TrpRS is homogeneous across species boundaries. They demonstrated that the aminoacyl-adenylates of 5FW, 6FW, 7AW, and 2AW could form in bovine pancreatic TrpRS. They showed that the aminoacyl-adenylates of 5MW, 6MW, 5HW, 6HW, ßMW and indolyl-2-L-alanine do not form. Some of these did, however, inhibit the formation of Trp-AMP, in the order ßMW >

5HW > 5MW = D-Trp >> 6MW, using a 200:1 ratio of analog to Trp. This study shows bovine TrpRS exhibits a clear *in-vitro* discrimination against the larger methyl or hydroxyl substituents at the 5 and 6 indole ring positions. 4,5,6,7-tetrafluorotryptophan was demonstrated to acylate yeast $tRNA^{Trp}$ using the bovine pancreatic TrpRS (Knorre et al., 1971). The $tRNA^{Trp}$ of these species share A73 as the discriminator base, and hence these will cross-react (Xue, 1993). 4FW, 5FW, 6FW, 7FW as well as 5,7-difluorotryptophan and 4,5,6,7-tetrafluorotryptophan were all shown to be bovine TrpRS substrates (Nevinsky et al., 1974). One report of the use of a ternary complex involving bovine TrpRS, 4MW and *E. coli* tRNA to purify *E. coli* $tRNA^{Trp}$ exists, (Preddie, 1969) although such a complex is dubious since *E. coli* $tRNA^{Trp}$ does not cross react with bovine pancreatic TrpRS (Xue, 1993). An attempt here to repeat this work, using *B. subtilis* TrpRS failed. No additional information on the possible incorporation or activity of 4MW could be found for bovine TrpRS.

Prokaryotic TrpRS specificity has been illustrated by many *in-vivo* studies with analogs, including the early work of Pardee et al. (1956) who demonstrated 7AW and 2AW incorporation into *E. coli* Trp auxotrophs and phage proteins, but asserted that 5MW was not incorporated. 5MW and 5HW were later demonstrated to be incorporated into protein of a *B. subtilis* auxotroph, however the incorporation halted when small amounts of Trp were added (Barlati and Ciferri, 1970). 5MW was shown as an *in-vitro* substrate for *E. coli* TrpRS, $tRNA^{Trp}$ aminoacylation (Thang et al., 1973) however it could be inhibited up to 50% by a tiny amount of Trp present (1/1000 Trp:5MW). Thang and coworkers overlooked the earlier relevant work of Barlati and Ciferri, but pointed out that important differences between incorporation experiments with auxotrophs and non-auxotrophs which result in conflicting results for the *in-vivo* incorporation of Trp analogs. Fluorinated analogs 4FW, 5FW and 6FW were demonstrated to be incorporated into *E. coli* proteins (Pratt and Ho, 1975). 5HW was first shown to be incorporable into *E. coli* proteins only recently (Hogue et al., 1992).

The inability of *B. subtilis* TrpRS to react with 1MW and 5MeOW are results with analogs not previously studied with TrpRS. These were chosen on the basis of promising spectral properties, however structural information may be obtained from these experiments. The failure of 1MW to form an aminoacyl-adenylate suggests that the indole N-H of substrate Trp may be required for enzymatic recognition by TrpRS, probably through hydrogen-bond interactions. This understanding is supported by the crystal structure, which shows the side chain of Asp-132 of *B. stearothermophilus* TrpRS within hydrogen bonding distance of the substrate indole N-H (Doublié et al., 1994).

The failure of 5MeOW to act as a substrate seems to define the steric limits of this TrpRS binding pocket as only being large enough to accommodate 5HW or 5MW. It should be possible to modify the Trp binding site of TrpRS through site-directed mutagenesis to accommodate both 5MeOW and 1MW. For example, a mutation of Ser-6 to Ala should enlarge the Trp binding site enough to accommodate 5MeOW, and the mutation of Asp-132 to Ala should accommodate 1MW. *E. coli* PheRS was recently modified at a conserved Ala-294 residue to Gly or Ser (Ibba et al., 1994). Using para-halogenated Phe analogs, they correlated PheRS activity with substrate size. The Gly-294 PheRS mutant was now capable of incorporating p-Cl-Phe into proteins, attributed to enlargening the size of the Phe binding pocket. Tyr was activated to an adenylate complex in this PheRS mutant, but hydrolytic proofreading prevented its aminoacylation onto $tRNA^{Phe}$. This study of PheRS indicates mutagenesis of TrpRS could be a successful strategy in developing biosynthetic incorporation techniques for these desirable analogs of Trp and allowing their use as intrinsic fluorescence probes.

4.5 Summary and Conclusions

Both 5HW and 7AW have unique spectral properties which could enhance the information available from protein fluorescence experiments. These experiments and those reported much earlier (Schlesinger, 1968) indicate that 7AW undergoes very large changes in its fluorescence properties on going from a polar to a non-polar environment. The longer decay time of a buried 7AW residue renders it more useful for dynamic studies with fluorescence anisotropy. The polarity dependence of the 7AW fluorescence could be used to monitor protein refolding events as well as conformational changes and ligand binding.

This work demonstrates that some non-protein amino acids should be considered when discussing aaRS specificity and proofreading, as evolutionary developments of more amino acids, like neurotransmitter precursors, could place additional strain on the fidelity of protein synthesis. The proofreading observed for 7AW and 5HW, but not for Trp and 4FW might be a result of their differences in hydrophobicity, as previously correlated for the TrpRS active site with fluorotryptophan analogs (Xu et al., 1989). The observations of non-reactivity with 1MW and 5MeOW and the previously unreported non-incorporation of 5MeOW, define structural limitations within the TrpRS Trp substrate binding site.

This work shows it is possible to obtain a preliminary determination of the potential for incorporation of Trp analogs in proteins. The fluorescence experiments with the Trp analogs as TrpRS substrates have shown the potential of their use as mechanistic probes of TrpRS functionality. The growing use of such analogs demonstrates their significant potential in protein studies. As a model system for future protein-protein interactions, this work cautions of the long absorbance tail of Trp residues in some proteins, which could contribute to the total fluorescence at 310 nm. Further extending the excitation to $\lambda > 315$ may be more suitable.

Chapter 5

TRP ANALOG REPLACEMENT OF TrpRS TRP-92

TRP ANALOG REPLACEMENT OF TrpRS TRP-92

5.1 Introduction

Intracellular protein synthesis begins with the specific activation of each of the 20 amino acids by their cognate aminoacyl-tRNA synthetase. Protein engineering studies need not be limited to these 20 amino acids, but could be expanded to include other amino acids which can act as substrates for aminoacyl-tRNA synthetases. Recombinant protein expression has afforded methods which allow for the production of high yields of expressed proteins in bacteria. Simple modifications of these methods permit large amounts of proteins to be produced with certain amino acids which are usually toxic to bacteria (Hogue et al., 1992). Despite the possibilities for protein engineering, little use has been made of amino acid analogs with the important exception of fluorinated amino acids used for ^{19}F NMR, as stated in Section 1.3.2. This could be attributed to a lack of identifiable usefulness and to the unknown structural or functional consequences of the incorporation of amino acid analogs.

Fersht has made a classification of mutations based on amino acid structural considerations (Fersht et al., 1987). According to this scheme, it is not possible to replace Trp in a conservative manner with the other 19 protein amino acids, because it is the largest of the amino acids. Any other amino acid substituting for Trp in a hydrophobic core would result in a cavity that requires filling by solvent or by alteration of the protein structure. However isomorphous Trp analogs are expected to behave as conservative substitutions and provide similar packing volumes as Trp.

The enzyme tryptophanyl-tRNA synthetase is responsible for the recognition of these Trp analogs and their subsequent aminoacylation of $tRNA^{Trp}$. The single tryptophan residue at position 92 of *B. subtilis* TrpRS (Chow and Wong, 1988) has been identified as essential for the activity of the enzyme (Chow et al., 1992). Mutants of position 92, W92F, W92A and W92Q, were inactive. In Chapter 3, section 3.4.1 it

was concluded that the W92F mutant was fundamentally unstable, which was attributed to the inability of Phe to replace the side-chain volume of the conserved Trp. The replacement of Trp-92 with Trp analogs offers a similar side-chain volume, and a mutagenic route that could preserve enzymatic activity.

Both the single Trp-92 of TrpRS and substrate Trp have revealing fluorescence parameters, but these were difficult to independently measure due to their competing fluorescence. This was overcome somewhat by comparing the effects of D- and L- Trp in Chapter 3. In Chapter 4, it was suggested that TrpRS can be considered a model system for studying the utility of analogs for more complex protein-protein interactions. In this chapter, studies with the substrate $tRNA^{Trp}$ demonstrate that TrpRS, incorporated with Trp analogs, can be used to examine protein-nucleic acid interactions, as well as those with other chromophoric and fluorophoric substrates, such as Trp.

Incorporable Trp analogs with useful fluorescence properties have been identified and discussed in earlier chapters; 5HW, 7AW, and 4FW (Sections 1.3 and 2.4; Figure 2.16). Incorporation of these tryptophan analogs into proteins can allow previously ambiguous measurements of the fluorescence parameters of protein-protein and protein-nucleic acid interactions to be made using their intrinsic fluorescence. In order to examine the fluorescence properties of substrate Trp, removal of the intrinsic fluorophore Trp-92 was required. 4FW is nonfluorescent, and was used in Chapter 3 to facilitate fluorescence studies of Trp-92 in the enzyme. Since the site-directed mutant W92F was inactive, the one strategy remaining was to prepare an active enzyme without Trp fluorescence by replacing Trp-92 with 4FW. The fluorescence of Trp-92 of TrpRS is only marginally sufficient when examining complexation and interactions of enzyme with stoichiometric amounts of $tRNA^{Trp}$, and data collection is difficult. This is due to the competing absorbance of the $tRNA^{Trp}$. In order to overcome this,

incorporation of 5HW and 7AW which provide extended red absorbance that is well beyond that of $tRNA^{Trp}$ would be useful.

Tryptophan analogs which are toxic to bacteria, such as 4FW, 7AW and 5HW, can be incorporated into expressed proteins using a "bait and switch" approach (Hogue et al., 1992). This technique requires a controllable protein expression system that can be "switched-on" by some perturbation. Examples include substrate-sensitive or, heat-sensitive promoters which are attached to the gene encoding the protein of interest. An auxotrophic organism (bacteria or yeast) which does not produce its own Trp is also required. The analog is incorporated into the desired protein with a simple procedure. First the organism is grown in a limited fashion in the presence of Trp. Then the Trp containing media is replaced with media lacking Trp, but containing the Trp analog. At this point the expression of the recombinant protein is initiated, and protein synthesis is forced to incorporate the Trp analog into the newly-made protein, rather than Trp.

This technique allows substantial amounts of incorporated protein to be made, despite the toxicity of analogs. Here, cells are not required to duplicate in the presence of these toxic Trp analogs, instead duplication was allowed to occur in the presence of Trp. This allows a large number of cells populated with active protein synthetic machinery to be established prior to addition of the analog. The inactivity of a single essential protein which is incompatible with an analog substitution could halt cell duplication. This method separates cell duplication from the expression of the desired analog incorporated protein, so the yield of protein is expected to be less sensitive to analog inactivation of other proteins.

The requirements for analog incorporation are thus a controlled, inducible expression system for the desired protein in an auxotrophic host organism. A modification to the TrpRS expression system was required to achieve this for TrpRS production with analog incorporation. The plasmid pKSW1 (Shi et al., 1989) contains

the *trpS* gene (Chow and Wong, 1988) encoding *B. subtilis* TrpRS downstream to a *tac* promoter (Amann et al., 1983) in the pKK223-3 expression vector (Pharmacia) with ampicillin resistance. In the original expression system (Shi et al., 1989) TrpRS production is repressed by the *lac* repressor protein which is encoded by the *lacI*^{q} gene of the JM109 host *E. coli* strain. This protein binds to the *tac* promoter, and stops RNA polymerase from making mRNA, thereby limiting protein synthesis. Expression of TrpRS is derepressed when isopropyl-ß-D-thiogalactoside (IPTG) is added to the medium. IPTG binds to *lac* repressor protein, causing it to dissociate from the *tac* promoter. This allows mRNA to be made, and subsequent protein synthesis. The tryptophan auxotroph strains CY15077 (W3110 tnaA2 ΔtrpEA2), and W3110 A33 do not have the *lacI*^{q} gene and hence cannot maintain the *tac* promoter in a repressed state. In order to repress the expression of TrpRS in the auxotroph strains, a second plasmid containing the *lacI*^{q} gene was required. The plasmid pMS421 has *lacI*^{q} with streptomycin/spectinomycin resistance and is derived from pSC101 (Churchward et al., 1984). Hence pMS421 is compatible with pBR322 derived pKSW1, i.e. they can coexist in a single host cell. Selection with both ampicillin and streptomycin would maintain both plasmids simultaneously in the bacteria (Ross et al., 1992a).

In the process of preparing and characterizing these analog incorporated enzymes, the kinetic parameters for $tRNA^{Trp}$ aminoacylation were measured. In a previous study of TrpRS using fluorinated analogs as substrates, (Xu et al., 1989) a correlation between hydrophobicity and kinetic parameters was established. In Chapter 3 the importance of Trp-92 and its role in conformational changes was postulated. Here Trp analogs in position 92 are examined for their effects on $tRNA^{Trp}$ aminoacylation kinetics to further define the mechanistic role of Trp-92.

5.2 Methods and Materials

5.2.1 Materials

Purification of Trp analog mutants followed methods described in Chapter 3. Additional reagents used are listed here. The Trp auxotroph *E. coli* strains CY15077 (W3110 tnaA2 ΔtrpEA2) and the strain AB1899 pMS421 (originating from M. Susskind, Ammanson Center For Biol. Research, Los Angeles) were kind gifts of Dr. C. Yanofsky. The strain W3110 A33, (originating in the laboratory of Dr. C. Yanofsky) was a kind gift of Dr. E. Li. Molecular biology grade phenol, streptomycin, agarose, ethidium bromide, triton-X-100, CDTA, casamino acids, EcoR1, were all obtained from Sigma Chemical Co., St. Louis, Missouri. Electro-transformation was performed using a GenePulser apparatus, BioRad Laboratories, Richmond, California. Glucose and chloroform were obtained from BDH Inc., Toronto, Ontario. Antibiotics were used in media at a concentration of 0.5 g/l.

5.2.2 Transformations into Trp Auxotrophs

Construction of the TrpRS expression system followed the scheme depicted in Figure 5.1. First the plasmid pMS421 was isolated from the parent strain AB1899 pMS421. Isolation from a 500 ml culture was necessary since the pMS421 plasmid has a low copy-number (Sambrook et al. 1989). The strains W3110 A33 and CY15077 were transformed with pMS421. Transformants were selected on LB agar plates containing streptomycin. Mini-plasmid preparations (Sambrook et al. 1989) were used to isolate plasmid from positive colonies and the 5.7 kilobase pMS421 was identified from its 1.7 kilobase *lacI*^{q} containing EcoRI digest fragment after 8% agarose gel electrophoresis (not shown). The strains W3110 A33 pMS421 and CY15077 pMS421 were thus obtained. The TrpRS bearing plasmid pKSW1 was electrotransformed into

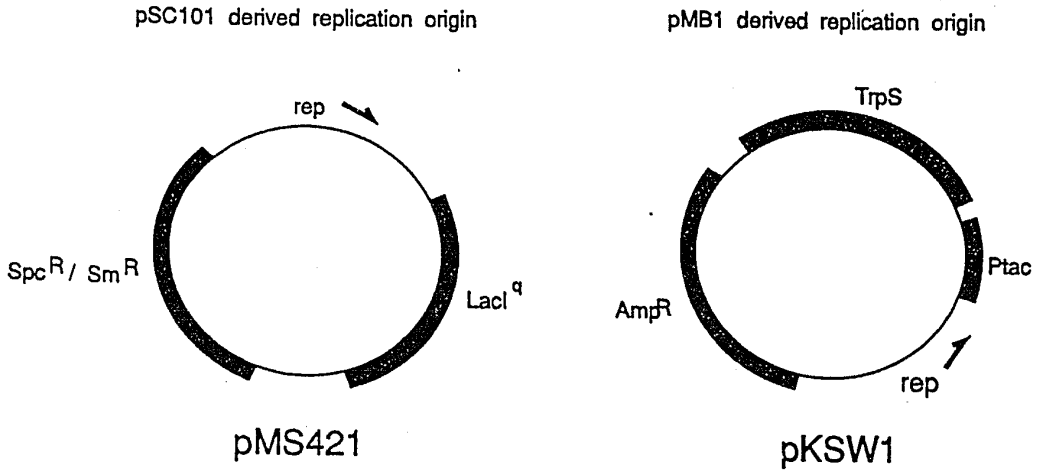

PARENT STRAIN
Eschericia coli CY15077 (W3110 tnaA2 ^trpEA2)

Transform with pMS421, screen colonies with Streptomycin.
Check Trp auxotrophy
INTERMEDIATE STRAIN
Cy15077 pMS421

Transform with pKSW1, screen with Ampicillin + Streptomycin
Check for inducible TrpRS expresion, Trp auxotrophy
DESIRED STRAIN
CY15077 pMS421 pKSW1

Figure 5.1: Schematic for the construction of the TrpRS expression system.

the strain CY15077 pMS421, creating the desired strain CY15077 pMS421 pKSW1. Positive transformants were screened on LB agar plates containing streptomycin and ampicillin.

Colonies were tested for remaining Trp auxotrophy after each transformation step on plates containing M9 minimal media (Sambrook et al., 1989) supplemented with 1% casein acid hydrolysate, (Casamino acids, Sigma) (Ross et al., 1992a) together with the appropriate antibiotic. Trp auxotrophs would only grow in the above media when L-Trp was included (0.001% was sufficient). Casamino acids are inherently Trp-free because the conditions of acid hydrolysis destroy Trp in its preparation. This could be shown by the lack of characteristic Trp fluorescence.

Four of the CY15077 pMS421 pKSW1 transformants were tested for IPTG-inducible TrpRS expression as follows: Duplicate 25 ml cultures of CY15077 pMS421 pKSW1 were inoculated with 100 μl of an overnight culture of each transformant. LB media was used with the antibiotics streptomycin, and ampicillin. Cells were grown for 3 h, then IPTG was added to one of the cultures to a final concentration of 1 mM. Cells were incubated a further 3 h, then centrifuged at 5000 x g. Cells were resuspended in a 1.5 ml microcentrifuge tube with 300 μl of a solution of 0.1 M NaCl, 10 mM Tris, 1 mM EDTA and 5% Triton X-100, pH 8.0. Then 100 μl of 1 mg/ml lysozyme dissolved in a pH 8.0 solution of 10 mM Tris, 1 mM EDTA was added to lyse the cells. After 10 minutes the lysed cells were centrifuged (15000 x g) and the supernatant was used for SDS-PAGE using the Pharmacia PhastSystem with 5-15% gradient gels. Overexpression of the characteristic 36 kDa TrpRS monomer (Shi et al., 1989) could be seen in the IPTG-treated samples. These results indicated that CY15077 pMS421 pKSW1 had the desired characteristics of Trp auxotrophy, and derepressable expression of TrpRS using IPTG.

5.2.3 Growth and Incorporation of Trp analogs

Four-litre erlenmeyer flasks with aeration vanes, added by a glassblower, were used as culture vessels in a constant temperature 37° C shaker. First, three vessels containing 2 l of Terrific Broth (TB) (Sambrook et al., 1989) supplemented with streptomycin, ampicillin and twice the usual amount of glycerol, were inoculated with 6 ml of an overnight culture of CY15077 pMS421 pKSW1. Cell growth was monitored by absorbance at 600 nm. When the absorbance reached 1.5, the culture was cooled on ice for 10 minutes, then the cells were collected by centrifugation. Cells were gently resuspended and washed with 500 ml ice cold distilled, sterilized water and divided into equal volumes for incorporation trials. After another centrifugation, the cells were resuspended in separate 4 l flasks, each containing 2 l of M9 media at room temperature, supplemented with 1% casamino acids, ampicillin and streptomycin. Cells were returned to the shaker and cultured for 1 hour to deplete residual Trp. Afterward, the Trp analog and control Trp was added. The analog solutions contained 40 mg of DL- or 20 mg of L- amino acid. 4-fluoro-DL-tryptophan, DL-7-azatryptophan, 5-hydroxy-L-tryptophan, and L-tryptophan were dissolved in 10 ml water with 100 μl of 1.0 M NaOH to solubilize the analogs. These solutions were filter-sterilized, then added to the 2 l culture. Ten minutes after adding the appropriate amino acid, a sterile solution of IPTG was added to a final concentration of 1 mM. Cells were allowed to grow a further 5 hours, after which the cells were isolated by centrifugation, weighed and frozen at -80° C until required for purification.

5.2.4 Purification of Analog Incorporated TrpRS

A detailed method for purification has been described in Chapter 3. The method involves a batch adsorption of the cell lysate, taking advantage of the high

affinity of TrpRS for hydroxyapatite. Following this step, TrpRS is the only protein visible on a SDS-PAGE gel. However ion-exchange chromatography using DEAE Sephacel and a KCl gradient was used to remove nucleic acids, then the TrpRS was applied to a 2.5 cm x 1.1 m column of S-200 HR (Pharmacia), from which elutes a single 72 kDa peak. Peak fractions after gel filtration were pooled and dialysed against 4 changes of 4 L of Milli-Q water. Fractions were lyophilized in tared vessels and the dried proteins were weighed.

5.2.5 Spectroscopy

Solutions for spectroscopy were prepared from lyophilized enzyme dissolved at 5 mg / ml in 200 mM Tris-HCL, 20 mM MgAcetate, pH 8.6. This was subjected to a 15 cm column of Sephadex G-25 fine (Pharmacia) equilibrated with 10 mM K_2HPO_4, 100 mM KCl, pH 7.5. For fluorimetry the solutions were diluted to an absorbance of 0.100 or less at the excitation wavelength. Absorbance spectra were collected using an SLM D200 spectrophotometer with a 1 nm bandpass, thermostated at 20° C. Fluorescence spectra were collected using an SLM 8000C instrument with 4 nm excitation and emission bandpasses, with Glan-Taylor polarizers oriented to eliminate anisotropic effects. Spectra were corrected for buffer-only blank and for the wavelength dependence of the instrument response. Quantum yields were computed using standards described in Chapter 4. DAS were collected as described in the two previous Chapters. Substrate studies such as those involving $tRNA^{Trp}$ were performed as described in Chapter 3. Thermal denaturation of TrpRS and mutants was monitored with fluorescence, and with absorbance at 330 nm to detect light scattering to determine protein aggregation. 5 μM solutions of protein were used, with fluorescence spectra collected at temperature intervals of 2.5° C integrated from the following excitation

wavelengths: 280 nm; 300 nm for wild-type TrpRS; and 310 nm for W92(7AW) and W92(5HW).

5.2.6 Kinetics

$tRNA^{Trp}$ aminoacylation kinetics were determined using $tRNA^{Trp}$ expressed and purified as previously described (peak I, Xue et al., 1993). Reactions at 25° C were carried out in 200 mM Tris-HCl, 20 mM MgAcetate, in a total volume of 110 μl. Final concentrations of TrpRS were 0.27 nM, ATP 2.9 mM, Trp 0.23 μM (1:1 ^{3}H labelled:unlabelled) and 60, 75, 90, 113, or 151 nM $tRNA^{Trp}$. Details for the assay were given in Chapter 3 (Joseph and Muench, 1971; Xu et al., 1989).

5.3 Results

5.3.1 Expression of TrpRS

The strain CY15077 pMS421 pKSW1 was demonstrated to have both Trp auxotrophy and IPTG-inducible expression of TrpRS. The latter is demonstrated by the gel in Figure 5.2 from untreated and IPTG treated cultures. The overexpression of TrpRS is seen in the IPTG treated samples. Upon close inspection, bands corresponding to this molecular weight were seen in the non-IPTG treated controls. This would suggest that this promoter is capable of TrpRS leakage, which would accumulate a portion of TrpRS with Trp instead of analog during growth. This leakage was characterized later by spectroscopic methods.

The growth curve for the analog incorporation using the *E. coli* expression system CY15077 pMS421 pKSW1 is shown in Figure 5.3. The first portion of the

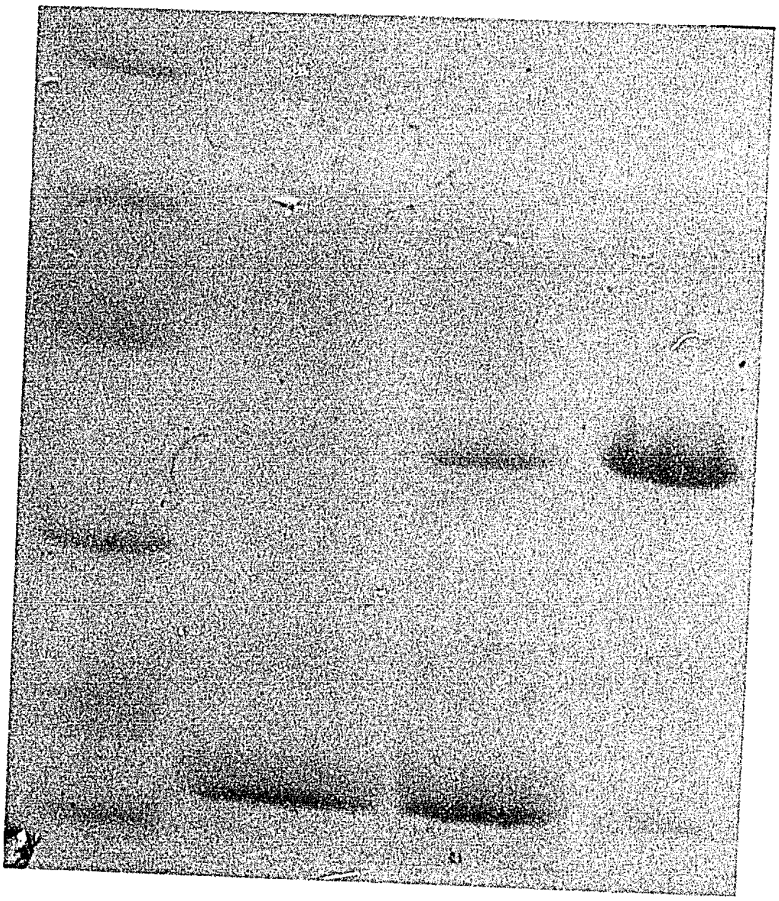

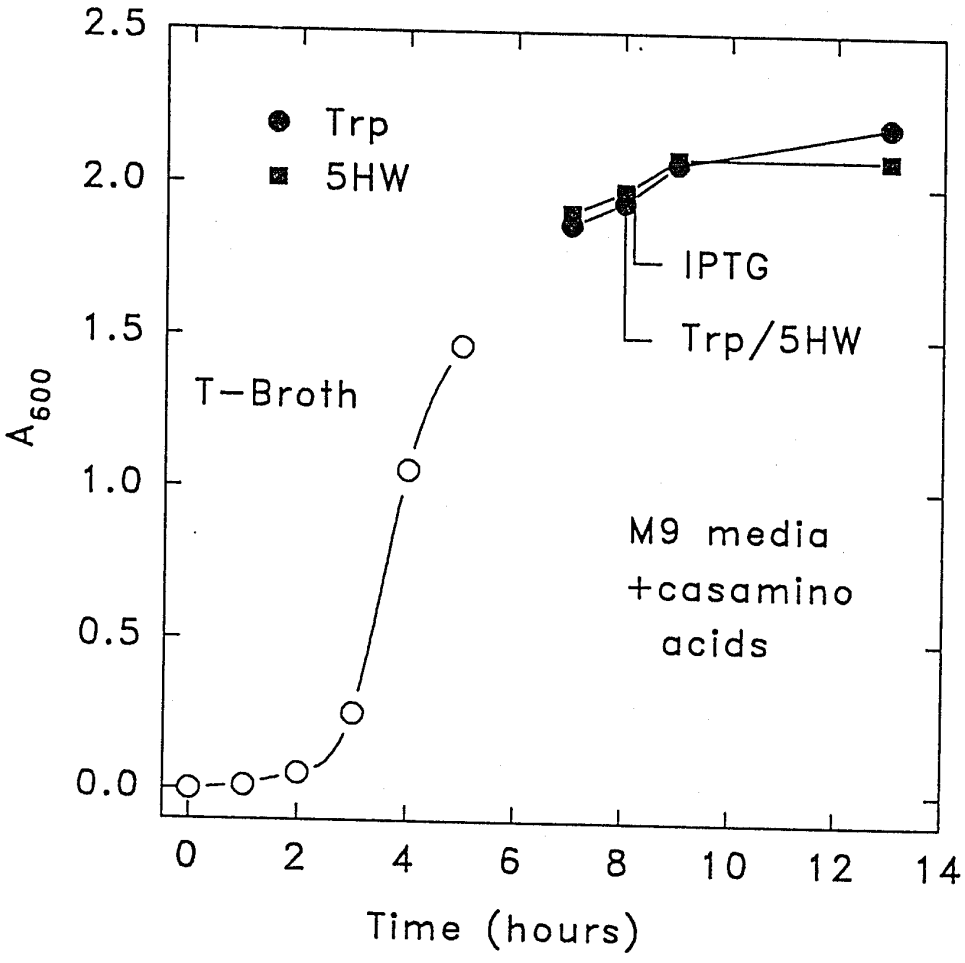

Figure 5.3: Growth curve of *E. coli* auxotroph CY15077 pMS421 pKSW1 containing the derepressable TrpRS expression system. Open circles represent the population of cells grown in Terrific Broth (see Materials and Methods). Filled circles are aliquots of cells cultured in M9 minimal media with casamino acids. The time of addition of Trp or analog, and the derepression of the expression system by IPTG are indicated. Circles represent Trp, and squares represent 5HW. 4FW and 7AW had data indistinguishable from that of 5HW.

growth curve represents the parallel growth of the whole population of cells in culture. The gap in the curve is due to the time required to perform the centrifugation steps to separate the cells from the first growth media (T-Broth) and to wash the cells with sterile distilled water. The last points on the curve represent the parallel incorporation of Trp and 5HW in M9 minimal media. Curves for 7AW and 4FW incorporation were indistinguishable from those of 5HW. Only the cells grown with control Trp showed measurable increases in absorbance due to light scattering. This result suggested that the analog treated cultures did not increase in number. Alternatively this increase in absorbance at 600 nm could represent an increase in cell size, as light scattering is also a function of cell size. Since the induction of the expression system committed the cell's resources to producing a large amount of protein, cell expansion is more likely than cell division. The relatively larger amounts of protein recovered from the cells (% Biomass, Table 5.1) grown with Trp compared to the analogs was consistent with this understanding.

Purification of these proteins followed the procedures described in section 3.2.2. An SDS-PAGE gel of each of the incorporated TrpRS samples is shown in Figure 5.4 after the batch hydroxyapatite extraction step, and prior to DEAE Sephacel chromatography. This gel illustrates the efficiency of this first batch purification step. UV spectra of these samples indicated that the absorbance of the expected chromophore, 4FW, 7AW, and 5HW was present in their respective samples, together with a contribution from nucleic acids at 260 nm (not shown). The typical chromatographic profiles are shown in Figure 5.5 with W92(5HW) TrpRS (compare the lower curve with Figure 3.3 curve a). The S-200 HR chromatography step may seem redundant after the DEAE Sephacel step, but it was important to establish a size-exclusion step in order to eliminate any possible higher-ordered aggregates. There was a small void-volume peak (< 1/10th of the 72 kDa peak) observed in the S-200-HR chromatography of W92(7AW) protein (not shown). Otherwise there was no

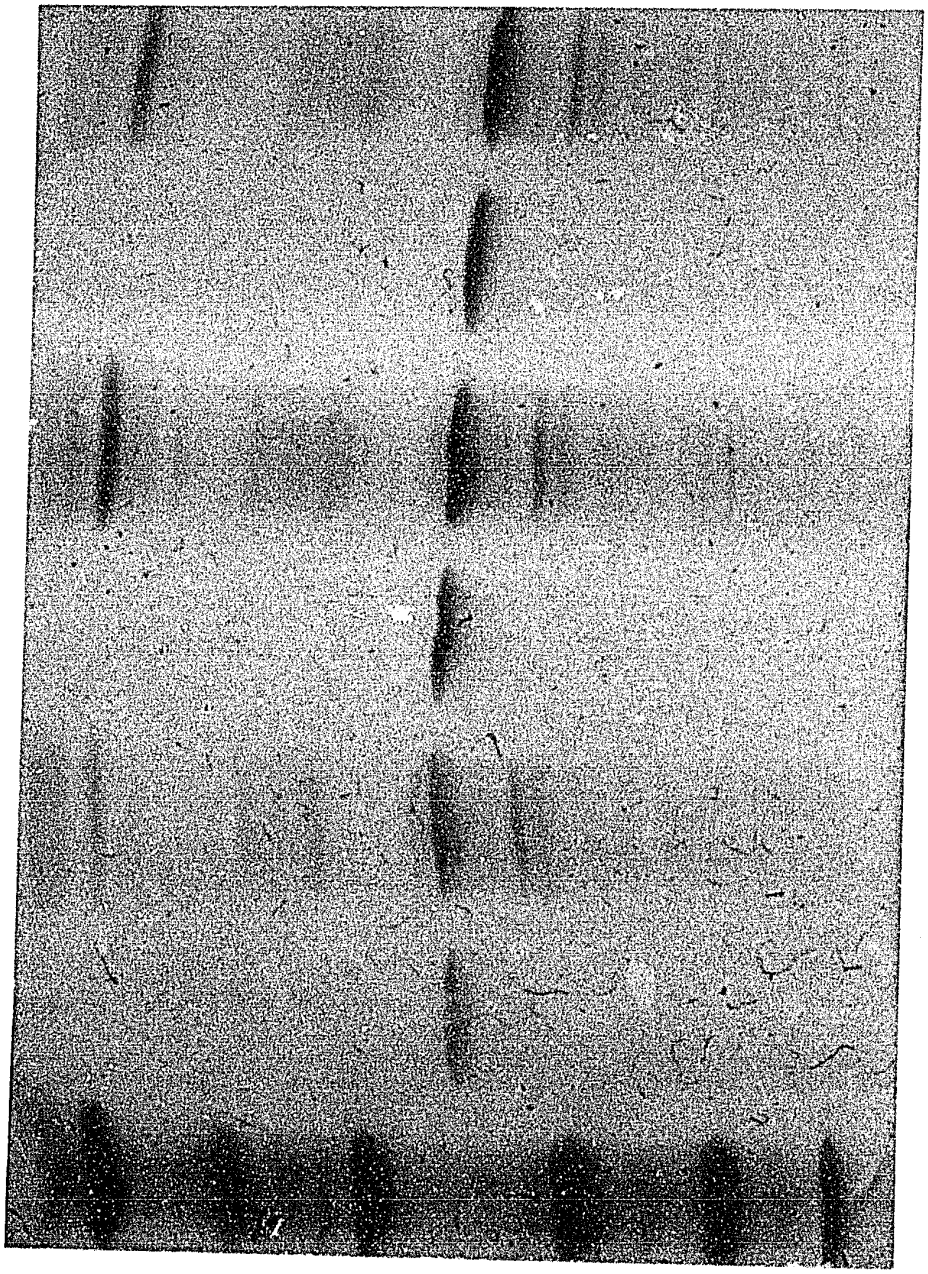

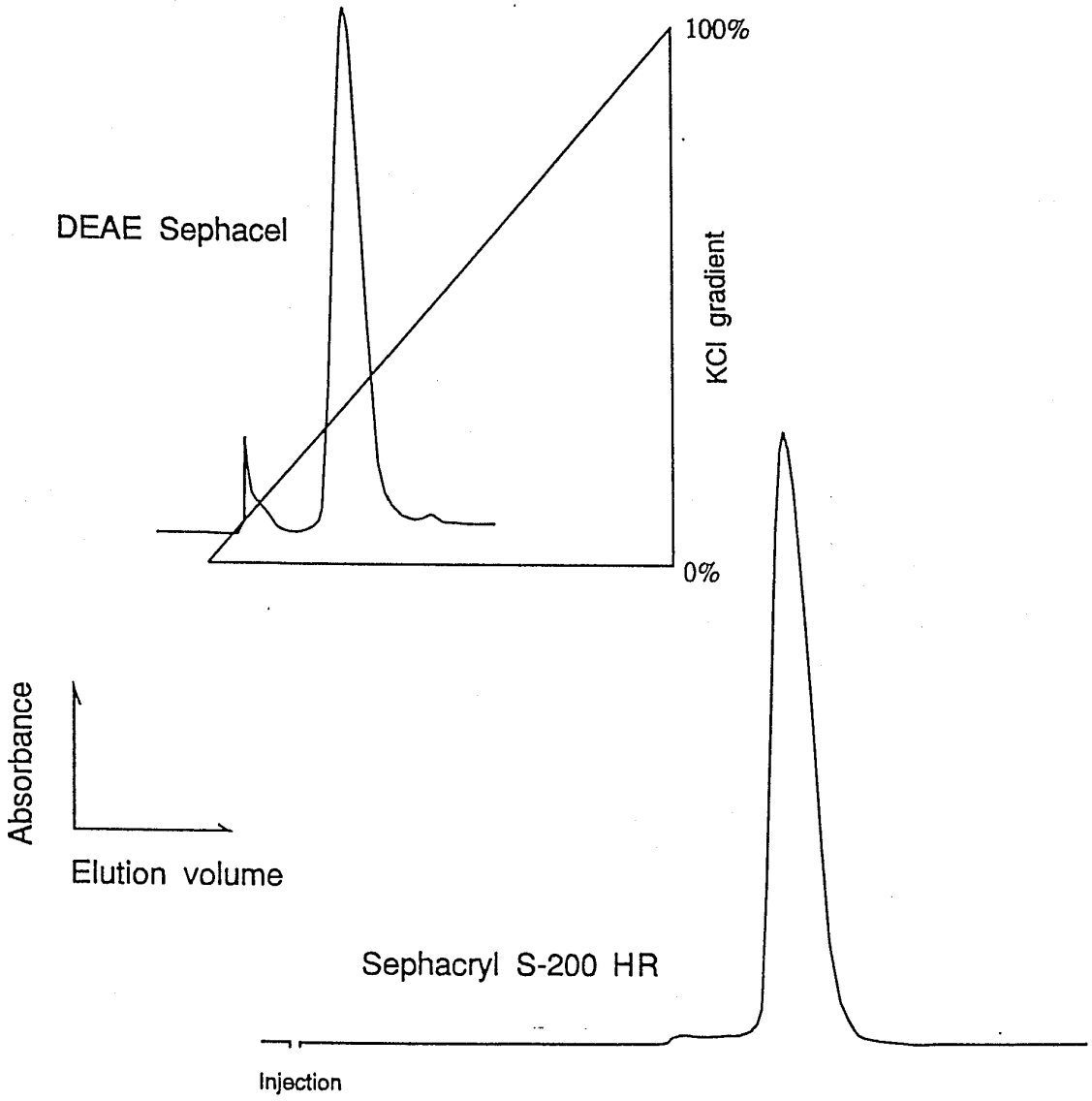

Figure 5.5: Chromatographic purification of W92(5HW) TrpRS. (Top) DEAE Sephacel chromatography after the batch hydroxyapatite TrpRS extraction. (Bottom) Sephacryl S-200 HR Chromatography.

observable difference between the performance of these mutants and the wild-type protein in the individual purification steps.

Cell wet weights and the final yield of purified TrpRS are listed in Table 5.1. Interestingly, all three analogs gave similar yields. Included in Table 5.1 is an estimate of the percent of endogenous *E. coli* TrpRS based on its purification from non-overexpressed cells. Maximizing yield with minimum biomass, as shown in the last example in Table 5.1, reduces the estimated amount of endogenous TrpRS to an insignificant amount.

Table 5.1: Yield of Purified TrpRS with Incorporated Analogs

Analog	Biomass[a] (g)	TrpRS[b] (mg)	% Biomass[c]	% Change[d]	% *E. coli* TrpRS[e]
L-Trp	9.68	122.0	1.2	-	0.12
L-5HW	9.22	67.6	0.73	-39	0.21
DL-4FW	9.71	64.3	0.66	-45	0.23
DL-7AW	9.69	62.6	0.65	-46	0.24
L-Trp[f]	12.32	210.0	1.7	+42	0.09

[a]Wet weight of cells. [b]Lyophilized, pure protein weight [c]TrpRS weight/biomass weight [d]Relative to L-Trp [e]Percent of lyophilized TrpRS of endogenous origin estimated from biomass Kuehl et al., 1976 (280 mg TrpRS from 18 kg *E. coli*). [f]Twice the amount of casamino acids in M9 media.

It was observed that the yield from a culture grown first with 2 l of T-Broth, then switched to 2 l of M9, gave as much TrpRS (120 mg) as did 6 l of T-Broth expressed with both cell growth and induction taking place in one volume of media (122 mg as in Chapter 3). By a further doubling of the amount of casamino acids in the media, the yield of TrpRS increased by 42% to 210 mg with an increase in biomass of only 27%. This indicated that something other than the concentration of L-

Trp may have limited the expression of TrpRS, possibly some other amino acid in the casamino acids.

Dialysis against distilled, deionized water caused *B. subtilis* TrpRS to form a characteristic microcrystalline precipitate, yet it remained fully active. In Chapter 3, the W92F mutant was found to irreversibly aggregate during and immediately after eluting from the S-200 HR gel filtration column. All three of the analog substituted proteins formed the microcrystalline precipitate upon dialysis with no premature aggregation. Some difficulty in resuspending the W92(7AW) enzyme was subsequently observed. For example 8 mg dry weight of protein resuspended in buffer left clumps and only about half passed through Sephadex G-25 gel filtration, the remainder clogged the column top. This suggested a degree of irreversible aggregation had occurred in W92(7AW) TrpRS during the precipitation and lyophilization steps. The protein retained activity, however, and prior to lyophilization, the relative $tRNA^{Trp}$ aminoacylation activities were: wild-type TrpRS = 1, W92(5HW) = 1, W92(4FW) = 0.8 and W92(7AW) = 0.7.

5.3.2 Absorbance Characterization

The absorption spectra of the analog incorporated TrpRS species are shown in Figure 5.6, compared to that of wild-type TrpRS. The absorbance of TrpRS is dominated by 14 Tyr residues, producing a λ_{max} at 277 nm. The incorporation of 4FW (Figure 5.6 A) produced an enzyme with a λ_{max} at 276 nm, and with a significant blue shift of wild-type. This was consistent with expected contribution from the absorbance spectrum of 4FW, which was blue shifted compared to Trp (Bronskill and Wong, 1988). Figure 5.6 B shows the absorbance of the W92(7AW) TrpRS. The spectrum of this enzyme gains the characteristic red-extended tail of 7AW, which was

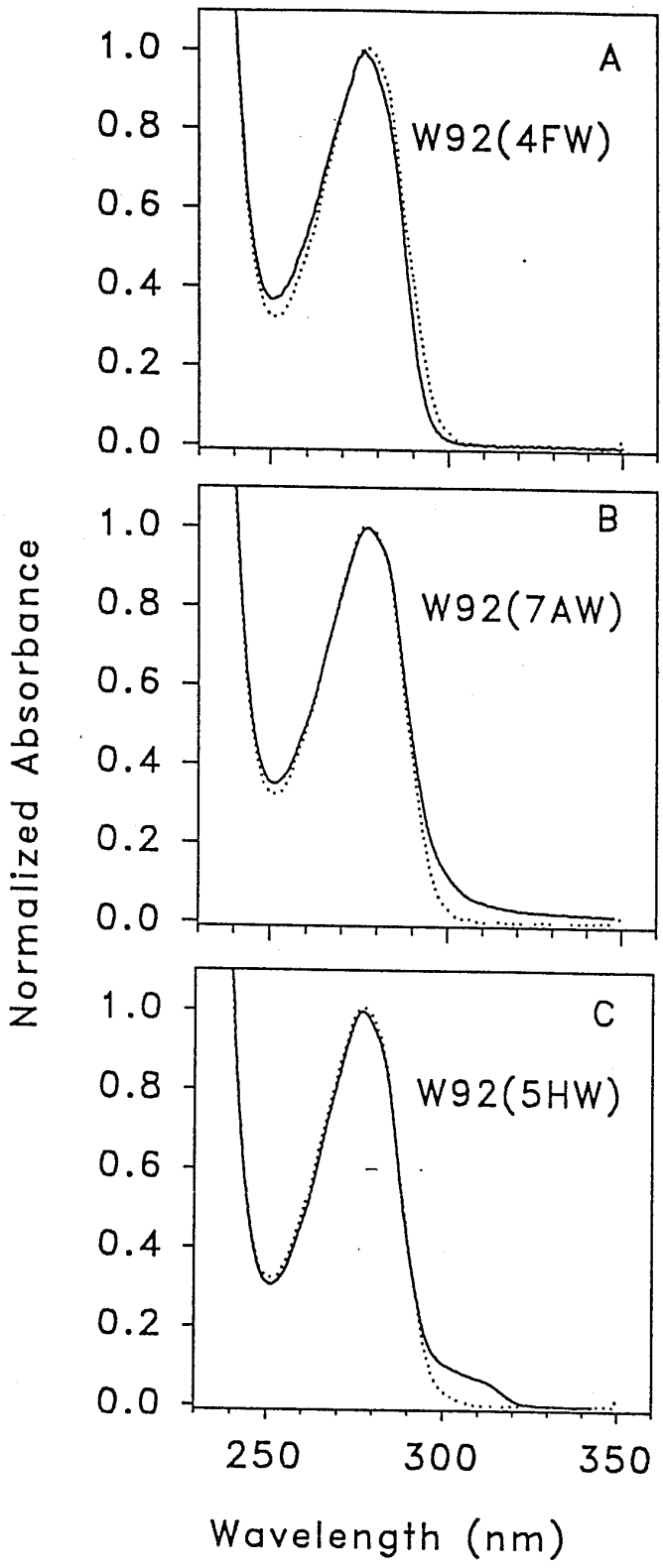

Figure 5.6: Normalized absorption spectra of analog incorporated TrpRS. Dotted line represents wild-type TrpRS. A. W92(4FW). B. W92(7AW). C. W92(5HW).

somewhat larger than expected. W92(5HW) enzyme had a spectrum (Figure 5.6 C) with the characteristic red-extended shoulder of 5HW (Hogue et al., 1992). Using a linear combination of absorbance (Waxman et al., 1993) at 280 nm and 310 nm, it was possible to estimate the incorporation of 5HW at 95%. The height of the shoulder of W92(5HW) was in proportion to the expected height of the individual chromophore in the presence of 14 Tyr residues. That of W92(7AW) was larger than that expected at 310 nm based on the absorbance of 7AW zwitterion. A similar increase in absorbance in 7AW at > 300 nm was observed in Chapter 4 for the 7AW-adenylate, and was observed in the Lys-7AW-Lys absorbance (Brennan et al., 1994). The enhanced red absorbance of 7AW is likely a consequence of peptide bond formation with 7AW. Subunit extinction coefficients for each protein were calculated (Gill and von Hippel, 1988) at 280 nm: W92(4FW) = 21609, W92(5HW) = 23364, W92(7AW) = 23533 M^{-1} cm^{-1} (wild-type = 24154) to be equivalent within a range of ±5% each, even with minor changes in absorbance of the chromophores due to protein inclusion considered.

5.3.3 $tRNA^{Trp}$ Aminoacylation Kinetics

$tRNA^{Trp}$ aminoacylation kinetics were performed to determine if the analogs had an effect on the overall enzymatic reaction of TrpRS. Joseph and Muench (1971) previously determined a K_m of 0.5 μM for the $tRNA^{Trp}$ aminoacylation step of *E. coli* TrpRS. Values obtained here for K_m and k_{cat} are listed in Table 5.2. Figure 5.7 is an Eadie-Hofstee plot of the kinetic data (Cornish-Bowden, 1979). This provides a graph of intercept V on the y axis and V/K_m, on the x axis, with a slope of $-K_m$. Since the V was expressed in arbitrary units (cpm) it is interchangeable here with the k_{cat} relative to the wild-type enzyme. It can be seen that both 5HW and 7AW in position 92 lowered both the K_m and k_{cat}, whereas 4FW had little effect on these parameters compared with

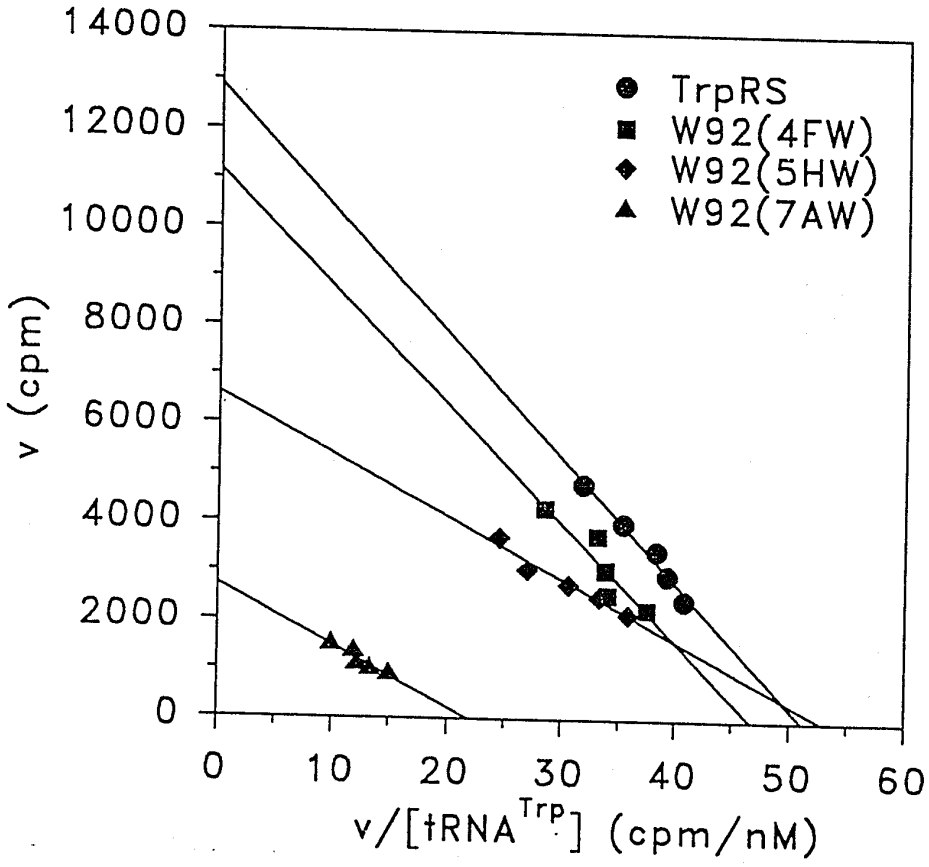

Figure 5.7: Kinetics of TrpRS tRNA aminoacylation. Eadie-Hofstee plot. V is cpm of duplicate counts of [^{3}H] Trp taken up by $tRNA^{Trp}$ in 5 minutes. $tRNA^{Trp}$ and assay kindly provided by H. Xue, University of Toronto. Errors are within the symbol contours.

wild-type. The lowest K_m is exhibited by the W92(5HW) enzyme. This enzyme had an overall higher ratio of k_{cat}/K_m compared to the wild type, indicating the W92(5HW) was *more specific* to its substrate $tRNA^{Trp}$ than the wild-type. However a lower k_{cat} suggests the presence of unproductive binding of substrates (Cornish-Bowden, 1979). Combined these two parameters could indicate that W92(5HW) binds to one substrate prematurely, possibly $tRNA^{Trp}$ or Trp. The catalytic rate of the W92(7AW) enzyme is certainly poor, which may be due to a proportion of aggregated or inactive enzyme in the assay.

Table 5.2: Kinetics of $tRNA^{Trp}$ Aminoacylation.

TrpRS	k_{cat}[a]	K_m (μM)	k_{cat}/K_m[b]
Wild-type	1	0.26	1
W92(5HW)	0.46	0.11	1.14
W92(4FW)	0.82	0.24	0.92
W92(7AW)	0.27	0.19	0.37

[a,b]relative to *B. subtilis* wild-type.

5.3.4 Fluorescence of Incorporated TrpRS

Spectra of the entire intrinsic fluorescence at 280 nm excitation, and the fluorescence excitation at 340 nm emission are depicted in Figure 5.8 for solutions of equal absorbance of 0.100 at 280 nm. Analog incorporated TrpRS are compared with the wild-type TrpRS. The W92(4FW) TrpRS fluorescence at 280 nm excitation (Figure 5.8 A) had a λ_{max} at 304 nm, indicating the dominance of Tyr fluorescence. Wong's group (Chow et al., 1992) reported an uncorrected emission λ_{max} of 307 nm for the inactive Trp-free W92F mutant, similar to this W92(4FW) TrpRS spectrum.

Interestingly, at 280 nm excitation, the emission intensity at 300 nm of W92(4FW) fluorescence was higher than that of the wild-type enzyme. This results suggest that quenching of Tyr fluorescence arises from Tyr → Trp-92 energy transfer in the wild-type protein. Tyr → 4FW-92 energy transfer may also occur in W92(4FW) enzyme but the present result would indicate it is less efficient than Tyr → Trp. The fluorescence from 280 nm excitation of the wild-type enzyme had an emission λ_{max} of 317 nm, partway between the fluorescence maximum of Trp-92 (325 nm) and that of Tyr (305 nm).

The emission spectra of W92(7AW) at 280 nm excitation had a λ_{max} at 306 nm, obviously dominated by Tyr fluorescence. Fluorescence from the 7AW-92 residue appeared as a shoulder between 340-370 nm, with a long tail out to 450 nm. The excitation spectrum at 340 nm emission of Fig. 4 B shows the additional excitation of W92(7AW) at $\lambda > 300$ nm. The emission of W92(5HW) had a distinct shape, with two unusual λ_{max} at 333 and 340.5 nm (not due to Raman scattering). The Tyr fluorescence at wavelengths below 310 nm was observed, largely unobstructed by 5HW fluorescence which did not begin until $\lambda > 310$ nm (Hogue et al., 1992). The emission of the Tyr fluorescence at 305 nm in W92(5HW) was diminished relative to that of W92(4FW) or wild-type enzyme. These indicate that Tyr → 5HW energy transfer is a more efficient process than Tyr → Trp as suggested by Ross et al. (1992a). The blue edge of the emission spectra of W92(7AW) was coincident with that of the wild-type TrpRS, suggesting that there may be no additional efficiency of a Tyr → 7AW-92 energy transfer process compared to Tyr → Trp.

The spectra of the individual fluorophores incorporated in place of Trp-92 are shown in Figure 5.9 using 300 nm excitation and the same solutions used for Figure 5.8. These spectra give an indication of the sensitivity of each fluorophore at 300 nm excitation. W92(5HW) had a λ_{max} at 333.5 nm, compared to 336 nm for 5HW in solution and 334 nm for the 5HW-adenylate bound in the hydrophobic active site of

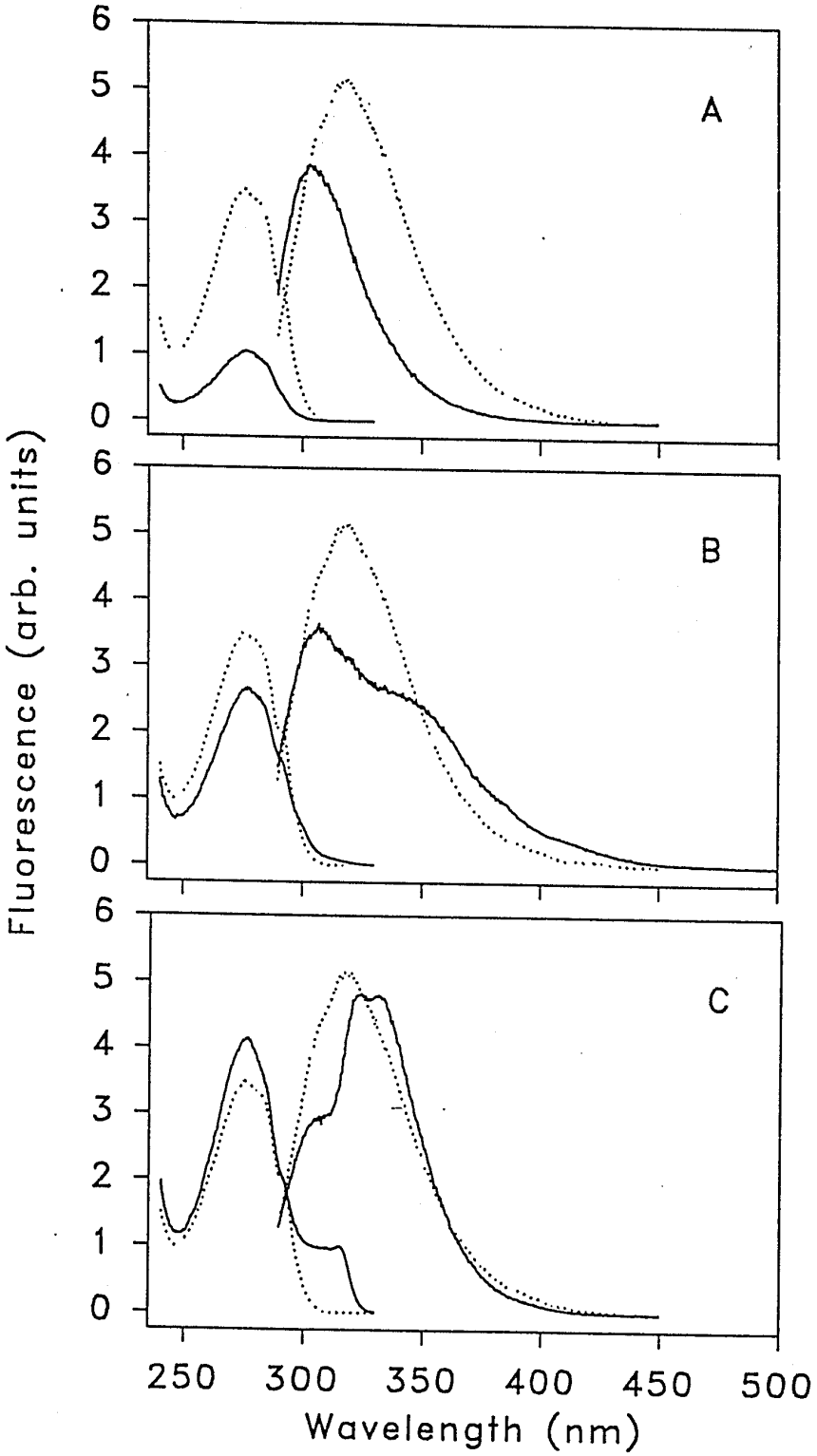

Figure 5.8: Fluorescence spectra of analog incorporated TrpRS. Emission spectra at 280 nm excitation; and excitation spectra at 340 nm emission. Solutions of analog incorporated and wild type TrpRS with an absorbance of 0.100 at 280 nm. Dotted line represents wild-type TrpRS. A. W92(4FW). B. W92(7AW). C. W92(5HW).

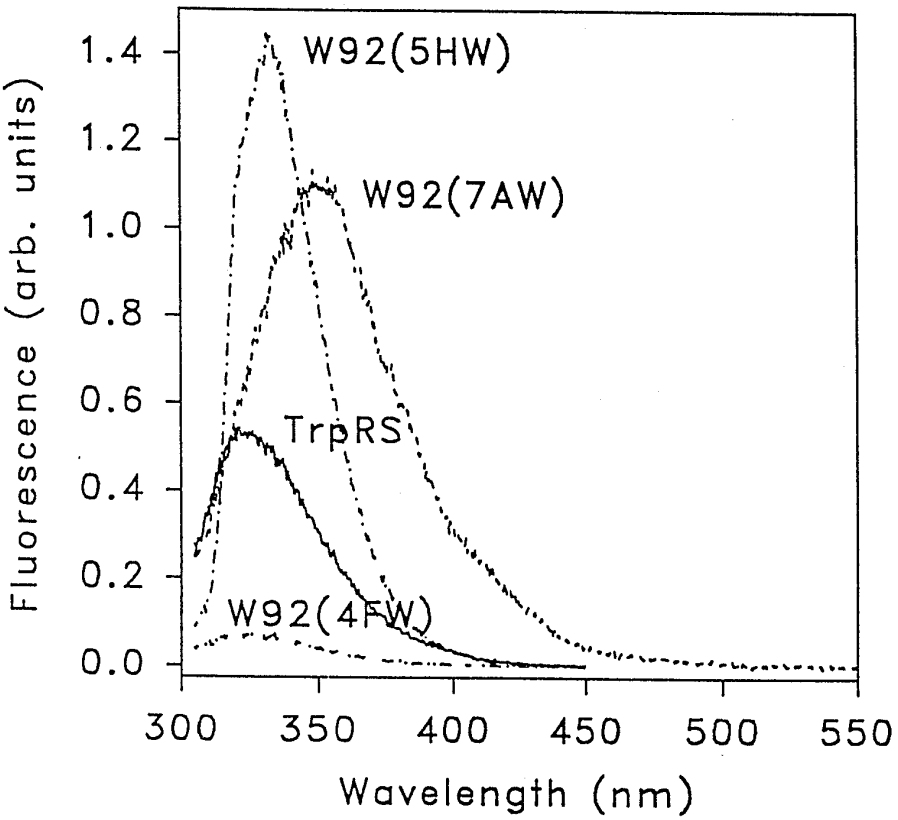

Figure 5.9: Fluorescence emission spectra at 300 nm excitation of analog incorporated TrpRS. Each solution had an absorbance of 0.100 at 280 nm.

TrpRS. Denaturation of W92(5HW) by 6 M GdHCl caused the maximum to shift to 336 nm (not shown). It is not unusual that the W92(5HW) emission maxima were different with 280 nm excitation compared to the single maxima with 300 nm excitation. The additional blue maxima with 280 nm excitation corresponds to the additive combination of a rising Tyr emission component together with the structured blue edge of the 5HW-92 emission spectrum.

The λ_{max} of W92(7AW) TrpRS at 350 nm was similar to that of 7AI in acetonitrile (Chapman and Maroncelli, 1992), and unlike that of 7AW in water (402 nm). Schlesinger (1968) observed similar blue-shifted fluorescence of 7AW in alkaline phosphatase. 7AW-adenylate in the hydrophobic active site of TrpRS exhibited a λ_{max} of 361 nm, with a large increase in quantum yield as shown in Chapter 4. The fluorescence of a buried, incorporated 7AW is therefore more like that of 7AI in aprotic solvents, rather than 7AI in alcohols as has been suggested (Négrerie et al., 1990).

Fluorescence at 300 nm excitation from the W92(4FW) TrpRS appeared (Figure 5.9) with the same maximum and fluorescence decay properties (data not shown) as the wild-type TrpRS, revealing its identity as wild-type TrpRS from promoter leakage. From the ratio of intensity of the same concentration of wild-type and W92(4FW) incorporated TrpRS, the amount of contaminating wild-type enzyme was calculated to be 5% of the total enzyme. This, unfortunately, was a significant fraction for fluorescence measurements with time-resolved techniques. However it was in agreement with the analysis of efficiency of incorporation using absorbance ratios of the W92(5HW). 4FW is thus useful to determine the amount of inherent expression system leakage.

5.3.5 7AW-92 As An Environmental Probe For TrpRS

It was of interest to further demonstrate the effect of solvent exposure on the fluorescence of the buried 7AW-92 residue, despite the low activity of the enzyme. Figure 5.10 shows the steady-state spectra and DAS from W92(7AW) TrpRS in the absence and presence of 6 M GdHCl. Time-resolved fluorescence revealed 3 decay components for W92(7AW) of 10.1 ns, 3.9 ns and 0.5 ns (values of α were 0.53, 0.33 and 0.14; SVR = 1.72). Three decay times corresponded with the number observed with the wild-type and W92(5HW) enzymes. The long, 10.1 ns decay component was comparable to that observed from the 7AW-adenylate in Chapter 4. Upon denaturation, the time-resolved decay was poorly resolved, owing to the low quantum yield of exposed 7AW. A fit to three-exponential decay times gave 4.3 ns, 1.5 ns and 0.51 ns lifetimes whose preexponentials were 0.34 0.30 and 0.36 (SVR = 1.34) Notably the relative concentration of the short decay component increased substantially, which had a DAS λ_{max} at 400 nm in GdHCl. This component was attributed to a mean value for solvent-exposed conformers of 7AW-92. A 75% decrease in the quantum yield (0.15 to 0.025) is affected by the denaturation, however a small amount of apparently solvent-shielded fluorescence persisted with maxima at 360 nm. The decrease in $<\tau>$ corresponding to the denaturation was 60%, indicating that the quenching was largely of a dynamic character, consistent with the mechanism for H_2O quenching described in section 2.4.2. The very high values of τ_r that can be calculated of 61 ns for the native and 136 ns for the denatured 7AW-92 fluorophore are striking. These values are much larger than any observed with Trp (Szabo and Faerman, 1988), and also larger than those observed with 5HW, as shown later.

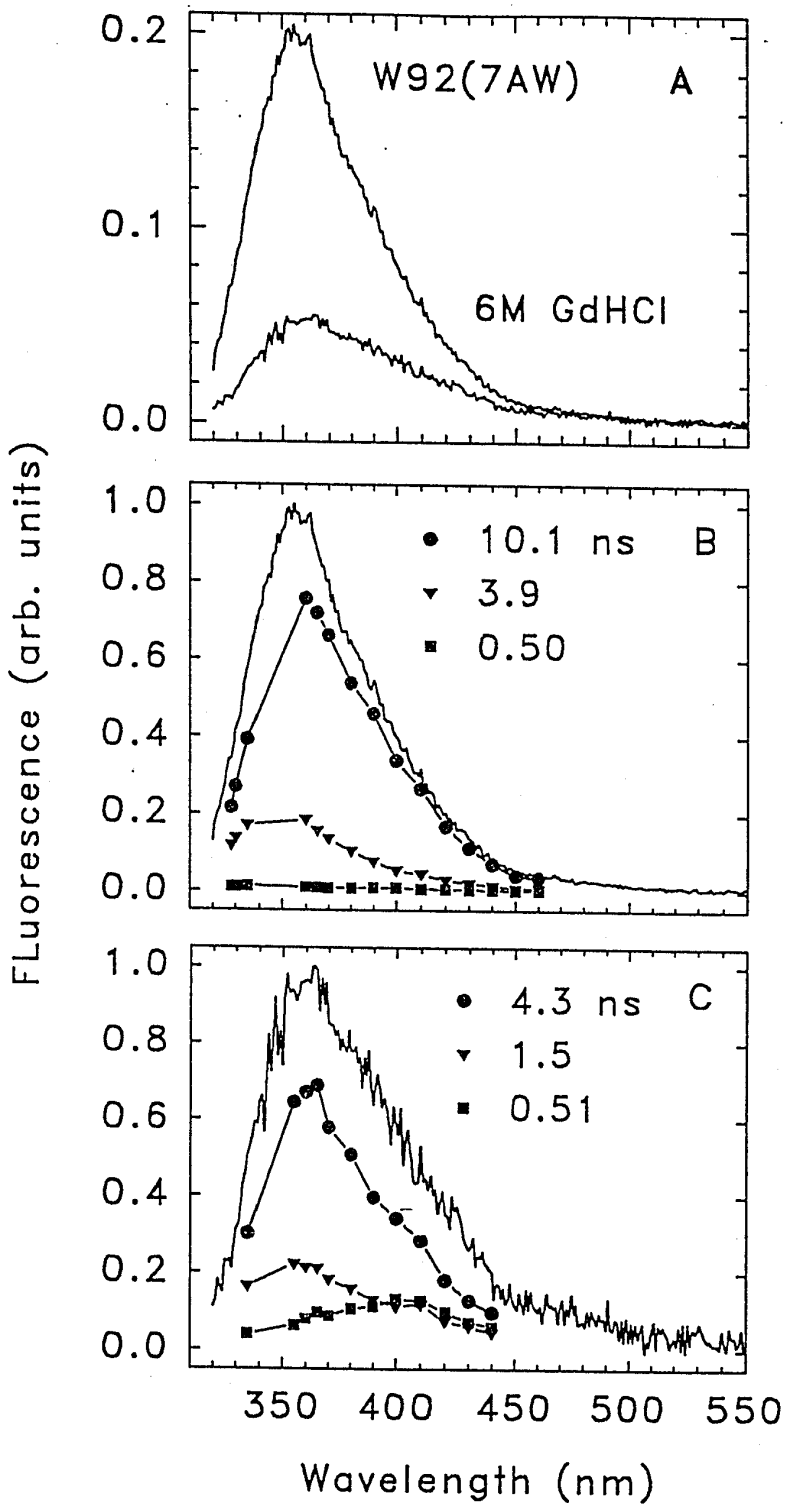

Figure 5.10: Fluorescence of W92(7AW) TrpRS. A. Steady-state spectra at 310 nm excitation of W92(7AW) TrpRS before and after denaturation with 6 M GdHCl. B. DAS of W92(7AW) TrpRS. C. DAS of W92(7AW) TrpRS after denaturation with 6 M GdHCl.

5.3.6 Thermal Denaturation of TrpRS

The fluorescence response of these enzymes were further studied as a function of temperature, as shown in Figure 5.11. The fluorescence of Trp-92 undergoes a monotonic decrease in fluorescence with increasing temperature. At 44° C, wild-type TrpRS and W92(5HW) began to noticeably aggregate, as monitored by light scattering. No clear thermal transitions were evident with Trp-92 fluorescence. However the fluorescence of 7AW-92 shows a dramatic transition starting at 36° C, with a large relative decrease in fluorescence. 5HW-92 also showed a transition, with a decrease in its fluorescence at 42° C. At 42° C, the fluorescence of W92(7AW) TrpRS was reduced by half. At the same temperature the aggregation of W92(7AW) TrpRS began. In both cases, the transitions indicated by the fluorescence of 7AW or 5HW began at lower temperatures than the observed aggregation, indicating two independent events.

Further studies of the thermal aggregation using light scattering of W92(4FW) TrpRS were carried out. It was found that W92(4FW) displayed a 5° C increase in aggregation temperature over that of the wild-type enzyme. The W92(4FW) enzyme also had a lower baseline aggregation between 35-45° C. This result was significant, as 5° C increases in thermal stability are often desired in protein engineering efforts.

A more dramatic demonstration of this thermostability was made with a solution of 2.5 mg/ml W92(4FW) TrpRS heated at 42° C for 15 minutes and then cooled. This sample was gel-filtered using the S-200 HR column to examine if any high-molecular weight forms had accumulated. The predominant 72 kDa peak was the only significant eluant, and this peak retained aminoacyl-adenylate forming activity. Wild-type protein irreversibly aggregates and is inactivated under these conditions, and cannot be resuspended. Clearly a more thermostable enzyme was created by the incorporation of 4FW.

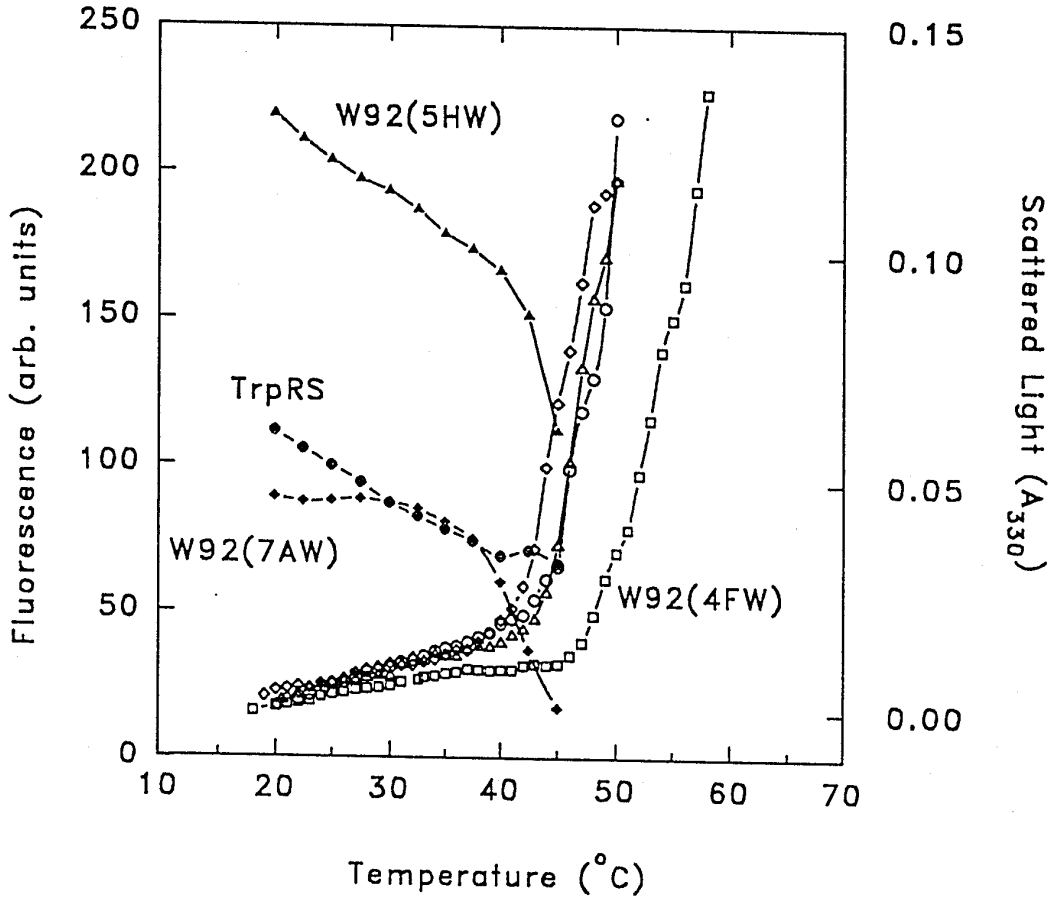

Figure 5.11: Thermal denaturation of analog incorporated TrpRS. Solid symbols are fluorescence intensity, and open symbols are scattered light. Circles = TrpRS wild-type, Diamonds = W92(7AW), Squares = W92(4FW), Triangles = W92(5HW). Fluorescence is integrated over the bandwidth, at 300 nm excitation for wild-type, and 310 nm excitation for W92(5HW) and W92(7AW).

5.3.7 Fluorescence of W92(5HW) TrpRS with Substrates

The fluorescence of 5HW in W92(5HW) TrpRS was examined with substrates, and it retained a significant indication of activity, unlike W92(7AW). Since the enzyme kinetics suggested an unproductive complex in the reaction, the effect of substrates on W92(5HW) steady-state and time-resolved fluorescence was investigated, using techniques similar to those in Chapter 3. In this case, the improved sensitivity and selectivity of the 5HW residue fluorescence enabled the use of Trp as a substrate in this study. The samples, their concentrations, quantum yields and λ_{max} are listed in Table 5.3.

Table 5.3: W92(5HW) Steady-State Fluorescence Parameters.

Sample	Φ_f ($\pm$0.01)	λ_{max} (nm)
5HW	0.25	336
A = W92(5HW) 7 μM	0.32	333
A + ATP 30 μM	0.30	334.5
A + L-Trp 30 μM	0.23	335
A + DL-4FW 60 μM	0.23	332.5
B = W92(5HW) 2.2 μM + $tRNA^{Trp}$ 6.7 μM	0.27	333.5
B + ATP 50 μM	0.25	335.0
B + L-Trp 25 μM	0.22	334.3
C = W92(5HW) 12 μM		
C + ATP 500 μM + DL-4FW 250 μM	0.09	332.5
C + ATP 207.2 μM + L-Trp 49 μM	0.11	337.0

Note that lower concentrations were used here compared to the previous studies of wild-type TrpRS in Chapter 3. This was allowed by the higher fluorescence sensitivity of 5HW. Despite lower concentrations, changes in quantum yield were demonstrated

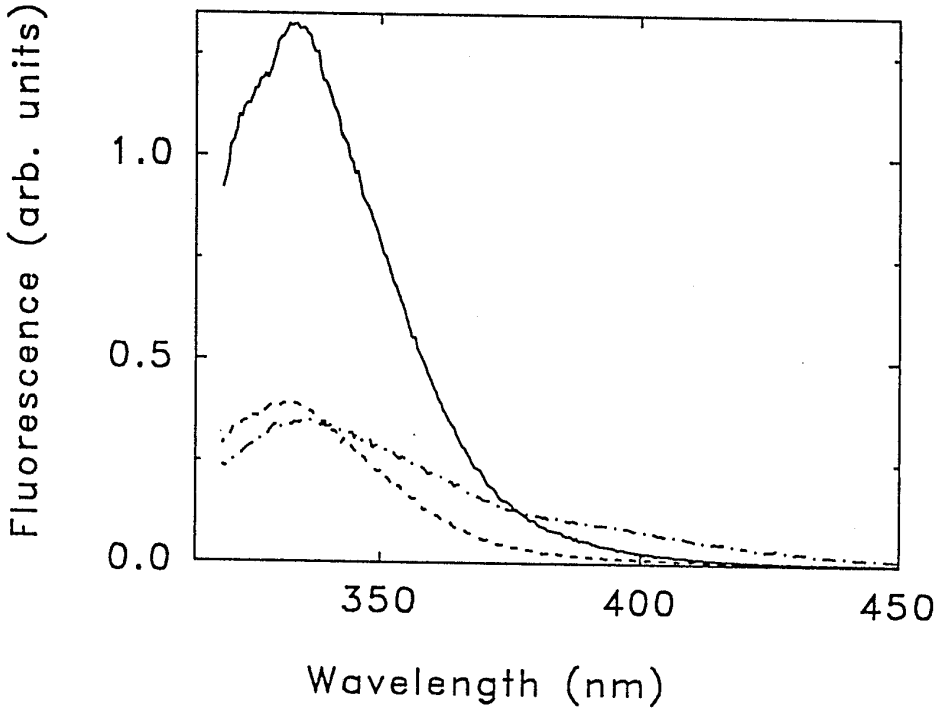

Figure 5.12: Fluorescence of W92(5HW) upon aminoacyl-adenylate formation. Corrected steady-state emission spectra at 310 nm excitation of (solid line) W92(5HW) TrpRS; (dashed line) W92(5HW) TrpRS·4FW-AMP complex; (dashed-dotted line) W92(5HW) TrpRS·Trp-AMP complex at 310 nm excitation. Compare with Figure 3.6.

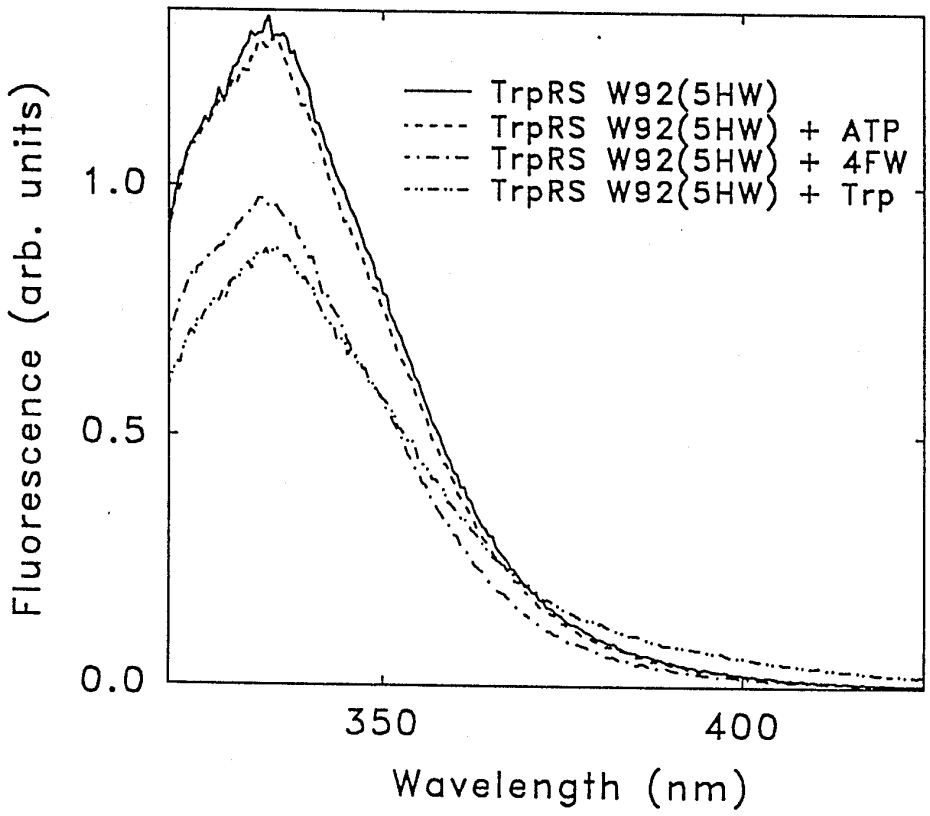

Figure 5.13: Steady-state spectra of W92(5HW) with substrates.

by every substrate. This is in sharp contrast to those of wild-type TrpRS in Table 3.2 where only the adenylate containing samples showed significant quantum yield changes. The steady-state fluorescence spectra of W92(5HW) with these substrates are shown in Figures 5.12-5.14.

The W92(5HW) samples containing adenylates (last two in Table 5.3) had the largest decreases in 5HW fluorescence. These spectra are shown in Figure 5.12 with 310 nm excitation. A 72% decrease in quantum yield was evident with the W92(5HW)·4FW-AMP complex, within experimental error of the quenching observed for the wild-type protein with Trp-92 (70%). There was a long red-tail in the fluorescence spectrum of the sample containing the W92(5HW)·Trp-AMP complex which could be attributed to a small amount of Trp fluorescence with 310 nm excitation. Nonetheless, this experiment is important in demonstrating that the same quenching of the position 92 fluorophore, was caused by both 4FW-AMP and by Trp-AMP. Quenching of 5HW is also demonstrated by the sole addition of either 4FW or Trp to the enzyme, as depicted in Figure 5.13. Trp-92 was not affected by 4FW in wild-type enzyme. Quenching of 5HW-92 fluorescence is also shown by the addition of $tRNA^{Trp}$ in Figure 5.14. It would seem the quantum yield of 5HW is sensitive enough to detect differences from the addition of these substrates.

The time-resolved fluorescence parameters of the samples described in Table 5.3 are presented in Tables 5.4 and 5.5, fit to three- and four-exponential decays. W92(5HW) in the absence of substrate exhibited an excellent fit to 3-exponential decay components. The corresponding DAS is shown in Figure 5.16 A. It is important to note that the λ_{max} of these DAS components varied in the same manner as those of Trp-92; the longest component = 335 nm, intermediate = 325, and short = 320 nm. This was also the case for DAS including substrates, as shown in Figure 5.16 and 5.17. The fitting of the fluorescence decay data from the 4FW-AMP and Trp-AMP complexes of W92(5HW) TrpRS did not give fully satisfactory statistics. Hence a

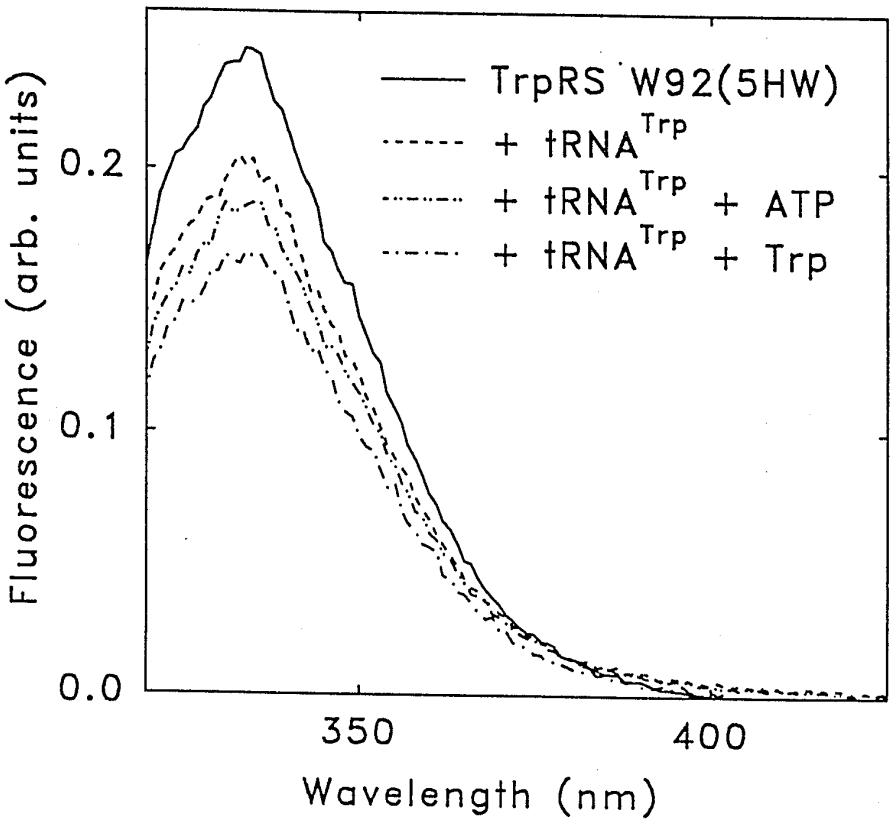

Figure 5.14: Steady-state spectra of W92(5HW) with $tRNA^{Trp}$ and other substrates.

4-exponential decay model was used to fit the data. Figure 5.15 shows examples of the weighted residuals for the one to four-exponential decay models fit to the W92(5HW) TrpRS·4FW-AMP complex. The longest exponential component in the W92(5HW) TrpRS·Trp-AMP DAS was clearly that of substrate Trp, exhibiting a much longer λ_{max} (not shown).

While the statistics for a triple-exponential decay fit for the sample of W92(5HW) + $tRNA^{Trp}$ were adequate (Table 5.4), the fractional fluorescence values from global analysis deviated from a smooth spectrum at certain wavelengths (not shown). Since this was on the threshold of a poor three-exponential fit, a four-exponential decay was computed for this sample, as shown in Table 5.5. Remarkably, the resolved four-exponential decay of the sample including $tRNA^{Trp}$ had similar lifetimes as those exhibited by the adenylate samples. Comparing the preexponential values in boldface in Table 5.5, the long decay component virtually disappears from $\alpha_1 = 0.57$ in the apo-enzyme to $\alpha_1 = 0.01$ in the 4FW-AMP complexed enzyme, with the simultaneous increase of short decay component from $\alpha_4 = 0$ to $\alpha_4 = 0.63$ in the adenylate complexed enzyme. It would seem that the long decay component was associated with the apo-enzyme, and the short decay component was associated with the adenylate-enzyme complexe.

It is most interesting that the same interpretation of the sample of W92(5HW) + $tRNA^{Trp}$ can be made. The fractional contributions of both the long and shortest components add to 60% of the total. From the ratio of these decay times it may be considered that about 1/3 of this sample represents the apo-enzyme conformer with the long component, and 2/3 represents a conformer with the short component, having a conformation like that of the adenylate complexed enzyme, yet caused by complexation with $tRNA^{Trp}$.

The mechanism of quenching of 5HW-92 via the addition of $tRNA^{Trp}$ or formation of the adenylate complex can be accounted for by comparing the ratios of

Table 5.4: Triple-exponential Fits to W92(5HW) Fluorescence Decays.[a]

Sample[b]	τ_1	τ_2	τ_3	τ_m	$<\tau>$	τ_r	c_1	c_2	c_3	X^2	SVR
W92(5HW) TrpRS	4.64	1.65	0.25	4.2	3.1	10	0.57	0.26	0.17	1.05	1.90
+ ATP	4.61	1.60	0.21	3.9	2.5	9	0.42	0.35	0.23	1.06	1.83
+ W	4.73	1.83	0.26	3.6	2.1	9	0.28	0.36	0.37	1.08	1.76
+ 4FW	4.58	1.49	0.20	3.8	2.1	9	0.35	0.32	0.32	1.07	1.80
+ $tRNA^{Trp}$	4.37	1.21	0.11	3.5	1.5	5	0.25	0.26	0.49	1.05	1.81
+ $tRNA^{Trp}$ + ATP	4.58	1.56	0.25	3.8	2.5	10	0.42	0.35	0.23	1.03	1.98
+ $tRNA^{Trp}$ + W	4.57	1.62	0.27	3.7	2.3	11	0.37	0.33	0.30	1.02	1.99
standard errors	±0.01	±0.02	±0.002				< 5%	< 5%	< 5%		

[a]Excitation at 310 nm. Parameters are given for a global fit to data sets collected as a function of emission wavelength.
[b]Concentrations as in Table 5.3, all values of τ in ns.

Table 5.5: Four-exponential Fits to W92(5HW) Fluorescence Decays.[a]

Sample[b]	τ_1	τ_2	τ_3	τ_4	τ_m	$<\tau>$	τ_r	α_1	α_2	α_3	α_4	X^2	SVR
W92(5HW) TrpRS	4.64	1.65	0.25		4.2	3.1	10	**0.57**	0.26	0.17		1.05	1.90
+ $tRNA^{Trp}$	4.79	2.00	0.57	0.080	3.7	1.6	6	**0.21**	0.21	0.17	**0.40**	1.01	1.97
·(4FW-AMP)[c]	5.63	2.03	0.38	0.089	1.8	0.38	4	**0.01**	0.08	0.28	**0.63**	1.11	1.67
·(Trp-AMP)	6.42[d]	2.35	0.38	0.097	[e]	[e]	[e]	0.03	0.11	0.29	0.57	1.09	1.82

[a] The excitation wavelength was 310 nm. Parameters are given for a global fit to data sets collected as a function of emission wavelength. [b]Concentrations as in Table 5.3, all values of τ in ns with standard errors as previously reported. [c] Weighted residuals shown in Figure 5.15. [d] This decay component was attributed to free Trp due to a 350 nm maxima. [e] Component emitting from Trp precludes calculation or comparison of this parameter.

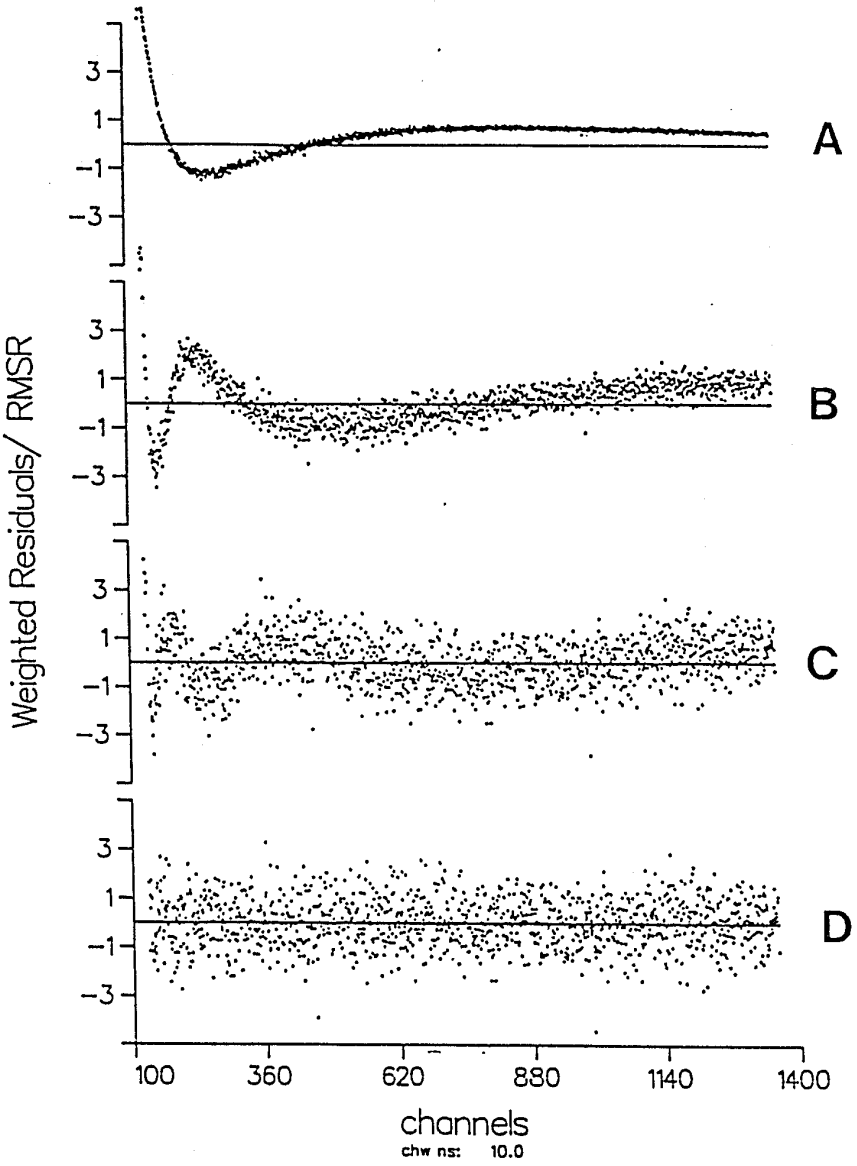

Figure 5.15: Weighted residuals of the four-exponential decay fit of the W92(5HW)·(4FW-AMP) complex. A. single-exponential, B. two-exponential, C. three-exponential and D. four-exponential decay models.

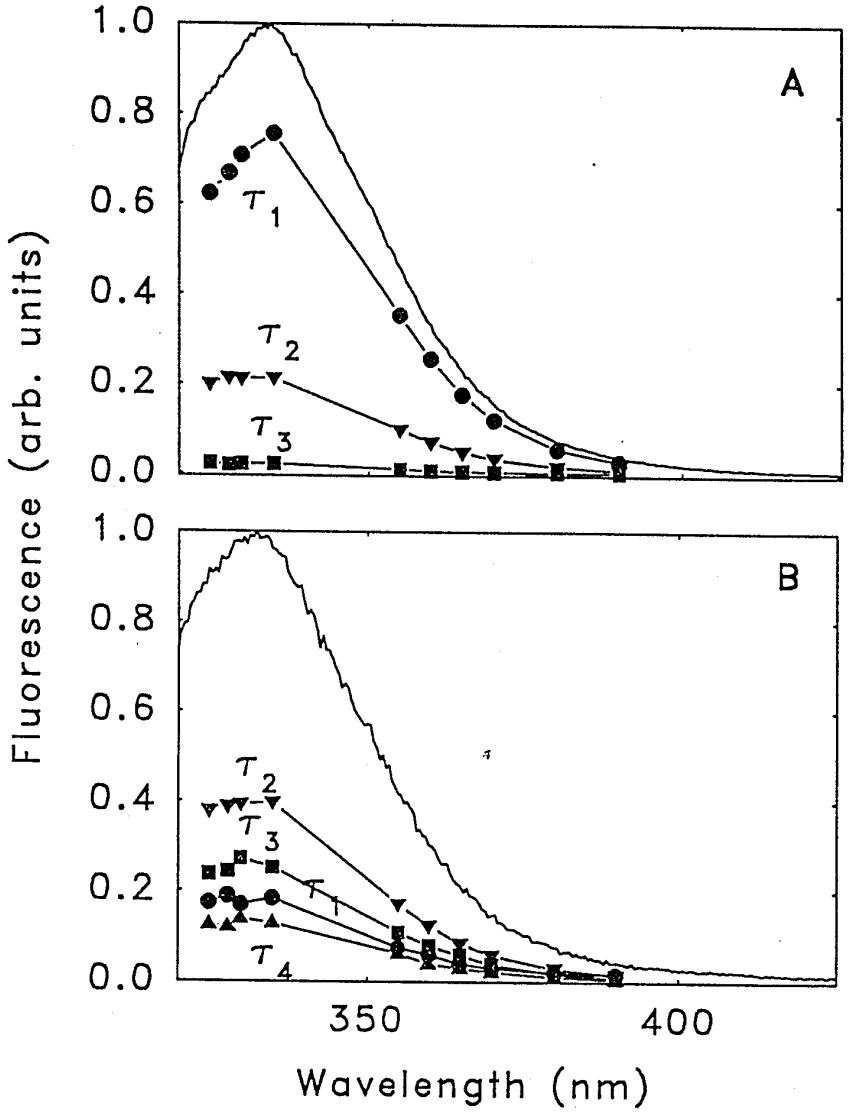

Figure 5.16: DAS of W92(5HW). A. DAS of W92(5HW) TrpRS at 310 nm excitation. B. DAS of W92(5HW)·4FW-AMP at 310 nm excitation..

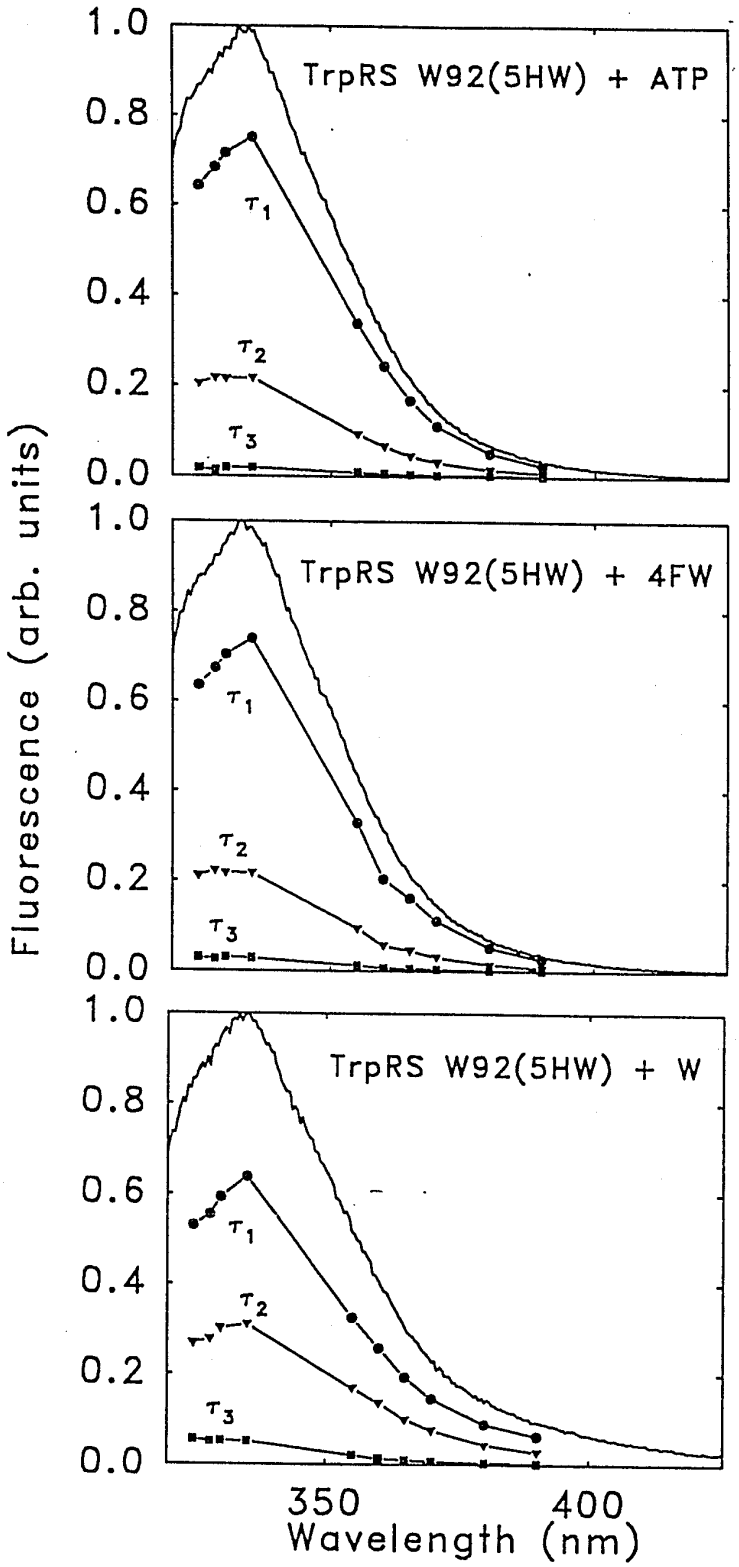

Figure 5.17: DAS corresponding to samples in Figure 5.13. Note that the short component maxima contribute to the structure seen on the blue-edge of the spectra.

decrease in Φ_f with decrease in $<\tau>$. From apo-W92(5HW) TrpRS to the W92(5HW)·(4FW-AMP) complex, the decrease in Φ_f was 72%, but the decrease in $<\tau>$ was 87%. An alteration of the radiative lifetime of 5HW-92 must be considered to account for the larger decrease in $<\tau>$ compared to Φ_f (Appendix A). From apo-W92(5HW) TrpRS to the W92(5HW)·$tRNA^{Trp}$ complex, the decrease in Φ_f was 16%, and the decrease in $<\tau>$ was 50%. Again, a larger decrease in $<\tau>$ compared to Φ_f was observed that can be explained by a change in τ_r (Appendix A). The decreases in τ_r of 5HW-92 (Table 5.5) further confirms that the conformation of adenylate complexation and $tRNA^{Trp}$ complexation were similar.

5.4 Discussion

5.4.1 Expression of Analog Incorporated Proteins

Since 5HW, 7AW and 4FW behave very differently as substrates for TrpRS as shown in the previous chapters, it was expected that they would give different yields of incorporation, as observed earlier for fluorinated Trp analogs (Pratt and Ho, 1975). Instead they gave equivalent yields of incorporation in parallel growths. Thus the extent of analog incorporation seems here to be limited by something that is unrelated to the properties of the individual analog, provided it is incorporable. This may be consistent with the accumulation of one or more inactivated proteins which inhibit the extent of protein biosynthesis - with inactivation arising equally from each of the analogs tested here.

The incorporation technique used here did not result in any significant increase in the number of cells after IPTG was added (Fig. 5.2). This is fundamentally different from earlier attempts at analog incorporation (Pratt and Ho, 1975), where protein synthesis and cell duplication are coupled, and the fraction of analog

incorporated protein much lower. By using the "bait and switch" technique to decouple cell growth from the desired protein expression, the yield and fraction of incorporated analog into the protein becomes independent of the toxicity of the analog for cell growth.

TrpRS expression reported by Wong and co-workers, (Ala et al., 1993) using LB media in a 14 l fermenter resulted in recovery of 7.1 mg/l. Previously in Chapter 3, 122 mg of TrpRS was recovered from a conventional growth using three 2 l batches of T-Broth, or a total of 20.3 mg/l. Here, with the "bait and switch" technique, the same recovery was achieved using 2 l of T-Broth and 2 l of M9 with casamino acids - a result which gives 30.5 mg/l of TrpRS. Doubling the amount of casamino acids produces 52.5 mg/l of TrpRS. There seems to be an advantage of the "bait and switch" technique, even when analog incorporation is not the desired outcome. Practitioners of recombinant protein expression may be encouraged by these results to use the "bait and switch" technique to increase yields.

5.4.2 Kinetics of Analog Incorporated TrpRS

The fact that each of the Trp analog replacements of Trp-92 produced active enzyme was gratifying, in the light of earlier failures to mutate this residue. Evidently TrpRS enzymatic activity is preserved when an indole structure is present in the conserved location.

4FW was incorporated into *E. coli* proteins by earlier workers without using expression systems (Pratt and Ho, 1975), together with 5FW and 6FW. In their study, 4FW exhibited the smallest perturbations in enzymatic activity and antigenic recognition. This result is also demonstrated here, by the similar kinetics of the W92(4FW) TrpRS compared to the wild-type. The W92(7AW) enzyme had the lowest

catalytic rate k_{cat}, but it also had a decreased K_m compared to the wild-type TrpRS. Unfortunately, while W92(7AW) was active, it suffered from a propensity to aggregate and was difficult to resuspend. This limited its utility in further characterization with substrates. The hydrophobicity of these amino acids increases in the order 5HW < 7AW < Trp < 4FW (Xu et al., 1989). No obvious correlation could be made between hydrophobicity and kinetic parameters in this case. The extra hydroxyl group of the 5HW-92 residues may somehow afford a stabilizing effect, either through space-filling or through hydrogen-bonding, which might offset a more simple effect of decreased hydrophobicity. Nonetheless, the incorporation of 5HW is better tolerated in TrpRS than 7AW. Like other amino acid substitutions, these differential effects may be difficult to rationalize without three-dimensional structural data for each mutant.

The kinetic parameters k_{cat}/K_m for W92(5HW) enzyme suggest an increase in specificity for $tRNA^{Trp}$ as a substrate over the wild-type TrpRS. Yet the combination of a lower K_m and a lower catalytic turnover k_{cat}, implies non-productive binding species, which slow the overall reaction rate (Cornish-Bowden, 1979). Considering the reaction mechanism binding ATP first, a non-productive species could be a complex involving either $tRNA^{Trp}$ or Trp substrates. Either of these could block the binding site for further substrate binding, causing a decrease in catalytic turnover k_{cat}. Most interestingly, the fluorescence studies herein with both $tRNA^{Trp}$ and DL-4FW (or L-Trp) show that complexes involving these lone substrates form with W92(5HW) but not with wild-type TrpRS. Therefore it can be concluded that the Trp-92 is crucial for preserving the mechanism order of TrpRS.

5.4.3 4FW and Promoter Leakage

The distinct red-extended absorption properties of the incorporated analogs 7AW and 5HW can be seen in Figure 5.9. However the blue-shift of the W92(4FW) enzyme is also visible. 4FW has been shown to be susceptible to photodamage (Hott and Borkman, 1989). Since 4FW is blue-shifted relative to Trp, Trp fluorescence can be excited at 300 nm, where 4FW does not absorb, thereby preventing 4FW photodamage. Hence the utility of 4FW to remove Trp fluorescence in studies of protein-protein interactions is not diminished by its photosensitivity. However the problem of 5% leakage of normal Trp containing protein must be overcome in order to make the 4FW incorporation more useful.

The expression system used for 5HW incorporation in Y57W oncomodulin employed an oxygen-sensitive promoter (Khosla and Bailey, 1989) that was extremely susceptible to leakage (50%, Hogue et al., 1992). The success of Ross and co-workers (1992a) in achieving under 5% leakage using a *tac* expression system prompted the attempt here at TrpRS analog incorporation with a very similar expression system. However the 5% contamination still remained with the *tac* promoter. Heyduk and Heyduk (1993) have recently reported the incorporation of analogs using two other promoters, one a temperature-sensitive λP_L promoter, and another a T7 polymerase based promoter (Studier, 1990). The temperature-sensitive λP_L promoter gave between 67-90% 5HW incorporation for a cAMP receptor protein, and the T7 polymerase promoter gave 88% 5HW incorporation into the α-subunit of RNA polymerase. Hence both these promoters share a basal level of leakage, no better than that of the *tac* promoter. In additional work, not presented in this thesis, the author prepared a T7 polymerase expression system for expression of rat parvalbumin F102W, but with an additional plasmid which was shown to more tightly restrict the basal expression (Studier, 1990). But this expression system also had a significant level of

leakage, as shown by low levels of Trp fluorescence in preparations of F102(4FW) parvalbumin.

Studier et al. (1990) describe a tandem T7 polymerase/*lac* promoter expression system (pET10 and pET11) which may eliminate the approximately 5% leakage that seems inherent to these two individual promoters. Other promoters may also exhibit less leakage if they could be somehow combined in tandem. However if a small amount of Trp is liberated through proteolysis, a basal level of Trp leakage may always be present after induction, no matter how tightly regulated the promoter. The *B. subtilis* strain reported by Wong which was de-adapted away from Trp towards 4FW may be a more appropriate vehicle for preparing proteins lacking Trp fluorescence with 4FW. Unfortunately *B. subtilis* is not as widely used for protein expression systems as *E. coli*. A similar *E. coli* strain adapted towards 4FW and de-adapted from Trp may be useful, and such a strain may be viable at higher temperatures.

5.4.4 W92(4FW) and Trp-AMP Fluorescence Decay

It may still be possible to do meaningful studies with a low-level of Trp background fluorescence if it is properly accounted for in a blank solution. An attempt was made to collect time-resolved decay of substrate Trp-AMP prepared in W92(4FW) TrpRS, using an equally elaborate blank prepared with W92(4FW) with 4FW-AMP bound. It was hoped this blank would subtract the 5% Trp-92 decay contribution from the adenylate-bound conformer. Single wavelength data collected was fit to four-exponential decay times at 300 nm excitation, 340 and 345 nm emission (SVR = 2.00). Decay parameters as τ/α pairs were: 6.12 ns/0.07 , 2.15 ns/0.06, 0.38 ns/0.12 and 0.03 ns/0.75. These were first thought uninterpretable, so the sample and blank were sacrificed by PP_i addition, and the fluorescence decay measured again. Yet the

two short components completely disappeared after treatment with excess PP_i (SVR = 1.96); 5.73 ns/0.52 and 2.0 ns/0.48. This gave confidence to the blanking procedure, as three lifetimes that could be attributed to Trp-92 were not observed. These latter long decay times were unfortunately not consistent with free Trp, but could represent some persistent interaction or complex involving W92(4FW) TrpRS and Trp. The significant disappearance of the two short decay times 0.38 and 0.03 ns after PP_i treatment, allows their assignment to the Trp-AMP species. The observation of at least two decay times associated with Trp-AMP is consistent with two decay times observed for 5HW-AMP in Chapter 4. Therefore conformational heterogeneity in the Trp-AMP or its binding pocket is likely. Previous workers have attributed fluorescence quenching and decrease in lifetime to esterification or amidation of the carboxyl-group (Weinryb and Steiner, 1971), consistent with the observed shorter decays attributed to Trp-AMP here. The TrpRS·7AW-AMP substrate fluorescence seems not to be quenched at all.

5.4.5 Trp Analog Fluorescence in TrpRS

Fluorescence excitation of 5HW and 7AW at $\lambda > 310$ nm seemed sufficient to avoid the fluorescence excitation of Trp from any leakage product in fluorescence emission and decay measurements. Excitation spectra, however would have artefacts from the 5% Trp, as was seen by the slight features in Figure 5.8 at 292 nm attributed to the ^1L_b dipole of Trp.

Fluorescence results here indicate that the λ_{max} of 5HW was relatively insensitive to changes in environment, with changes of only a few nm, observed between 334 and 336 nm. In this respect 5HW is much like Tyr (Ross et al., 1992b), which undergoes changes only between 303 and 305 nm. However there were

significant changes in the quantum yield of 5HW. The observation of larger deviations in DAS component λ_{max} was noteworthy, as these approach values for 5HI in nonpolar solvents, and contribute to the structured blue-edge observed for buried 5HW residues. That these higher energy λ_{max} did not dominate the steady-state spectrum of 5HW buried in a protein was unexpected. A dipolar relaxation caused by the protein, and not attributed to solvent exposure, could result in the dominance of the lower energy λ_{max} in the steady-state spectra.

It is noteworthy that 5HW, which is less sensitive to solvent dielectric relaxation than Trp, and is a single dipole absorbing/fluorescing species, exhibits triple-exponential decay kinetics. This experiment, as suggested by Hudson et al., (1986), is important additional evidence that the origin of multi-exponential fluorescence decay of Trp is due to conformational heterogeneity from rotamers (Szabo and Rayner, 1980).

Ross and coworkers (1992a) predicted that energy transfer from Tyr to 5HW would be about 3 times more efficient than energy transfer from Tyr to Trp, based on the spectral overlap integral. The intensity of Tyr fluorescence in the W92(5HW) enzyme at 300 nm emission, 280 nm excitation was 28% less than the intensity of the W92(4FW) enzyme. The Tyr fluorescence of the wild-type was 6% less than that of the W92(4FW) enzyme. This suggests that Tyr fluorescence was quenched more efficiently by 5HW, and that energy transfer from Tyr to 5HW was indeed more efficient than from Tyr to Trp. The R_o for Tyr - Trp RET is about 15 Å (Lakowicz, 1983). Factoring in the J value of Ross et al. (1992a) the R_o for Tyr - 5HW RET should be close to 18 Å. The Tyr-65 in W57(5HW) Oncomodulin was also well within this 18 Å range, yet it was not quenched by 5HW. An observations of lower than expected Tyr $\rightarrow$ 5HW RET may be attributed to a stricter orientational (κ^2) dependence of Tyr $\rightarrow$ 5HW RET, as only the ^1L_b state of 5HW is involved for RET > 300 nm.

5.4.6 7AW As an Indicator for Protein Denaturation

The protein W92(7AW) TrpRS provides another demonstration of the large magnitude changes of 7AW fluorescence upon denaturation with chaotropic agents, as first published by Schlesinger (1968). The intense, blue shifted, long-lived fluorescence of 7AI is therefore characteristic of a buried 7AW. Schlesinger (1968) showed the fluorescence from 7AW-incorporated alkaline phosphatase had a high intensity and uncorrected λ_{max} near 370, which was diminished and red-shifted in the presence of 6 M GdHCl. Aqueous quenching of 7AW fluorescence was eliminated by protecting the N1 and N7 side of the 7-azaindole ring from solvent hydroxyls which were capable of catalyzing an excited state tautomerization (section 2.4.2, Figure 2.13). Consequently 7AW fluorescence is very sensitive to its exposure to water. Experiments here have clearly demonstrated the response of the buried 7AW-92 in TrpRS to solvent exposure. In addition, the high quantum yield and 360 nm maxima of W92(7AW) indicates the residue at position 92 was not accessible to water.

Fluorescence and phosphorescence have been used to monitor denaturation processes (e.g. Fersht, 1993; Mersol et al., 1993), in addition to other optical and NMR spectroscopies. The ideal denaturation curve appears as a graph of spectroscopic signal versus denaturing conditions (e.g. fluorescence versus [GdHCl]). An ideal single-transition curve would appear as a flat pre-transition region, a sharp change in signal indicating the transition, and a flat post-transition region. Such curves were found with the urea denaturation of barnase, following fluorescence at 279 nm excitation, 320 nm emission (Pace et al., 1992). Unfortunately TrpRS is not an ideal model system for protein denaturation. On the other hand it is not an atypical example, as many proteins denature irreversibly and aggregate.

Ahmad (1993) advises against using Trp fluorescence to monitor thermal unfolding. His argument is based on the significant decrease of Trp fluorescence with

temperature (>1% per degree). This introduces steep, temperature-sensitive pre- and post- transition baselines into the ideal curve. This has been well documented (Kronman, 1976; Palleros et al., 1992; Dungan and Horowitz, 1993). Although Trp fluorescence is generally poor for detecting thermal unfolding transitions, it has demonstrated some success.

Figure 5.11 plainly illustrates that, for TrpRS, no transition could be perceived from Trp-92 fluorescence. The steep decline in fluorescence of Trp-92 from 20-30° C is in stark contrast to the steady fluorescence of 7AW-92 over the same temperature range. This suggests that the pre-transition baseline of incorporated 7AW may be much less steep than that of Trp. 5HW-92 also exhibits a steep baseline like that of Trp, yet it has a perceptible temperature transition, unlike Trp. In this case, both 5HW and 7AW show greater responses for monitoring thermal transitions than Trp.

5.4.7 Local Environment of 5HW-92

The formation of an α-helical structure placing Cys-96 close to either Trp-92 or 5HW-92 is put forth as the conformational change causing the approximately 70% steady-state quenching for each of these fluorophores. That these were not quenched to an even greater extent, and that longer decay times of Trp which persist is most unusual. This is one case where a conformation predisposed to dominant static quenching complex could be expected. Since a variation in radiative lifetimes is evident as discussed in Appendix A, the 70% decrease in quantum yield is largely attributed to dynamic quenching from the nearby Cys residue, which is within 3.58 Å of the indole N of Trp-91 in the *B. stearothermophilus* TrpRS structure (Doublié et al., 1994).

Nonetheless it is important that both 5HW-92 and Trp-92 detect the same steady-state conformational change with Trp-AMP formation, arguing they are in the same local microenvironments in wild-type and mutant proteins. That their radiative lifetimes, τ_r, change in different directions may have to do with the alternate orientations of their different emissive dipole transitions, which are almost at right angles to one another (Figure 2.4).

5.4.8 W92(5HW) TrpRS Conformers With Substrates

The mechanism of TrpRS has been earlier demonstrated to be highly ordered, as discussed in Chapter 1, section 1.2.5.1, Figure 1.13, and in Chapter 4, section 4.4.2. Here there is both strong kinetic and spectroscopic evidence that this mechanism ordering was lost with W92(5HW). That a short decay time appears upon the addition of $tRNA^{Trp}$ and in the W92(5HW)·4FW-AMP complexed enzyme is significant. This short decay component was not detected in the uncomplexed W92(5HW) enzyme, so two conformers were probably not in equilibrium prior to the introduction of $tRNA^{Trp}$. Therefore an induced-fit complex is evident. This is a strong indication that the adenylate-bound enzyme conformer is the same as the $tRNA^{Trp}$ binding enzyme conformer. It could be argued that a similar induced-fit complex between $tRNA^{Trp}$ and the wild-type TrpRS was seen, but only after a third substrate was present, explaining the observations of Chapter 3.

The changes to W92(5HW) fluorescence due to substrate ATP 4FW or Trp binding are also noteworthy. The 4FW substrate, at an even higher concentration, had no affect on Trp-92 fluorescence in Chapter 3. Here, the patterns of fluorescence decay of W92(5HW) due to 4FW substrate binding were unlike those from the adenylate or $tRNA^{Trp}$ complexes, thus it is unlikely that Trp binding alone placed the

enzyme into the correct conformation for binding $tRNA^{Trp}$. The combinations of Trp and $tRNA^{Trp}$, or ATP and $tRNA^{Trp}$, did not provide fluorescence decay patterns which mimicked the adenylate complex, rather they more closely resembled the decays from mixtures of enzyme with ATP and Trp respectively. In the case of the mixture of enzyme with $tRNA^{Trp}$ and ATP, the values of c_i match those from the mixture of enzyme and ATP without $tRNA^{Trp}$. These patterns seem to argue against the observation of tertiary complexes, as were seen with wild-type TrpRS. This observation further suggests that the overall stabilization of certain enzyme-substrate complexes has been altered by 5HW-92.

5.4.9 TrpRS Mechanism Order and Residue 92

No evidence has been reported of $tRNA^{Trp}$ binding to TrpRS in the absence of Trp, ATP or Trp-AMP. The 5HW-92 residue somehow stabilizes the $tRNA^{Trp}$-bound conformer in the absence of Trp-AMP, allowing induced-fit $tRNA^{Trp}$·TrpRS conformers to be observed. This 5HW-92 residue also allows the premature binding of substrate Trp out of mechanistic order. From this and previous work, clearly this one Trp residue plays a very large role in maintaining activity and proper ordering of the entire TrpRS mechanism. There is no homologous residue in the mammalian TrpRS enzymes. This may account for their very different mechanisms, as mentioned in Chapter 1, section 1.2.5.3.

A molecular envelope determined for a crystals of an alternate TrpRS conformer shows each monomer has a loosely-tethered C-terminal domain. This is also supported by limited proteolysis studies of *E. coli* TrpRS (Omnaas et al., 1979), where the C-terminus was shown to be cleaved. However as discussed in section 1.2.5.1, both the molecular envelopes of TrpRS monomers (Carter Jr. et al., 1994) were too small in the

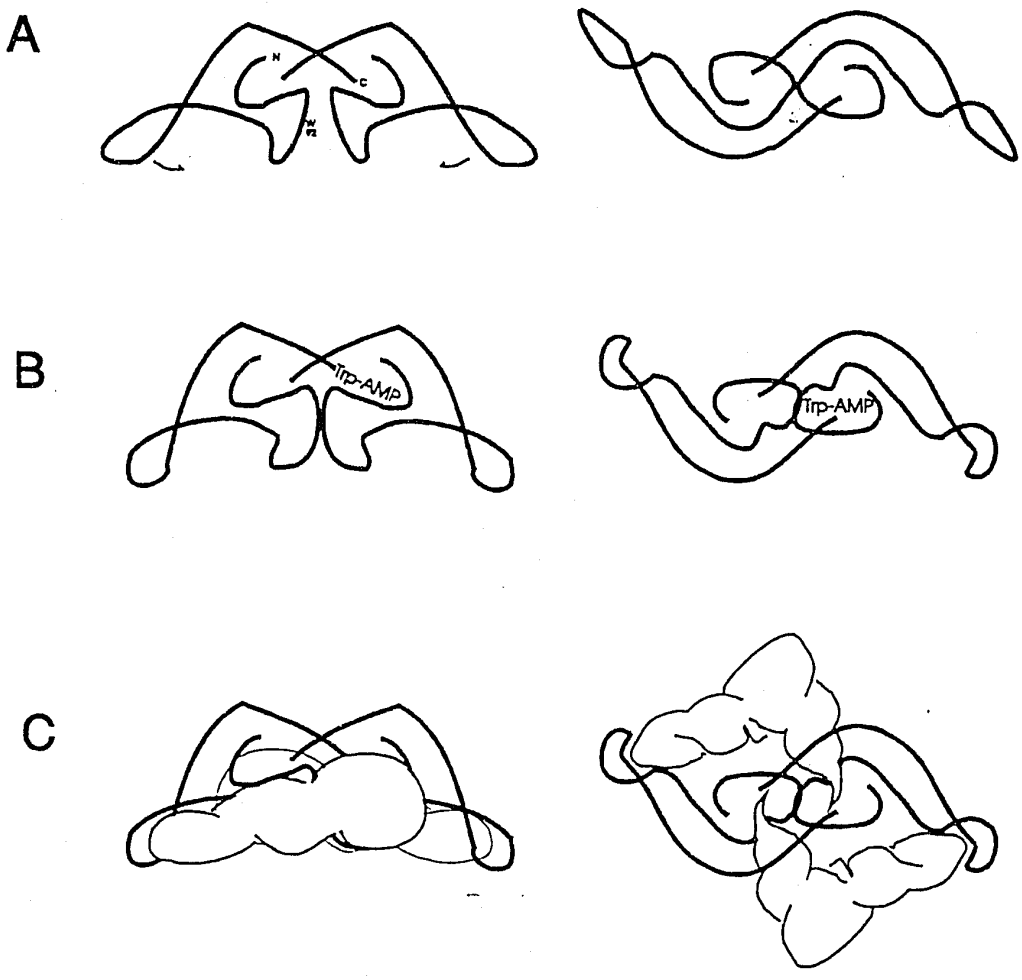

Figure 5.18: Cartoon showing possible dynamic substrate-dependent conformational changes of TrpRS. Left and right images correspond to side and top views A. Uncomplexed enzyme conformation, with loosely tethered C-termini. B. The adenylate-binding conformer (compare with Figure 1.6) based on the crystal structure. C. The $tRNA^{Trp}$ binding conformer is expected to be similar to B., and accommodate the ends of two $tRNA^{Trp}$ molecule as shown here. Geometric constraint arguments are used to indicate the possible orientation of $tRNA^{Trp}$.

two crystal conformations to accommodate a $tRNA^{Trp}$ molecule, hence the $tRNA^{Trp}$ must be bound across the subunit interface of TrpRS, like TyrRS (Carter et al., 1986). A concerted conformational change would be expected therefore to alter the conformation of both subunits symmetrically allowing $tRNA^{Trp}$ to bind across the dimer in either orientation. This gives a structural and mechanistic rationalization for why TrpRS requires a concerted conformational change.

The dynamic conformational changes evident in TrpRS are depicted in the cartoon in Figure 5.18. The side and top views are drawn based on a cartoon to depict a simplified backbone. The C-terminal domains on the ends of the enzyme are shown first in an extended conformation, and upon Trp-AMP binding they are shown to adopt a $tRNA^{Trp}$ anticodon-binding conformer. The existing geometric constraints for $tRNA^{Trp}$ leave few possibilities other than the C-terminal location for anticodon binding. It is interesting that the C-terminal end has connectivity to the subunit interface, and that there may be a direct conformational link between the C-terminus and the region near Trp-92 (Doublié et al., 1994) through the two large outer helices. The conformational change induced by binding Trp-AMP alters the subunit interface portion of the enzyme, as evidenced by this body of work. This is expected to propagate to the CP1 domain which could bind the 3' terminus of $tRNA^{Trp}$. The expected orientation of binding of $tRNA^{Trp}$ is also shown.

5.4.10 An Aggregation Mechanism for TrpRS

The obvious temperature transition which can be seen for the W92(7AW) fluorescence results in a 50% decline by 42° C. This temperature corresponds to the point where significant aggregates begin to form in solution. A large decrease in the fluorescence yield of 7AW corresponds to solvent exposure, hence it is concluded that

the drop in the intense fluorescence of 7AW-92 corresponds to its exposure to bulk solvent, starting at 36° C. The temperature transition of W92(5HW) fluorescence is similarly at lower temperature (42° C) than the temperature of aggregation (44° C).

Considering the location of the single Trp-92, buried deep within the subunit interface of TrpRS, it can be concluded that this transition corresponds to a process that disrupts the subunit interface. It is expected that these fluorescence transitions mark the temperature at which subunits dissociate. From the fluorescence of 7AW-92, the aggregation phenomenon did not begin until a significant fraction (e.g. 50%) of TrpRS molecules had dissociated into subunits. This aggregation is expected to vary with TrpRS concentration, pH, and buffer composition, which were constant in these studies. It is evident that TrpRS aggregation probably follows subunit dissociation.

Interesting comparisons with an early in-vivo study of a *B. subtilis* strain with a temperature-sensitive mutant of TrpRS can be made (Steinberg and Anagnostopoulos, 1971). This strain ceased to grow at 42° C, which is indicative of the *in-vivo* thermal destabilization of TrpRS. These authors were unable to observe *in-vitro* activity at 30° C in either pyrophosphate exchange or tRNA aminoacylation. This is similar to the in-vivo behavior of the Trp-92 mutants reported by Chow et al. (1992). Steinberg and Anagnostopoulos concluded that, at the restrictive temperature, the temperature-sensitive event was an irreversible step leading to inactivation of TrpRS and suggested it may be correlated with subunit dissociation.

Inadvertent aggregation was suggested as the underlying reason for the inactivity of the TrpRS mutants at position 92 W92F, W92A, and W92Q (Chow et al., 1992) in section 3.4.1 of this work. It can be further concluded that substitution of Trp-92 destabilizes the subunit interface in these mutants which renders them inactive and likely to aggregate. The irreversible nature of aggregation, and the observed disulfide bond formation (section 3.3.1) upon denaturation corresponds to the potential exposure

of Cys-96. This also indicates subunit dissociation as a mechanism preceding aggregation.

Hence a proposed mechanism for irreversible aggregation of TrpRS involves a disruption of the subunit interface, whereupon Cys-96 is exposed and allowed to form disulfide bonds with Cys residues from other subunits. The exposure of the hydrophobic subunit interface is expected to nucleate further aggregation.

5.4.11 Hydrophobicity of Fluorinated Analogs.

The unexpected observation of thermostabilization of TrpRS by 4FW substitution deserves further comment. Wong and coworkers (Xu et al., 1989) used fluorotryptophans as substrates for *B. subtilis* TrpRS, and demonstrated that the fluorotryptophans were more hydrophobic than Trp in the order: Trp < 4FW < 6FW < 5FW in increasing hydrophobicity. The effect of a fluoro-substituent is minimal in terms of increased molecular volume (Pauling, 1960), hence these analogs could be considered isomorphous with Trp. The hydrophobic series of incorporable isomorphous Trp analogs 7AW < Trp < 4FW < 6FW < 5FW may prove itself useful in studies of the kinetic, dynamic and stability properties of other proteins and enzymes. The hydrophobic effect is accepted as the dominant force for protein folding (Dill, 1990). The dynamics and flexibility of some enzymes are carefully tuned by their hydrophobicities to the viable temperature range of the organism in which they are found (Nosoh and Sekiguchi, 1993). This work hints that enzyme thermostabilization may be a beneficial effect of fluorotryptophan substitution. Further study of this unusual phenomenon is warranted.

5.5 Summary and Conclusions

B. subtilis tryptophanyl-tRNA synthetase (TrpRS) has a single conserved Trp-92. 5HW and 7AW are useful new intrinsic fluorescence probes, capable of exclusive excitation at 310-320 nm. The nonfluorescent 4FW could be used to make proteins free of Trp fluorescence. Using a Trp auxotroph of *E. coli*, efficient replacement of Trp-92 has been achieved using 4FW, 5HW, and 7AW. The technique used here for analog incorporation also resulted in superior yields for the wild-type enzyme. 7AW-92 exhibited useful properties as a probe of environment and solvent exposure.

The three Trp analogs in position 92 have different effects on $tRNA^{Trp}$ aminoacylation kinetics. W92(4FW) TrpRS was most similar to native TrpRS. W92(7AW) TrpRS had depressed kinetics compared to the wild-type protein which could result from a fractional inactivation of a portion of the enzyme. W92(5HW) TrpRS exhibited unusual kinetic behavior compared to the wild-type, suggesting formation of unproductive complexes with the enzyme binding prematurely to either $tRNA^{Trp}$ or Trp. Both of these unproductive complexes were confirmed by the fluorescence of 5HW-92. The formation of Trp-AMP induces a quenching of 5HW-92 of the same magnitude experienced by Trp-92. This is accounted for by a conformational change which places Cys-96 nearby 5HW-92 on an α-helix. The observation that residue 92 plays a substantial role in $tRNA^{Trp}$ aminoacylation suggests its importance in stabilizing different conformations associated with the TrpRS mechanism and its ordering.

Appendix A: Static Quenching or Radiative Lifetimes?

The singlet lifetime τ_s of a Trp residue is mainly a function of two rate parameters, k_r and k_{nr}:

$$\tau_s = 1 /(k_r+k_{nr}) \qquad (A.1)$$

The rate of fluorescence depopulation of a molecule k_r is related to the radiative lifetime of the molecule, τ_r:

$$\tau_r = 1 / k_r \qquad (A.2)$$

The quantum yield of a fluorophore Φ_f, is related by definition to both the singlet lifetime and the radiative lifetime:

$$\Phi_f = \tau_s / \tau_r \qquad (A.3)$$

Substituting equation A.2 into A.1:

$$\tau_s = 1 /((1/\tau_r)+k_{nr}) \qquad (A.4)$$

In a previous report (Szabo and Faerman, 1992) values of τ_r have been demonstrated to vary from 8.8 ns up to 56.8 ns (Szabo and Faerman, 1992) for many different single-Trp proteins with quantum yields in the range $0.05 < \Phi_f < 0.35$. The presence of a static quenching component which reduces the value of Φ_f could account for unusually high values of τ_r, and thus the variation observed could be considered

false. But physical static quenching complexes cannot always be assigned to account for this wide range of values (Chen et al., 1991; Szabo and Faerman, 1992, Vos and Engelborgs, 1994), hence the variations in τ_r might inherently originate from processes other than static quenching. Static quenching is most clearly demonstrated by a decrease in Φ_f but with constant τ_s. If only those values of $\Phi_f > 0.3$ are compared, ensuring competing external non-radiative processes are minimal, a large variation in τ_r values remains. As shown in Table A.1, the two largest values of τ_r correspond to larger λ_{max} values.

Table A.1 Radiative Lifetimes of Trp.

PROTEIN	Φ_f	$<\tau>$ (ns)	τ_r (ns)	λ_{max}
[a]Apo Azurin	0.31	5.10	15.5	308
[b]Apo Rat Parvalbumin F102W	0.36	3.77	10.5	313
[b]Holo Rat Parvalbumin F102W	0.41	4.04	9.85	313
[c]Phosphofructokinase	0.31	3.28	10.6	328
[d]Troponin C mutant	0.33	7.24	21.9	337
[e]Phosphoglycerate Mutase	0.31	16.4	53.0	368

a (Szabo et al., 1983); *b* (Pauls et al., 1993); *c* (Kim et al., 1993); *d* (I.D. Clark, personal communication); e (Schauerte and Gafni, 1989). *a* and *b* are unambiguous single-exponential decays *c,d* are from double-exponential decays and *e* is estimated from the resolved single-exponential decay of a unique Trp in a multi-Trp protein.

Equation A.4 shows that the differences in τ_s that were observed in multi-exponential fluorescence decay of a single Trp could come from either differences in τ_r or k_{nr}. If radiative processes (τ_r) are different for different rotamers or ground-state conformers, multi-exponential decay would be certainly observed. However differences of τ_r are not widely considered as the underlying origin of multi-exponential *single*-Trp luminescence. In the majority of studies, τ_r are assumed to be equal for different conformers in the data analysis. Instead, changes in non-radiative processes (k_{nr}) are invoked to explain observed τ_s, e.g. examining the near-neighbors of a Trp residue and their quenching efficiencies, and attributing differences to non-radiative

rates for each conformer. An example is the style of treatment of Harris and Hudson (1990) in which any nearby potential quencher of a Trp residue was considered.

The observed quenching of either Trp-92 or 5HW-92 in this thesis upon adenylate formation, represents about a 70% drop in quantum yield. It is remarkable that the same complex yields similar changes in Φ_f for these two different fluorophores, yet the changes in their fluorescence decay behaviour do not correspond. After complexation, the calculated τ_r of Trp-92 increases twofold, but for 5HW-92 τ_r decreases to about half its value. These stark differences warrant a closer examination of the underlying assumptions (as shown by Hutnik and Szabo, 1989). The quantum yield is the sum of the quantum yield of each component:

$$\Phi_f = \Phi_1 c_1 + \Phi_2 c_2 + \Phi_3 c_3 \qquad (A.5)$$

Equation A.3 substituted into A.5 gives:

$$\Phi_f = (\tau_{s1}/\tau_{r1})c_1 + (\tau_{s2}/\tau_{r2})c_2 + (\tau_{s3}/\tau_{r3})c_3 \qquad (A.6)$$

Using the values in Table 3.4 (Sample 1 TrpRS) for τ_{si} and c_i, and assuming the radiative lifetime for Trp-92 was 17 as calculated, the quantum yield equates to 0.18 (as it should, since the value of τ_r was determined from 0.18). Yet if the values of τ_r were varied, the quantum yield of 0.18 could be also obtained from certain combinations of τ_r, for example: $\tau_{r1} = 40$; $\tau_{r2} = 15$ and $\tau_{r3} = 10$. Note that these values are reasonable given Table A.1 and the maxima observed of 340, 325 and $\lambda <$ 320 nm for the three decay components. If the same lifetimes are used, but altered values of $c_1 = 0.2$, $c_2 = 0.3$ and $c_3 = 0.5$, are inserted into equation A.6, the quantum yield becomes 0.14. Alternatively the values: $c_1 = 0.1$, $c_2 = 0.8$ and $c_3 =$ 0.1 give a quantum yield of 0.21. *Therefore alterations to the component population*

could lower or raise the quantum yield provided variations in τ_r *exist*. The resulting τ_r calculated from equation A.3 might represent a mean value, and either increase or decrease depending on the c_i values. An increase in τ_r is observed with Trp-92, and a decrease of τ_r is observed in 5HW-92. Since both these changes are evident, static quenching is unlikely to be affecting the fluorescence of Trp-92, rather it is more likely to have different values of τ_r associated with each conformer. In the case of the His quenching of the single Trp fluorescence of anantin, static quenching could also not explain the observed changes in fluorescence parameters (Vos and Engelborghs 1994). Varying values of τ_r would necessitate changes in the values of c_i calculated from DAS, as these would not reflect the solution concentration of components. It is important to note that variations in τ_r between 10-50 ns cannot account for the wide variety of lifetimes displayed by single Trp residues (ps to ns), and that alterations to k_{nr} must also occur. The patterns observed in DAS as mentioned near the end of section 2.3.2 indicate that these parameters, τ_r and k_{nr} and λ_{max} are probably correlated, and these may all reflect nuclear coordinate alterations.

Appendix B: 5HW In Oncomodulin

Appendix C: Curriculum Vitae

Christopher Warren Victor Hogue

Date of Birth	11 May, 1965
Place of Birth	Windsor, Ontario
Citizenship	Canadian
Academic Background	
Sept 1990 - Present	Postgraduate Studies - Biochemistry
	University of Ottawa
Sept 1984 - June 1990	Bachelor of Science - Honours Biochemistry
	University of Windsor
1984	Honours Secondary School Graduate Diploma
	Sandwich Secondary School, LaSalle Ont.

Membership To Professional Bodies

American Association for the Advancement of Science.
Biophysical Society
Canadian Society of Chemistry
Society for Teaching and Learning in Higher Education
International Society for Exploring Teaching Alternatives

Scholarships and Awards

NSERC Postdoctoral Fellowship (29,000/a)	1995-6
NSERC Postgraduate Scholarship PGS3 U. of Ottawa ($20,500/a)	1993,94
Ontario Graduate Scholarship U. of Ottawa ($12,000/a)	1991,92
Research Achievement Award U. of Ottawa, Tuition Waiver	1990,91,92
Winbaum Memorial Bursary U. of Windsor ($150)	1989
Academic Scholarship U. of Windsor, Tuition Waiver	1984,85,86
NSERC Undergraduate Research Award U. of Windsor, Summer Research ($750/m)	1986
Physics Dept. Entrance Award U. of Waterloo (Declined)	1984
Ford of Canada Scholarship U. of Windsor ($500)	1984
Kelley-England Bursary/CAW Local 200 U. of Windsor ($200)	1984
Ontario Scholar Sandwich Secondary School	1984
Telesat Canada Space Shuttle "Getaway Special" contest, National Finalists, Sandwich Secondary.	1984

Publications

Publications in Refereed Journals:

13 Hogue, C.W.V., MacManus, J.P., Szabo, A.G. (1994) Efficient sites for Terbium (III) luminescence enhancement energy donors in Oncomodulin. In preparation.

12 Hogue, C.W.V., Xue, H., and Szabo, A.G. (1994) Biosynthetic incorporation of tryptophan analogs in place of the essential Trp-92 of *B. subtilis* tryptophanyl-tRNA synthetase. In preparation.

11 Hogue, C.W.V., Doublié, S., Carter, C.W. Jr., Xue, H., Wong, J.T. and Szabo, A.G. (1994) A tryptophanyl-adenylate dependent concerted conformational change in *B. subtilis* tryptophanyl-tRNA synthetase revealed by the fluorescence of Trp-92. In preparation.

10 Brennan, J.D., Clark, I.D., Hogue, C.W.V., Ito, A., Juliano, L., Pavia, A., Rajendran, B., and Szabo, A.G. (1994) Interaction of enantiomers of lysyl-7-azatryptophyl-lysine with acidic phopholipid vesicles: A Fluorescence Study. Applied Spectroscopy. In Press.

9 Clark, I.D., Bruckman, A.J., Hogue, C.W.V., MacManus, J.P., and Szabo, A.G. (1993) Effects of Metal Ion Binding on an Oncomodulin Mutant Containing a Novel Calcium-Binding Loop. **J. Fluorescence.** In Press.

8 Hill, I., Hogue, C.W.V., Clark, I.D., MacManus, J.P., and Szabo, A.G. (1993) Detection of calcium-binding proteins on polyacrylamide gels using time-resolved lanthanide luminescence photography. **Anal. Biochem.** 216, 439-443.

7 Hogue, C.W.V. and Szabo, A.G. (1993) Characterization of aminoacyl-adenylates in *B. subtilis* tryptophanyl-tRNA synthetase, by the fluorescence of tryptophan analogs 5-hydroxytryptophan and 7-azatryptophan. **Biophys. Chem.** 48, 159-169.

6 Hogue, C.W.V., Rasquinha, I., Szabo, A.G., and MacManus, J.P. (1992) A new intrinsic probe for proteins - biosynthetic incorporation of 5-hydroxytryptophan into oncomodulin **FEBS Letters** 310, 269-272.

5 Hogue, C.W.V., MacManus, J.P., Banville, D., and Szabo, A.G. (1992) Comparison of Terbium(III) Luminescence Enhancement in Mutants of EF-hand Calcium-binding Proteins. **J. Biol. Chem.** 267, 13340-13348.

4 MacManus, J.P., Hogue, C.W., Marsden, B.J., Sikorska, M., Szabo, A.G. (1990) Terbium Luminescence in Synthetic Peptide Loops From Calcium-Binding Proteins With Different Energy Donors. **J. Biol. Chem.** 265.18, 10358-10366.

3 Habowsky J.E.J., Sands, T.W., Hogue, C.W.V., and Stager, R.A. (1990) The Database as a Learning Tool. **Journal of College Science Teaching** May, 363-367.

2 Habowsky J.E.J., Sands, T.W., Hogue, C.W.V., Stager, R.A. and Postlethwait, S.N. (1990) An Audio-directed Multimedia Lab. **Journal of College Science Teaching** February, 232-234.

1 Hogue, C.W.V. and Fackrell, H.B. (1987) The Menu Workbench: An Automatic Menu Generator for Biomedical Programs. **International Journal of Bio-Medical Computing** 21, 253-264.

Publications in Non-Refereed Journals:

Habowsky J.E.J., Sands, T.W., Hogue, C.W.V., and Stager, R.A. (1987) Interactive Audio Cassette. The Unifying Thread in Multi-Media and Computer Assisted Instruction. **Connexions - Journal of the International Society for Exploring Teaching Alternatives** 3:1-2.

Conference Proceedings:

20 Hogue, C.W.V., Cyr, S., Brennan, J.D., Pauls, T.L., Cox, J.A., Berchtold, M.W., and Szabo, A.G. Efficient Incorporation of Tryptophan Analogs In Recombinant Rat F102W Parvalbumin For Fluorescence and ^{19}F NMR Studies. **39th Annual Meeting of the Biophysical Society,** Feb 1995. San Francisco USA. (Submitted to the **Biophysical Journal**)

19 Clark, I.D., Hogue, C.W.V., Dufor, D., Pauls, T.L., Cox, J.A., Berchtold, M.W. and Szabo, A.G. Near Neighbors of Trp-102 in Rat Parvalbumin Mutated To Residues of Oncomodulin. Why is the Multi-Exponential Fluorescence Decay of Oncomodulin Not Exhibited In This Mutant? **39th Annual Meeting of the Biophysical Society,** Feb 1995. San Francisco USA. (Submitted to the **Biophysical Journal**)

18 Hogue, C.W.V. Multiexponential Fluorescence Decay of A Single 5-Hydroxytryptophan Containing Protein. **77th CSC Conference**, May 29 - June 2. 1994 Winnipeg, MN, Canada. Abstract 505.

17 Brennan, J.D., Hogue, C.W.V., and Szabo, A.G. Photophysics of 7-Azatryptophan: An Intrinsic Fluorescent Probe of Protein Folding. **77th CSC Conference**, May 29 - June 2. 1994 Winnipeg, MN, Canada. Abstract 506.

16 Szabo, A.G., Hogue, C.W.V., and Brennan, J. Biosynthetic incorporation of tryptophan analogs in proteins: Exciting prospects for protein interaction studies. **38th Annual Meeting of the Biophysical Society,** March 6-10 1994. New Orleans, Louisiana, USA. **Biophysical Journal** 66.2.2:A252.

15 Hogue, C.W.V. ß-strand structures in simulations of emerging polyalanine: The excluded volume effect. **38th Annual Meeting of the Biophysical Society,** March 6-10 1994. New Orleans, Louisiana, USA. **Biophysical Journal** 66.2.2:A395.

14 Szabo, A.G., and Hogue, C.W.V. A fluorescence study of 5-hydroxytryptophan-92 in *B. subtilis* tryptophanyl-tRNA synthetase. **38th Annual Meeting of the Biophysical Society,** March 6-10 1994. New Orleans, Louisiana, USA. **Biophysical Journal** 66.2.2:A187.

13 Hogue, C.W.V. Protein Engineering with the isomorphous Trp analogs 7-azatryptophan and 4-fluorotryptophan. **38th Annual Meeting of the Biophysical Society,** March 6-10 1994. New Orleans, Louisiana, USA. **Biophysical Journal** 66.2.2:A296.

12 Szabo, A.G., and Hogue, C.W.V. Structural changes of aminoacyl-adenylate formation in 5-hydroxytryptophan-92 incorporated *B. subtilis* tryptophanyl-tRNA synthetase. **11th International Biophysics Congress**, July, 1993 Budapest, Hungary.

11 Hogue, C.W.V., and Szabo, A.G. Mechanistic studies of *B. subtilis* tryptophanyl-tRNA synthetase using the fluorescent substrates 5-hydroxytryptophan and 7-azatryptophan. **11th International Biophysics Congress**, July, 1993 Budapest, Hungary.

10 Hogue, C.W.V., Xue, H., Wong, J.T. and Szabo, A.G. Fluorescence of *B. subtilis* tryptophanyl-tRNA synthetase and tRNA aminoacylation intermediates with 4-fluorotryptophan. **37th Annual Meeting of the Biophysical Society,** Feb, 1993. Washington DC., USA. **Biophysical Journal** 64.2.2:M-Pos179.

9 Hogue, C.W.V. The excluded volume effect examined with kinetic, self-avoiding, off-lattice random walk polypeptides. **37th Annual Meeting of the Biophysical Society,** Feb, 1993. Washington DC., USA. **Biophysical Journal** 64.2.2:W-Pos127.

8 Hogue, C.W.V., Szabo, A.G., and Wong, J.T. *B. subtilis* tryptophan tRNA synthetase - Fluorescent studies of the single-tryptophan enzyme and the W92F mutant. **36th Annual Meeting of the Biophysical Society,** Feb, 1992. Houston, Texas, USA. **Biophysical Journal** 61.2.2:1040

7 Rasquinha, I., Hogue, C.W.V., Szabo A.G., and MacManus, J.P. *E. Coli* tryptophan tRNA synthetase will incorporate 5-hydroxy-tryptophan into expressed proteins - A new intrinsic fluorescent probe. **36th Annual Meeting of the Biophysical Society,** Feb, 1992. Houston, Texas, USA. **Biophysical Journal** 61.2.2:2610

6 Hogue, C.W.V., Szabo, A.G., MacManus, J.P., and Banville, D. (1991) Studies of Tb^{3+} Luminescence Amongst Mutants of Ca^{2+} binding proteins - Engineering A Highly Luminescent Tb^{3+} Binding Protein. **35th Annual Meeting of the Biophysical Society, San Francisco Feb 24-28. Biophysical Journal** 59:355a.

5 Habowsky, J.E.J., Sands, T.W., Hogue, C.W.V., and Doyle, R.J. (1990) Two Decades Using Media Technologies in Education: Have They Improved The Instructional Process? **10th Annual Conference on Teaching and Learning in Higher Education.** Junt 16-19 McGill University, Canada. 5.

4 Hogue, C.W.V., Thomas, D., and Mutus, B. (1990) Glutathione levels in *Achlya ambisexualis* using HPLC and the fluorescent thiol label monobromobimane. **Awarded 2nd Prize at the 18th Annual Southwestern Ontario Undergraduate Student Chemistry Conference,** March 24. Ryerson Polytechnical Institute. Toronto, Canada. 4-4.

3 Habowsky, J.E.J., Sands, T.W., Hogue, C.W.V., and Stager, R.A. (1988) Interactive Audio: The Unifying Thread in Multi-Media and Computer Assisted Instruction. **Proceedings of Ontario Universities Instructional Technology Conference,** April 20-22. University of Guelph, Canada. 93-94.

2 Habowsky, J.E.J., Sands, T.W., Hogue, C.W.V., and Stager, R.A. (1988) Educational Delivery Models Using Computer Databases. **Proceedings of Ontario Universities Instructional Technology Conference,** April 20-22. University of Guelph, Canada. 85-86.

1 Habowsky, J.E.J., Stager, R.A., Hogue, C.W.V., Sands, T.W., Glasgow, A., and Postlethwait, S.N., (1986) Audio-Tutorial/Individualized Instruction Using Computers. **Proceedings of the Annual Conference of the International Society for Individualized Instruction.** Atlanta, USA. 1-2.

Papers Presented:

14 Hogue, C.W.V, Random-Walk Polyalanine: A Diversion from Engineering Spectrally Enhanced Proteins. **National Center for Biotechnology Information, NIH,** Bethesda, MD. 15 August, 1994.

13 Hogue, C.W.V, Random-Walk Polyalanine: A Diversion from Engineering Spectrally Enhanced Proteins. **Dép. d'Informatique and Recherche Opérationelle, Université de Montréal,** 11 August, 1994.

12 Hogue, C.W.V, Tryptophanyl-tRNA synthetase and its role in the incorporation of tryptophan analogs: New Intrinsic Fluorescent Probes. **Dept. of Chemistry and Biochemistry, University of Windsor,** May, 6 1994.

11 Szabo, A.G., and Hogue, C.W.V. Unraveling the mechanism of tryptophan aminoacyl t-RNA synthetase using tryptophan analogs. **SPIE's International Symposium, Time-Resolved Laser Spectroscopy in Biochemistry IV,** Jan 24-26 1994. Los Angeles, CA. USA.

10 Hogue, C.W.V., Kinetic, Self-Avoiding, Non-Lattice Random Walk Polypeptides, Sizes and Shapes. **Patterns in Biology,** Oct 8-12, 1992. Albany, NY. USA.

9 Szabo, A.G., Hogue, C.W., Rasquinha, I., and MacManus, J.P. (1992) Site specific incorporation of 5-hydroxytryptophan into proteins: An intrinsic fluorescent probe to study protein-protein interactions. **Protein Engineering Network Centres of Excellence.** June 8-9. Montreal.

8 Hogue, C.W.V., Szabo, A.G., MacManus, J.P., and Banville, D. (1991) Studies of Tb^{3+} Luminescence Amongst Mutants of Ca^{2+} binding proteins - Engineering A Highly Luminescent Tb^{3+} Binding Protein. **IVth International Symposium on Quantitative Luminescence Spectrometry in Biomedical Sciences** May 27-31. State Univ. of Ghent, Belgium.

7 Hogue, C.W.V, Thomas, Des. S., and Mutus, B. (1990) Glutathione levels in *Achlya ambisexualis* using HPLC and the fluorescent thiol label monobromobimane. **Presented at the Metropolitan Detroit American Chemical Society Student Affiliate Symposium.** March 23. University of Detroit. USA.

6 MacManus, J.P., Hogue C.W.V., Hutnik, C.M.L., Banville. D., and Szabo, A.G., (1990) Fluorescent monitoring of metal-binding to tryptophan mutants of oncomodulin. **Seventh International Symposium on Calcium-Binding Proteins in Health and Disease,** March, 1990. Banff, Alberta, Canada.

5 Habowsky, J.E.J., Sands T.W., Hogue, C.W.V, and Stager, R.A. (1988) Interactive Audio: The Unifying Thread in Multi-Media and Computer Assisted Instruction. **Proceedings of the Canadian Society of Microbiologists Conference,** June 19-22. University of Windsor, Canada.

4 Hogue, C.W.V. (1988) Ten Minute Programming. **Presented at Ontario Universities Instructional Technology Conference,** April 20-22. University of Guelph, Canada.

3 Hogue, C.W.V., Sands, T.W. Habowsky J.E.J. and Stager R.A. (1987) Database Creation and Use in a Learning Environment. **Presented at Ontario Universities Instructional Technology Conference,** May 1-3. University of Guelph, Canada.

2 Habowsky, J.E.J., Postlethwait, S.N., Stager, R.A. Hogue, C.W.V. and Glasgow A. (1987) The Interactive Audio Cassette (IAC). **Presented at Ontario Universities Instructional Technology Conference,** May 1-3. University of Guelph, Canada.

1 Stager, R.A., Habowsky, J.E.J., and Hogue, C.W.V (1987) Teaching Decision-Making with Microcomputers. **Presented at Ontario Universities Instructional Technology Conference,** May 1-3. University of Guelph, Canada.

Patents:

Banville, D., MacManus, J.P., Marsden, B., Szabo, A.G., Hogue, C.W.V., Sikorska, M., and Clark, I. **Engineered Protein Chelates Suitable for Fluorescent Lanthanide [E.G. Terbium (III)]** Canadian Serial no. 590,950. Canadian Filing date Feb. 2, 1989 (pending).

Contributions to Commercially Viable Products:

LIFO - LIposome inFOrmation. 1990- Avestin Inc. (formerly MM Developments), 404-60 MacLaren St., Ottawa, Ont. Canada. An electronic database of over 10000 references relating to liposomes. Stand-alone search and retrieval software by C.W.V. Hogue.

ProtoGen (c) 1988, 1989, 1990 C.W.V. Hogue and D.G. Peel. A computer program that allows a user to prototype computer software and generate programming code from the prototype to allow completion in the C or Pascal languages. ProtoGen is a trademark of MacCulloch, Prymak Assoc. Inc., Windsor, Ontario, Canada.

Work Experience

Teaching Assistant, U. of Ottawa, Dept. of Biochemistry

Experimental Biochemistry BCH 3946 — 09/93-12/93,09/92-12/92 09/91-12/91,09/90-12/90

Physical Biochemistry BCH 3928 — 01/94-04/94,01/92-04/92 01/91-04/91,01/89-04/89

Teaching Assistant, U. of Windsor, Dept. of Biological Sciences

Cytology 55-228 — 09/89-12/89,09/87-12/87 09/86-12/86

Cellular Physiology 55-231 — 01/90-04/90 01/88-04/88

U. of Ottawa, Dept. of Biochemistry — 09/90-Present
Postgraduate Research Project: Tryptophanyl-tRNA synthetase and the incorporation of new intrinsic fluorescence probes into proteins.

U. of Windsor, Dept. of Chemistry and Biochemistry — 09/89-05/90
Undergraduate Research Project: HPLC quantitation of fluorescent labelled thiols in *Achlya ambisexualis*.

NRC Center for Protein Structure and Design, Ottawa — 08/88-09/89
Lab Technician. Terbium (III) luminescence enhancement in peptide and proteins based on EF-hand calcium(II) binding proteins.

U. of Windsor, Dept. of Biological Sciences. — 05/86-09/86
Programming immunoassay analysis software and computer assisted instruction.

U. of Windsor, Dept. of Biological Sciences. — 05/85-08/85
Laboratory assistant, Molecular biology of the soybean chloroplast.

Canadian Forces Militia, Windsor, 21 Service Battalion — 05/82-11/82
Private, Casualty Aide (Medic) Technical Qualification Level 1

References

Adams, R.L.P., Burdon, R.H., Campbell, A.M., and Smellie, R.M.S. (1976) *Davidson's The Biochemistry of the Nucleic Acids, 8th Ed.* Chapman and Hall, London.

Adler, T.K. (1962) The fluorescence of azaindoles. *Anal. Chem. 34*, 685-689.

Ahmad, F. (1993) Measuring the Conformational Stability of Enzymes. in *Thermostability of Enzymes* (Ed. M.N. Gupta). Springer-Verlag, New York, USA. pp 96-113.

Ala, P., Xue, H., Leung, L., Xue, Y.Q., Wong, J. T., and Yang, D.S.C. (1993) Crystallization of *Bacillus subtilis* tryptophanyl-tRNA synthetase. *J. Mol. Biol. 230*, 1089-1090.

Albinsson, B., and Nordén, B (1992) Excited-State Properties of the Indole Chromophore. Electronic Transition Moment Directions from Linear Dichroism Measurements: Effects of Methyl and Methoxy Substituents. *J. Phys. Chem 96*, 6204-6212.

Alcala, J.R., Gratton, E., and Predergast, F.G. (1987) Fluorescence lifetime distributions in proteins. *Biophys. J. 51*, 597-604.

Amann, E., Brosius, J., and Ptashne, M. (1983) Vectors bearing a hybrid *trp-lac* promoter useful for regulated expression of cloned genes in *Escherichia coli*. *Gene 25*, 167-178.

Andrews, D., Trezeguet, V., Merle, M., Graves, P.-V., Muench, K.H., and Labouesse, B. (1985). Tryptophanamide formation by *Escherichia coli* tryptophanyl-tRNA synthetase. *Eur. J. Biochem. 146,* 201-209.

Andrews, J., and Forster, L.S., (1972) Protein Difference Spectra. Effect of Solvent and Charge on Tryptophan. *Biochemistry 11*, 1875-1879.

Atkins, P.W. (1986) *Physical Chemistry, Third Edition*. W.H. Freeman, New York.

Avouris, P., Yang, L.L., and El-Bayoumi, M.A. (1976) Excited State Interactions of 7-Azaindole with Alcohol and Water. *Photochim. Photobiol. 24*, 211-216.

Backlund, B.-M., and Gräslund, A. (1992) Structure and dynamics of mollitin. Time-resolved fluorescence of a peptide hormone with a single Tyr residue. *Biophys. Chem. 45*, 17-25.

Barlati, S., and Ciferri, O. (1970) Incorporation of 5-methyl- and 5-hydroxy-tryptophan into the protein of *Bacillus subtilis*. *J. Bacteriol. 101*, 166-172.

Barstow, D.A., Sharman, A.F., Atkinson, T., and Minton, N.P. (1986) Cloning and complete nucleotide sequence of the *Bacillus stearothermophilus* tryptophanyl-tRNA synthetase gene. *Gene 46*, 37-45.

Beechem, J.M., and Brand, L. (1985) Time-Resolved Fluorescence of Proteins. *Ann. Rev. Biochem.* 54, 43-71.

Berlman, I. (1970) On an Empirical Correlation between Nuclear Conformation and Certain Fluorescence and Absorption Characteristics of Aromatic Compounds. *J. Phys. Chem. 74*, 3085-3093.

Bhattacharyya, T., and Roy, S, (1993) A Fluorescence Spectroscopic Study of Substrate-Induced Conformational Changes in Glutaminyl-tRNA Synthetase *Biochemistry 32*, 9268-9273.

Bhattacharyya, T., Bhattacharyya, A., and Roy, S. (1991) A fluorescence spectroscopic study of glutaminyl-tRNA synthetase from *Escherichi coli* and its implications for the enzyme mechanism. *Eur. J. Biochem. 200*, 739-745.

Birks, J.B. (1970) *Photophysics of Aromatic Molecules*, John Wiley and Sons, New York. pp 353-369.

Birks, J.B. (1975) *Organic Molecular Photophysics*. John Wiley and Sons, New York. pp 557-585.

Bollum, F.J. (1966) Filter paper disc techniques for assaying radioactive macromolecules. In *Procedures for Nucleic Acid Research* (Cantoni, G.L., and Davies, D.R. Eds.) Harper and Row, New York., pp 296-300.

Brennan, J.D., Clark, I.D., Hogue, C.W.V., Ito, A., Juliano, L., Pavia, A., Rajendran, B., and Szabo, A.G. (1994) Interaction of Enantiomers of Lysyl-7-Azatryptophyl-Lysine With Acidic Phospholipid Vesicles: A Fluorescence Study. *Applied Spectroscopy* (In Press).

Brick, P., and Blow, D.M. (1987) Crystal Structure of a Deletion Mutant of a Tyrosyl-tRNA Synthetase Complexed with Tyrosine. *J. Mol Biol. 194*, 287-297.

Brick, P., Bhat, T.N., and Blow, D.M. (1988) Structure of Tyrosyl-tRNA Synthetase Refined at 2.3 Å Resolution. *J. Mol. Biol. 208*, 83-98.

Bridges, J.W., and Williams, R.T. (1968) The Fluorescence of Indoles and Aniline Derivatives. *Biochem J. 107*, 225-237.

Bronskill, P.M. and Wong, J.T. (1988) Suppression of fluorescence of tryptophan residues in proteins by replacement with 4-fluorotryptophan. *Biochem. J. 249*, 305-308.

Brunie, S., Zelwer, C., and Risler, J.L. (1990) Crystallographic study at 2.5 Å resolution of the interaction of methionyl-tRNA synthetase from Escherichia coli with ATP. *J. Mol. Biol. 216*, 411-424.

Bryant, J.T., Green, R., Gurusadaiah, T., and Ryan, C.A. (1976) Proteinase inhibitor II from potatoes: isolation and characterization of its protomer components. *Biochemistry 15*, 3418-3424.

Bucci, E., and Steiner, R.F. (1988) Anisotropy decay of fluorescence as an experimental approach to protein dynamics. *Biophys. Chem. 30*, 199-224.

Burbaum, J.J., and Schimmel, P. (1991) Structural Relationships and the Classification of Aminoacyl-tRNA Synthetases. *J. Biol. Chem. 266*, 16965-16968.

Burbaum, J.J., Starzyk, R.M., and Schimmel, P. (1990) Understanding Structural Relationships in Proteins of Unsolved Three-Dimensional Structure. *Proteins: Structure Funtion and Genetics 7*, 99-111.

Carter Jr., C.W. (1988) Cloning heterologous genes into *E. coli* for enzyme production and crystal growth: Problems of expression and microheterogeneity. (1988) *J. Crystal Growth 90*, 168-179.

Carter Jr., C.W. (1993) Cognition, Mechanism and Evolutionary Relationships in Aminoacyl-tRNA Synthetases. *Annu. Rev. Biochem, 62,* 715-748.

Carter Jr., C.W. Crumley, K.V., Coleman, D.E., and Hage, F. (1990) Direct phase determination for the molecular envelope of tryptophanyl-tRNA synthetase from *Bacillus stearothermophilus* by X-ray contrast variation. *Acta Cryst. A46*, 57-68.

Carter Jr., C.W., and Carter, C.W. (1979) Protein Crystallization Using Incomplete Factorial Experiments. *J. Biol. Chem. 254*, 12219-12223.

Carter Jr., C.W., Doublié, S., and Coleman, D.E., (1994) Quantitative Analysis of Crystal Growth: Tryptophanyl-tRNA Synthetase Crystal Polymorphism and Its Relationship to Catalysis. *J. Mol. Biol. 238*, 346-365.

Carter, P., Bedouelle, H., Winter, G. (1986) Construction of heterodimer tyrosyl-tRNA synthetase shows $tRNA^{Tyr}$ inteacts with both subunits. *Proc. Natl. Acad. Sci. USA 83,* 1189-1192.

Caskey, C. Th., (1980) Peptide chain termination. *Trends Biochem. Sci. 5*, 234-237.

Chabbert, M., Lukas, T.J., Watterson, D.M., Axelsen, P.H., and Prendergast, F. (1991) Fluorescence Analysis of Calmodulin Mutants Containing Tryptophan: Conformational Changes Induced by Calmodulin-Binding Peptides from Myosin Light Chain Kinase and Protein Kinase II. *Biochemistry 30*, 7615-7630.

Chan, K.W., and Koeppe II, R.E. (1993) The "TIGN" sequence in E. coli tryptophanyl-tRNA synthetase serves as a Class I aminoacyl-tRNA synthetase "HIGH" sequence. *Biophys. J. 64,* A368.

Chang, M.C., Petrich, J.W., McDonald, D.B., and Fleming, G.R. (1983) Nonexponential Fluorescence Decay of Tryptophan, Tryptophylglycine, and Glycyltryptophan. *J. Am. Chem. Soc. 105,* 3819-3824.

Chapeville, F., Lipmann, F., Ehrenstein, G., Weisblum, B., Ray, W.J., and Benzer, S. (1962) On the role of soluble ribonucleic acid in coding for amino acids. *Proc. Natl. Acad. Sci. 48,* 1086-1092.

Chapman, C.F., and Maroncelli, M. (1992) Excited-state tautomerization of 7-azaindole in water. *J. Phys. Chem. 96*, 8430-8441.

Chen, R.F., Knutson, J.R., Ziffer, H., and Porter, D. (1991) Fluorescence of Tryptophan Dipeptides: Correlations with the Rotamer Model. *Biochemistry 30*, 5184-5195.

Chen, Y., Gai, F., and Petrich, J.W. (1994a) The single exponential fluorescence decay of the nonnatural amino acid, 7-azatryptophan and the nonexponential decay of tryptophan. *J. Phys. Chem. 98*, 2203-2209.

Chen, Y., Gai, F., and Petrich, J.W. (1994b) Solvation and excited-state proton transfer of 7-azaindole in alcohols. *Chem. Phys. Lett. 222*, 329-334.

Chen, Y., Rich, R.L., Gai F., and Petrich, J.W., (1993) Fluorescent Species of 7-Azaindole and 7-Azatryptophan in Water *J. Phys. Chem. 97*, 1770-1780.

Chou, P., Martinez, M.L., Cooper, W.C., McMorrow, D., Collins, S.T., and Kasha, M. (1992) Monohydrate Catalysis of Excited-State Double-Proton Transfer in 7-Azaindole. *J. Phys Chem. 96.* 5203-5205.

Chou, P.Y., and Fasman, G.D. (1974a). Conformational parameters for amino acids in helical, ß-sheet, and random coil regions calculated from proteins. *Biochemistry 13*, 222-245.

Chou, P.Y., and Fasman, G.D. (1974b). Prediction of protein conformation. *Biochemistry 13*, 222-245.

Chow, K., and Wong, J.T. (1988) Cloning and nucleotide sequence of the structural gene coding for *Bacillus subtilis* tryptophanyl-tRNA synthetase. *Gene 73*, 537-543.

Chow, K.C., Xue, H., Shi, W., and Wong, J.T-F., (1992) Mutational identification of an essential tryptophan in tryptophanyl-tRNA synthetase of *Bacillus subtilis*. *J. Biol. Chem. 267*, 9146-9149.

Churchward, G., Belin, D., and Nagamine, Y., (1984) A pSC101-derived plasmid which shows no sequence homology to other commonly used cloning vectors. *Gene 31*, 165-171.

Clark, B. (1980) The elongation step of protein biosynthesis. *Trends Biochem. Sci. 5*, 207-210.

Coates, P.B. (1968) The correction for photon "pile-up" in the measurement of radiative lifetimes. *J. Phys. E. 1*, 878-879.

Coleman, D.E., and Carter Jr., C.W. (1984) Crystals of *Bacillus stearothermophilus* Tryptophanyl-tRNA Synthetase Containing Enzymatically Formed Acyl Transfer Product Tryptophanyl-ATP, an Active Site Marker for the 3' CCA Terminus of Tryptophanyl-tRNA^{Trp}. *Biochemistry 23*, 381-385.

Cornish-Bowden, A. (1979) *Fundamentals of Enzyme Kinetics* Chapter 5.10, Butterworths, London.

Cowgill, R.W. (1976) Tyrosyl Fluorescence in Proteins and Model Peptides. In *Biochemical Fluorescence Concepts,* (Chen, R.F., and Edelhoch, H., Eds.) Marcel Dekker Inc. New York, NY., USA. pp 441-486.

Cowgill, R.W., (1967) Fluorescence and Protein Structure, XI. Fluorescence Quenching by Disulfide and Sulfhydryl Groups. *Biochim. Biophys. Acta. 140*, 37-44.

Creed, D. (1984) The Photophysics and Photochemistry of the Near-UV Absorbing Amino Acids. Parts 1-3. *Photochim. Photobiol 39*, 537-575.

Cusack, S. (1993) Aminoacyl-tRNA synthetases. *Current Opinion in Structural Biology 3,* 39-44.

Cusack, S., Berthet-Colominas, C., Härtlein, M., Nassar, N., and Leberman, R. (1990) Seryl-tRNA synthetase from *Eschericha coli* at 2.5 Å resolution: A second class of synthetase structure. *Nature 347*, 249-255.

Dahms, T.E.S., Willis, K.J., and Szabo, A.G. (1993) Fluorescence Decay Kinetics of a Tryptophyl Residue in a Protein Crystal. *Biophys. J. 64*, A55.

Davie, E.W., Koningsberger, V.V., and Lipmann, (1956) The isolation of a tryptophan-activating enzyme from pancreas. *Arch. Biochim. Biophys. 65*, 21-38.

Demas, J.N., and Crosby, G.A. (1971) The measurement of photoluminescence quantum yields. A Review. *J. Phys. Chem. 75*, 991-1024.

Demtröder, W. (1988) *Laser Spectroscopy. Basic Concepts and Instrumentation.* Corrected Third Printing. Springer-Verlag. Berlin, Germany.

Dignam, J.D., and Deutscher, M.P. (1979) Relation between aminoacyl-tRNA synthetase stimulatory factors and inorganic pyrophosphatase. *Federation Proceedings 38,* Abstract 3115.

Dill, K.A. (1990) Dominant Forces in Protein Folding. *Biochemistry 29*, 7133-7145.

Donzel, B., Gauduchon, P., and Wahl, Ph. (1974) Study of the conformation in the excited state of two tryptophanyl diketopiperazines. *J. Am. Chem. Soc. 96*, 801-808.

Doublié, S., and Carter Jr., C.W. (1993) Structural Studies of *B. stearothermophilus* tryptophanyl-tRNA synthetase. *Biophysical Journal 64*, A57.

Doublié, S., Bricogne, G., Gilmore, C., and Carter, Jr. C.W. (1994) Tryptophanyl-tRNA Synthetase crystal structure and its homology to tyrosyl-tRNA synthetase. (Submitted to J. Mol. Biol. Sept. 1994).

Dungan, J.M., and Horowitz, P.M. (1993) Thermally Perturbed Rhodanase Can Be Protected From Inactivation by Self-Association. *Journal of Protein Chemistry 12*, 311-321.

Eftink, M.R. (1991) Fluorescence Techniques for Studying Protein Structure. in *Protein Structure Determination: Methods of Biochemical Analysis, Vol 35*, (Suelter, C.H., Ed.) John Wiley and Sons Inc., New York, pp 127-207.

Eftink, M.R., and Ghiron, C.A. (1976) Exposure of tryptophanyl residues in proteins. Quantitative determination by fluorescence quenching studies. *Biochemistry 15*, 672-679.

Eftink, M.R., and Ghiron, C.A. (1977) Exposure of Tryptophanyl Residues and Protein Dynamics *Biochemistry 16*, 5546-5551.

Eftink, M.R., and Ghiron, C.A. (1981) Fluorescence Quenching Studies with Proteins. *Analytical Biochemistry 114*, 199-227.

Eisinger, J. (1969) A variable temperature UV luminescence spectrograph for small samples. *Photochim. Photobiol. 9*, 241-258.

Eisinger, J., and Dale, R.E. (1976) What has energy transfer done for Biochemistry lately? *In Excited States of Biological Molecules* (Birks, J.B. Ed.) John Wiley and Sons, New York, pp 579-590.

Engh, R.A., Chen, L.X.-Q., and Fleming, G.R. (1986) Conformational Dynamics of Tryptophan: A Proposal For the Origin of the Non-Exponential Fluorescence Decay. *Chem. Phys. Lett. 126*, 365-372.

Eriani, G., Delarue, M., Poch, O., Gangloff, J., and Moras, D. (1990) Partition of tRNA synthetases into two classes based on mutually exclusive sets of sequence motifs. *Nature 247,* 203-206

Evers, U., Franceschi, F., Böddeker, and Yonath, A. (1994) Crystallography of halophilic ribosome: the isolation of an internal ribonucleoprotein complex. *Biophysical Chemistry 50*, 3-16.

Fasman, G.D (1989) *Prediction of Protein Structure and the Principles of Protein Conformation.* 193-301.

Fasman, G.D. Ed. (1988) *Handbook of Biochemistry and Molecular Biology, 3rd. Ed.*, Vol. II. CRC Press Inc. Boca Raton, FL., USA. p233.

Favorova, O.O., Madoyan, I.A., and Drusta, V.L. (1981) 'Half-Site' Affinity Modification of Tryptophanyl-tRNA Synthetase Leads to Freezing of the Free Subunit. *FEBS Lett. 123*, 161-164.

Fersht, A.R. (1993) Protein folding and stability: the pathway of folding of barnase. *FEBS letts. 325*, 5-16.

Fersht, A.R., Jakes, R. (1975) Demonstration of two reaction pathways for the aminoacylation of tRNA. Application of the pulsed quenched flow technique. *Biochemistry 14*, 3350-3356.

Fersht, A.R., Leatherbarrow, R.J., and Wells, T.N.C (1987) Structure-activity relationships in engineered proteins: Analysis and use of binding energy by linear free energy relationships. *Biochemistry 26*, 6030-6038.

Foote, J., Ikeda, D.M., and Kantrowitz, E.R. (1980) The role of tryptophan in aspartate transcarbamylase. *J. Biol. Chem. 255*, 5154-5158.

Förster, Th. (1951) *Fluoresenz Organischer Verbindungen*, Vanderhoeck and Rupprect, Göttingen.

Freist, W. (1989) Mechanisms of Aminoacyl-tRNA Synthetases: A Critical Consideration of Recent Results. *Biochemistry 28*, 6787-6795.

Frolova. L.Y., Fleckner, J., Justesen, J., Timms, K.M., Tate, W.P., Kisselev, L.L., and Haenni, A. (1993) Are the tryptophanyl-tRNA synthetase and the peptide-chain-release facto from higher eukaryotes on and the same protein? *Eur. J. Biochem. 212*, 457-466.

Frolova, L.Y., Sudomoina, M.A., Grigorieva, A.Y., Zinovieva, O.L., and Kisselev, L.L. (1991) Cloning and nucleotide sequence of the structural gene encoding for human tryptophanyl-tRNA synthetase. *Gene 109*, 291-296.

Fromant, M., Fayat, G., Laufer, P., and Blanquet, S. (1981) Affinity Chromatography of aminoacyl-tRNA synthetases on agarose-hexyl-adenosine-5'-phosphate. *Biochimie. 63*, 541-553.

Gai, F., Chen, Y. and Petrich, J.W. (1992) Nonradiative Pathways of 7-Azaindole in Water. *J. Am. Chem. Soc. 114*, 8343-8345.

Gai, F., Rich, R.L., and Petrich, J.W. (1994) Monophotonic Ionization of 7-Azaindole, Indole, and Their Derivatives and the Role of Overlapping Excited States. *J. Am. Chem. Soc. 116*, 735-746.

Garret, M., Pajot, B., Trézéguet, V., Labouesse, J., Merle, M., Gandar, J-C., Benedetto, J-P., Sallafranque, M-L., Alterio, J., Gueguen, M., Sarger, C., Labouesse, B., and Bonnet, J. (1991) A mammalian tryptophanyl-tRNA synthetase shows little homology to prokaryotic synthetases but near identity with mammalian peptide chain release factor. *Biochemistry 30*, 7809-7817.

Gill, S.C., and von Hippel, P.H., (1989) Calculation of Protein Extinction Coefficients from Amino Acid Sequence Data. *Analytical Biochemsitry 182*, 319-326.

Goodsell, D.S., and Olson, A.J. (1993) Soluble Proteins: size, shape and function. *Trends. Biochem. Sci. 18*, 65-68.

Gordon, H.L., Jarrel, H.C., Szabo, A.G., Willis, K.J., and Somorjai, R.L. (1992) Molecular Dynamics Simulations of the Conformational Dynamics of Tryptophan. *J. Phys. Chem. 96*, 1915-1921.

Graves, P.V., deBony, J., Mazat, J.P., and Labouesse, B. (1980) Tryptophanyl-tRNA synthetase from beef pancreas. Spectroscopic analysis of the stoichiometry of formation of the enzyme-tryptophanyl-adenylate complex. *Biochimie, 62*, 33-41.

Gregoret, L.M., Rader, S.D., Fletterick, R.J., and Cohen, F.E (1991) Hydrogen Bonds Involving Sulfur Atoms in Proteins. *Proteins: Structure Function, and Genetics 9*, 99-107.

Grinvald, A., and Steinberg, I.Z. (1976) The fluorescence decay of tryptophan residues in native and denatured proteins. *Biochem. Biophys. Acta. 427*, 663-678.

Gros, C., Lemaire, G., VanRapenbusch, R., and Labouesse, B. (1972) The Subunit Structure of Tryptophanyl Transfer Ribonucleic Acid Synthetase from Beef Pancreas. *J. Biol. Chem. 247*, 2931-2943.

Gudgin-Templeton, E.F., and Ware, W.R. (1984) The Time Dependence of the Low-Temperature Fluorescence of Tryptophan. *J. Phys. Chem. 88*, 4626-4631.

Hall, C.V., and Yanofsky, C. (1981) Cloning and Characterization of the Gene for *Escherichia coli* Tryptophanyl-Transfer Ribonucleic Acid Synthetase. *J. Bacteriology 148*, 941-949.

Hall, C.V., vanCeemput, M., Muench, K.H., and Yanofsky, C. (1982) The Nucleotide Sequence of the Structural Gene for Escherichia coli Tryptophanyl-tRNA Synthetase. *J. Biol. Chem. 257*, 6132-6136.

Halvorson, H., Spiegelman, S., and Hinman, R.L., (1955) The effect of tryptophan analogs on the induced synthesis of maltase and protein synthesis in yeast. *Arch. Biochim. Biophys. 55*, 512-525.

Harris, D.L., and Hudson, B.S. (1990) Photophysics of Tryptophan in Bacteriophage T4 Lysozymes. *Biochemistry 29*, 5276-5285.

Hasselbacher, C.A., Rusinova, E., Waxman, E., Lam, W., Guha, A., Rusinova, R., Nemerson, Y., and Ross, J.B.A. (1994) Probing the structure of human tissue factor by site-directed mutagenesis of tryptophan residues and in-vivo incorporation of tryptophan analogs. *SPIE Proceedings, 2137*, 312-323.

Haydock, C. (1993) Protein side chain rotational isomerization: A minimum perturbation mapping study. *J. Chem. Phys. 98*, 8199-8214.

Hershberger, M.V., Lumry, R., and Verrall, R. (1981) The 3-Methylindole/n-Butanol Exciplexes: Evidence for Two Exciplex Sites in Indole Compounds. *Photochim. Photobiol. 33*, 609-617.

Heyduk, E., and Heyduk, T., (1993) Physical Studies on Interaction of Transcription Activator And RNA-Polymerase: Fluorescent Derivatives of CRP and RNA Polymerase. *Cellular and Molecular Biology Research 39*, 401-407.

Heyduk, T. and Callaci, S. (1994) Fluorescence probes for studying the mechanism of transcription activation. *SPIE Proceedings 2137*, 719-724.

Hogue, C.W., MacManus, J.P., Banville, D., and Szabo, A.G. (1992) Comparison of Terbium(III) Luminescence Enhancement in Mutants of EF Hand Calcium Binding Proteins. *J. Biol. Chem. 267*, 13340-13347.

Hogue, C.W.V., and Szabo, A.G., (1993) Characterization of aminoacyl-adenylates in *B. subtilis* tryptophanyl-tRNA synthetase, by the fluorescence of tryptophan analogs 5-hydroxytryptophan and 7-azatryptophan. *Biophys. Chem. 48*, 159-169.

Hogue, C.W.V., Rasquinha, I., Szabo, A.G., and MacManus, J.P., (1992) A new intrinsic fluorescent probe for proteins: Biosynthetic incorporation of 5-hydroxytryptophan into oncomodulin. *FEBS Letts. 310*, 269-272.

Hott, J.L., and Borkman, R.F. (1989) The non-fluorescence of 4-fluorotryptophan. *Biochem. J. 264*, 297-299.

Hou, Y. and Schimmel, P. (1992) Novel Transfer RNAs That Are Active in *Escherichia coli*. *Biochemistry 31*, 4157-4160

Hudson B.S., Harris, D.L., Ludescher, R.D., Ruggiero, A., Cooney-Freed, A., and Cavalier, S. (1986) Fluorescence Probe Studies of Proteins and Membranes. in *Applications of Fluorescence in the Biomedical Sciences.* Eds. D. L. Taylor et al. A.R. Liss Inc. New York. pp. 159-202.

Hunt, T. (1980) The initiation of protein synthesis. *Trends Biochem. Sci. 5*, 178-181.

Hutnik, C.M.L., 1990 *The Conformational Heterogeneity of Proteins.* Ph.D. Thesis, University of Ottawa.

Hutnik, C.M.L., and Szabo, A.G. (1989) A Time-Resolved Fluorescence Study of Azurin and Metalloazurin Derivatives. *Biochemistry 28*, 3935-3939.

Hutnik, C.M.L., MacManus, J.P., Banville, D., and Szabo, A.G. (1990) Comparison of Metal Ion-induced Conformational Changes in Parvalbumin and Oncomodulin as Probed by the Intrinsic Fluorescence of Tryptophan 102. *J. Biol. Chem. 265*, 11456-11464.

Hutnik, C.M.L., MacManus, J.P., Banville, D., and Szabo, A.G. (1991) Metal-Induced Changes in the Fluorescence Properties of Tyrosine and Tryptophan Site-Specific Mutants of Oncomodulin. *Biochemistry 39*, 7652-7660.

Ibba, M., Kast, P., and Hennecke, H. (1994) Substrate Specificity Is Determined by Amino Acid Binding Pocket Size in *Escherichia coli* Phenylalanyl-tRNA Synthetase. *Biochemistry 33*, 7107-7112.

Illich, P., Axelsen, P., and Prendergast, F.G. (1988) Electronic transitions in molecules in static external fields. I. Indole and Trp-59 in ribonuclease T1. *Biophys. Chem. 29*, 341-349.

Imoto, T., and Yamada, H. Chemical Modification in *Protein Functin, A Practical Approach*, (Creighton, T.E., Ed.) IRL Press, New York. pp 266-268.

Ito, A.S., de L. Castrucci, A.M., Hruby, V.J., Hadley, M.E., Krajcarski, D.T., and Szabo, A.G. (1993) Structure-Activity Correlations of Melanotropin Peptides in Model Lipids by Tryptophan Fluorescence Studies. *Biochemistry 32*, 2264-12272.

Jablonski, A. (1935) Über den mechanismus des photolumineszenz von farbstoff-phosphoren. *Z. Phys. 94*, 38-46.

Jakubowski, H., and Pawelkiewicz, J. (1975) The Plant Aminoacyl-tRNA Synthetases. Purification and Characterization of Valyl-tRNA, Tryptophanyl-tRNA and Seryl-tRNA Synthetases from Yellow Lupin Seeds. *Eur. J. Biochem. 52*, 301-310.

James, D.R., and Ware, W.R. (1986) Chem Phys. Lett. 126, 7-11

Johnson, A.D. (1974) A biologically active aminoacyl-tRNA analogue: ε-N-acetyl-Lys-tRNA. *Federation Proceedings 33*, part II Abstract 1189.

Joseph, D.R., and Muench, K.H. (1971a) Tryptophanyl Transfer Ribonucleic Acid Synthetase of *Escherichia coli* I. Purification of the Enzyme and of Tryptophan Transfer Ribonucleic Acid. *J. Biol. Chem. 246*, 7602-7609.

Joseph, D.R., and Muench, K.H. (1971b) Tryptophanyl Transfer Ribonucleic Acid Synthetase of *Escherichia coli* II. Molecular Weight, Subunit Structure, Sulfhydryl Content and Substrate-Binding Properties. *J. Biol. Chem. 246*, 7610-7615.

Judice, J.K., Gamble, T.R., Murphy, E.C., deVos, A.M., and Schultz, P.G (1993) Probing the Mechanism of Staphylococcal Nuclease with Unnatural Amino Acids: Kinetic and Structural Studies. *Science 261*, 1578-1581.

Khosla, C., and Bailey, J.E. (1989) Characterization of the Oxygen-Dependent Promoter of the Vitreoscilla Hemoglobin Gene in *Escherichia coli*. *J. Bacteriol 171*, 5995-6004.

Kim, S.-J. Chowdhury, F.N., Stryjewski, W., Younathan, E.S., Russo, P.S., and Barkley, M.D. (1993) Time-resolved Fluorescence of the Single Tryptophan of *Bacillus stearothermophilus* Phosphofructokinase. *Biophys. J. 65*, 215-226.

Kimber, B.J., Feeney, J., Roberts G.C.K., Birdsall, B., Griffiths, D.V., Burgen, A.S.V., and Sykes, B.D. (1978) Proximity of two tryptophan residues by dihydrofolate reductase determined by ^{19}F NMR. *Nature 271*, 184-185.

Kingdon, H.S., Webster, L.T., and Davie, E.W. (1958) Enzymatic formation of adenyl-tryptophan: Isolation and Identification. *Proc. Natl. Acad. Sci. U.S.A. 44*, 757-765.

Kishi, T., Tanaka, M., and Tanaka, J. (1977) Electronic Absorption and Fluorescence Spectra of 5-Hydroxytryptamine (Serotonin). Protonation in the Excited State. *Bull. Chem. Soc. Japan, 50,* 1267-1271.

Kisselev, L., Frolova, L., and Haenni, A.L. (1993) Interferon inducibility of mammalian tryptophanyl-tRNA synthetase: new perspectives. *Trends. Biochem. Sci. 18*, 263-267.

Kisselev, L.L., Favorova, O.O., Nurbekov, M.K., Dmitriyenko, S.G., and Engelhardt, W.A. (1981) Bovine Tryptophanyl-tRNA Synthetase: A Zinc Metalloenzyme. *Eur. J. Biochem. 120*, 511-517.

Klapper, M.G. (1977) The independent distribution of amino acid near neighbor pairs into polypeptides. *Biochem. Biophys. Res. Commun. 78*, 1018-1024.

Klotz, I.M. (1989) Ligand-protein binding affinities. in *Protein function, a practical approach* (Creighton, T.E. Ed) IRL Press, New York. pp 25-54.

Knorre, D.G., Lavrik, O.I., Petrova, T.D., Savchenko, T.I., and Yakobson, G.G. (1971) 4,5,6,7-Tetrafluorotryptophan: A Substrate For Tryptophanyl-tRNA Ligase, *FEBS Letts. 12*, 204-206.

Knutson, J.R., Beechem, J.M., and Brand, L. (1983) Simultaneous Analysis of Multiple Fluorescence Decay Curves: A Global Approach. *Chem. Phys. Lett. 102*, 501-507.

Knutson, J.R., Walbridge, D.G., and Brand, L., (1982) Decay-Associated Fluorescence Spectra and the Heterogeneous Emission of Alcohol Dehydrogenase. *Biochemistry 21*, 4671-4679.

Kohno, T., Kohda, D., Haruki, M., Yokoyama, S., and Miyazawa, T. (1990) Nonprotein amino acid furanomycin, unlike isoleucine in chemical structure, is charged to isoleucine tRNA by isoleucyl-tRNA synthetase and incorporated into protein. *J. Biol. Chem. 265*, 6931-6935.

Koide, H., Yokoyama, S., Kawai, G., Ha, J-M., Oka, T., Kawai, S., Miyake, T., Fuwa, T., and Miyazawa, T. (1988) Biosynthesis of a protein containing a nonprotein amino acid by *Escherichia coli*: L-2-aminohexanoic acid at position 21 in human epidermal growth factor. *Proc. Natl. Acad. Sci. USA. 85*, 6237-6241.

Krishnaswamy, P.R., and Meister, A. (1960) Enzymatic Synthesis and Reactions of Amino Acyl Adenylates. *J. Biol. Chem. 235,* 408-415.

Kronman, M.J. (1976) Changes in Emission Band Shape of Proteins Undergoing Conformational Changes. In *Biochemical Fluorescence Concepts.* (Chen., R.F., and Edelhoch, H., Eds). Vol. 2. Marcel Dekker Inc., New York pp.487-514.

Kuehl, G.V., Lee, M.L., and Muench, K.H. (1976) Tryptophanyl Transfer Ribonucleic Acid Synthetase of *Escherichia coli*: Character of required thiol group and structure of thiol peptides. *J. Biol. Chem. 251, 3254-3260.*

Lakowicz, J.R. (1983) *Principles of Fluorescence Spectroscopy.* Plenum Press, New York.

Lami, H. (1976) On the possible role of mixed valence-Rydberg state in the fluorescence of indoles. *J. Chem. Phys. 67*, 3274-3281.

Lark, K.G. (1969) Incorporation of 5-methyltryptophan into the protein of *Escherichia coli* I5T- (555-7). *J. Bacteriol. 97*, 980-982.

Laue, T.M., Senear, D.F., Eaton, S., and Ross, J.B.A. (1993) 5-Hydroxytryptophan as a New Intrinsic Probe for Investigating Protein-DNA Interactions by Analytical Ultracentrifugation. Study of the Effect of DNA on Self-Assembly of the Bacteriophage λ *c*I Repressor. *Biochemistry 32*, 2469-2472.

Laws, W.R., and Brand, L. (1979) Analysis of two-state excited-state reactions. The fluorescence decay of 2-napthol. *J. Phys. Chem. 83*, 795-802.

Laws, W.R., and Contino, P.B. (1992) Fluorescence Quenching Studies: Analysis of Nonlinear Stern-Volmer Data. *Methods in Enzymology 210*, 448-463.

Lee, C.C., Craigne, W.J., Muzny, D.M., Harlow, E., and Caskey, C.T. (1990) Cloning and expression of a mammalian peptide chain release factor with sequence similarity to tryptophanyl-tRNA synthetase *Proc. Natl. Acad. Sci. U.S.A. 87*, 3508-3512.

Lee, M.L. (1974) Nicked Isoleucyl-tRNA synthetase with partial retention of activities. *Federation Proceedings 33*, part II, Abstract 1115.

Lemaire, G., Dorizzi, M., Spotorono, G., and Labouesse, B. (1968) Purification de la tryptophanyl tRNA synthétase de pancréas de boeuf. *Bull. Soc. Chim Biol. 51*, 495-510

Lemaire, G., VanRapenbusch, R., Gros, C., and Labouesse, B. (1969) Beef Pancreas Tryptophanyl-tRNA Synthetase: Molecular Weight, Composition and Spectral Properties. *Eur. J. Biochem. 10*, 336-344.

Li, E., Qian, S., Nader, L., Yang, N.C., d'Avignon, A., Sacchettini, J.C. and Gordon, J.I. (1989) Nuclear Magnetic Resonance Studies of 6-fluorotryptophan-substituted rat cellular retinol-binding protein II produced in *Escherichia coli*. *J. Biol. Chem. 264*, 17041-17048.

Lian, Chenyang, Le, Honbiao, Montez, B., Patterson, J., Harrel, S., Laws, D., Matsumura, I., Pearson, J., and Olfield, E. (1994) Fluorine-19 Nuclear Magnetic Resonance Spectroscopic Study of Fluorophenylalanine- and Fluorotryptophan-Labeled Avian Egg White Lysozymes. *Biochemistry 33*, 5238-5245.

Lim, V., Venclovas, C., Spirin, A., Brimacombe, R., Mitchell, P and Muller, F. (1992) How are tRNAs and mRNA arranged in the ribosome? An attempt to correlate the stereochemistry of the tRNA-mRNA interaction with constraints imposed by the ribosomal topography. *Nucleic Acids Research 20*, 2627-2637.

Lindahl, P., Raub-Segall, E., Olson, S.T., and Björk, I. (1991) Papain labelled with fluorescent thiol-specific reagents as a probe for characterization of interactions between cysteine proteinases and their protein inhibitors by competitive titrations. *Biochem J. 276*, 5074-5082.

Longworth, J.W. (1971) Luminescence of Polypeptides and Proteins. in *Excited States of Proteins and Nucleic Acids.* (Eds. Steiner, R.F., and Weinryb, I) Plenum Press. pp 319-484.

Longworth, J.W. Luminescence of Polypeptides and Proteins. (1970) in *Excited States of Proteins and Nucleic Acids* (Steiner, R.F., and Weinryb, I., Eds) Plenum Press, New York., USA, pp 319-484.

MacManus, J.P., Hutnik, C.M.L., Sykes, B.D. Szabo, A.G., Williams, T.C., and Banville, D. (1989) Characterization and Site-specific Mutagenesis of the Caclium-binding Protein Oncomodulin Produced by Recombinant Bacteria. *J. Biol Chem. 264*, 3470-3477.

Marquardt, D.W. (1963) An algorithm for least-squares estimation of nonlinear parameters. *J. Soc. Ind. Appl. Math. 11*, 431-441.

Mazat, J.P., Merle, M., Graves, P.V., Merault, G., Gandar, J.C. and Labouesse, B. (1982) Kinetic Anticooperativity in Pre-Steady-State Formation of Tryptophanyl Adenylate by Tryptophanyl-tRNA Synthetase from Beef Pancreas: A Consequence of Tryptophan Anticooperative Binding. *Eur. J. Biochem. 128*, 389-398.

McClain, W.H. (1993) Rules that govern tRNA identity in protein synthesis. *J. Mol. Biol. 234*, 257-280.

McKinnon, A.E., Szabo, A.G., and Miller, D.R. (1977) The Deconvolution of Photoluminescence Data. *J. Phys. Chem. 81*, 1564-1570.

Meech, S.R., and Phillips, D. J. (1983) Photophysics of Some Common Fluorescence Standards. *J. of Photochem. 23* 193-217.

Mendel, D.M., Ellman, J.A., Chang, Z., Veenstra, D.L., Kollman, P.A., and Schultz, P.G. (1992) Probing Protein Stability with Unnatural Amino Acids. *Science 256*, 1798-1802.

Merault, G., Labouesse, J., Graves, P.V., and Labouesse, B. (1981) Kinetics of formation of tryptophanyl-adenylate by tryptophanyl-tRNA synthetase from beef pancreas. *FEBS Lett. 123*, 165-168.

Merle, M., Trezeguet, V., Graves, V., Andrews, D., Muench, K.H., and Labouesse, B. (1986) Tryptophanyl-Adenylate Formation by Tryptophanyl-tRNA Synthetase from *Escherichia coli. Biochemistry 25*, 1115-1123.

Mersol, J.V., Steel, D.G., and Gafni, A. (1993) Detection of intermediate protein conformations by room temperature phosphorescence spectroscopy during denaturation of *Escherichia coli* alkaline phosphatase. *Biophysical Chemistry 48*, 281-291.

Mersol, J.V., Wang, H., Gafni, A., and Steel, D.G. (1992) Consideration of dipole orientation angles yields accurate rate equations for energy transfer in the rapid diffusion limit. *Biophys. J. 61*, 1647-1655.

Miller, J.N. (1981) *Standards in Fluorescence Spectrometry*. Chapman and Hall, London, UK.

Milton, J.G., Purkey, R.M., and Galley, W.C. (1978) The kinetics of solvent reorientation in hydroxylated solvents from the exciting-wavelength dependence of chromophore emission spectra. *J. Chem. Phys. 68*, 5396-5404.

Mirande, M. (1991) Aminoacyl-tRNA Synthetase Family from Prokaryotes and Eukaryotes: Structural Domains and Their Implications. *Progress in Nucleic Acids Research and Molecular Biology 40*, 95-142.

Montgomery, R., and Swenson, C.A., (1976) Quantitative Problems in the Biochemical Sciences, 2nd Ed. W.H. Freeman and Co., San Francisco, pp 292-295.

Moras, D. (1992) Structural and Functional Relationships Between Aminoacyl-tRNA Synthetases. *Trends. Biochem. Sci. 17*, 159-164.

Muench, K.H. (1976) Two Substrate Binding Sites on Tryptophanyl Transfer Ribonucleic Acid Synthetase of Escherichia coli. *J. Biol. Chem. 251*, 5195-5199.

Muench, K.H., Lipscomb, M.S., Lee, M., and Kuehl, G.V. (1975) Homologous cysteine-containing sequences in Tryptophanyl-tRNA synthetases from *Eschercia coli* and human placentas. *Science 187*, 1089-1091.

Myers, A.A and Tzagoloff, A. (1985) MSW, A Yeast Gene Coding for Mitochondrial Tryptophanyl-tRNA Synthetase *J. Biol. Chem. 260*, 15371-15377.

Négrerie, M., Bellefeuille, M., Whitham, S., Petrich, J.W., and Thornburg, R.W. (1990) Novel Noninvasive in Situ Probe of Protein Structure and Dynamics. *J. Am. Chem. Soc. 112*, 7419-7421.

Négrerie, M., Gai, F., Bellefeuille, M., and Petrich, J.W. (1991) Photophysics of a Novel Optical Probe,: 7-Azaindole. *J. Phys. Chem. 95*, 8663-8670.

Négrerie, M., Gai, F., Lambry, J.-C. Martin, J.-L. and Petrich, J.W. (1993) Photoionization and Dynamic Solvation of the Excited States of 7-Azaindole. *J. Phys. Chem. 97*, 5046-5049.

Nevinsky, G. A., Favorova, O.O., Kavrik, O.I., Petrova, T.D., Kochkina, L.L., and Savchenko, T.I. (1974) Fluorinated tryptophans as substrates and inhibitors of the ATP-[^{32}P]PP$_i$ exchange reaction catalysed by tryptophanyl-tRNA synthetase. *FEBS Lett. 43*, 135-138.

Nosoh, Y., and Sekiguchi, T. (1993) Protein Engineering for Thermostabilization. in *Thermostability of Enzymes*, (Gupta, M.N ed.), pp 182-203.

O'Connor, D.V., and Phillips, D. (1984) *Time-correlated Single Photon Counting.* Academic Press, London, UK.

Omnaas, J., Bonura, M., Chang, P., Safille, P.A., and Muench, K.H. (1979) Limited Tryptic Digestion of Native Tryptophanyl-tRNA Synthetase From a Superproducing Strain of *Escherichia coli. Federation Proceedings. (FASEB) 38*, 821 Abstract 3113.

Orgel, L.E. (1994) The Origin of Life on the Earth. *Scientific American, 271*, 76-83.

Pace, C.N., Laurents, D.V., and Erickson, R.E. (1992) Urea Denaturation of Barnase: pH Dependence and Characterization of the Unfolded State. *Biochemistry 31*, 2728-2734.

Pak, M., Pallanck, L., and Shulman, L.H. (1992) Conversion of a Methionine Initiator tRNA into a Tryptophan-Inserting Elongator tRNA *in vivo. Biochemistry 31*, 3303-3309.

Palleros, D.R., Reid, K.L., McCarty, J.S., Walker, G.C., and Fink, A.L. (1992) DnaK, hsp73, and Their Molten Globules. *J. Biol. Chem. 267*, 5279-5285.

Pardee, A.B., Shore, V.G., and Prestidge, L.S. (1956) Incorporation of azatryptophan into proteins of bacteria and bacteriophage. *Biochim. et Biophys Acta 21*, 406-407.

Parker, C.A. (1968) *Photoluminescence of Solutions.* Elsevier, Amsterdam, Netherlands.

Parker, C.A., and Rees, W.T. (1960) Corrections of fluorescence spectra and measurement of fluorescence quantum efficiency. *Analyst 85*, 587-600.

Pauling, L. (1960) *The Nature of the Chemical Bond, 3rd ed.* Cornell Univ. Press, Ithaca N.Y. pp 257-260.

Pauls, T.L., Durussel, I., Cox, J.A., Clark, I.D., Szabo, A.G., Gagné, S.M., Sykes, B.D., and Berchtold, M.W. (1993) Metal Binding Properties of Recombinant Rat Parvalbumin Wild-type and F102W Mutant. *J. Biol. Chem. 268*, 20897-20903.

Pavia, D.L., Lampman, G.M., and Kriz Jr., G.S. (1979) *Introduction to Spectroscopy: A Guide for Students of Organic Chemistry.* Saunders College Press, Philadelphia, pp 183-220.

Penneys, N.S., and Muench, K.H. (1974) Human Tryptophanyl Transfer Ribonucleic Acid Synthetase. Comparison of the Kinetic Mechanism to that of *Escherichia coli* Tryptophanyl Transfer Ribonucleic Acid Synthetase. *Biochemistry 13*, 566-571.

Penzer, G.R. (1980) Molecular Emission Spectroscopy (Fluorescence and Phosphorescence) in *An Introduction to Spectroscopy for Biochemists* (Brown, S.B., Ed.) Academic Press, New York, pp. 70-107.

Perona, J.J., Rould, M.A., and Steitz, T.A. (1993) Structural Basis for Transfer RNA Aminoacylation by *Escherichia coli* Gluaminyl-tRNA Synthetase. *Biochemistry 32*, 8758-8771.

Petrich, J.W., Chang, M.C., McDonald, D.B., and Fleming, G.R. (1983) On the Origin of Nonexponential Fluorescence Decay in Tryptophan and Its Derivatives. *J. Am. Chem. Soc. 105*, 3832-3836.

Phillips, D., Drake, R.C., O'Connor, D.V., and Cristensen, R.L. (1985) Time correlated single-photon counting (TCSPC) using laser excitation. *Anal. Instr. 14*, 267-292.

Piel, N., Freist, W., and Cramer, F. (1983) Synthesis of Modified Tryptophanyl-Adenylates and of Modified Adenosine-Triphosphates and their Use as Tools for Elucidation of the Mechanism of Tryptophanyl-tRNA Synthetase from Yeast. *Bioorg. Chem. 12*, 18-33.

Pratt, F. A. and Ho, C. (1975) Incorporation of fluorotryptophans into proteins of *Escherichia coli*. *Biochemistry 14*, 3035-3040.

Preddie, E.C., (1969) Tryptophanyl Transfer Ribonucleic Acid Synthetase for Bovine Pancreas, III A complex of tryptophanyl transfer ribonucleic acid synthetase and transfer ribonucleic acid that accepts tryptophan: The purification of ^{32}P-tryptophan transfer ribonucleic acid. *J. Biol. Chem.* 244, 3969-3972.

Prince, J.B., Gutell, R.R., and Garrett, R.A. (1983) A consensus model of the *E. coli* ribosome. *Trends Biochem. Sci. 8*, 359-363.

Quigley, G.L., and Rich, (1976) A. Structural Domains of Transfer RNA Molecules. *Science 194*, 796-806

Rayner, D.M., and Szabo, A.G. (1978) Time resolved fluorescence of aqueous tryptophan. *Can. J. Chem. 56*, 743-745.

Rich, R.L., Chen, Y. Neven, D. Négrerie, M., Gai, F., and Petrich, J.W. (1993a) Steady-State and Time-Resolved Fluorescence Anisotropy of 7-Azaindole and Its Derivatives. *J. Phys. Chem. 97*, 1781-1788.

Rich, R.L., Gai, F., Chen, Y. and Petrich, J.W. (1994) Using 7-Azaindole to Probe Condensed Phase Dynamics. *Proceedings of SPIE 2137*, 435-446.

Rich, R.L., Négrerie, M., Li, J., Elliot, S., Thornburg, R.W., and Petrich, J.W. (1993b) The Photophysical Probe, 7-azatryptophan, in Synthetic Peptides. *Photochim. Photobiol. 58*, 28-30.

Rogers, M.J., and Soll, D. (1990) Inaccuracy and the Recognition of tRNA. *Progress in Nucleic Acids Research and Molecular Biology. 39*, 185-208.

Ross, J.B.A., Laws, W.R., Rousslang, K.W., and Wyssbord, H.R. (1992b) Tyrosine fluorescence and phosphorescence from proteins and polypeptides. In *Topics in Fluorescence Spectroscopy, Vol. 3: Biochemical Applications* (Lackowitcz, J.R., Ed), Plenum Press, New York. pp. 1-63.

Ross, J.B.A., Senear, D.F., Waxman, E., Kombo, B.B., Rusinova, E., Huang, Y.T., Laws, W.R., and Hasselbacher, C.A., (1992a) Spectral enhancement of proteins: Biological incorporation and fluorescence characterization of 5-hydroxytryptophan in bacteriophage λ cI repressor *Proc. Natl. Acad. Sci. USA. 89*, 12023-12027.

Ross, J.B.A., Wyssbrod, H.R., Porter, R.A., Schwartz, G.P., Michaels, C.A. and Laws, W.R. (1992c). Correlation of tryptophan fluorescence intensity decay parameters with ^{1}H NMR-determined rotamer conformations: [tryptophan^{2}] oxytocin. *Biochemistry 31*, 1585-1594.

Rossmann, M.G., Moras, D., and Olsen, K.W. (1974) Chemical and biological evolution of a nucleotide-binding protein. *Nature 250*, 194-199.

Rould, M.A., Perona, J.J., Söll, D., and Steitz, T.A., (1989) Structure of *E. coli* glutaminyl-tRNA synthetase complexed with tRNA-Gln and ATP at 2.8 Å resolution. *Science 246*, 1135-1142.

Royer, C.A., Gardner, J.A., Beechem, J.M., Brochon, J-C., and Matthews, K.S (1990) Resolution of the fluorescence decay of the two tryptophan residues of *lac* repressor using single tryptophan mutants. *Biophys. J. 58*, 363-378.

Ruff, M., Krishnaswamy, S., Boeglin, M., Poterszman, A., Mitschler, A., Podjary, A., Rees, B., Thierry, J.C., and Moras, D. (1991) Class II aminoacyl transfer RNA synthetases: crystal structure of yeast aspartyl-tRNA synthetase complexed with $tRNA^{Asp}$. *Science 252*, 1682-1689.

Saito, I., Sugiyama, H., Yamamoto, A., Muramatsu, S., and Matsuura, T. (1984) Photochemical Hydrogen-Deuterium Exchange Reaction of Tryptophan. The Role in Nonradiative Decay of Singlet Tryptophan. *J. Am. Chem. Soc.* 106, 4286-4287.

Sambrook, J., Fritsch, E.F., and Maniatis, T., (1989) *Molecular Cloning, a laboratory manual, 2nd Ed.* Cold Spring Harbor Laboratory Press, New York.

Sato, A., Bitten, E., Lambert, D., and Rousslang, K. (1994) Steady-state and time-resolved phosphorescence of 5-hydroxy-L-tryptophan λ *c*I repressor bound to DNA. *SPIE Proceedings 2137*, 343-352.

Schauerte, J.A., and Gafni, A. (1989) Long-Lived Tryptophan Fluorescence in Phosphoglycerate Mutase. *Biochemistry 28*, 3948-3954.

Schimmel, P. (1987) Aminoacyl tRNA Synthetases: General Scheme of Structure-Function Relationships in the Polypeptides and Recognition of Transfer RNA. *Ann. Rev. Biochem. 56*, 125-158.

Schlesinger, S. (1968) The effect of amino acid analogues on alkaline phosphatase formation in *Escherichia coli* K-12 II. Replacement of tryptophan by azatryptophan and by tryptazan. *J. Biol. Chem. 243*, 3877-3883.

Schlyer, B.D., Schauerte, J.A., Steel., D.G., and Gafni, A. (1994) Time-Resolved Room Temperature Protein Phosphorescence: Nonexponential Decay from Single Emitting Tryptophans. *Biophysical Journal 67*, 1192-1202.

Segel, I.R., *Biochemical Calculations*, 2nd Ed. (Wiley, New York, 1976) pp. 225-229.

Senear, D.F., Laue, T.M., Ross, J.B.A., Waxman, E., Eaton, S. and Rusinova, E. (1993) The Primary Self-Assembly Reaction of Bacteriophage λ *c*I Repressor Dimers Is to Octamer. *Biochemistry 32,* 6179-6189.

Sharon, N., and Lipmann, F. (1957) Reactivity of analogs with pancreatic tryptophan activating enzyme. *Arch. Biochim. Biophys. 69*, 219-227.

Shen, F., Triezenberg, S.J., Porter, D., Knutson, J.R., and Hensley, P. (1994) Fluorescence Analysis of the Transcriptional Activation Domain of the Herpesvirus Protein VP16 Reveals A Highly Flexible Structure. *Biophys. J. 66.26*, A241.

Shi., W., Chow, K.C., and Wong, J.T. (1989) High-level expression of *Bacillus subtilis* tryptophanyl-tRNA synthetase in *Escherichia coli. Can. J. Biochem. Cell Biol. 68*, 492-495.

Shiba, K., and Schimmel, P. (1992) Tripartite Functional Assembly of a Large Class I Aminoacyl tRNA Synthetase. *J. Biol. Chem. 267*, 22703-22706.

Shore, V.G., and Pardee, A.B. (1956) Fluorescence of some proteins, nucleic acids, and related compounds, Arch. Biochem. *Biophys. J. 60*, 100-107.

Skalski, B., Rayner, D.M., and Szabo, A.G. (1980) Ground-State Complexes Between Polar Solvents and 1-Methylindole: The Origin of the Stokes' Shift In Their Fluorescence Spectra. *Chem. Phys. Lett. 70*, 587-590.

Smith, C.J., Clarke, A.R., Chia, W.N, Irons, L.I., Atkinson, T., and Holbrook, J.J. (1991) Detection and Characterization of Intermediates in the Folding of Large Proteins by the Use of Genetically Inserted Tryptophan Probes. *Biochemistry 30*, 1028-1036.

Stäheli, P., Kradolfer, P., Niderberger, P., and Hütter, R. (1981) Inhibition of Yeast $tRNA^{Trp}$ Aminoacylation by 4-Methyltryptophan. *Arch. Microbiol 129*, 146-149.

Stanzel, M., Schon, A., and Sprinzl, M. (1994) Discrimination against misacylated tRNA by chloroplast elongation factor Tu. *Eur. J. Biochem. 219*, 435-439.

Steinberg, S., Gautheret, D., and Cedergren, R. (1994) Fitting the Structurally Diverse Animal Mitochondrial $tRNAs^{Ser}$ to Common Three-dimensional Constraints. *J. Mol. Biol. 236*, 982-989.

Steinberg, W., and Anagnostopoulos, C. (1971) Biochemical and Genetic Characterization of a Temperature-Sensitive, Tryptophanyl-Transfer Ribonucleic Acid Synthetase Mutant of *Bacillus subtilis*. *J. Bacteriol.* 105, 6-19.

Steiner, R.F., Albaugh, S., and Kilhoffer, M.C. (1991) Distribution of Separations Between Groups in an Engineered Calmodulin. *J. of Fluorescence 1*, 15-22.

Stokes, G.G., (1852) On the change of refrangibility of light. *Phil. Trans. R. Soc. London 142*, 463-562.

Stryer, L. (1978) Fluorescence Energy Transfer as a Spectroscopic Rule. *Ann. Rev. Biochem.* 47, 819-846.

Studier, F. W., Rosenberg, A.H., Dunn, J.J. and Dubendorff, J.W. (1990) Use of T7 RNA polymerase to direct expression of cloned genes. *Meth. Enzymol. 185*, 60-88.

Sun, M., and Song, P. (1978) Solvent Effects on the Fluorescent States of Indole Derivatives-Dipole Moments. *Photochim. Photobiol. 25*, 3-9.

Sussman, J.L., Holbrook, S.R., Warrant, R.W., Church, G.M., Kim, S-H. (1978) Crystal Structure of Yeast Phenylalanine tRNA. I. Crystallographic Refinement. *J. Mol. Biol. 123*, 607-630.

Sykes, B.D., Weingarte, H.I., and Schlesinger, M.J., (1974) Fluorotyrosine alkaline phosphatase from *Escherichia coli*: preparation, properties, and fluorine-19 nuclear magnetic resonance spectrum. *Proc. Natl. Acad. Sci. USA. 71*, 469-473.

Szabo, A.G. (1988) Laser instrumentation and data analysis in time correlated photon counting fluorescence decay measurements in biochemical investigations. in *Time-Resolved Laser Spectroscopy in Biochemistry, Proceedings of SPIE 909*, 2-7.

Szabo, A.G. (1989) The Fluorescence Properties of Aromatic Amino Acids: Their Role In The Understanding of Enzyme Structure and Dynamics. in *The Enzyme Catalysis Process* (Cooper, A., Houben, J.L., and Chien, L.C. Eds.) Plenum Publishing, New York, pp 1213-139.

Szabo, A.G., and Faerman, C (1992) Dilemma of Correlating Fluorescence Quantum Yields and Intensity Decay Times in Single Tryptophan Mutant Proteins. In Time-Resolved Laser Spectroscopy in Biochemistry III (Lakowicz, J.R., Ed.) *Proceedings of SPIE, 1640,* 70-80.

Szabo, A.G., and Rayner, D.M. (1980) Fluorescence Decay of Tryptophan Conformers in Aqueous Solution. *J. Am. Chem. Soc. 102*, 554-563.

Szabo, A.G., Stepanik, T.M., Wayner, D.M., and Young, N.M. (1983) Conformational Heterogeneity of the Copper Binding Site in Azurin, A Time-Resolved Fluorescence Study. *Biophys. J. 41*, 233-243.

Szabo, A.G., Willis, K.J., Krajcarski, D.T, and Alpert, B. (1989) Fluorescence Decay Parameters of Tryptophan in a Homogeneous Preparation of Human Hemoglobin *Chem. Phys. Lett. 163*, 565-570.

Teale, F.W.G., and Weber, G. (1957) Ultraviolet fluorescence of the aromatic amino acids. *Biochem J. 65*, 476-482.

Thang, M.N., Buckingham, R.H., and Dondon, L. (1973) Acylation of *Echericia coli* $tRNA^{Trp}$ with 5-methyltryptophan by *E. coli* tryptophanyl-tRNA ligase. *Biochim. Biophys. Acta.* 312, 685-694.

Thompson, R.C., (1988) EF-Tu provides an internal kinetic standard for translational accuracy. *Trends Biochem. Sci. 13*, 91-93.

Tonge, P.J., and Carey, P.R. (1990) Length of the Acyl Carbonyl Bond in Acyl-Serine Proteases Correlates with Reactivity. *Biochemistry, 29*, 10723-10727.

Valeur, B., and Weber, G. (1977) Resolution of the fluorescence excitation spectrum of indole into the ^1L_a and ^1L_b excitation bands. *Photochim. Photobiol. 25*, 441-444.

Vos, R., and Engelborghs, Y. (1994) A Fluorescence Study of Tryptophan-Histidine Interactions in the Peptide Anantin and in Solution. *Photochim. Photobiol. 60*, 24-32.

Walker, M.S., Bednar, T.W., and Lumry, R. (1967) Exciplex Studies. II. Indole and Indole Derivatives. *J. Chem. Phys.* 47, 1020-1028.

Waxman, E., Rusinova, E., Hasselbacher, C.A., Schwartz, G.P., Laws, W.R., and Ross, J.B.A., (1993) Determination of tryptophan:tyrosine ratio in proteins. *Anal. Biochem. 210*, 425-428.

Weber, G. (1960) Fluorescence-polarization spectrum and electronic-energy transfer in tyrosine, tryptophan and related compounds. *Biochem. J. 75*, 335-345.

Webster, T.A., Lathrop, R.H., and Smith, T.F. (1987) Prediction of a Common Structural Domain in Aminoacyl-tRNA synthetases through the Use of a New Pattern-Directed Inference System. *Biochemistry 26*, 6950-6957.

Weijland, A., and Parmeggiani, A. (1994) Why do two EF-Tu molecules act in the elongation cycle of protein biosynthesis? *Trends. Biochem. Sci. 19*, 188-193.

Weinryb, I., and Steiner, R.F. (1971)The Luminescence of the Aromatic Amino Acids. in *Excited States of Proteins and Nucleic Acids.* Plenum Press, New York. pp 277-318.

Werner, M.H., Clore, G.M., Gronenborn, A.M., Konkoh, A., and Fisher, R.J. (1994) Refolding proteins by gel filtration chromatography. *FEBS Letters 345*, 125-130.

Wetlaufer, D.B., (1962) Ultraviolet absorption spectra of proteins and amino acids. *Adv. Protein Chem.* 17, 303-390.

Willaert, K., and Engleborghs, Y. (1991) The quenching of tryptophan fluorescence by protonated and unprotonated imidazole. *Eur. Biophys. J. 20*, 177-182.

Willis, K.J., and Szabo, A.G. (1991) Fluorescence Decay Kinetics of Tyrosinate and Tyrosine Hydrogen-Bonded Complexes. *J. Phys. Chem. 95*, 1585-1589.

Willis, K.J., and Szabo, A.G. (1992) Conformation of Parathyroid Hormone: Time-Resolved Fluorescence Studies. *Biochemistry 31*, 8924-8931.

Willis, K.J., and Szabo, A.G., (1989) Resolution of Tyrosyl and Tryptophyl Fluorescence Emission From Subtilisins. *Biochemistry 28*, 4902-4908.

Willis, K.J., Neugebauer, W., Sikorska, M., and Szabo, A.G., (1994) Probing α-helical Secondary Structure at a Specific Site in Model Peptides Via Restriction of a Tryptophan Side-Chain Rotomer Conformation. *Biophysical Journal 66*, 1623-1630.

Willis, K.J., Szabo, A.G., and Krajcarski, D.T. (1990) The use of Stokes Raman scattering in time correlated single photon counting: Application to the fluorescence lifetime of tyrosinate. *Photochim. Photobiol. 51*, 375-377.

Willis, K.J., Szabo, A.G., and Krajcarski, D.T. (1991) Excited-state reaction and origin of the biexponential fluorescence decay of tryptophan zwitterion. *Chem. Phys. Lett. 182*, 614-616.

Winter, G., and Hartley, B.S. (1977) The amino acid sequence of tryptophanyl-tRNA synthetase from *Bacillus stearothermophilus. FEBS Lett. 80,* 340-342.

Wong, K.K., Meister, A., and Moldave, K. (1959) Enzymic formation of ribonucleic acid-amino acid from synthetic aminoacyladenylate and ribonucleic acid. *Biochim. Biophys. Acta. 36*, 531-533.

Xu, Z., Love, M.L., Ma, L.Y.Y., Blum, M., Bronskill, P.M., Bernstein, J., Grey, A.A., Hofmann, T., Camerman, N., and Wong, J.T. (1989) Tryptophanyl-tRNA synthetase from *Bacillus subtilis*: Characterization and role of hydrophobicity in substrate recognition. *J. Biol. Chem. 264*, 4304-4311.

Xue, H., Shen, W., and Wong, J.T. (1993a) Purification of hyperexpressed *Bacillus subtilis* $tRNA^{Trp}$ cloned in *Escherichia coli*. *J. Chromatog.* 613, 247-255.

Xue, H., Shen, W., Giegé, R., and Wong, J.T. (1993b) Identity Elements of $tRNA^{Trp}$: Identification and Evolutionary Conservation. *J. Biol. Chem. 268*, 9316-9322

Yamamoto, Y., and Tanaka, J. (1972) Polarized Absorption Spectra of Crystals of Indole and Its Related Compounds. *Bull. Chem. Soc. Japan 45*,1362-1366.

Yonath, A. (1993) Towards the Molecular Structure of the Ribosome. *Proceedings of the 11th International Biophysics Congress, July 25-30*, Budapest, Hungary. Abstract PL.4 p. 15.

Yoo, S.H., and Albanesi, J.P. (1990) Ca^{2+}-induced Conformational Change and Aggregation of Chromogranin A. *J. Biol. Chem. 265*, 14414-14421.

Zoller, M.J. and Smith, M. (1982) Oligonucleotide-directed mutagenesis using M13-derived vectors: an efficient and general procedure for the production of point mutations in any fragment of DNA. *Nucleic Acids Research 10*, 6487-6500.